NUFFIELD DEPARTMENT OF OBSTETRICS AND GYNAECOLOGY

NANOPARTICLE-MEDIATED DELIVERY TO MAMMALIAN GAMETES: DEVELOPMENT OF NOVEL RESEARCH TOOLS AND DELIVERY METHODS FOR THERAPEUTIC AGENTS

THESIS SUBMITTED FOR THE DEGREE OF
DOCTOR OF PHILOSOPHY

Natalia Barkalina

The Queen's College

Supervised by: Dr Kevin Coward

Michaelmas Term 2015

Table of Contents

List of Abbreviations

ALH	Amplitude of lateral head displacement
APTES	Aminopropyltrietoxysilane
ART	Assisted reproduction technology
BCF	Beat cross frequency
BTS	Beltsville thawing solution
CASA	Computer-assisted sperm analysis
CHAPS	3-[(3-cholamidopropyl) dimethylammonio]-1-propanesulfonate
CI	Confidence interval
CPP	Cell-penetrating peptide
CT	Computed tomography
CTAB	Hexadecyltrimethylammonium bromide
CTAC	Hexadecyltrimethylammonium chloride
DAPI	4',6-diamidino-2-phenylindole
DAR	Damaged acrosomal ridge
DEA	Diethanolamine
DGW	Density gradient washing
DNA	Deoxyribonucleic acid
EDC	1-ethyl-3-[3-dimethylaminopropyl]carbodiimide hydrochloride
EDVs	EnGeneIC Delivery Vehicles
EGFP	Enhanced Green Fluorescent Protein
EGFR	Epidermal growth factor receptor
ESHRE	European Society of Human Reproduction and Embryology
FACS	Fluorescence-activated cell sorting
FITC	Fluorescein isothiocyanate
GFP	Green Fluorescent Protein
hCG	Human chorionic gonatropin
HFEA	Human Fertilization and Embryology Authority
HIV	Human immunodeficiency virus
HLA	Human leucocyte antigen
HRT	Hormone replacement therapy
ICSI	Intracytoplasmic sperm injection
IVF	*In vitro* fertilization
LAC	Loosened acrosome cap
LIN	Linearity
MAR	Missing acrosomal ridge
MES	2-[n-morpholino]ethane sulfonic acid
MRI	Magnetic resonance imaging
MSNPs	Mesoporous silica nanoparticles
NAR	Normal apical ridge
NICE	National Institute for Health and Care Excellence
PAMAM	Poly(amidoamine)
PBS	Phosphate-based saline
PEG	Polyethylene glycol
PEI	Polyethileneimine
PGD	Preimplantation genetic diagnosis
PLA	Polylactic acid
PLCζ	Phospholipase C zeta
PLGA	Poly(lactic-co-glycolic acid)
PPI	Polypropyleneimine
RES	Reticuloendothelial system
ROS	Reactive oxygen species
RT	Room temperature
SEM	Scanning electron microscopy or Standard error of the mean
SFM	Swine Fertilization Medium
shRNA	Short hairpin ribonucleic acid
siRNA	Small interfering ribonucleic acid
SMGT	Sperm-mediated gene transfer
STR	Straightness
TEOS	Tetraethyl orthosilicate
TEM	Transmission electron microscopy
THPMP	(3-Trihydroxysilyl) propylmethylphosphonate
TNF-α	Tumor necrosis factor alpha
USPIO-NPs	Ultrasmall superparamagnetic iron oxide nanoparticles
VAP	Smoothed path velocity
VCL	Track velocity
VSL	Straight line velocity
WGA	Wheat germ agglutinin

CHAPTER 1

NANOTECHNOLOGY IN REPRODUCTIVE MEDICINE AND BIOLOGY: EMERGING APPLICATIONS OF NANOMATERIALS

Key messages:

- Nanotechnology allows the engineering of complex biocompatible nanoscale-sized platforms with high loading capacity, stability, highly selective affinity, and potential for simultaneous diagnostic and therapeutic applications.
- These platforms are increasingly introduced into various fields of medicine, including reproductive medicine, where they are currently being investigated as novel candidates for early and minimally-invasive treatment of malignant and benign diseases.
- The encouraging evidence obtained from the use of nanomaterials in medicine in general, and reproductive medicine in particular, has given rise to the hypothesis that nanotechnology could offer powerful solutions to reproductive biology via accurate and non-invasive tools for the transfer of molecular compounds into gametes and embryos for investigative and therapeutic purposes.
- Mesoporous silica is a nanomaterial with favourable features for reproductive biology, however it has not been previously studied in this specialised field.

1.1. BACKGROUND

Nanotechnology is an integrative discipline, which represents a unique combination of classical natural, mathematical, computer and materials sciences, investigating and manipulating physical matter on the nanometer scale (Koopmans and Aggeli, 2010). The unparalleled potential of engineered sub-micron structures, which are comparable in size to biological molecules, has been recognized ever since the 1950s (Feynman, 1960). However, the rapid development of applied nanotechnology only began in the 1990s following the discovery of the Nobel Prize-winning technique, scanning tunnelling microscopy (Binnig and Rohrer, 1982), and, several years later, atomic force microscopy (Binnig *et al.*, 1986). Both these methods, which allow the visualisation and handling of small-scale physical matter with exceptional accuracy, triggered an exponential growth in nanoscience.

By the year 2000, nanotechnology was universally recognised as a landmark innovation, and named “the sixth truly revolutionary technology introduced in the modern world” (Bromley, 2001). In response to the widespread practical applications of nanotechnology, many countries have introduced specialised courses in nanoscience as part of high school, undergraduate and graduate curricula, and promoted dedicated international research initiatives (European Commision (EC), 2004; Velez and Velez, 2011).

Over the last decade, nanotechnology has been extensively introduced into biomedical applications, including biological detection, drug delivery, diagnostic imaging, and tissue engineering (Koopmans and Aggeli, 2010; Kim *et al.*, 2013b; Lehner *et al.*, 2013; Tsai *et al.*, 2014). This action resulted in dramatic improvement in the diagnostic and therapeutic values of these methodologies (Uskokovic, 2013; Tsai *et al.*, 2014). Estimates suggest that the number of nanotechnology patents related to healthcare increased from less than 200 in the year 2000 to nearly 10,000 by the year 2010, doubling almost every three years, and thus reflecting the rapid expansion of the pioneering industries of nanobiotechnology and nanomedicine (**Figure 1–1**) (Antunes *et al.*, 2012).

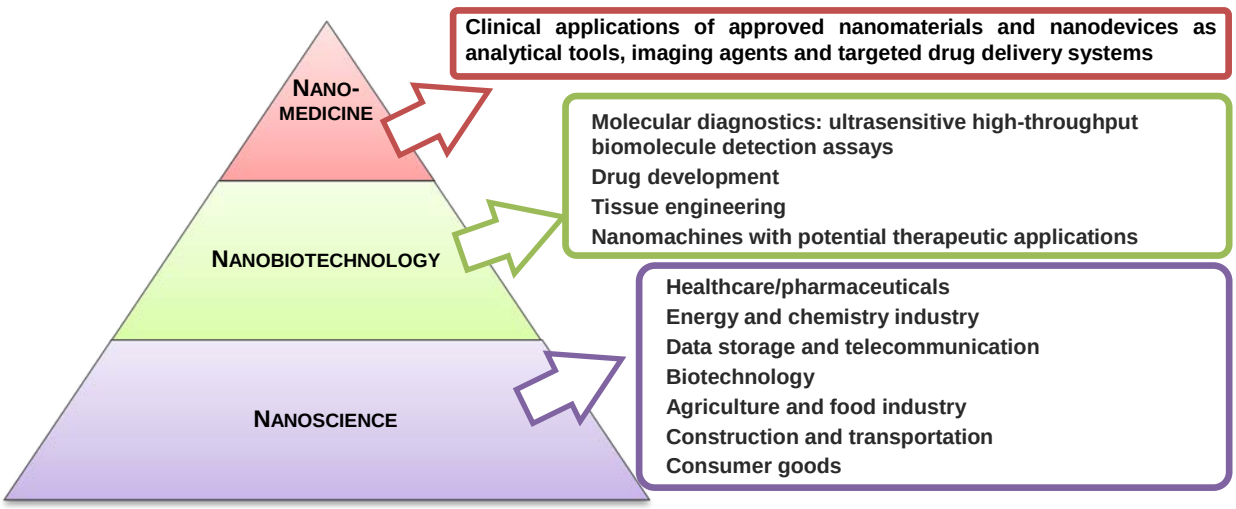

***Figure 1-1* – Nanoscience, nanobiotechnology and nanomedicine: inter-disciplinary relations and key fields of interest**. In general, nanoscience investigates the nature of atomic/molecular interactions at the 1-100 nm scale. Nanobiotechnology covers the diverse aspects of design, production and practical applications of nanostructures in biological systems. Finally, nanomedicine applies engineered nanomaterials in a clinical setting, targeting cellular and molecular levels of human biological systems for diagnostics and therapy (Webster, 2006; Jain, 2011; Lammers *et al.*, 2011).

Traditionally, the main scope of fundamental and applied nanobiotechnology lay in the field of cancer diagnostics and treatment, inseparable from the challenge of selecting and destroying affected cell populations with ultimate precision (Zamboni *et al.*, 2012). However, on-going improvement in the safety of biomedical nanomaterials, along with the accumulation of experimental evidence supporting the benefits of nanomaterial-based agents in terms of selectivity, sensitivity, affinity and detection limits (Riehemann *et al.*, 2009; Koopmans and Aggeli, 2010; Uskokovic, 2013; Tsai *et al.*, 2014), have led to the expansion of nanobiotechnological tools in a number of non-cancer applications, such as cardiovascular (Psarros *et al.*, 2012), neurological (Holmes, 2013), gastrointestinal (Brakmane *et al.*, 2012), autoimmune (Gharagozloo *et al.*, 2015; Serra and Santamaria, 2015), infectious (Mahajan *et al.*, 2012; Singh *et al.*, 2014; Choudhary and Kusum Devi, 2015) and, reproductive diseases, where they are increasingly applied for detection and treatment of cancer and experimental management of non-cancer pathologies.

This Chapter highlights the key benefits of nanotechnology in biomedicine, and introduces its emerging uses for applied reproductive medicine and fundamental reproductive biology. It addresses the benefits and concerns associated with the use of nanomaterials in a highly delicate

system of reproductive tissues and gametes, and discusses the feasibility of the innovative and controversial approach of nanomaterial-mediated delivery for research and manipulation of the mechanisms underlying reproductive pathologies, including infertility. Finally, this Chapter introduces mesoporous silica nanoparticles (MSNPs) as a potential nanovector for reproductive applications, and addresses the specific features of this nanomaterial, which could render it a promising tool for reproductive biology and medicine.

1.2. NANOMATERIALS: KEY FEATURES AND RELEVANCE FOR BIOMEDICAL APPLICATIONS

Nanotechnology, at its core, is a science investigating the engineering and application of nanomaterials – natural or manufactured objects with at least one of the three dimensions at the nanoscale (1-100 nm) (European Commision (EC), 2011). At this scale, physical, chemical and biological properties of materials fundamentally differ from the properties of single atoms of bulk solid matter, and are controlled by the effects of quantum mechanics, rather than classical physics. Regardless of natural and physicochemical properties, such as origin, size, structure, composition, and shape (**Figure 1–2)**, nanomaterials are universally characterised by one key feature, the combination of small size and immense surface area. Increased surface energy, and the altered chemical potential of nanomaterials, transforms their mechanical, magnetic, optical, and catalytic properties (European Commision (EC), 2004; Ashby *et al.*, 2009; Cao and Wang, 2011). These properties permit new levels of performance in a variety of industries, including chemical synthesis, energy supply, construction and transportation, food production, data storage and telecommunication, biotechnology, healthcare, and the manufacturing of consumer products (European Commision (EC), 2004).

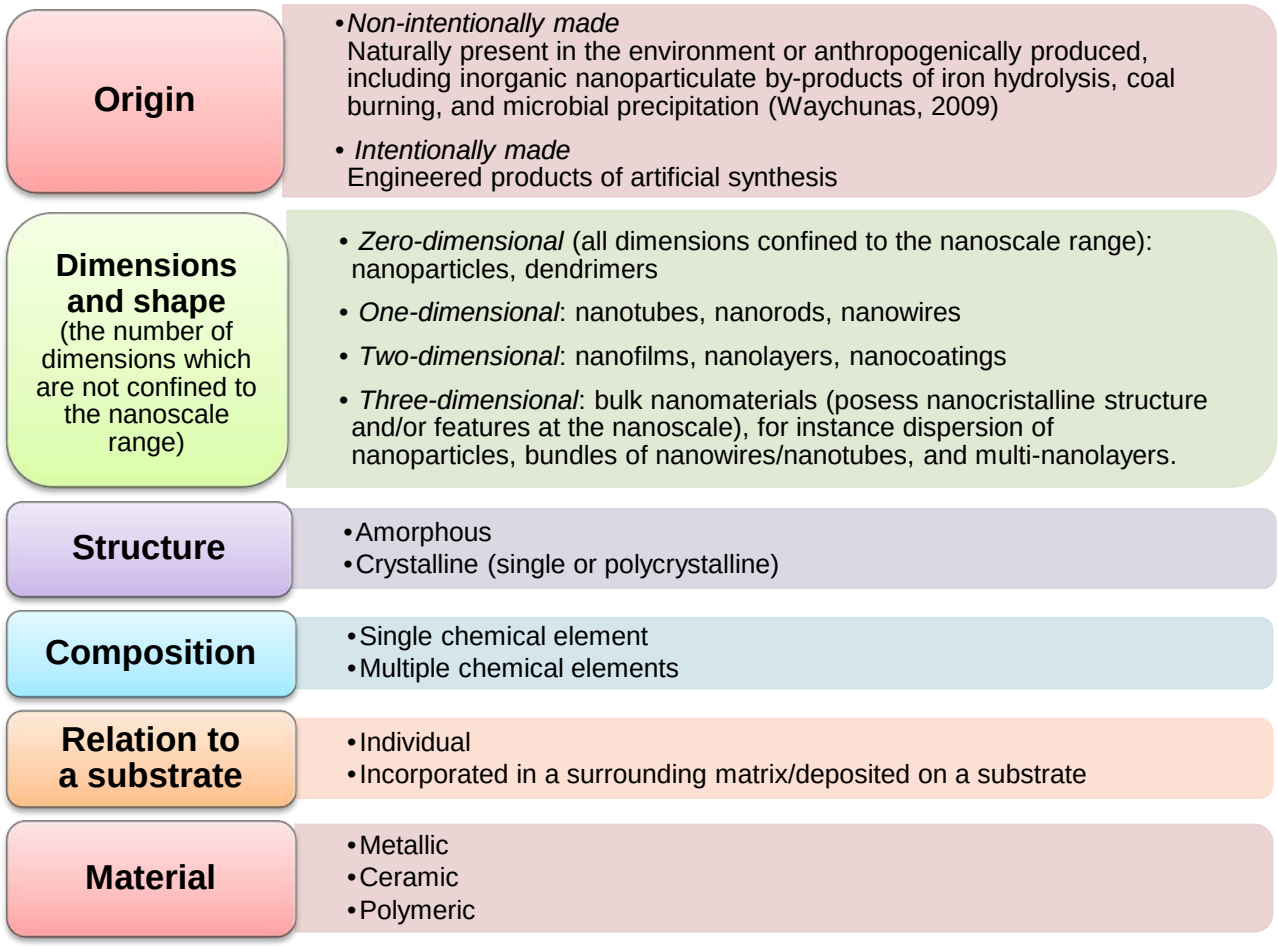

***Figure 1-2* – Summary of current nanomaterial classifications.** Nanomaterials can be classified into subtypes based on their origin, size and shape, structure, composition, relation to a substrate, and material (adapted from Ashby *et al.*, 2009). Biomedical research and clinical practice primarily utilise zero-and one-dimensional nanomaterials with various sizes, shapes and surface properties.

From the biological perspective, nanomaterials represent highly customisable and robust multifunctional platforms for the non-invasive transport of virtually any type of biological cargo, designed to mark, augment or suppress endogenous functional activity, into a selected target cell population for investigative, diagnostic and/or therapeutic purposes. Over the last few years, favourable biocompatibility has been demonstrated for a vast array of nanocarriers in combination with a wide variety of mammalian cell types (**Table 1–1, Figure 1–3)**. Furthermore, the constantly increasing awareness of the important physiological roles of natural phospholipid micro- and nanovesicles, referred to as ‘microparticles’ and ‘exosomes’, produced by mammalian cells and acting as powerful mediators of cell communication *in vivo*, highlights the possibility of

manipulating cell function using similar artificial nanostructures (El-Andaloussi *et al.*, 2013; Raposo and Stoorvogel, 2013).

***Table 1-1*– Common biomedically-applied nanomaterials**

Class	Subclass	Material	Structure	Description
Organic	**Lipids**	Phospholipids	Liposomes	Enclosed nanospheres comprised of a phospholipid bilayer
			Micelles	Enclosed nanospheres comprised of a phospholipid monolayer
		Solid lipids	Solid lipid nanoparticles	Nanospheres comprised of a lipid core stabilised by surfactants and/or polymers
	Polymers	Poly-L-lactide-co-glycolide (PLGA) Poly-L-lactic acid (PLA) Chitosan Gelatine	Nanoparticles	Variously shaped structures with all three physical dimensions on the nanoscale (<100nm)
		Polyamidoamine (PAMAM) Polypropyleneimine (PPI)	Dendrimers	Spherical nanomolecules consisting of a central core and sequential layers of branching groups
Inorganic	**Noble metals**	Gold Silver Platinum	Nanoparticles	Variously shaped structures with all three physical dimensions on the nanoscale (<100nm)
	Oxides	Magnetic and superparamagnetic iron oxides	Nanoparticles	Variously shaped structures with all three physical dimensions on the nanoscale (<100nm)
	Semi-conductors	Cadmium Selenium Tellurium Indium	Quantum dots	Semiconductor nanocrystals with optical properties
	Carbon-based	Carbon	Fullerenes	Hollow nanospheres, comprised of carbon atoms, forming cage-like structures
			Nanotubes	Cylindrical structures with two of the three physical dimensions on the nanoscale (<100nm)
	Other	Mesoporous silica	Nanoparticles	Variously shaped structures with all three physical dimensions on the nanoscale (<100nm) and mesoporous architecture (pore diameter: 2-50nm)

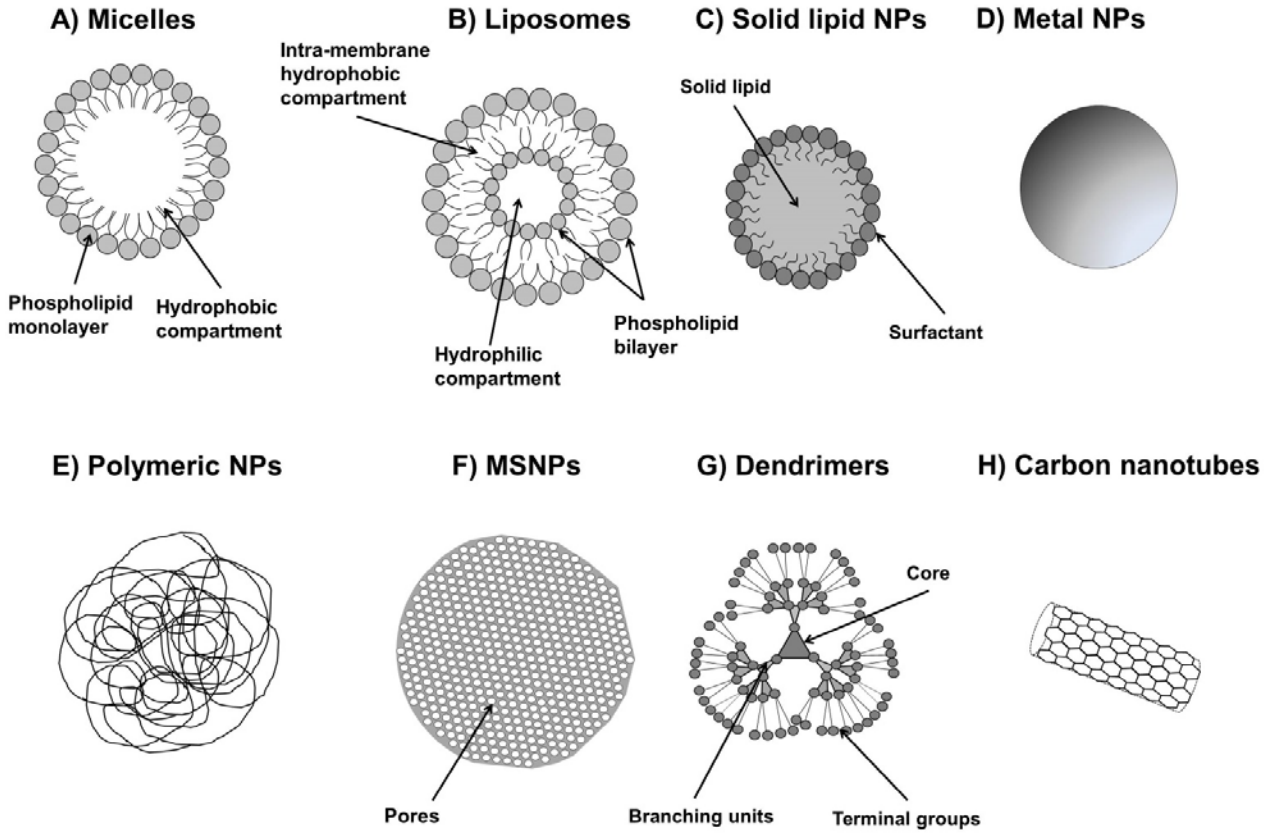

***Figure 1-3* – Common biomedically-applied nanomaterials**. A) Micelles. B) Liposomes. C) Solid lipid nanoparticles. D) Inorganic (metal) nanoparticles; quantum dots. E) Polymeric nanoparticles. F) Mesoporous silica nanoparticles. G) Dendrimers. H) Carbon nanotubes.

The enormous potential of nanomaterials in biomedicine arises from a number of features, which favour their use in the research and clinical setting (**Table 1–2)**. Firstly, their small size, comparable to the size of biomolecules, allows straightforward integration into physiological cellular processes, such as passage through the plasma membrane via innate uptake mechanisms, migration between intracellular compartments, and selective targeting of endogenous functional pathways (Petros and DeSimone, 2010; Kunzmann *et al.*, 2011).

Secondly, nanomaterials are intrinsically characterised by high stability, which results in long-distance action and, therefore, offers potential for systemic administration. Stability can be further enhanced through the use of biocompatible surface coatings, such as organic self-assembling monolayers, polyethyleneglycol (PEG), or polyethyleneimine (PEI), which prevent recognition and sequestration of a systemically administered nanocarrier by the reticuloendothelial system (RES) (Ashby *et al.*, 2009; Petros and DeSimone, 2010; Cao and Wang, 2011; Albanese *et al.*, 2012). In

the newest generations of nanomaterials, more sophisticated types of surface coatings can function as microenvironment-responsive gate-keeping mechanisms, which limit the off-target escape of cargo and allow its release upon the action of a specific endogenous or exogenous stimulus (pH, temperature, light, ultrasound) (Albanese *et al.*, 2012; Rosenholm *et al.*, 2012; Kim *et al.*, 2013b; Lehner *et al.*, 2013).

Table 1-2– **Key features of nanomaterials which favour their use in biomedicine**

Feature	**Relevance for biomedical applications**
Small size	Comparability with the size of biological molecules Potential for straightforward integration into cellular processes and physiological pathways
Large surface area	Capacity to carry large amounts of biological cargo, including simultaneous transport of various types of cargo on one nanocarrier
Versatility	Adjustable physicochemical properties (size, shape, surface charge and architecture) for increased efficacy of targeting Adjustable surface chemistry (addition of specific functional groups and/or coatings) for the covalent or non-covalent absorption of a particular type of payload Options for the 'fine-tuning' of surface chemistry through the addition of highly-specific ligands for molecular recognition and further enhanced selectivity of targeting
Targeted action	High sensitivity and specificity Reduced 'off-target' effects of cargo Improved accuracy of detection profiles for diagnostic agents Increased bioavailability and/or decreased toxicity for therapeutic agents
Stability	Distance of action Options for systemic administration Protection of 'sensitive' payloads and optimised biodistribution

In addition, nanomaterials provide enormous options for passive and active targeting. Passive targeting is based primarily on the phenomenon of enhanced permeability and retention: an ability of tissues with increased microvascular permeability, mainly malignant, to passively accumulate systemically administered nanomaterials (Matsumura and Maeda, 1986). Passive targeting, therefore, is mostly relevant for the management of cancer. In contrast, active targeting relies upon the concept of molecular recognition, and is achieved through the intentional enrichment of the nanoparticle surface with specific ligands, such as antibodies, peptides and

aptamers. These functionalities direct the nanocarrier towards a particular anatomical region, cell population and/or intracellular compartment, significantly improving the selectivity of action, both in cancerous and non-cancerous conditions (Riehemann *et al.*, 2009; Petros and DeSimone, 2010; Albanese *et al.*, 2012; Marrache and Dhar, 2012).

Finally, the versatility and immense loading capacity of nanomaterials permits the binding and targeted delivery of large payload volumes (**Figure 1–4)**. As mentioned previously, the biodistribution of cargo adsorbed on a nanomaterial differs dramatically from that of a free molecule, being driven primarily by the biodistribution profile of the nanocarrier, which was specifically engineered to recognise a particular molecular target (Chiannilkulchai *et al.*, 1989). This permits increased total circulation times for payloads, and limits their action to a selected population of cells – a particular benefit for expensive pharmaceutical products with poor biodistribution and/or agents with high unselective cytotoxicity (Damascelli *et al.*, 2001; Gelperina *et al.*, 2002). Recently, the versatility of nanomaterials, and their capacity to simultaneously bind various types of cargo, have laid the foundation for the concept of a theranostic nanomedicine (‘nanotheranostic’) – a multifunctional delivery platform, which combines diagnostic and therapeutic action through the selective targeting and contrasting of a pathological lesion during clinical diagnostic imaging, followed by spontaneous or triggered drug release, the pattern of which can be tracked in real time (Lammers *et al.*, 2010; Xie *et al.*, 2010).

Collectively, all these features explain the growing interest towards the use of nanomaterials in the research and clinical setting in order to enhance the diagnostic and therapeutic value of existing techniques.

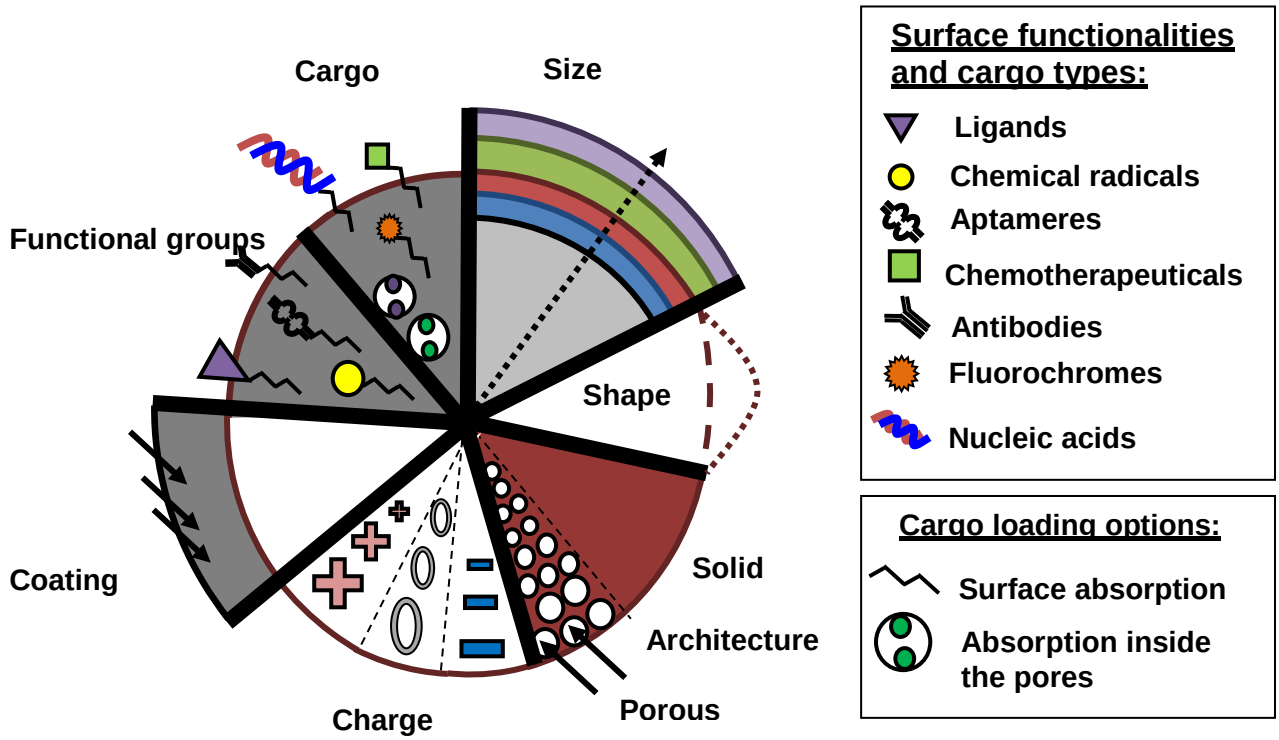

***Figure 1-4* – Versatility of nanomaterials.** Nanomaterials represent highly versatile structures with adjustable physical and chemical properties. Changes in the size, shape, architecture, surface charge and coating of nanomaterials allow us to manipulate their interaction with cells, improving uptake by the target cell population and minimising non-specific interaction. Surface functional groups (ligands, chemical radicals, aptamers, antibodies) play the role of targeting moieties and/or independent functional cargo. Nanomaterials can be optionally loaded with biological payloads (chemotherapeutics, proteins, nucleic acids) through either absorption on the surface of the nanocarrier or inside the pore channels for porous nanomaterials.

1.3. Reproductive science and medicine: challenges requiring a new vision

Reproductive science is an exciting and continuously developing field which aims to provide theoretical insight into the mechanisms of gametogenesis, fertilization, early embryo development, pregnancy establishment, and to develop applied tools for the intentional manipulation of these processes to address fertility issues across different biological species. Assisted reproductive technology (ART) represents a collection of sophisticated laboratory techniques and approaches for the *in vitro* manipulation of gametes and embryos that were developed to enhance the chances of fertilization and development to full-term, respectively. Today, ART is deemed essential for the treatment of human infertility (Gianaroli *et al.*, 2012; Aitken, 2014), but also for the preservation of animal species (Holt *et al.*, 2014) and production of livestock (Galli *et al.*, 2014; Knox, 2014;

Martin, 2014). In addition, reproductive science investigates an array of fundamental biological processes underlying reproduction, including cell division and fusion, genetic recombination, maintenance of pluripotency, and cell migration and differentiation, which are very similar to the events involved in tumour biogenesis and tissue regeneration. Therefore, research into reproductive biology has an inherent translational component, and permits advancement in our understanding of cell-based regenerative therapies for cardiovascular, renal, neurological and other diseases (Felsenstein *et al.*, 2014; Freire *et al.*, 2014; Katari *et al.*, 2014), and the fine mechanisms of cancer (Pardal *et al.*, 2003; Kim and Dirks, 2008).

The role of assisted reproductive technology, primarily *in vitro* fertilization (IVF), in the management of reproductive disorders has been growing steadily since the 1980s. Ever since the birth of the first IVF baby, Louise Brown, in 1978 (Steptoe and Edwards, 1978), the continuous progress in fundamental reproductive biology has been increasingly fuelling the field of clinical assisted reproduction (Gianaroli *et al.*, 2012). In fact, over the last few decades, the field of reproductive science has expanded tremendously, now incorporating the principles of cell culture, micromanipulation, live cell microscopy, cryobiology, laser technology, proteomics, metabolomics, molecular genetics and biology. The integration of data arising from state of the art fundamental research concerning the selection and micromanipulation of gametes and embryos, *in vitro* culture, preimplantation genetic testing, and reproductive cryopreservation, into routine clinical practice has resulted in improved treatment success and safety of ART. It has also increased the 'patient-friendliness' of treatments and the total number of available options, now spanning from conventional IVF/ICSI to intracytoplasmic morphologically selected sperm injection, time-lapse imaging of embryo development, next-generation sequencing of pre-implantation embryos, and nuclear genome transfer (Bartoov *et al.*, 2002; Lemmen *et al.*, 2008; Fragouli and Wells, 2012a; Wells, 2014).

Indeed, ART has revolutionised the field of infertility treatment, resulting in the birth of more than 5 million children worldwide ever since its first successful use in humans (Adamson *et*

al., 2013). Over the last four decades, pregnancy rates following ART have increased by nearly six-fold, from 6% (Wang and Sauer, 2006) to approximately 35% (ESHRE, 2014, HFEA, 2014), and the procedure now allows us to achieve pregnancy in a range of male and female endocrine, anatomic and genetic conditions. Although ART has expanded and improved, perhaps even more than anticipated in its early days, and transformed from a controversial experimental procedure to a routine medical treatment, its success rates, from the modern perspective, remain insufficient to consider this technique a reliable solution to the problem of infertility. At the same time, the average live birth rate after ART globally still remains reasonably low, and does not exceed 30% per started cycle (ESHRE, 2014). At the same time, according to recent estimations, infertility affects nearly 48.5 million couples globally (Mascarenhas *et al.*, 2012), and in approximately 25% of cases, the exact cause of reproductive failure cannot be established (National Institute for Health and Care Excellence (NICE), 2013). Furthermore, the demands for successful ART, especially in post-industrial economies, are continuously growing under the pressure of an increasing prevalence of age-related infertility due to the intentional postponement of parenthood (Schmidt *et al.*, 2012), and expansion of assisted reproduction into 'non-infertility' indications. These indications include: fertility preservation in patients undergoing gonadotoxic treatment for cancer and severe systemic immune conditions (Oktay and Karlikaya, 2000), preimplantation genetic diagnosis (PGD) of hereditary diseases (Handyside *et al.*, 1992), PGD with human leukocyte antigen (HLA) genotyping for conception of 'saviour siblings', who can donate bone marrow to a family member with a haematological malignancy (Verlinsky *et al.*, 2001). In addition, ART is being used for minimisation of the risks of human immunodeficiency virus (HIV) transmission in HIV-discordant couples (Marina *et al.*, 1998). Collectively, these factors contribute to an acute demand for increased success in ART, which cannot be achieved without the development of novel research and clinical techniques to investigate, and selectively manipulate, the sensitive physiological mechanisms underlying gametogenesis, fertilization and early embryo development.

However, the goals of reproductive medicine are not limited exclusively to allowing the conception and delivery of healthy offspring, but also encompass the wider concept of physical and emotional patient well-being throughout their lives. Therefore, another current challenge in reproductive medicine, equally relevant for other clinical fields, is that existing diagnostic and therapeutic options for many chronic diseases, which ultimately lead to a significant reduction in quality of life and/or infertility, do not interfere with the requirements of a 'gold standard' of care. These requirements generally include simplicity, non-invasiveness, high diagnostic value, ability to accurately detect diseases at early preclinical stages, and high therapeutic efficacy combined with safety and minimal side effects. To address this challenge, numerous research groups are investigating possibilities for the non-invasive detection and minimally invasive treatment of reproductive pathologies, for example, endometriosis, uterine fibroids, or ectopic pregnancy, which are currently believed to inevitably require surgical intervention at a certain stage, either for diagnosis or treatment. Candidate approaches include the use of systemic biomarkers (May *et al.*, 2010; Van Gorp *et al.*, 2011; Levy *et al.*, 2013), along with improvement of the diagnostic accuracy of non-invasive imaging techniques, such as ultrasound, computed tomography (CT) and magnetic resonance imaging (MRI) (Ammar *et al.*, 2012; Langer *et al.*, 2012), as well as the selectivity of pharmaceutical products targeting the reproductive system (Janat-Amsbury *et al.*, 2009).

In summary, current approaches in reproductive medicine are becoming increasingly fertility-sparing, with particular focus upon possibilities for the early non-invasive detection of diseases (Fassbender *et al.*, 2013; Levy *et al.*, 2013; Senapati and Barnhart, 2013), thereby permitting non-surgical or minimally-invasive surgical treatment to maximise the chances of conception, either spontaneous or assisted (Lipskind and Gargiulo, 2013). The field of reproductive biology is in need of more robust and targeted research tools to allow the selective and precise manipulation of molecular and cellular mechanisms underlying reproduction to advance our understanding of the multi-faceted issue of infertility. Therefore, it is not surprising that in the last few years there has been a steady increase in the number of attempts to utilise the principles of

nanotechnology for reproductive applications. It is anticipated that, similarly to other areas of medicine, the use of nanomaterial-based techniques, with their revolutionary robustness and targeting potential, will aid in the development of next-generation diagnostic and treatment modalities to ultimately benefit patient care.

1.4. APPLICATIONS OF NANOTECHNOLOGY IN REPRODUCTIVE MEDICINE AND REPRODUCTIVE BIOLOGY

Today, nanomaterial-based diagnostic and therapeutic approaches have been investigated for a number of reproductive medicine and biology scenarios **(Table 1–3**). The majority of publications describe the use of nanomaterials for the detection and targeted therapy of reproductive cancers. However, a growing number of experimental studies assess the use of nanotechnology for the diagnosis and treatment of non-cancerous conditions, including endometriosis (Lee *et al.*, 2012; Zhao *et al.*, 2012; Wang *et al.*, 2014), uterine fibroids (Ali *et al.*, 2013b), ectopic pregnancy and trophoblastic diseases (Kaitu'u-Lino *et al.*, 2013), and in drug delivery systems (Cohen *et al.*, 2011; McGowan *et al.*, 2011; Tomoda *et al.*, 2012a; Tomoda *et al.*, 2012b; Ali *et al.*, 2013a). From the fundamental reproductive biology perspective, nanomaterials are being applied as research tools to manipulate gene expression in offspring (Yang *et al.*, 2009; Kim *et al.*, 2010b; Campos *et al.*, 2011a; Campos *et al.*, 2011b; Yang *et al.*, 2011), investigate molecular pathways in gametes and early-stage embryos (Makhluf *et al.*, 2008), or mark and select specific populations of gametes (**Table 1–3)** (Barchanski *et al.*, 2011; Feugang *et al.*, 2012; Rath *et al.*, 2013; Odhiambo *et al.*, 2014).

The use of nanomaterials for reproductive biology represents a much ‘younger’ field, with a limited amount of specific evidence. Therefore, in **Subsections 1.4.1.** and **1.4.2.** I will firstly present practical examples of diagnostic and therapeutic uses of nanotechnology in a more applied reproductive medicine setting, in order to demonstrate the key translational benefits of nanomaterials for targeted delivery. Then, in **Subsections 1.5.1** and **1.5.2.**, a brief review of the far

smaller body of evidence concerning the use of nanomaterials for reproductive biology and, particularly, the manipulation of gametes, will be presented.

***Table 1-3*– Applications of nanomaterials in reproductive medicine**

Reproductive oncology	**Non-cancer conditions**
Cancer detection: • Nanobiosensors for cancer biomarkers • Contrast agents for clinical diagnostic imaging **Cancer treatment:** • Targeted delivery for improved efficacy and decreased toxicity • Combined therapy: simultaneous delivery of therapeutic payloads • Reversal of resistance to chemotherapy • Nanosensitisation: potentiation of anti-tumour effect of chemotherapy by simultaneous exposure of cancer cells to nanomaterials • Effective delivery of drugs with poor biodistribution profile • Experimental gene therapy	• **Endometriosis** o Contrast agents for MRI o Targeted delivery of experimental treatment agents, including gene therapy • **Uterine fibroids** o Nanosensitisation during minimally-invasive surgery o Targeted delivery of experimental treatment agents • **Ectopic pregnancy and trophoblastic diseases** o Targeted delivery of chemotherapy drugs • **Drug delivery systems** o Topical o Transdermal o Transplacental o Intravaginal

***Table 1-4* – Applications of nanomaterials in reproductive biology**

Gene therapy for reproductive diseases
Sperm-mediated gene transfer of genes and biological compounds
Direct intracellular delivery of biological compounds into oocytes and embryos
Selection of gametes and embryos • Sex sorting of sperm • Non-invasive bioimaging • Labelling of pre-implantation embryos

1.4.1. REPRODUCTIVE MEDICINE

1.4.1.1. Detection and treatment of cancer: nanobiosensors, contrast agents and targeted delivery tools

Reproductive cancers represent one of the most commonly diagnosed malignancies in the majority of geographic regions around the world. In developed countries, prostate cancer represents the leading type of malignancy in males, and the second largest cause of cancer-related deaths (Office for National Statistics, 2011; U.S. Cancer Statistics Working Group, 2013). According to global data relating to females, reproductive cancer, including ovarian, uterine and cervical forms, consistently remain among the twenty most prevalent and lethal (Office for National Statistics, 2011; U.S. Cancer Statistics Working Group, 2013).

Early diagnosis of cancer is crucial for adequate treatment success and acceptable survival rates. However, as mentioned previously, many current screening approaches, particularly those that are biomarker-based, fail to yield accurate, reproducible and, most importantly, quick and cost-effective results. These concerns arise as a result of the sub-optimal sensitivity and specificity of commonly applied biomarkers, as well as sophisticated design strategies and the high costs of common laboratory immunoanalysers.

The use of nanobiosensors, which rapidly and directly transform the large number of simultaneous biological events (binding and/or reaction) into electronic signals without additional labelling steps, has proven advantageous in various fields of biodetection, including the identification of antigens, proteins, nucleic acids, and reactive oxygen and nitrogen species (Medina-Sanchez *et al.*, 2012; Perfezou *et al.*, 2012; Kumar *et al.*, 2013). Recently, this approach has been successfully attempted in reproductive oncology. Today, nanoparticle (NP)-based biosensors are being widely introduced for the detection of well-characterised and novel cancer biomarkers, including cancer antigen 125 and human epididymis secretory protein 4 for ovarian cancer, and prostate-specific antigen for prostate cancer, respectively (Suwansa-ard *et al.*, 2009; Yuan *et al.*, 2012). Current evidence universally supports the advantages of these label-free,

straightforward, quick, portable, and cost-effective detection techniques, which can be used directly at the 'point of care', in preference to conventional immunoassays (Thaxton *et al.*, 2009; Medina-Sanchez *et al.*, 2012; Perfezou *et al.*, 2012).

Diagnostic imaging, including CT, MRI and ultrasound scanning, forms the first-line approach for the visualisation of cancer, and aims to establish the location of primary tumours along with the detection of regional and systemic metastases in order to stage the disease. In this field, nanomaterials are being increasingly considered as the next generation of image enhancers. Their unique optical properties, along with the potential for active targeting towards malignant cells and improved detection limits, result in major benefits compared to previous contrast agents (Wang *et al.*, 2008). The use of nanomaterial-based formulations, for instance super-paramagnetic iron oxides and aptamere-conjugated gold NPs, has been extensively described in the treatment of prostate cancer patients, particularly for the detection of small tumours and lymph node staging, both of which represent a significant challenge for standard imaging approaches (Wang *et al.*, 2008; Thoeny *et al.*, 2009; Kim *et al.*, 2010a). More recently, a similar technique has been developed and tested for the imaging of ovarian cancer (Zhou *et al.*, 2013). Over the last few years, NP-guided imaging of prostate cancer has progressed into the concept of image-guided therapy, which utilises nanomaterials with contrasting properties, additionally loaded with a chemotherapeutic agent, for precise and traceable drug delivery and release (Yu *et al.*, 2011; Gao *et al.*, 2012).

Nanomaterial-mediated delivery of chemotherapeutics permits marked improvements in their efficiency, and also helps reduce systemic toxicity. Many studies have demonstrated the potential of various types of NPs, such as derivatives of polylactic acid (PLA) and poly(lactic-co-glycolic) acid (PLGA) (Dhar *et al.*, 2008; Liang *et al.*, 2011; Le Broc-Ryckewaert *et al.*, 2013), bovine serum albumin (Zhao *et al.*, 2010), magnetic iron (Lee *et al.*, 2013), and gold (de Oliveira *et al.*, 2013), functionalised with different targeting ligands, such as follicle-stimulating hormone receptor-binding peptides (Zhang *et al.*, 2013), folates (Zhao *et al.*, 2010; Liang *et al.*, 2011) and aptamers (Dhar *et al.*, 2008) to facilitate the delivery of chemotherapeutic agents into ovarian,

endometrial and prostate cancer cells, which significantly potentiated their anti-tumour effects, compared to their respective free molecules.

The use of nanomaterials for intracellular delivery can reverse the resistance of tumours to chemotherapy via active targeting and the activation of alternative mechanisms of cellular uptake. Liang *et al*. (2010) described the potential of metallofullerene NPs to overcome the resistance of human prostate cancer cell lines to cisplatin via the reactivation of dysfunctional endocytosis (Liang *et al.*, 2010). Similar effects were described for a specific formulation of cisplatin, encapsulated in F3 peptide-functionalised polyacrylamide NPs, and targeted specifically to ovarian tumour vessels in an *in vivo* mouse model of human tumour vascularisation. The use of this formulation resulted in strong anti-tumour activity, attributed to vascular necrosis, both in platinum-sensitive and platinum-resistant cell lines (Winer *et al.*, 2010). In another study, Nair *et al.* (2011) reported that the encapsulation of letrozole, an aromatase inhibitor used to suppress oestrogen biosynthesis in post-menopausal patients with hormone-responsive breast cancer, into hyaluronic acid-bound polymeric (PLGA-PEG), NPs restored drug sensitivity in letrozole-resistant cells *in vitro* and *in vivo* via the interaction of hyaluronic acid with CD44 receptors upon the tumour cell surface (Nair *et al.*, 2011). Collectively, these findings demonstrate that nanomaterial-mediated delivery can effectively alter the pharmacokinetics and pharmacodynamics of common drugs for chemotherapy to overcome the mechanisms of drug resistance.

In addition, the efficiency of anti-tumour therapies can be potentiated by the simultaneous independent exposure of reproductive cancer cell lines to certain nanomaterials. The use of such targeted sensitizers would allow us to use milder regimens of chemotherapy or irradiation, thereby improving the safety and tolerability of these procedures, without compromising their anti-tumour efficacy. Nanosensitisers, such as nanoparticulate magnetic iron oxide, gold nanoshells and gold NPs, have been widely applied for selective thermal ablation and radiotherapy in patients with prostate cancer since the mid-2000s (Johannsen *et al.*, 2005; Stern *et al.*, 2008; Roa *et al.*, 2009). More recently, Geng *et al. (*2011) reported that thio-glucose bound gold NPs (Glu-GNPs) exhibited

a similar radio-sensitizing effect upon a human ovarian cancer cell line SK-OV-3. The use of these NPs resulted in an approximately 30% increase in the inhibition of cell proliferation compared to the irradiation alone, primarily due to the elevation of reactive oxygen species (ROS) production. Similarly, Zhang *et al.* (2012) observed a sensitizing effect of carbon nanotubes to the chemotherapeutic agent paclitaxel in the human ovarian cancer cell line OVCAR3, mediated through the increase of apoptosis.

Nanomaterials allow the simultaneous targeted intracellular delivery of various types of payloads absorbed on one type of nanocarrier, thus providing an effective means of combined treatment for cancer. In a study by Qi *et al. (*2011), PLGA NPs were used to simultaneously deliver a pro-apoptotic human PNAS-4 (hPNAS-4) gene and cisplatin into mouse ovarian carcinoma cells. The authors reported significant anti-tumour activity associated with PLGA NPs loaded with hPNAS-4, mediated through the induction of apoptosis and the suppression of cell proliferation and angiogenesis. The anti-tumour effects of hPNAS-4-carrying PLGA NPs were further potentiated by the simultaneous loading of cisplatin, thus highlighting the feasibility of using this combined approach for cancer treatment.

Nanomaterial-mediated delivery can also increase the efficacy of anti-cancer chemotherapeuticals and preventative agents, the previous use of which has been limited by poor biodistribution and lack of specific affinity towards the malignant tissue (Nair *et al.*, 2010). Several groups have described the successful encapsulation of the chemopreventative agent (-)-epigallocatechin 3-gallate into PLA-PEG or polysaccharide NPs, and subsequent delivery of the formulation into prostate cancer cells (Rocha *et al.*, 2011; Sanna *et al.*, 2011). In a study by Long *et al. (*2013), a PEGylated liposomal formulation of quercetin, a flavonoid compound with anti-free radical and proposed anti-cancer activity, demonstrated significantly improved ability to suppress tumour growth in models of human ovarian cancer, both *in vitro* and *in vivo,* that proved resistant to conventional treatment with cisplatin, compared to free quercetin.

Finally, nanomaterials are being increasingly investigated for targeted intracellular gene delivery in experimental gene therapy approaches for cancer. The spontaneous uptake of nanocarriers by target cells is associated with a number of benefits, compared to conventional electro- and viral transfer. Nanomaterials combine the main advantages of viral vectors (such as selectivity, non-invasive delivery, and stable expression of genetic constructs), with the main benefit of electroporation using plasmid DNA (total avoidance of viral integration into the host genome). In reproductive oncology, the use of nanovectors has been investigated for the experimental gene therapy of ovarian, cervical and prostate cancer, pre-cancer cervical lesions, and choriocarcinoma (Peng *et al.*, 2013).

Numerous publications describe the use of dendrimers, polymeric and lipid NPs for the delivery of suicide DNAs, tumour suppressor genes (p53), and short interfering RNAs (siRNAs) against genes expressed in malignant phenotypes (heat shock protein 27, androgen receptors, cofilin-1) into prostate cancer cells, resulting in anti-tumour activity (Peng *et al.*, 2007; Liu *et al.*, 2009; Sharma *et al.*, 2011; Perez-Martinez *et al.*, 2012; Yang *et al.*, 2012a). Several groups have utilised PLGA and chitosan NPs to transfer short hairpin ribonucleic acids (shRNAs) and siRNAs into ovarian cancer cells, that were designed to interfere with the expression of target genes associated with cancer phenotypes and metastatic progression, including focal adhesion kinase, CD44, claudine-3 and Jagged1. In all cases, target genes were successfully knocked-down, resulting in a pronounced anti-tumour effect, attributed to a reduction in cell proliferation and angiogenesis, and a concomitant increase in apoptosis (Steg *et al.*, 2011; Sun *et al.*, 2011; Zou *et al.*, 2013).

A similar approach was attempted by Yang *et al. (*2013), who also used chitosan NPs to deliver siRNAs against the E6 and E7 oncoproteins of human papillomavirus into a cervical cancer cell line. Inactivation of these proteins, which are currently held responsible for malignant epithelial transformation and preservation of the malignant phenotype, resulted in significant induction of apoptosis in target cells. Another study described the synthesis of magnetic iron oxide (Fe(3)O(4))-dextran-anti-β-human chorionic gonadotropin (hCG) NPs and their successful use in

choriocarcinoma tissue in an *in vivo* mouse model of disease, highlighting the potential use of this system as a nanovector for the use of gene therapy in trophoblastic diseases (Jingting *et al.*, 2011).

1.4.2. NON-CANCER APPLICATIONS: DIAGNOSTIC IMAGING AND ALTERNATIVES TO SURGICAL TREATMENT

There is increasing awareness that treatment approaches in reproductive medicine should be as fertility-sparing as possible (Gianaroli *et al.*, 2012), since in the case of conditions with high recurrence rates, for example endometriosis and uterine fibroids, repeated surgeries can reduce the chances of spontaneous and assisted conception in the future, occasionally requiring third-party reproduction (Bongioanni *et al.*, 2011). Currently, several experimental nanomaterial-based approaches have been investigated as a safer and less invasive alternative to standard diagnostic and therapeutic techniques for the management of several traditionally 'surgical' reproductive diseases. These studies highlight the growing trust of scientific and medical community into biomedical nanotechnology, which is now expanding to more 'benign' and, therefore, more physiologically and ethically sensitive scenarios.

1.4.2.1. Endometriosis

Endometriosis, a chronic gynaecological condition associated with the presence of endometrial-like tissue outside of the uterine cavity, affects nearly 2-22% of women of reproductive age (Kennedy *et al.*, 2005; Johnson and Farquhar, 2007) and manifests with mild to severe pelvic pain and/or infertility. In recent large-scale epidemiological studies, endometriosis has been proven to have a profound negative impact upon health-related quality of life and work productivity, exacerbated by an average delay in diagnosis, on all healthcare levels, of 7 to 10 years (Nnoaham *et al.*, 2011; Hudelist *et al.*, 2012). Early non-invasive diagnosis of this disease remains highly challenging due to the lack of sensitive serum biomarkers and limitations associated with the imaging techniques used, such as ultrasound and MRI, in peritoneal endometriosis (Stratton *et al.*, 2003; May *et al.*, 2010; Fassbender *et al.*, 2013). Therefore, for more than 50 years, the gold standard of detection for

ectopic endometrial lesions has been laparoscopy (Steptoe, 1969), an invasive procedure with inherent surgical and anaesthesiological risks.

In a recent study, Lee *et al. (*2012) evaluated the performance of intravenously administered ultra-small super-paramagnetic iron oxide NPs (USPIO-NPs) as MRI-signal enhancers in a rat model of surgically-induced endometriosis. The authors hypothesised that the affinity of USPIO-NPs towards macrophages could allow these NPs to be used as novel contrast agents, and extend applications of MRI to the detection of ectopic endometrial lesions without a prominent haemorrhagic component, such as pelvic adhesions or intraperitoneal implants. Results arising from this study confirmed that the use of USPIO-NPs increased the diagnostic accuracy of MRI in the detection of non-haemorrhagic ectopic endometrial lesions, and, therefore, represents a promising strategy for the non-invasive diagnosis of endometriosis.

Endometriosis represents not only a diagnostic, but also a therapeutic challenge. Current treatments, including surgical and medical hormonal approaches, are primarily symptomatic and have a temporary effect, with pain recurrence rates after various treatments reported to range from approximately 25% to nearly 50% (Kim *et al.*, 2013a). A number of alternative approaches for the management of endometriosis are currently being investigated, such as anti-angiogenesis and anti-inflammatory agents, anti-cytokines, and gene therapy (Kennedy *et al.*, 2005; Laschke and Menger, 2012; Lu *et al.*, 2013), with several recent publications describing the use of nanomaterials in the delivery of these experimental compounds.

In particular, Zhao *et al. (*2012) reported the use of lipid-grafted chitosan micelles loaded with a therapeutic gene encoding pigment-epithelium derived factor, a multi-functional protein with anti-tumour and anti-angiogenic properties, in gene therapy approaches for endometriosis. The intravenous administration of micelles to rats with surgically-induced endometriosis resulted in similar therapeutic efficiency as the commonly-used agent danazol, in terms of reducing the volume of ectopic lesions and the inhibition of endometriod cyst growth, and demonstrated a significantly stronger effect than placebo. In another study, Chaudhury *et al*. (2013) described the beneficial

effects associated with the intraperitoneal administration of cerium oxide NPs with proven anti-inflammatory, anti-angiogenic and anti-free radical properties in a mouse model of endometriosis. These authors reported a reduction in the systemic levels of ROS and angiogenic factors (vascular endothelial growth factor and adrenomedullin), along with a reduction in CD34 expression and endometrial gland density in ectopic lesions, compared to an active control (N-acetyl-cystein) and placebo.

1.4.2.2. Uterine fibroids

Uterine fibroids (leiomyomas) are benign hormone-dependent tumours originating from the myometrial smooth muscle cells. Leiomyomas represent the most prevalent type of pelvic tumours in women of reproductive age, and affect between 60% to 80% of the population (Laughlin *et al.*, 2010). Clinical manifestations of the disease include abnormal uterine bleeding, anaemia, genitourinary symptoms and infertility, which collectively lead to a reduction in the health-related quality of life (Williams *et al.*, 2006). Current approaches to the treatment of uterine fibroids are primarily surgical, comprising a range of techniques with an increasing degree of invasiveness: focused ultrasound ablation, uterine artery embolisation, myomectomy and, finally, hysterectomy (Falcone and Parker, 2013). In view of the fact that the prevalence of uterine fibroids decreases dramatically in women aged over 30 years (Huyck *et al.*, 2008), which coincides with the time of first parenthood, the need for minimally invasive and fertility-sparing treatment approaches is being increasingly recognised.

Nanomaterial-mediated delivery of anti-tumour cytokines has been investigated for the improvement of selectivity and potentiation of the effects of minimally-invasive surgical removal of fibroids. Jiang and Bischof (2010) reported the use of nanogold-conjugated tumour nectosis factor alpha (TNF-α) as a nanosensitiser during cryosurgery for uterine leiomyoma in a mouse model of disease. Although an improvement of anti-tumour efficacy and post-surgery relapse times was observed after administration of both the nanoparticulate and free form of TNF-α, compared to

cryosurgery alone, the nanoparticulate formulation demonstrated a superior safety profile, than intra- or peri-tumour injections of free TNF-α.

An alternative approach was reported by Ali *et al*. (2013) and involved the use of PLA-PLGA NPs for the delivery of 2-methoxyoestradiol, a biologically-active metabolite of oestradiol with anti-tumour and anti-angiogenic activity, into a human leiomyoma cell line as an investigational fertility-preserving alternative to hysterectomy. In a manner similar to other research groups investigating the effects of nanomaterial-mediated delivery, these authors observed an increase in anti-tumour activity of the nanoparticulate formulation of the drug, compared to the free molecule.

1.4.2.3. Ectopic pregnancy

Medical management of early-stage ectopic pregnancies is being increasingly adopted in clinical practice, particularly for patients with rare locations of extra-uterine pregnancy, such as the cervix, the interstitial part of the fallopian tube, or post-caeserian scar (van Mello *et al.*, 2012). In these cases, fertility-preserving surgical treatment often represents a significant challenge, requiring the use of alternative methods. Methotrexate, an anti-folate agent for chemotherapy with proven affinity towards the trophoblast, is the treatment of choice for the medical management of ectopic pregnancy (American Society for Reproductive Medicine (ASRM), 2008). However, treatment with methotrexate is effective only in early gestational age, and often requires prolonged monitoring of hCG levels and multiple administrations of the drug (American Society for Reproductive Medicine (ASRM), 2008).

To overcome existing limitations in the medical management of ectopic pregnancy and trophoblastic diseases, Kaitu'u-Lino *et al.* (2013) engineered bacterial-derived nanospheres (EnGeneIC Delivery Vehicles (EDVs)) actively targeted towards epidermal growth factor receptors (EGRF), which are abundantly expressed in human placenta, and loaded the EDVs with doxorubicin. EDVs represent a novel class of easily synthesised organic NPs with high loading capacity, versatility and low toxicity, and are currently undergoing a phase I clinical trial. This

engineered delivery system was characterized by high specific affinity towards the trophoblast, which allows it to be used for the treatment of both ectopic pregnancy and trophoblastic diseases. The administration of doxurubicin-loaded EGFR-targeted EDVs resulted in more pronounced anti-tumour activity in a mouse model of human choriocarcinoma, compared to non-targeted doxorubicin-loaded EDVs and the free drug. An increase in anti-tumour activity was attributed to the increased intracellular uptake of EGFR-targeted EDVs and a higher rate of apoptosis, compared to non-targeted EDVs. Based on the results of this study, the authors hypothesised that this new delivery system could not only increase efficacy of the medical management of ectopic pregnancy and trophoblastic diseases in future, but was also relevant for the delivery of placental-specific drugs in general.

1.4.2.4. Drug delivery systems

Several studies report positive outcomes from the use of NPs in investigational drug delivery systems for hormone replacement therapy (Tomoda *et al.*, 2012a; Tomoda *et al.*, 2012b), medical treatment of foetal diseases *in utero* (Ali *et al.*, 2013a), and topical intravaginal therapeutic agents (Menjoge *et al.*, 2010; Navath *et al.*, 2011).

Tomoda *et al. (*2012) described the advantages of encapsulating oestradiol into PLGA NPs for delivery through the *stratum corneum* of the skin. The same research group had previously attempted a similar approach for the transdermal delivery of indomethacin with encouraging results (Tomoda *et al.*, 2012a). In both studies, nanoparticulate formulations of the products demonstrated greater permeability, compared to free drugs, which was further enhanced by the simultaneous application of physical factors (iontophoresis).

Ali *et al*. (2013a), for the first time, presented a prototype of a versatile trans-placental delivery system for the medical therapy of foetal diseases. Previously, trans-placental penetration of nanocarriers was repeatedly found to be regulated by their physicochemical properties, including size, shape and surface chemistry, which creates immense opportunities for the manipulation of their pharmacokinetics (Menezes *et al.*, 2011; Refuerzo *et al.*, 2011). Ali et al. (2013a) applied

PLGA NPs loaded with dexamethasone in an *in vitro* model of human placental trophoblast cells as an experimental treatment for congenital adrenal hyperplasia, and observed an increase in permeability of the nanoencapsulated drug, compared to the free form, from the maternal to foetal compartment. Further research in this direction could aid in the development of a trans-placental delivery nanoplatform for the targeted medical therapy of foetal diseases *in utero*.

Another series of studies describe the use of a polyamidoamine (PAMAM) dendrimer-based topical intravaginal delivery system to restrict the effect of antimicrobial drugs to the vaginal compartment, which prevents the passage of drugs through the foetal membranes in pregnant women with ascending genital infections, minimizing the risk of foetotoxicity (Menjoge *et al.*, 2010; Navath *et al.*, 2011).

1.5. REPRODUCTIVE BIOLOGY

The sub-optimal success rates of ART, allowing the achievement of live birth only in only approximately 1 in 3 couples initiating treatment (ESHRE, 2014), are generally attributed to two key factors. Firstly, the conventional techniques used to select embryos to be transferred back into the patient's uterus have inherent limitations, since they are based exclusively upon the morphological assessment of embryos, and not the evaluation of their chromosomal status and, therefore, developmental potential in the long-term (Fragouli *et al.*, 2014). Secondly, *in vitro* handling of gametes and embryos, which forms an integral part of ART, has been reported to induce microstructural and functional damage in these delicate structures, with consequential reduction in developmental competency. There is mounting evidence that gamete processing *in vitro* during ART also promotes the fragmentation of sperm DNA (Toro *et al.*, 2009; Matsuura *et al.*, 2010; Rougier *et al.*, 2013), reduces the levels of sperm-borne oocyte-activating factor phospholipase C zeta (Kashir *et al.*, 2011; Yelumalai *et al.*, 2013), and facilitates oxidative stress in unfertilized oocytes (Martin-Romero *et al.*, 2008; Otsuki *et al.*, 2009), all of which, in the case of gametes with already compromised fertility, can have profound negative effects. Optimisation of *in vitro* culture conditions, such as the supplementation of culture media with antioxidants, small

molecules and growth factors (Kawamura *et al.*, 2012; Yun *et al.*, 2013; Tardif *et al.*, 2014), or embryo incubation in time-lapse monitoring systems, which do not require repeated interruptions of culture for morphology assessment (Meseguer *et al.*, 2012), has been reported to increase gamete/embryo survival and improve developmental potential. These observations elegantly indicate that the potential to improve ART success rates via the wider adoption of such approaches is both exciting and necessary. Nevertheless, substantial breakthroughs in the field of clinical ART can only be achieved via ongoing fundamental reproductive biology studies into the physiological mechanisms underlying reproduction, enabling the discovery of targeted molecular tools to investigate or manipulate these fine mechanisms at the cellular level. In this view, the universal evidence that nanomaterials improve the selectivity and efficacy of cargo delivery across a variety of cell types (Ryan and Brayden, 2014; Tsai *et al.*, 2014) and do not compromise cell function, render them particularly attractive candidates for intracellular delivery into reproductive tissues, gametes and embryos.

1.5.1. GENE TRANSFER INTO REPRODUCTIVE TISSUES

Research into the specific mechanisms underlying reproduction is increasingly demonstrating an association between various forms of previously unexplained infertility, such as specific types of gonadal insufficiency (O'Flynn O'Brien *et al.*, 2010; Cordts *et al.*, 2011), failure of fertilization (Amdani *et al.*, 2013) and recurrent pregnancy loss (Su *et al.*, 2011), and abnormal gene expression and/or genetic polymorphisms. In view of these findings, targeted genetic modification of reproductive tissues, allowing the production of transgenic gametes and subsequently embryos could evolve into a powerful tool for studying and manipulation of the fine pathophysiological mechanisms underlying infertility or, in a broader sense, any genetic pathology.

A series of studies have described successful *in vivo* intra-testicular gene transfer in rodents using electroporation and viral vectors, resulting in the production of transgenic epididymal sperm (Muramatsu *et al.*, 1997; Kubota *et al.*, 2005; Coward *et al.*, 2006). Several publications report that intra-testicular and intra-ovarian gene transfer using viral vectors restores gametogenesis in mouse

models of genetic gonadal failure (Ikawa *et al.*, 2002; Kojima *et al.*, 2008; Ghadami *et al.*, 2010); however data regarding the safety of such methodology remain highly contradictory (Raper *et al.*, 2003; Woods *et al.*, 2006). Therefore, the availability of a technique, which is devoid of the biological risks associated with traditional gene transfer approaches, could support research into reproductive gene transfer as a possible treatment for specific forms of infertility in future (Lamb, 2008). From this perspective, spontaneous internalisation of nanovectors into target cells is associated with a number of benefits, compared to conventional electro- and viral transfer. In particular, nanomaterials combine the main advantages of viral vectors, such as high specificity and non-invasiveness of delivery, with the key benefit of electroporation: an avoidance of viral integration into the host genome, which renders them a viable alternative to traditional gene therapy tools.

The feasibility of nanomaterial-mediated gene transfer into foetal tissues *in utero* for investigating gene therapy for monogenic diseases was demonstrated by Yang *et al.* (2011). In this pilot study, the authors utilised intra-amniotic injections of chitosan NPs conjugated with enhanced green fluorescent protein (EGFP) gene into mouse embryos and observed expression of the transgene in the alveolar epithelium of the lungs and the luminal intestinal epithelium, coinciding with penetration of NPs through respiratory and gastrointestinal pathways. Expression of the transgene, however, was temporary and localised exclusively to these tissues, justifying that further research was required to optimise the techniques and timings of this procedure in order to achieve more stable outcomes. In a more recent study, (Tseng *et al.*, 2013) applied gelatine nanoparticles loaded with a reporter plasmid pEGFP-C1 for gene transfer into chick embryos, and observed GFP gene expression in embryos just 4 days after transfection. However, the stability of transgenesis along with long-term safety outcomes has not been evaluated in this set of experiments, prompting further investigations.

1.5.2. INTRACELLULAR DELIVERY OF MOLECULAR COMPOUNDS INTO GAMETES

The use of molecular research tools, including oligonucleotides, nucleic acids, peptides, antibodies, fluorescent markers and small molecules, forms the cornerstone of experimental studies in developmental and reproductive biology. These tools allow the precise mapping of specific cellular structures and molecular pathways, and tracking of their activity and fate at the different stages of gamete/embryo development. However, this seemingly straightforward approach, which is universally applied for experiments in biology, is associated with substantial challenges when used for studies of gamete structure and function *in vitro*. These highly specialised cells, especially in their mature form and after isolation from the natural microenvironment, acquire remarkable resistance towards the uptake of exogenous compounds. The specific molecular structure of the sperm membrane, characterised by an increased proportion of polyunsaturated fatty acids and the presence of rare ether-linked phospholipids, plasmalogens (Lenzi *et al.*, 2000; Tapia *et al.*, 2012), along with high structural and functional compartmentalisation (James *et al.*, 2004) and low activity of endocytotic processes (Jones *et al.*, 2013), render sperm a particularly difficult target for the intracellular delivery of investigative compounds *in vitro*. Similarly, the oocyte, throughout its maturation *in vivo*, maintains an intimate relationship with the surrounding cumulus cells which deliver essential nutrients into the oocyte via a system of gap junctions between the long cumulus cell processes penetrating the *zona pellucida* and the oocyte plasma membrane (Eppig *et al.*, 2005). Studies of oocyte structure and function *in vitro* often require the mechanical removal of these surrounding nurturing cells to facilitate visualisation of the female gamete, and, subsequently, compromise the physiological mechanisms of cargo internalisation.

In its current form, the *in vitro* intracellular delivery of research compounds into gametes, and particularly into sperm, often requires the use of powerful membrane-disrupting agents, such as cholamidopropyl-dimethylammoniopropanesulfonate hydrate (CHAPS), Tween 20 and Triton X-100 (Jakop *et al.*, 2009) with subsequent fixation, which renders gametes entirely unsuitable for further use (Garcia-Vazquez *et al.*, 2009; Yamauchi *et al.*, 2012). Consequently, this approach does

not allow for the evaluation of how differences in gamete structure relate to their functionality, especially the ability to initiate and sustain normal embryo development. Improvement of intracellular delivery into gametes in a non-aggressive fashion and without effects upon developmental potential is, therefore, pre-exquisite for the improvement of our existing knowledge of reproductive biology, and, consequently, the advancement of ART.

From a rather more applied perspective, tools for efficient and non-damaging intra-gamete delivery could hold a therapeutic promise for patients with infertility caused by specific molecular deficiencies in gametes, for example deficiency of the sperm-borne oocyte activating factor phospholipase C zeta (PLCζ), resulting in oocyte activation failure post-fertilization, even following ICSI (Amdani *et al.*, 2013). Similarly, these tools could be used in applied ART to supplement gametes with fertility-enhancing compounds, either promoting sperm motility or protecting gametes from deterioration during long-term culture *in vitro* (Kawamura *et al.*, 2012; Yun *et al.*, 2013; Tardif *et al.*, 2014), especially for such indications as the *in vitro* maturation of oocytes or the *in vitro* culture of oocytes from primordial follicles for experimental fertility preservation programmes (Telfer and McLaughlin, 2012). The versatility and large loading capacity of nanomaterials, along with evidence of spontaneous internalisation into a variety of cell types, render them attractive candidates for intra-gamete delivery of biological compounds in diverse research and therapeutic scenarios.

1.5.2.1. Sperm-mediated transfer of genes and/or biological compounds

One of the promising applications of nanomaterials in reproductive biology is to enhance the efficacy of sperm-mediated gene transfer (SMGT). During SMGT, sperm spontaneously incorporate exogenous DNA during simple co-incubation and serves as a natural vector for transfection of the oocyte and, therefore, a developing embryo, via IVF (**Figure 1–5**) (Brackett, 1971; Lavitrano *et al.*, 1989). SMGT is used to breed transgenic animals applied as pre-clinical models of human diseases, bioreactors for pharmaceutical products, and in xenotransplantation experiments (Parrington *et al.*, 2011). In many livestock species, including cows, pigs and sheep,

SMGT is reported to be more cost-effective than conventional genetic modification, which historically, has involved complex micromanipulation procedures, and the injection of foreign DNA into the pronucleus of a fertilized egg, or the injection of a genetically-modified embryonic stem cell population into the inner cell mass of the blastocyst (Parrington *et al.*, 2011). Nevertheless, the overall reproducibility of this technique remains questionable, with large variation in the reported rates of successful exogenous DNA uptake by sperm and expression of the transgene in the offspring (Oddi *et al.*, 2012; Eghbalsaied *et al.*, 2013).

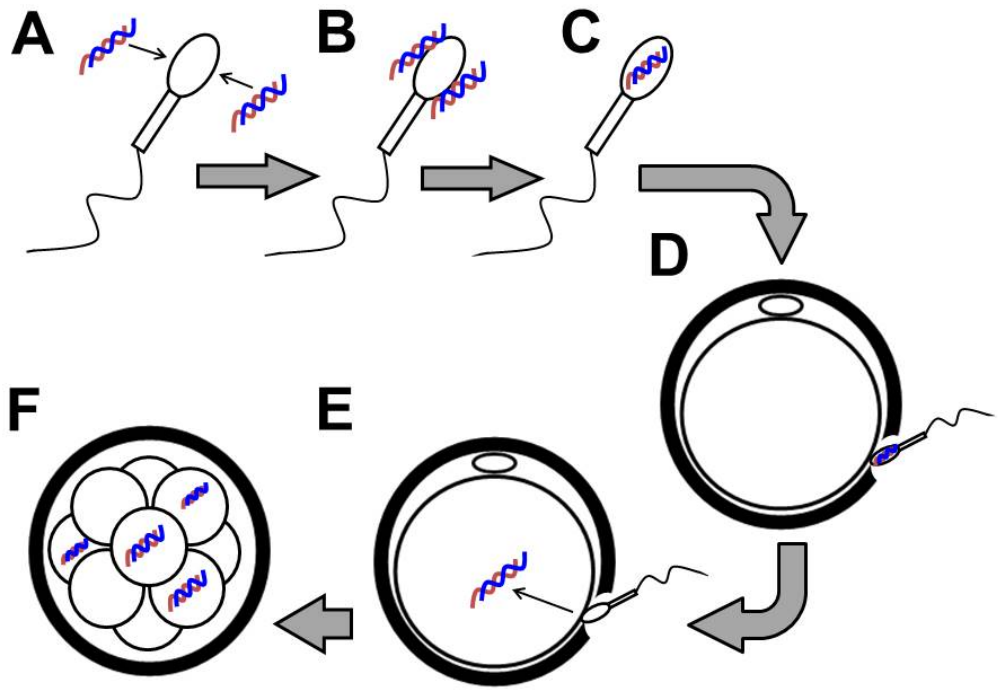

***Figure 1-5*– Sperm-mediated gene and compound transfer**. A-C) Sperm spontaneously bind, internalise and incorporate exogenous DNA into the genome upon incubation *in vitro*. D-E) The construct is subsequently delivered into the oocytes at the time of fertilization. F) Transgenic/mosaic embryos are produced. Nanomaterial-mediated delivery is a promising technique to increase the efficiency of sperm transfection and internalize into sperm alternative molecular compounds (proteins, antibodies, fluorescent markers), which can target specific physiological processes in the oocytes and early stage embryos for investigative purposes.

Several studies show that adsorption of exogenous DNA on nanocarriers improves the efficacy of construct internalisation into sperm for SMGT (Kim *et al.*, 2010b; Campos *et al.*, 2011a). Kim *et al*. (2010) described more than a 2-fold increase in plasmid DNA uptake by boar sperm after its simultaneous exposure to an enhanced green fluorescent protein (EGFP) gene

construct and magnetic iron NPs, compared to the plasmid DNA combined with only lipofectamin. This effect was further potentiated by the application of a magnetic field, resulting in an almost 3-fold increase of exogenous DNA uptake, compared to lipofection. This construct was successfully transferred via SMGT into fertilized oocytes, as evidenced by the expression of EGFP in morulae and blastocysts. Similar results were obtained in a more recent set of experiments. Specifically, Campos *et al*. (2011) used a commercially available nanopolymer along with halloysite clay nanotubes to deliver an EGFP construct into bull sperm (Campos *et al.*, 2011a). The use of both types of nanocarriers resulted in an almost 4 fold increase in DNA uptake, compared to lipofectamine, and a 5-fold increase compared to free plasmid DNA. However, despite the successful PCR-based detection of the EGFP construct in embryos produced after using sperm loaded with exogenous DNA, none of the resultant embryos expressed EGFP (Campos *et al.*, 2011a).

In theory, and in a manner similar to SMGT, sperm could be used to deliver alternative biological cargo into the oocyte such as proteins, peptides, antibodies, fluorescent markers, or, in a broader sense, any agents designed to suppress, enhance, or detect endogenous biological activity. From the research perspective, this approach could provide invaluable insight into the physiological pathways associated with fertilization and early embryo development. Preliminary work in this direction has been carried out by Makhluf *et al.* (2008), who synthesised polyvynylalcohol-coated magnetic iron oxide NPs coupled with an antibody towards protein kinase C (antiPKC-Ab) and delivered them inside bovine sperm without the antibody losing functional activity. However, this technique continues to remain controversial due to an absence of data regarding the functionality of sperm loaded with an exogenous biological agent. Currently, the use of such sperm for IVF has not been reported, and therefore, prediction of their fertilization potential, and capability of delivering and releasing the agent into the oocyte, is not possible, unless relevant studies are carried out.

1.5.2.2. Direct intra-cellular delivery of molecular compounds into oocytes and embryos

The use of nanomaterials loaded with putative molecular compounds, supporting the development and function of oocytes and pre-implantation embryos, could represent a valuable addition to existing *in vitro* culture systems. Although these potential applications have not been extensively studied, there is a series of reports concerning the beneficial effects of silver, heparan sulfate-conjugated gold and diamond nanoparticles upon the metabolic rate and anabolic processes, in particular associated with myogenesis, in chicken embryos after injections into the fertilized egg (Zielinska *et al.*, 2011; Pineda *et al.*, 2012; Grodzik *et al.*, 2013). Although the precise molecular mechanisms of these effects remain to be elucidated, these studies have already given rise to the concept of embryo 'nano-nutrition' as a means to supplement the quantitative and qualitative deficiencies of endogenous nutrients, stored in the female gamete, and promote more favourable developmental profiles.

1.5.2.3. Selection of gametes and embryos

The use of nanoparticles to target specific markers, unique to selected cell populations is being increasingly investigated for cell sorting purposes. Since NPs demonstrate improved optical properties and greater internalisation potential, they have been recently proposed as an alternative to traditional fluorophores for flow cytometry and fluorescent-activated cell sorting (FACS) (Chattopadhyay *et al.*, 2010). This concept has been explored in reproductive biology, and several recent publications report the use of NPs to label populations of gametes in a specific manner. Barchanski *et al*. observed the internalisation of gold NPs functionalised with a cell-penetrating agent into mammalian sperm, an approach that can be implemented in future for bioimaging applications in reproductive research (Barchanski *et al.*, 2011; Barchanski *et al.*, 2015).

In addition, a substantial body of research is currently investigating the potential to apply noble metal NPs, which are capable of recognising and binding with specific DNA sequences on the sex chromosomes, for high-throughput sex sorting of sperm in livestock breeding (Taylor *et al.*,

2010b; Barchanski *et al.*, 2011; Rath *et al.*, 2013). Research in a similar direction was implemented by Feugang *et al*. (2012) who reported the possibility of labelling boar sperm with CdSe/ZnS quantum dots conjugated with an arginine-rich cell penetrating peptide and a luciferase enzyme to permit bioluminescence (Feugang *et al.*, 2012). Sperm labelling was not shown to affect sperm membrane integrity or fertilization potential, indicating favourable biocompatibility of the nanomaterial with gametes. This experimental approach, therefore, has been proposed for *in vivo* tracking purposes in reproductive biology studies to investigate sperm transport utilizing fluorescence endo-microscopy.

Nanomaterials have also been evaluated as potential 'tags' for preimplantation embryos in IVF for identification purposes. (Fynewever *et al.*, 2007) applied and microinjected polysterene and polyacrylonitrile NPs into mouse embryos for external and cytoplasmic tagging, respectively. This study provided valuable insight into the variability of developmental effects of nanomaterials in an embryo, depending upon their specific spatial localisation. While external attachment of polysterene NPs to the *zona pellucida* of mouse embryos did not affect their development, intracytoplasmic injections of the same NPs resulted in a reduced proportion of developing embryos, compared to control groups. Negative effects of polyacrilonitrile NPs were more pronounced, and affected embryo development, both after intracytoplasmic microinjection and simple exposure.

1.6. CONCERNS ASSOCIATED WITH THE USE OF NANOBIOTECHNOLOGY FOR REPRODUCTIVE MEDICINE AND BIOLOGY

Despite mounting evidence of the superiority of nanobiotechnological methods in a variety of clinical applications, this approach remains inseparable from concerns relating to the potential risks of the systemic and local toxicity of engineered nanomaterials. Nanocarriers are able to accumulate in organs, tissues and intracellular structures, and, in theory, can cause long-term metabolic, immune and carcinogenic effects (Petros and DeSimone, 2010; Kunzmann *et al.*, 2011). In contrast to the treatment of cancer, where local cytotoxicity of nanomaterials is a neutral feature, because the

primary goal of treatment lies in the destruction of the affected cell population, in non-cancer fields of nanomedicine, this effect is extremely undesirable.

Concerns over the potential long-term negative effects of biomedical nanomaterials are further increased in the field of reproductive medicine and biology. Reproductive tissues and gametes represent highly specialised and sensitive biological systems with the essential function of transmitting genetic information to the offspring. Whereas nanomaterial accumulation in somatic cells can result in inflammation and, potentially, carcinogenesis, accumulation in reproductive cells can impair fertility and affect the resulting offspring (Taylor *et al.*, 2012). Nanomaterials used in reproductive medicine should, therefore, be entirely devoid of acute toxicity and the capability to induce long-term trans-generational effects. Moreover, they should not affect the viability and functionality of gametes/embryos, packaging and integrity of DNA, gene expression profiles, protein biosynthesis, energy production, cell division, or induce apoptosis, the release of ROS, or promote alternative mechanisms of cell breakdown.

Assessment of nanotoxicity represents a significant challenge, since the mechanisms governing interaction of nanomaterials with cells and their final effects depend upon a combination of factors, including physical and chemical properties of the nanocarrier (size, surface charge, coating, presence of functional groups) and morphological/physiological features of the particular target cell population. Since reproductive tissues and gametes are characterised by unique structure and functions, and safety and efficacy of nanomaterials, when applied in this delicate system, can fundamentally differ from those observed in somatic cells.

Unfortunately, detailed nanotoxicology studies involving reproductive tissues and gametes have yet to be carried out. At present, biocompatibility with mammalian sperm has been demonstrated for only a limited number of nanomaterials: magnetic iron NPs (Ben-David Makhluf *et al.*, 2006; Kim *et al.*, 2010b), halloysite clay nanotubes and commercial nanopolymer-based transfectants (Campos *et al.*, 2011a), a specific type of CdSe/ZnS quantum dots (Feugang *et al.*, 2012). At the same time, data regarding the toxicity of nanogold, one of the most commonly used

and inert nanomaterials, in sperm remain highly contradictory. While several research groups have observed detrimental effects of exposure to nanoparticulate gold upon motility, morphology and DNA integrity of mammalian sperm (Wiwanitkit *et al.*, 2009; Skuridin *et al.*, 2010; Taylor *et al.*, 2010b; Taylor *et al.*, 2012), others have failed to detect any effects of this nanomaterial upon sperm functionality, unless extreme concentrations were applied (Moretti *et al.*, 2012). It should, however, be noted that collective interpretation of these findings remains difficult due to the use of various sources, synthesis procedures and modifications of NPs, as well as different protocols of exposure and toxicity assays (Taylor *et al.*, 2014c).

Regarding the effects of nanomaterials upon embryo development, numerous publications support the biocompatibility of chitosan, CdSe/ZnS quantum dots, and externally applied polysterene NPs with early embryogenesis in mammals (Fynewever *et al.*, 2007; Ema *et al.*, 2010; Yang *et al.*, 2011). However, even slight modifications in the physicochemical properties of NPs, and their delivery route, can dramatically alter their safety profiles. For instance, Fynewever et al. (2007) showed that while the external application of polysterene NPs to mouse embryos does not compromise early embryo development, intracytoplasmic injection of the same NPs induces developmental toxicity (Fynewever *et al.*, 2007). Similarly, removal of ZnS coating from the surface of CdSe quantum dots affects the maturation profiles of mouse oocytes *in vitro*, and increases mortality rates in early post-implantation embryos (Hsieh *et al.*, 2009).

Another significant concern is that successful nanomaterial-mediated delivery requires the penetration of nanocarriers into the target cell. Nanomaterial uptake by gametes and reproductive tissues can differ from that by somatic cells due to their unique structure and function. These cells, particularly gametes, lack strong endocytotic mechanisms, and generally have low physiological permeability to foreign substances. For instance, the sperm plasma membrane contains a significantly higher proportion of unsaturated fatty acids, compared to most somatic cells. These chains are crucial for membrane fluidity and elasticity, thus promoting active cell movement (Tapia *et al.*, 2012). In sperm, the plasma membrane also bears a stronger negative charge, demonstrates

limited permeability to exogenous molecules, and exhibits an increased degree of functional compartmentalisation (Parrington *et al.*, 2007). Consequently, even those nanomaterials with proven uptake by a variety of somatic cells, for instance nano-gold, are not readily internalised into sperm (Taylor *et al.*, 2010a), who failed to deliver gold NPs, rapidly uptaken by a variety of cell types, into sperm. Similar findings were obtained by other research groups, who observed that binding of various NPs to the sperm surface represented the preferential type of interaction, with intracellular uptake observed for a much smaller proportion of the NPs (Makhluf *et al.*, 2008; Kim *et al.*, 2010b; Feugang *et al.*, 2012; Taylor *et al.*, 2014a; Barchanski *et al.*, 2015). Interestingly, most publications have emphasised that the lack of cellular NP internalisation did not compromise the performance of the specific research techniques investigated. This could suggest that although the mechanisms of cellular uptake in sperm are not sufficient for internalisation of a nanocarrier, transmembrane penetration of the payloads can still occur.

In the case of oocytes, cellular transport throughout the maturation stages occurs via the transzonal projections of adjacent granulosa cells, which penetrate the *zona pellucida* and terminate at the oocyte plasma membrane. At present, it remains unclear whether nanomaterials can spontaneously cross the *zona pellucida* via transzonal channels and internalize into the oocytes (Courbiere *et al.*, 2013), and moreover, what the ‘fate’ of internalised nanomaterials would be during embryo cleavage.

Collectively, these concerns justify further detailed studies into the nanoxocitity of candidate nanomaterials for reproductive applications, since these tools could form a highly valuable addition to the field of reproductive biology, markedly increasing the success rates of techniques associated with internalisation of compounds into gametes.

1.7. MESOPOROUS SILICA AS A POTENTIAL DELIVERY TOOL FOR REPRODUCTIVE APPLICATIONS

Mesoporous silica originates from a special class of synthetically modified colloidal silica with highly ordered mesoscale-sized pores (2-50nm) (Kresge *et al.*, 1992), which began to receive attention as a promising tool for targeted drug and gene delivery, bioimaging, and tissue engineering, since the early 2000s (Vallet-Regi *et al.*, 2007) **(Figure 1–6).**

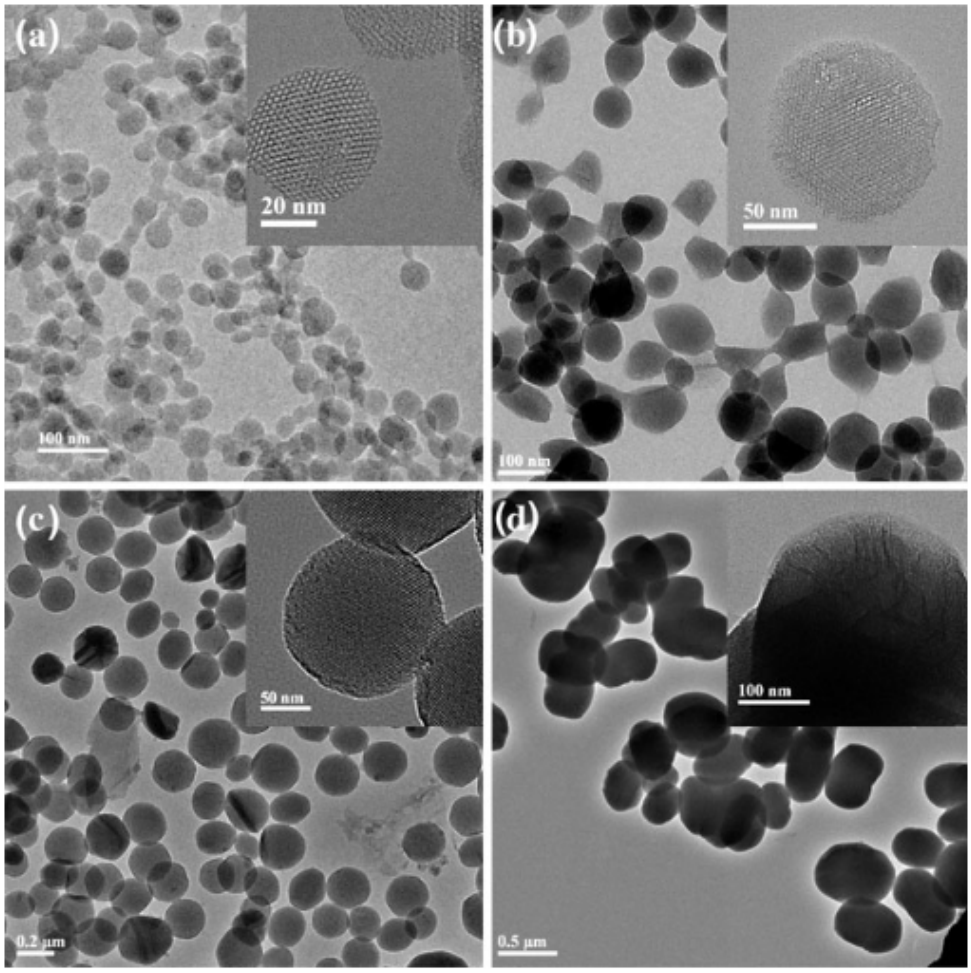

***Figure 1-6*– Mesoporous silica nanoparticles with various diameters: scanning electron microscopy.** (a) 50 nm. (b) 100 nm. (c) 200 nm. (d) 440 nm. (Adapted from Gan *et al.*, 2012).

Today, mesoporous silica is universally recognised as a powerful biomedical nanomaterial, and a solid body of evidence now supports its low cytotoxicity across a variety of cell types (Yang *et al.*, 2012b). Mesoporous silica is characterised by a number of features, which make it particularly attractive as a targeted delivery vector for reproductive biology (summarised in **Table 1–5).**

***Table 1-5* – Mesoporous silica: main benefits for reproductive biology**

Feature	Benefits
Robustness	Stable cytoplasmic/surface tag for cell proliferation, differentiation and migration studies
Chemical inertness	Minimisation of free radical–associated cell damage
Versatility and ease of production	Reduced need for large-scale synthesis
Porous architecture	Lower dose of nanocarrier to carry the required dose of cargo
Encouraging safety profiles	Expected long-term safety for highly-specialised cells

Firstly, mesoporous silica is robust, and, therefore, has an increased likelihood to persist in a targeted cell population after internalisation, compared to organic biodegradable materials. Hence, fluorescent modifications of targeted mesoporous silica can be used as highly-selective cytoplasmic/surface cell tags with which to investigate patterns of cellular proliferation, differentiation, and migration in cell tracking studies (Huang *et al.*, 2005), which represent the cornerstone of reproductive biology and stem cell research. Secondly, mesoporous silica is chemically inert, and is not prone to induce free radical formation when internalised inside cells, unlike, for example, magnetic iron oxides. This minimises the risks of free radical-associated DNA damage in gametes and early stage embryos – a proven cause of aberrant embryo development, implantation failure and recurrent spontaneous abortion (Robinson *et al.*, 2012). In fact, mesoporous silica has even been shown to suppress the production of ROS in a model of malignant growth – a finding necessitating further investigation, particularly in a reproductive biology setting (Huang *et al.*, 2010). Thirdly, this nanomaterial is highly versatile, but, at the same time, relatively easy to manufacture. Indeed, mesoporous silica can be modified with specific features (size, pore architecture and diameter, surface functionalities/coatings, fluorescent labels) by a series of reasonably straightforward and inexpensive wet-chemistry reactions without significant implications to overall cost (Gan *et al.*, 2012).

Furthermore, the unique porous structure of this nanomaterial rapidly increases its total surface area, and, therefore, loading capacity. In addition, it allows the absorption of functional cargo both on the surface and inside the pore channels, protecting payloads from degradation and

preventing off-target escape. Mesoporous silica has high structural integrity, and large amounts of payloads can be attached to silica scaffold without its disruption (Rosenholm *et al.*, 2012). This minimises the dose of nanovector required to deliver required amounts of biological cargo, and thus avoids the over-exposure of highly specialised and sensitive reproductive tissues and gametes. Ultimately, the primary function of these highly specialised cells is to transmit genetic material to the offspring and are widely known to be vulnerable to sub-optimal culture conditions (temperature, light, oxygen tension, culture media), when handled *in vitro*. Finally, although mesoporous silica has been extensively studied in a variety of somatic cell types, data regarding its biocompatibility with gametes is lacking, which, alongside its other promising features, renders it an interesting subject for the specific research described in this thesis.

1.8. ASPECTS OF GAMETE STRUCTURE AND BIOLOGY RELEVANT TO THIS THESIS

The majority of experiments, described in this thesis, involved evaluation of effects of MSNPs upon sperm structure and function using the boar and human models. A smaller subset of experiments evaluated the use of MSNPs in mouse oocytes – the most conventional model in reproductive biology. Given the small number of these experiments and the fact that they did not aim to provide in-depth assessment of effects of MSNPs upon oocyte function, details of mouse oocyte morphology and function will not be discussed in this subsection.

Boar sperm are traditionally used in reproductive biology as a model for human sperm, given their morphological and functional similarities. Same as human sperm, boar sperm contain three distinct morphological regions: head, midpiece and tail – and are obtained via ejaculation, which ensures that epididymal maturation had already taken place. In addition, boar sperm represent an important subject reproductive biology studies themselves, given the wide introduction of assisted reproduction techniques into breeding of farm animals.

The ejaculated boar and human sperm consists of a compact head (oval-shaped for boar and paddle-shaper for human), acrosome, which comes in close contact with the nucleus, prominent

mitochondrial sheath and tail (**Figure 1–7A**). Comparison of dimensions of normal mature boar and human sperm is presented in **Table 1–6**.

***Table 1-6* – Physical dimensions of normal mature boar and human sperm: comparative analysis**

	Boar (Bonet *et al*., 2013)	**Human** (Hafez and Kenemans, 2012)
Sperm length	45 μm	48 μm
Head		
Length	7.0 μm	4.5 μm
Width	3.7 μm	3.0 μm
Thickness	0.4 μm	N/A
Tail	37.4 μm	43.8 μm
Midpiece		
Length	9.0 μm	5-7 μm
Width	0.7 μm	1 μm
Principal piece		
Length	26.2 μm	45 μm
Width	0.4 μm	Decreasing
Terminal piece		
Length	2.2 μm	5 μm
Width	0.2 μm	Thinner than the principal piece

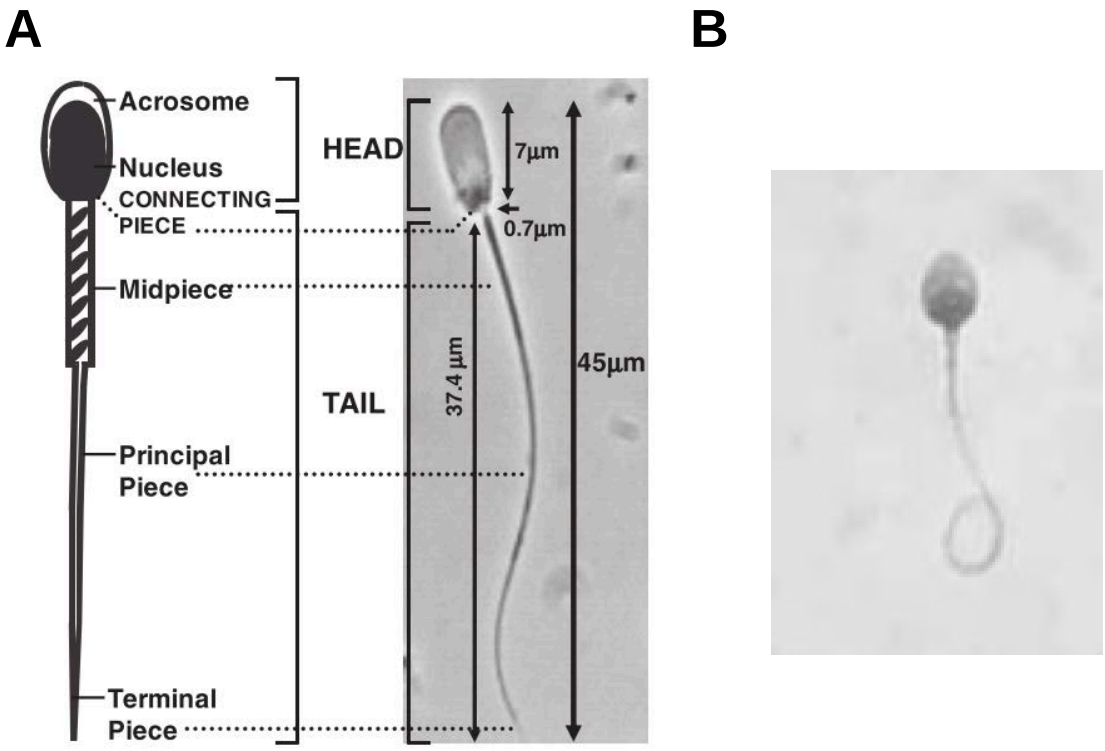

***Figure 1-7* – Morphology of boar and human sperm.** A) Boar. B) Human. Boar and human sperm share substantial morphological similarities: the head contains the nucleus and the acrosome, and the tail consists of three regions: the midpiece, the principal piece, and the terminal piece. A short linking segment between the head and details if often referred to as connecting piece (or neck). Boar sperm have slightly larger and more oval-shaped heads compared to human sperm, and shorter tails which approximate 80% of the total sperm length versus 90% in humans (images sourced from Bonet *et al*. (2013) and www.who.int (accessed on 4 December 2015)).

As mentioned previously, sperm represent a subset of cells with highly specialised morphology and function. Although sperm contain organelles, which are characteristic of any cell type, for example, the nucleus and plasma membrane, the structure of these organelles can differ substantially from that in somatic cells. A general outline of the differences between structure and function of intracellular organelles in sperm compared those in somatic cells, and their relevance for intracellular uptake of cargo, is presented in **Table 1–7**.

***Table 1-7* – Structural and functional differences between intracellular organelles in sperm and somatic cells**

	Key differences	**Relevance for intracellular uptake of molecular cargo**
Nucleus	• Chromatin packaging by protamines ensures tight compaction in small space and low accessibility of chromatin to external factors • Nuclear envelope is largely devoid of nuclear pore complexes (Ho and Suarez, 2003)	• Low accessibility of the nuclear compartment in mature sperm • Low efficacy of spontaneous integration of molecular cargo
Cytoplasm	• Almost redundant (is gradually removed during the process of spermiogenesis) • Cytoplasmic compartment in the sperm head is reduced to perinuclear theca (PT) – a rigid structure containing cross-linked structural proteins and other protein molecules	• 'Lack' of space for uptake of large extracellular cargo • Challenges associated with free migration of molecules within the cytoplasm and their incorporation into intracellular pathways
Plasma membrane	• Organised into lipid domains, which display differences in fluidity and lipid content • High degree of mosaicism with regards to domain distribution, surface antigens and charge • Constantly undergoes structural and functional reorganisation during transit through the make and female reproductive tract	• Interaction with cargo can be limited by the localisation and size of relevant domains • Targeting towards surface receptors can inadvertently block fertilization potential

1.9. AIM OF THIS THESIS

Recent progress in biomedical nanotechnology has transformed the concept of targeted biological delivery, allowing the engineering of complex biocompatible nanoscale-sized platforms with high loading capacity, stability, highly selective affinity, and potential for simultaneous diagnostic and therapeutic applications. These versatile delivery vehicles with spontaneous internalisation into target cells can hold great promise for the field of reproductive science and medicine, and may

represent elegant targeted tools for clinical and/or research application. Such tools could substantially improve performance of reproductive science techniques, based upon the internalisation of molecular compounds into reproductive tissue and gametes. These techniques include, but are not limited to, gene transfer into reproductive tissues, sperm-mediated gene/ compound transfer into the oocyte, direct supplementation of gametes with fertility-enhancing compounds *in vitro*, and highly selective labelling of gametes for sorting or bioimaging. The use of nanomaterials as delivery platforms for these methodologies could help achieve physiological and safe uptake of large amounts of different molecular cargo types, and bypass the need for aggressive chemical agents or viral vectors. Mesoporous silica, combining the features of robustness, chemical inertness, large loading capacity and promising safety profiles, represents an attractive novel candidate for use in reproductive science and medicine. However, its performance in gametes, characterised by highly specialised morphology and function, has never been tested previously.

The primary aim of this project was to design a versatile mesoporous silica nanoparticles-based 'platform', capable of delivering different molecular compounds, such as nucleic acids, peptides/proteins or fluorescent markers, into mammalian gametes during simple *in vitro* co-incubation, which, at the same time, would not compromise gamete function, allowing the subsequent use of these cells for fertilization.

To achieve this primary aim, the following study objectives were pursued:

1. In-house synthesis of fluorescent and non-fluorescent MSNPs in a surfactant-templated base-catalysed sol-gel gel reaction, followed by optional surface functionalisation to permit subsequent loading with molecular cargo (nucleic acids and proteins;), and physicochemical characterisation of various modifications of synthesised MSNPs

2. Evaluation of the toxicity and spontaneous binding of various modifications of MSNPs with mammalian gametes during co-incubation *in vitro* under conditions, similar to those used in the

ART setting, to determine the appropriate incubation times and doses of MSNPs from the perspective of safety/efficacy balance. These experiments were carried out using boar sperm and mouse oocytes as well-characterised models for reproductive biology. In the case of oocytes, the potential for assisted internalisation of MSNPs via micromanipulation techniques was also assessed.

3. Optimisation of binding rates between MSNPs and sperm via the selection of MSNP-bound sperm, via modification of the physico-chemical properties of MSNPs or via the active targeting of MSNPs towards sperm.

4. Evaluation of the delivery potential of various modifications of MSNPs in previously optimised doses for DNA and protein transfer into mammalian sperm during co-incubation *in vitro* under conditions similar to those used in the ART setting.

5. Evaluation of toxicity, spontaneous binding of various modifications of MSNPs, and their potential to deliver DNA into human sperm during co-incubation *in vitro* under conditions, similar to those used in the ART setting.

CHAPTER 2

GENERAL MATERIALS AND METHODS

Key messages:

- This chapter presents a description of the general materials and methods used throughout this thesis
- To facilitate clarity, detailed information regarding the specific experimental conditions and particular tests applied only at certain stages of this thesis, is presented in the relevant experimental chapters

2.1. SYNTHESIS, FUNCTIONALISATION AND CHARACTERISATION OF MESOPOROUS SILICA NANOPARTICLES (MSNPS)

2.1.1. SYNTHESIS OF MSNPS

Synthesis of MSNPs was performed in a surfactant-templated base-catalysed sol-gel reaction as previously described by Hom *et al.* (2010) and Zhu *et al.* (2011). Essentially, the reaction is based upon mixing of the templating agent cetyltrimethylammonium bromide or cetyltrimethylammonium chloride (CTAB or CTAC) with silica source tetraethylorthosilicate (TEOS) in hot basic aqueous solution (pH>7.0), followed by amine and phosphonate surface modification, and final removal of the template via refluxing in acidic methanol (**Figure 2–1**). A summary of the types and surface modifications of MSNPs, and types of cargo used in this project, as well as the main rationale for the use of each kind of synthesised MSNPs, is presented in **Figure 2–2**.

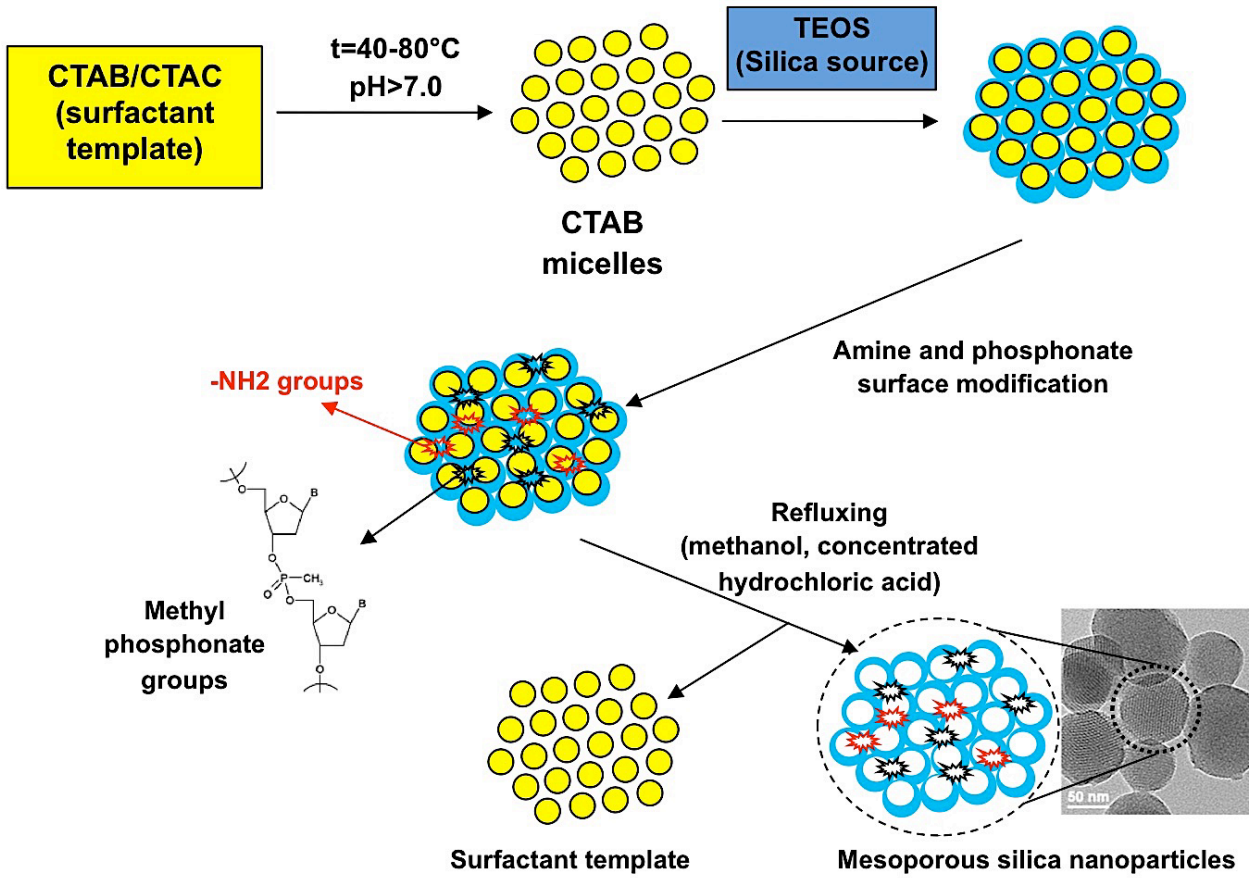

***Figure 2-1*– Surfactant-templated base-catalysed sol-gel MSNPs synthesis.** Under high temperature conditions and alkaline pH, the surfactant (CTAB or CTAC) assembles into micelles, around which the silica scaffold is synthesized from a precursor (TEOS). Amine and phosphonate surface modification provides the functional groups for cargo loading, and determines the surface chemistry. To remove the surfactant from the pores, nanoparticles are refluxed in acidic methanol, which exposes the characteristic mesoporous structure (MSNP image source: www.wikipedia.org, accessed on 27/07/2015).

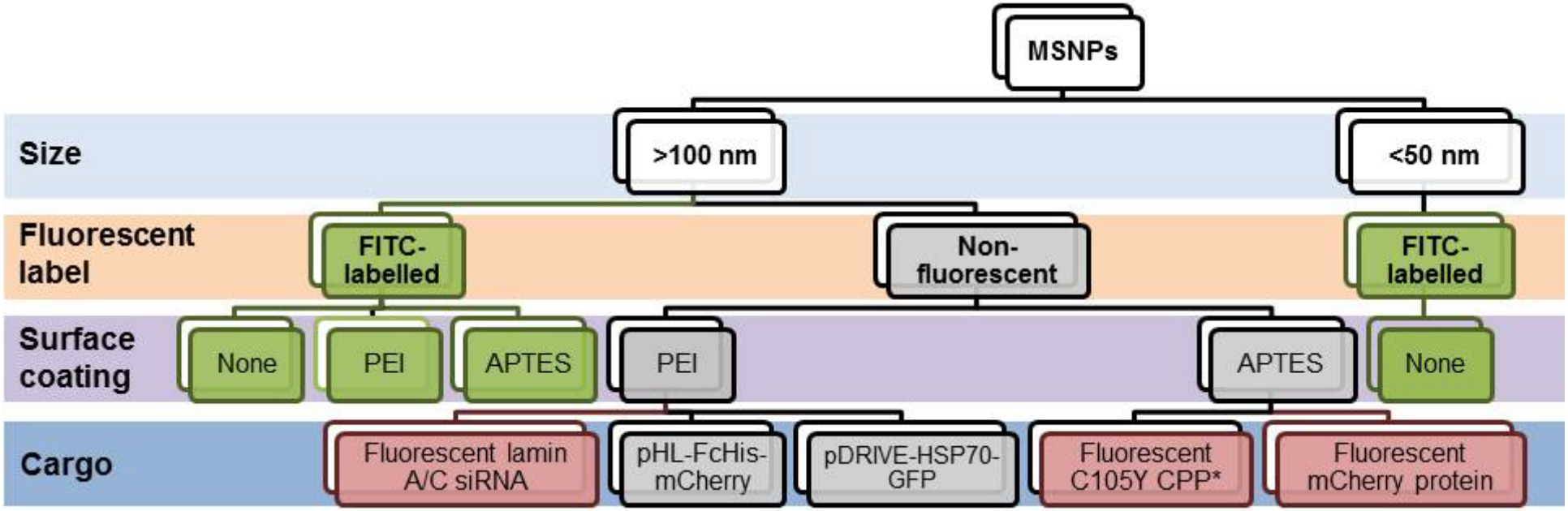

Figure 2-2 **- Modifications of mesoporous silica nanoparticles (MSNPs) and types of cargo used in the project.** The project primarily evaluated the performance of MSNPs with a physical diameter >100 nm. MSNPs with a physical diameter <50nm were synthesised to evaluate the effects of particle size upon gamete binding capacity, and exclusively applied for experiments described in **Section 4.2.2**. MSNPs were synthesised either in fluorescent form via the incorporation of FITC into the silica scaffold to permit visualisation in gametes during fluorescence/confocal microscopy, or non-fluorescent form for subsequent loading with cargo. Synthesised fluorescent MSNPs were optionally functionalised with PEI and APTES, representing the common surface modifications of nanomaterials, permitting loading with nucleic acids or peptides/proteins, respectively. Surface coating of fluorescent MSNPs was carried out to visualise, how the different surface chemistry of MSNPs affects toxicity and binding profiles with gametes, and compare the behaviour of 'empty' and 'loaded' vehicles in these cells. Finally, non-fluorescent PEI- and APTES-coated MSNPs were loaded with fluorescent 'prototypes' of molecular cargo: fluorescent nucleic acid (lamin A/C siRNA) or protein (mCherry) to visualise the effects of cargo loading upon the toxicity and binding of MSNPs with gametes. To evaluate the delivery capacity of MSNPs into sperm, non-fluorescent PEI-coated MSNPs were loaded with plasmids (pHL-FcHis-mCherry or pDRIVE-HSP70-GFP), and APTES-coated MSNPs – with mCherry. * Fluorescent C105Y cell-penetrating peptide was used as a targeting agent towards sperm.
MSNPs: mesoporous silica nanoparticles; FITC: fluorescein isothiocyanate, PEI: polyethileneimine; APTES: (3-aminopropyl)triethoxysilane; CPP: cell-penetrating peptide.

2.1.1.1. Reagents for the synthesis and functionalisation of MSNPs

Anhydrous sodium hydroxide (NaOH, ≥98%), hexadecyltrimethylammonium bromide (CTAB, >99%), hexadecyltrimethylammonium chloride (CTAC, >98%), tetraethyl orthosilicate (TEOS, 98%), diethanolamine (DEA, ≥99.5%), 3-(trihydroxysilyl)propyl methylphosphonate (3-THPMP, monosodium salt, 42 wt.% solution in water), fluorescein isothiocyanate (FITC, ≥90%), (3-aminopropyl)triethoxysilane (APTES, ≥98%), polyethileneimine (PEI, 50 wt.% solution in water, MW 1.3kD, Mn 1,200g/mol), concentrated hydrochloric acid (HCL; 37.2 wt.% solution in water, 12.1M) and Dulbecco's phosphate based saline (DPBS) were sourced from Sigma-Aldrich (UK). Methanol (≥99.8%) was sourced from Rathburn Chemicals (UK). Absolute ethanol (≥99.8%) was sourced from Riedel-de Haën (Germany).

2.1.1.2. Synthesis of MSNPs

A) Synthesis of MSNPs > 100 nm

In a round-bottomed flask, 0.1g of CTAB was dissolved in a mixture of 48ml double distilled water (DDW) and 0.35ml of 2M NaOH. The solution was heated in a silicone oil bath to 80°C with magnetic stirring. After the temperature had stabilised, 0.5ml of TEOS was added to the reaction. After 15 minutes, 0.127ml of 3-THPMP was added, and the reaction stirred for 2 hrs at 80°C. The solution was then cooled to room temperature (RT), and MSNPs were recovered and washed twice with methanol via centrifugation. Particles were redispersed in a mixture of 40ml of methanol and 2ml of 12.1M HCL, and refluxed for 24 hrs at 80°C with magnetic stirring to remove CTAB. After refluxing, MSNPs were recovered and washed twice in absolute ethanol via centrifugation, and vacuum dried overnight.

To synthesise fluorescent MSNPs, FITC was introduced into the silica framework in the form of FITC-APTES conjugate during the main reaction. The conjugate was prepared by mixing 100µl of APTES with 25mg of FITC in 5ml of absolute ethanol, and stirring magnetically for 12 hrs under a dry nitrogen atmosphere. To produce fluorescent particles, 50µl of FITC-APTES conjugate

was added to the reaction 10 minutes after 0.5ml of TEOS had been introduced. After 5 minutes, 0.127ml of 3-THPMP was added, and the remaining steps were carried out in accordance with the standard procedure.

B) Synthesis of MSNPs <50 nm

Briefly, in a round-bottomed flask, 50.4ml of DDW, 6.3g of absolute ethanol, 1.82g of CTAC, and 0.14g of DEA were mixed and stirred magnetically in a heated silicone bath at 40°C for 30min. Then 5.11mL of TEOS was slowly added into the mixture, followed by 100µl of FITC-APTES conjugate 10 minutes after TEOS had been introduced. The reaction was stirred for a further 2 hours. The solution was then cooled to RT, and MSNPs were recovered and washed twice with methanol via centrifugation. Particles were redispersed in a mixture of 40ml of methanol and 2ml of 12.1M HCL, and refluxed for 24 hrs at 80°C with magnetic stirring to remove CTAC. After refluxing, MSNPs were recovered and washed twice in absolute ethanol via centrifugation, and vacuum dried overnight.

2.1.1.3. Surface functionalisation of MSNPs with PEI

Functionalisation of the surface of MSNPs with the cationic polymer PEI aimed to reduce particle agglomeration, improve cell interaction and provide a positively charged surface for electrostatic binding of nucleic acids (Xia *et al.*, 2009). To perform the coating, 5mg of dry MSNPs with a size >100nm was redispersed in a mixture of 75µl of PEI and 30ml of absolute ethanol in a round-bottomed flask, and stirred at RT for 1 hour. MSNPs were recovered and washed by centrifugation in absolute ethanol and sterile DDW, and vacuum dried overnight.

2.1.1.4. Surface functionalisation of MSNPs with APTES

Coating of MSNPs with APTES aimed to provide amine groups for covalent cross-linking with carboxyl groups of payloads (Can *et al.*, 2009). To achieve this, MSNPs were redispersed in DDW to a concentration of 10mg/ml, and APTES was added to 5% by volume. The reaction was stirred

magnetically for 1 hour at RT. Coated particles were recovered and washed in sterile DDW by centrifugation, and vacuum dried overnight.

2.1.1.5. Surface functionalisation of APTES-coated MSNPs with C105Y

For active targeting of MSNPs towards sperm, APTES-coated MSNPs were functionalised with C105Y-TMR fluorescent peptide (tetramethylrhodamine-CSIPPEVKFNKPFVYLI-CONH2, Covalab, France) via the cross-linking of amine groups on the functionalised surface of MSNPs with carboxyl groups of the peptide using 1-ethyl-3-[3-dimethylaminopropyl]carbodiimide hydrochloride coupling agent (EDC, Fisher Scientific, UK). In brief, 2mg of APTES-functionalised MSNPs were redispersed in 200µl of 0.1M 2-[n-morpholino]ethane sulfonic acid-buffered saline (MES-buffered saline, Fisher Scientific, UK) and mixed with 200µl of C105Y-TMR (2mM in 10% acetic acid, Sigma-Alrdich, UK). The resulting suspension was diluted with 1500µl of 0.1M MES buffer, and 100µl of EDC (10mg/ml in DDW) was immediately added to the reaction. The reaction was incubated for 2 hours at RT on a shaker plate. C105Y-TMR-functionalised MSNPs were recovered through centrifugation, and redispersed in phosphate-buffered saline (PBS, Oxoid, UK). Binding of C105Y-TMR with APTES-coated MSNPs was confirmed by the calculation of peptide concentration in solution using spectrophotometric measurements at 280nm before and after the reaction (BiophotometerPlus, Eppendorf, UK).

2.1.2. Characterisation of MSNPs

For transmission electron microscopy (TEM), dry non-coated MSNPs were redispersed in absolute ethanol, sonicated for 30s, and loaded on a TEM grid coated with lacey carbon film (Agar Scientific, UK). Imaging was performed on a JEOL JEM-2010 analytical TEM (JEOL Ltd., Japan). Acquired images were processed using Digital Micrograph 3.7.4 for GMS 1.2 Build 45 (Gatan Inc., Pleasanton, CA, USA). The physical size of the particles and diameter of pores, where available, was measured in a minimum of 100 MSNPs with an anticipated diameter of >100nm and 50 MSNPs with an anticipated diameter of <50nm.

For scanning electron microscopy (SEM), dry samples of non-coated MSNPs were dusted onto a carbon taped SEM stub, and 3nm layer coating of platinum was applied. Nanoparticle size and morphology was investigated using a JEOL JSM-840F SEM (JEOL Ltd., Japan). Images were collected in the secondary electron (SE) imaging mode.

Unless specified otherwise, the hydrodynamic size of synthesised MSNPs (non-coated, PEI-coated and APTES-coated) was analysed using a disc centrifuge (CPS DC24000, CPS Instruments Europe, Netherlands), which determined the diameter of particles in solution based upon their sedimentation profiles during centrifugation in a liquid gradient, or NanoSight. For disk centrifuge analysis, particle size was measured at a disk speed 24,000rpm and pH 7.0. External calibration with a kit calibration standard (0.377μm-sized polyvinyl chloride latex particles dispersed in distilled water, density 1.385g/ml; CPS Instruments, Netherlands) was performed before each test to maintain accuracy.

Electrokinetic (ζ) potential of synthesised MSNPs (non-coated, PEI-coated and APTES-coated) was measured using the dynamic light scattering (DLS) technique using a Zetasizer Nano ZS (Malvern Instruments, UK). The Zetasizer recorded the phase/frequency shift of a laser beam coming in contact with charged particles moving in the electric field to the oppositely charged electrode, and converted their velocity to ζ potential. Measurements were performed at 25ºC and pH 7.0.

2.1.3. LOADING OF MSNPS > 100 NM WITH CARGO

2.1.3.1. Loading with nucleic acids (siRNA or plasmid DNA)

To load particles with nucleic acids, non-fluorescent PEI-coated MSNPs with a size > 100nm were redispersed in 1.0ml of nuclease-free water (Millipore, UK) to 1.5-2mg/ml concentration. Fluorescent lamin A/C siRNA (siGLO Lamin A/C Control siRNA (human/mouse/rat), Dharmacon RNAi Technologies, Thermo Scientific, UK) was added to the resulting MSNP dispersion to 0.2μM for siRNA; pHL-FcHis-mCherry (for transfer into boar sperm; plasmid prepared earlier by a past member of the group Dr Junaid Kashir) or pDRIVE-HSP70-GFP

(for transfer into human sperm; plasmid prepared by a current group member Miss Lien Davidson) were added in a 10:1 mass ratio (MSNP:plasmid) (**Figure 2–3**). The mixture was incubated for 24 hrs at 4°C with rotation. MSNPs were recovered through centrifugation and redispersed in 1.0ml of nuclease-free water. Loading was confirmed by calculation of nucleic acid concentration in solution before and after the reaction via the measurement of absorbance at 260nm by spectrophotometry (BiophotometerPlus, Eppendorf, UK).

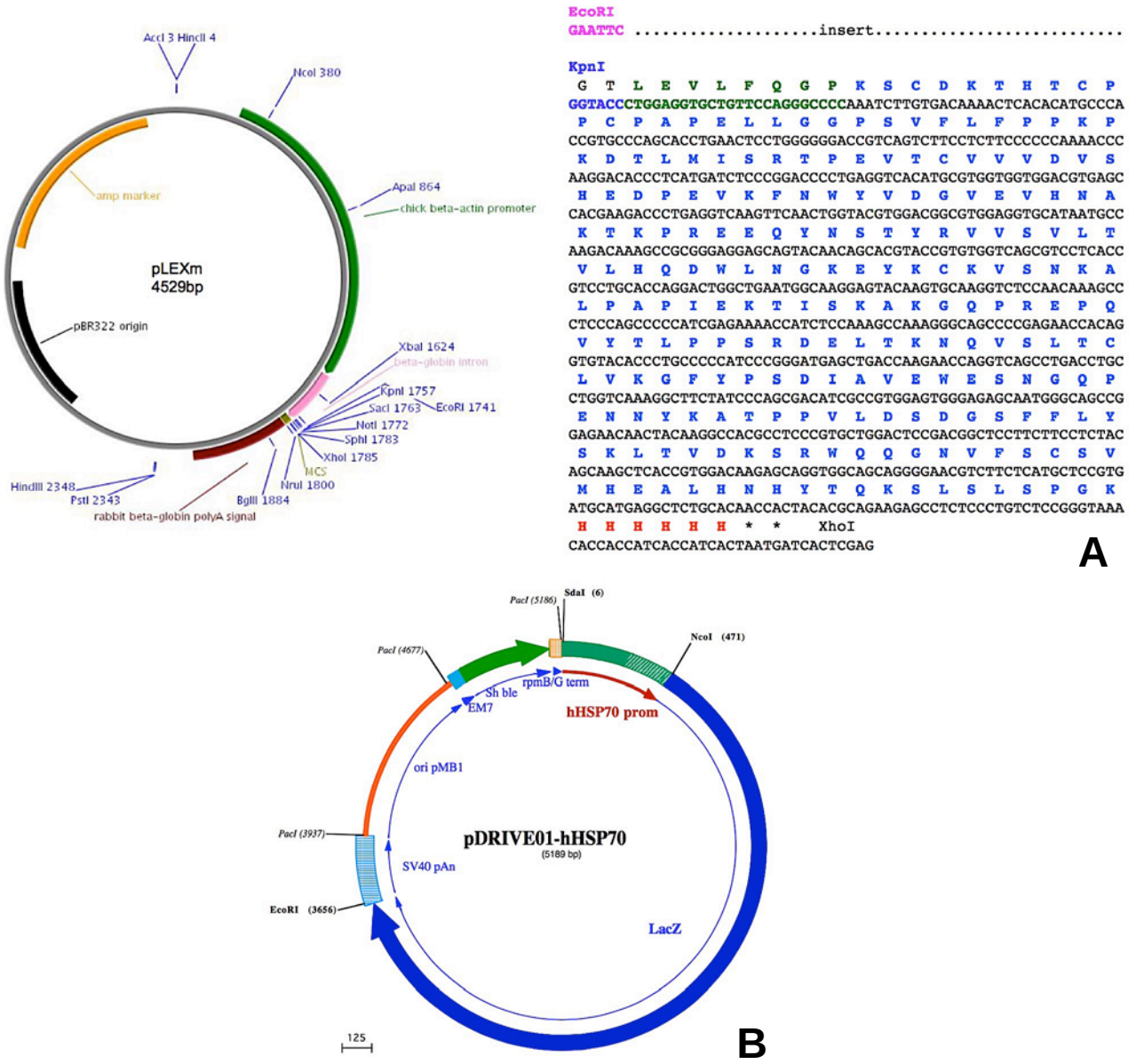

***Figure 2-3* – Maps of plasmid vectors used for molecular cloning of mCherry and GFP sequences.** Plasmids were loaded onto PEI-coated MSNPs via electrostatic association and used for subsequent delivery into sperm**. A) pHL-FcHis vector used for delivery into boar sperm.** The vector is based upon the pLEXm backbone and contains a 3C protease cleavage site (in green) followed by the human IgGγ1 hinge and Fc regions (blue) and finally a KHis6 tag (red), all cloned between the KpnI site (purple) and the XhoI site (black) (Aricescu *et al.* (2006)). **B) pDRIVE-HSP70 vector used for delivery into human sperm** (available from www.invivogen.com, accessed on 14/09/2015).

To evaluate the profile of pDNA adsorption on the MSNPs, spectrophotometric quantification of free pDNA concentration in the supernatant was carried out at hourly intervals during the first 6 hours of incubation, and then after 24 hours. Measurements were performed at 260nm in a minimum of three replicates.

To additionally confirm the loading of pDNA onto MSNPs, an agarose gel retardation test was carried out. To perform this test, 10µl of a 2mg/ml suspension of PEI-coated MSNPs, loaded with pHL-FcHis-mCherry, was mixed with 2µl loading dye (6X Orange DNA Loading Dye, Thermo Scientific, UK) and loaded onto a 0.8% agarose gel (Agarose LE Analytical Grade, Promega). The gel was prepared with tris-acetate-ethylenediaminetetraacetic acid buffer (TAE; Life Technologies, UK) and pre-stained with ethidium bromide (final concentration: 0.5µg/ml, Fisher Scientific, UK). An equivalent amount of free pHL-FcHis-mCherry was loaded onto the same gel as a control. The gel was run in TAE at 90V for 1 hour, and imaged by a gel documentation system (BioDoc-It, UVP, USA).

2.1.3.2. Loading with mCherry protein

A) Mammalian cell culture and mCherry expression

Transformed human embryonic kidney cells (HEK293T) were cultured under standard conditions and seeded into 175cm^3 tissue culture flasks at a confluency of 30-50%. Transfection with pHL-FcHis-mCherry was performed at 50-70% confluency using the jetPEI DNA transfection kit (Polyplus-transfection SA, France) according to the manufacturer's protocol. Cells were cultured in Dulbecco's Modified Eagle Medium supplemented with 10% fetal bovine serum (FBS), 1%v/v 5000U penicillin, 5mg/ml streptomycin, 2mM L-glutamine and sodium pyruvate (all reagents sourced from Sigma-Aldrich, UK) for 24 hrs, after which the medium was changed to FBS-free.

B) Purification of mCherry protein

Culture media was collected on day 6 of culture, supplemented with phenylmethanesulfonylfluoride (PMSF; Sigma-Aldrich, UK) and ethylenediaminetetraacetic acid (EDTA; Sigma-Aldrich, UK) to a final concentration of 1mM, and centrifuged for 30min at 6,000g at 4^{o}C. The supernatant was

filtered through a 0.45µm polyethersulfone membrane filter, and passed through a column containing Protein A Sepharose beads (GE Healthcare Lifesciences, UK) to bind the Fc-tag. The column was washed with 20 column volumes of PBS, followed by 10 column volumes of TNED buffer (50mM Tris (pH 8.0), 150mM NaCl, 10mM EDTA, and 1mM diothiothreitol; all reagents from Sigma-Aldrich, UK). 3C protease was added in 1 column volume of TNED buffer and left to shake overnight to cleave the Fc-tag. Protein was eluted with TNE (50mM Tris (pH 8.0), 150mM NaCl, 10mM EDTA). Purified protein identity was verified by liquid chromatography/mass spectrometry (Professor Benedikt Kessler, Centre for Cellular and Molecular Physiology, Nuffield Department of Medicine, University of Oxford, UK).

C) Loading of MSNPs with mCherry protein

Loading of APTES-coated MSNPs was performed via cross-linking of amine groups on the functionalised surface of mesoporous silica with the carboxyl groups of mCherry protein using 1-ethyl-3-[3-dimethylaminopropyl]carbodiimide hydrochloride (EDC) coupling agent (Fisher Scientific, UK). For EDC coupling, 2mg of APTES-functionalised MSNPs were redispersed in 200µl of 0.1M 2-[n-morpholino]ethane sulfonic acid (MES) buffer (Fisher Scientific, UK) and mixed with mCherry protein dissolved in 1500µl 0.1M MES buffer. For experiments investigating the potential for cargo loading onto MSNPs and effects of such loading upon MSNP binding with sperm (***Section 3.5.***), MSNPs were mixed with mCherry in a 1:6 mass ratio. For experiments investigating the delivery capacity of MSNPs as cargo transporters into sperm (***Section 5.3.4.***), MSNPs were mixed with mCherry in a 2:1 mass ratio. Then, 10mg of EDC was dissolved in 1ml of DDW, and 100µl of the solution was added immediately to the MSNP-mCherry mixture. The reaction was incubated for 2 hours at RT on a shaker plate. MSNPs were recovered through centrifugation, and redispersed in PBS. Loading was confirmed by calculation of protein concentration in solution before and after the reaction via the measurement of absorbance at 650nm by spectrophotometry (BiophotometerPlus, Eppendorf, UK) using the Bio-Rad DC Protein Assay kit (Bio-Rad, UK) in accordance with the manufacturer's instructions.

2.2. PREPARATION AND EXPOSURE OF SPERM TO MSNPS

2.2.1. BOAR SPERM

A substantial amount of biological experimentation in this project was carried out with boar sperm, which represents a common animal model for human sperm in pilot experiments involving reproductive biology. This is due to similarities in morphology and physiology, and overall robustness. Boar sperm was sourced from a licensed pig breeding company (JSR Genetics, UK), and delivered in a commercial extender at ~17ºC. Sperm motility was activated by incubation for 15 minutes at 35°C, according to the supplier's instructions. Sperm concentration was assessed in a Bürker-Turk haemocytometer at 200x magnification using a negative contrast phase objective (Nikon UK Ltd.). Following activation, 1ml aliquots were withdrawn from each sample, centrifuged at 500g for 10 minutes, washed from the extender with PBS (Oxoid, UK), and resuspended in 'incubation medium' (PBS, Beltsville Thawing Solution or Swine Fertilization Medium, as appropriate). Washed sperm were then subject to treatment with MSNPs or control treatment. A detailed description of the types and doses of MSNPs, incubation conditions (medium and time) and respective controls is provided in the relevant subsections in **Chapters 3-5**. Incubation was carried out for up to 4 hrs at 37ºC under low-oxygen atmosphere, with this time point falling within the conventional timeframe for sperm handling prior to IVF. Samples were gently mixed by rotation every 20 minutes throughout incubation. Each experiment was replicated for a minimum of three times.

2.2.2. HUMAN SPERM

Human sperm samples were sourced from a licensed human sperm cryobank, based in Germany, in accordance with ethical permission from the Oxford Tropical Research Ethics Committee (OxTREC Ref # 31-09). Cryopreserved sperm from individual subjects were supplied in 300µl aliquots in separate colour-coded sealed straws along with supporting documentation detailing the date of freezing and baseline sperm parameters. Samples were shipped in liquid nitrogen and thawed at RT. For experiments, samples from each shipment were pooled together to enable easier

handling and therefore, minimise the loss of sperm prior to the experiment. A pooled sperm sample was briefly washed from cryopreservation media via two rounds of centrifugation at 500g for 5 min and resuspended in PureSperm Wash medium (Nidacon, Sweden). Sperm concentration was assessed in a Bürker-Turk haemocytometer at 200x magnification using a negative contrast phase objective (Nikon UK Ltd.). The sample was then divided into aliquots, which were subsequently subject to treatment with MSNPs or control treatment. A detailed description of the types and doses of MSNPs, incubation times and respective controls are provided in the relevant subsections of **Chapter 6**. Incubation was carried out for up to 4 hrs at 37ºC under low-oxygen atmosphere, with gentle mixing by inversion at regular intervals throughout incubation.

2.3. ASSESSMENT OF SPERM FUNCTIONAL STATUS

2.3.1. MOTILITY ASSESSMENT

Motility assessment was performed using a computer-assisted sperm analysis system (CASA; HTM-Ceros v.12.3, Hamilton Thorne, MA, USA). Analysed parameters included total motility (%), progressive motility (%), smoothed path velocity (VAP, µm/sec), straight line velocity (VSL, µm/sec), track velocity (VCL, µm/sec), straightness (STR: ratio of VSL/VAP, %), linearity (LIN: ratio of VSL/VCL, %), amplitude of lateral head displacement (ALH, µm), and beat cross frequency (BCF, Hz) (**Figure 2–4**).

For CASA, 6µl of each sample was loaded into a 20µm-deep Leja counting chamber, and equilibrated on a warm stage (37°C) for 2 minutes. Images were acquired at 100x magnification using a negative contrast phase objective (Nikon UK Ltd.) and pre-set ‘boar’ and ‘human’ capture and analysis algorithms. A minimum of 5 fields, containing at least 200 sperm, were evaluated in each sample.

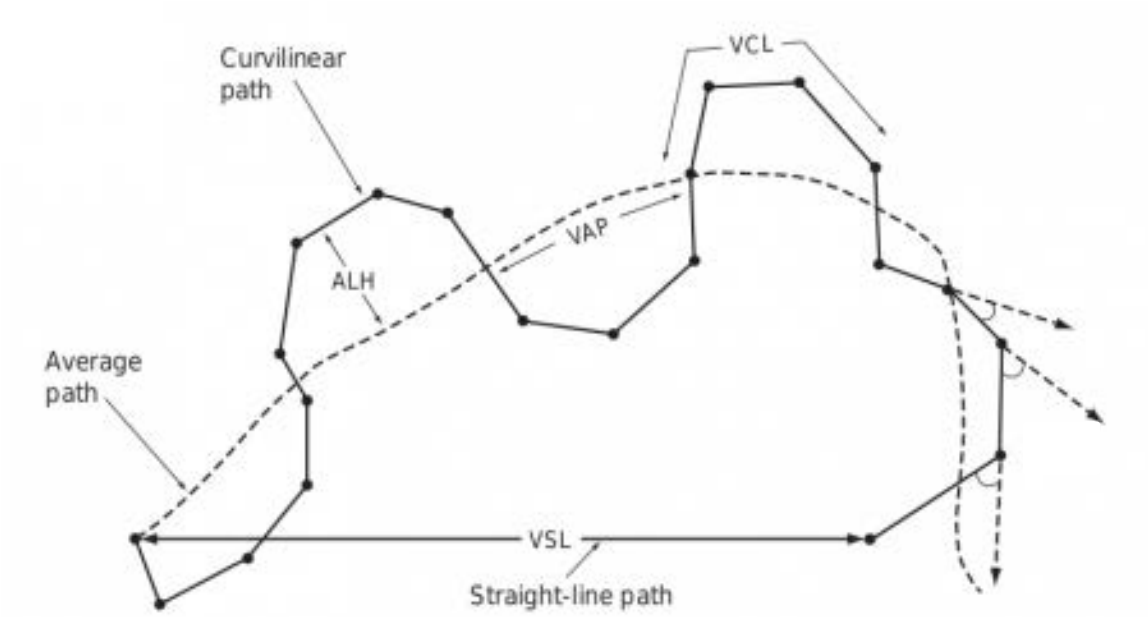

***Figure 2-4* – Computer-assisted analysis of sperm kinematic parameters.** CASA allows to perform quantitative assessment of sperm motion parameters (image sourced from www.mibio.org, accessed on 10/07/2015).

2.3.2. VIABILITY ASSESSMENT

For the viability evaluation of boar sperm in **Chapter 3**, a 5µl drop of each sample was mixed with 5µl of eosin Y (1% w/v in saline, VitalScreen, Microm, UK) on a microscope slide, covered with a coverslip, and equilibrated for 30 seconds. The number of stained (red or dark-pink; 'dead') and unstained (white or light-pink; 'live') sperm was counted at 400x magnification, in a minimum of 200 sperm.

For the viability evaluation of boar and human sperm in **Chapters 5 and 6**, dual fluorescent staining with SYBR 14 and propidium iodide was performed (LIVE/DEAD Sperm Viability Kit Life Technologies, UK). In brief, analysed sperm samples were diluted with incubation medium to a concentration of $1x10^6$ sperm/ml, and stained in 500µl aliquots with 0.5µl of SYBR 14 (Component A; final concentration: 100nM) in the dark at 36°C for 10 minutes. For counterstaining, 2.5µl of propidium iodide (Component B; final concentration: 12µM) was added. After 5 minutes, slides were examined at 400x magnification under a fluorescent microscope with a 465-495nm (SYBR 14) and 580-588nm (Propidium iodide) excitation wavelength filters (Nikon

UK Ltd.). The number of viable (green; 'live') and unviable (red; 'dead') sperm was counted at 400x magnification, in a minimum of 200 sperm.

2.3.3. EVALUATION OF ACROSOME MORPHOLOGY

Acrosome morphology was evaluated only in boar sperm by examining the integrity of the acrosomal apical ridge in unstained fixed sperm samples. To perform the evaluation, analysed sperm samples were fixed with 4.5% phosphate buffered formalin solution (Sigma-Aldrich, UK) for 10 minutes. A 'wet drop' for analysis was prepared by placing 10µl of the sample on a microscope slide and covering with a coverslip. Slides were examined at 1000x magnification using a positive contrast phase oil-immersion objective (Leica Microsystems UK Ltd).

A minimum of 200 sperm were assessed for acrosome morphology, and classified into 4 categories according to reference images (**Figure 2–5)**: normal apical ridge (NAR), damaged apical ridge (DAR), missing apical ridge (MAR), and loose acrosomal cap (LAC) (Pursel *et al.*, 1972).

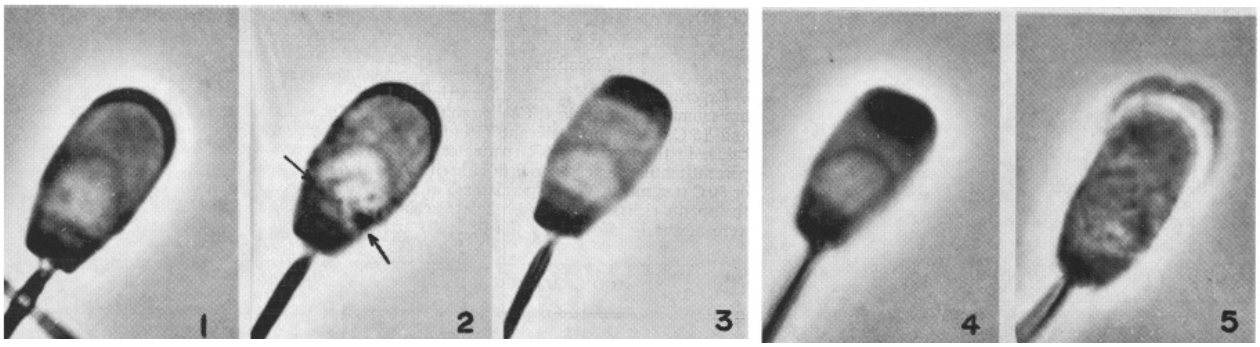

***Figure 2-5* – Acrosomal apical ridge in boar sperm: reference images (adapted from Pursel *et al.* (1972)).** Images produced at x4000 using the phase-contrast objective. 1) Normal Apical ridge (NAR). 2) Normal Apical ridge with particles (arrows). 3) Damaged apical ridge (DAR). 4) Missing apical ridge (MAR). 5) Loose acrosomal cap.

2.3.4. CALCULATION OF SPERM DNA FRAGMENTATION INDEX

Sperm DNA fragmentation index was assessed using the sperm chromatin dispersion technique, using a *Halomax* family of kits (Halotech DNA SL, Spain), according to the manufacturer's instructions.

For boar sperm, the *Sus-halomax* kit was utilised. In brief, analysed sperm samples were diluted in PBS to a concentration of 15-20x10^6 sperm/ml, and 25µl of each sample was mixed with 50µl of molten agarose, cooled to 37°C. A 2µl drop of the cell suspension from each sample was

transferred into an individual well on pre-treated slides, covered with a cover slip, and incubated at 4°C on a pre-cooled plate for 5 minutes. The cover slips were then removed, and slides immersed for 5 minutes into the lysis solution, followed by washing with double distilled water (DDW), and dehydration in a series of increasing ethanol concentrations (70-90-100% for 2 minutes each). After drying, processed slides were stained with 2µl of 4',6-diamidino-2-phenylindole (DAPI)-containing mounting medium (Vectashield H-1200, Vector Laboratories, UK) per well, and examined at 400x magnification under a fluorescent microscope with a 330-380nm (DAPI) excitation wavelength filter (Nikon UK Ltd.). A minimum of 300 sperm per sample were examined for the presence of a large halo of chromatin dispersion (fragmented DNA), and classified into either fragmented or non-fragmented DNA accordingly.

For human sperm, the *Halosperm* kit was used. In brief, analysed sperm samples were diluted in PBS to a concentration of 5-10x10^6 sperm/ml, and embedded in agarose microgels on individual pre-treated slides as described above. Samples were then immersed into acid denaturation solution for 7 minutes, and subsequently transferred into lysis solution for 25 minutes. Slides were washed with double distilled water, and dehydrated in a series of increasing ethanol concentrations (70-90-100% for 2 minutes each). After drying, processed slides were stained with 10µl of 4',6-diamidino-2-phenylindole (DAPI)-containing mounting medium (Vectashield H-1200, Vector Laboratories, UK), and examined at 400x magnification under a fluorescent microscope with a 330-380nm (DAPI) excitation wavelength filter (Nikon UK Ltd.). A minimum of 300 sperm per sample were examined for the absence of a large halo of chromatin dispersion (fragmented DNA), and classified into either fragmented or non-fragmented DNA accordingly. Both for boar and human samples, sperm DNA fragmentation index was calculated as a percentage of sperm with fragmented DNA from the total sperm population studied.

2.4. CALCULATION OF MSNP-SPERM BINDING RATE

To quantify the number of boar and human sperm binding with MSNPs, samples were fixed with 10% formalin solution (Sigma-Aldrich, UK) for 10 minutes at appropriate time points during incubation, and then washed from the fixative in PBS via centrifugation. A specific description of time points at which binding rates were analysed, is given in the relevant experimental chapters. Washed sperm were transferred to poly-L-lysine pre-coated slides, incubated in a humidifying chamber for 30 minutes at room temperature, washed twice in PBS, and mounted with 10µl of DAPI-containing medium. Slides were examined at 400x magnification under a fluorescent microscope with 330-380nm (blue), 465-495nm (green) and 540-588nm (red) excitation wavelength filters (Nikon UK Ltd.). The number of sperm bound with MSNPs was counted in a minimum of 200 cells. Higher resolution imaging was performed at 600x magnification with an oil-immersion objective under a confocal laser microscope with a 405nm (blue), 488nm (green) and 559nm (red) excitation lines (Olympus UK Ltd.; The Dunn School Bioimaging Facility, University of Oxford). Acquired images were processed and analysed with Fiji/ImageJ 1.48t (Schindelin *et al.*, 2012).

2.5. TRANSMISSION ELECTRON MICROSCOPY (TEM) OF BOAR SPERM EXPOSED TO MSNPS

To investigate the localisation of MSNPs in boar sperm after incubation, samples were subject to thin-section TEM. After 4 hours of incubation, sperm samples exposed to unmodified and PEI-coated MSNPs were washed from the unbound particles in PBS via centrifugation, and fixed in 4% gluteraldehyde (Sigma-Aldrich, UK). TEM was carried in the Nuffield Division of Clinical Laboratory Sciences (Professor David JP Ferguson, Ultrastructural Morphology Group, John Radliffe Hospital, University of Oxford).

2.6. MSNP-MEDIATED TRANSFER OF DNA INTO SPERM

2.6.1. BOAR SPERM

2.6.1.1. Preparation and exposure of sperm to MSNPs and free/adsorbed DNA

For MSNP-mediated transfer of pHL-FcHis-mCherry into boar sperm, a modification of the protocol described by Lavitrano *et al.* (2013) was used. Specifically, sperm motility was activated by incubation for 15 minutes at 35°C, according to the supplier's instructions. Sperm concentration was assessed in a Bürker-Turk haemocytometer at 200x magnification using a negative contrast phase objective. Following activation, aliquots containing $5x10^7$ sperm each were withdrawn from the sample, centrifuged at 500g for 10 minutes, washed from the extender with PBS, and resuspended to 500µl in pre-warmed (37°C) sperm fertilisation medium (SFM: 62.5mM glucose, 34mM sodium citrate dihydrate, 12.5mM ethylenediaminetetraacetic acid (EDTA) dihydrate, 15.5mM citric acid hydrate, 53.3mM Tris; pH 6.8; all reagents sourced from Sigma-Aldrich, UK), supplemented with 0.3% bovine serum albumin (BSA; Sigma-Aldrich, UK). Washed sperm were then subject to the following treatments: (1) SFM (control); (2) free pHL-FcHis-mCherry; (3) PEI-coated MSNPs, loaded with pHL-FcHis-mCherry; (4) unmodified MSNPs and pHL-FcHis-mCherry; (5) C105Y-functionalised MSNPs and pHL-FcHis-mCherry. All stock suspensions of nanoparticles (concentration: 2mg/ml) were prepared with nuclease-free water. The doses used for each type of experimental treatment are presented in **Table 2–1**. Incubation was carried out for 2 hrs at 37ºC under a low-oxygen atmosphere, with gentle mixing by inversion at regular intervals throughout incubation.

***Table 2-1* – Doses for each type of experimental treatment in MSNP-mediated DNA transfer experiments (boar sperm)**

Type of treatment	Dose per 10^7 sperm
Free pHL-FcHis-mCherry	Equivalent to the dose absorbed on 10µg PEI-coated MSNPs
PEI-coated MSNPs, loaded with pHL-FcHis-mCherry	10µg
Unmodified MSNPs and pHL-FcHis-mCherry	MSNPs: 10µg per 10^7 sperm; pHL-FcHis-mCherry: equivalent to the dose absorbed on 10µg PEI-coated MSNPs
C105Y-functionalised MSNPs and pHL-FcHis-mCherry	MSNPs: 10µg per 10^7 sperm; pHL-FcHis-mCherry: equivalent to the dose absorbed on 10µg PEI-coated MSNPs

After incubation, 10µl aliquots were removed from each sample, diluted with 50µl of warm SFM+BSA (0.3%), and analysed for motility and viability using CASA and dual fluorescent staining with SYBR 14 and propidium iodide, as described in **Section 2.3.1.**

2.6.1.2. Removal of non-internalised plasmid DNA from sperm samples

The remaining aliquots were diluted with SFM to 1.5ml and washed twice in SFM by centrifugation at 500g for 5 minutes. To eliminate the free plasmid, which had not been incorporated by the sperm, samples were treated with DNase I. To achieve this, samples were resuspended in 500µl of DNase buffer (10mM Tris, 2.5mM $MgCl_2$, 0.5mM $CaCl_2$; pH 7.5; Life Technologies, UK) and incubated with 20 units DNase I (Life Technologies, UK) for 30 minutes at 37ºC. DNase was then inactivated by heating at 75°C for 5 minutes, and sperm were washed in 1.0ml pre-lysis buffer (150mM sodium chloride, 10mM EDTA, pH 8.0; all reagents sourced from Sigma-Aldrich, UK) by centrifugation at 700g for 10 minutes.

2.6.1.3. DNA extraction

To extract sperm DNA, each sperm aliquot was resuspended in 750µl lysis buffer (4.24M guanidine thiocyanate, 10mM sodium chloride, 1% sodium laurylsarcosinate, 150mM dithiothreitol, 200µg/ml proteinase K (Life Technologies, UK); chemical reagents sourced from Sigma-Aldrich, UK). Lysis was carried out for 2 hours at 56°C. After 1 hour of incubation, the reaction was gently mixed by inversion.

After the completion of lysis, DNA was precipitated with isopropanol. To perform the precipitation, 750µl of pure isopropanol (Sigma-Aldrich, UK) was added to each tube, and the contents were mixed by inversion until DNA strands formed, followed by centrifugation at 5000g for 3 minutes to sediment the DNA. The pellet was washed twice in 70% ethanol (Sigma-Aldrich, UK), air-dried, resuspended in nuclease-free water and stored at 5°C. DNA concentration in the supernatant was determined via the measurement of absorbance at 260nm by spectrophotometry.

2.6.1.4. Qualitative assessment of pHL-FcHis-mCherry delivery into boar sperm

Qualitative assessment of pHL-FcHis-mCherry delivery into boar sperm was performed using polymerase chain reaction (PCR) with primers designed to detect mCherry (sequenced by Miss Siobhan Coote, an ex-member of the Coward laboratory) and swine leptin gene fragments (GenBank Accession number: U66254.1) in DNA extracted from sperm after exposure to various treatments. Specific primer pairs were designed using Primer-BLAST algorithm (Ye *et al.*, 2012) in accordance with the following specifications: length – 18-30 base pairs (bp) length, melting temperature (Tm) – 65-75°C, GC content – 40-60%. Primer characteristics for the amplification of mCherry and swine leptin target fragments are presented in **Table 2–2**.

Table 2-2 **- Primer pairs for amplification of target mCherry and swine leptin gene fragments using PCR**

	Sequence length (bp)	**Primer**	**Sequence (5'->3')**	**Primer length (bp)**	**Start**	**Stop**	**Product length (bp)**
mCherry	708	Forward	ACCGCCAAGCTGAAGGTGACCA	22	142	163	**437**
		Reverse	TGCACGGGCTTCTTGGCCTTGT	22	578	557	
Swine leptin	5920	Forward	GACTGTCCCCTGAGCCAGCTAGTGT	25	5761	5785	**151**
		Reverse	ACAAAACAGCCTCCTCCCTCCAGGC	25	5911	5887	

Primers were synthesised by Invitrogen, UK.

Singleplex PCR for the amplification of target mCherry and swine leptin fragments from each individual sample were set up in PCR tubes in a final volume of 25µl by mixing 12.5µl High Fidelity PCR Master (Roche Diagnostics, Switzerland) with 1.5µl forward and reverse primers (stock concentration: 5µM; final concentration: 300nM), 50-100ng template DNA, and then nuclease-free water to the final volume. Amplification was carried out in a G-Storm GS1 thermal cycler (G-Storm, UK) using the protocol described in **Table 2–3.**

Table 2-3 **– PCR protocol for the amplification of target mCherry and swine leptin gene fragments**

	Cycles	**Time**	**Temperature**
Initial denaturation	1	2 min	94°C
Denaturation	10	10 s	94°C
Annealing		70 s	65°C
Elongation		1 min	72°C
Denaturation	15-20	15 s	94°C
Annealing		30 s	65°C
Elongation		1 min	72°C
Final elongation	1	7 min	72°C

PCR products were analysed for size by electrophoresis on a 1.3% TAE agarose gel pre-stained with ethidium bromide (final concentration: 0.5µg/ml). The gel was run in TAE at 100V for 1 hour, and imaged by a gel documentation system.

2.6.1.5. Quantitative assessment of pHL-FcHis-mCherry delivery into boar sperm

Quantitative assessment of pHL-FcHis-mCherry delivery into boar sperm was performed via the quantification of band density, corresponding to the mCherry target fragment, *versus* the density of swine leptin bands (internal control), on digital images acquired from agarose gels. Relative density was expressed as arbitrary units (AU) and subsequently adjusted for relative density of mCherry *versus* swine leptin in samples treated with free plasmid only. Quantification was performed using the Gel Analysis tool in Fiji/ImageJ 1.48t (Schindelin *et al.*, 2012).

2.6.1.6. Quality control for detecting DNA transfer into boar sperm

Primer specificity was confirmed via the PCR amplification of target sequences using stock pHL-FcHis-mCherry and control pig genomic DNA (Novagen, Merck Millipore, UK) as templates. PCR products were analysed for length by electrophoresis on a 1.3% TAE agarose gel pre-stained with ethidium bromide. In addition, PCR products were purified using a QIAquick PCR purification kit (QIAgen, UK) in accordance with the manufacturer's instructions, eluted with nuclease-free water and subject to Sanger sequencing (sequencing performed by Source BioScience, UK). Sequences obtained were visualised in 4Peaks v.1.8 (Nucleobytes BV, The Netherlands; available from www.nucleobytes.com; accessed on 03/08/2015) and aligned with source sequences using Pairwise Sequence Alignment algorithm (http://www.ebi.ac.uk/Tools/psa, accessed on 04/08/2015) to check identity.

To confirm the efficacy of digesting free pHL-FcHis-mCherry with DNase I under the conditions used during this protocol, a dose of pHL-FcHis-mCherry, equivalent to the dose added to sperm samples during the steps described in **Section 2.6.1.1.** was subjected to treatment with 20 Units of DNase I under conditions identical to those applied to remove free plasmid from sperm

samples (**Section 2.6.1.2.** Amplification of the digestion product was carried out using the PCR protocol described in **Section 2.6.1.4.** A 1:10 dilution of the stock pHL-FcHis-mCherry solution, which was subject to DNase I treatment, was used as a positive control. PCR products were analysed for length by electrophoresis on a 1.3% TAE agarose gel pre-stained with ethidium bromide, as described above.

2.6.2. HUMAN SPERM

2.6.2.1. Preparation and exposure of sperm to MSNPs and free/adsorbed DNA

For the MSNP-mediated transfer of pDRIVE-HSP70-GFP into human sperm, a similar modification of the protocol described by Lavitrano *et al.* (2013), which was applied in **Section 2.6.1.**, was used. Specifically, sperm samples were thawed at room temperature and pooled together to increase the number of sperm for subsequent experiments. Sperm concentration was assessed in a Bürker-Turk haemocytometer at 200x magnification using a negative contrast phase objective. The pooled sample was separated into 250µl aliquots containing $1x10^7$ sperm each. Sperm were then subject to the following treatments: (1) PBS; (2) free pDRIVE-HSP70-GFP; (3) PEI-coated MSNPs, loaded with pDRIVE-HSP70-GFP; (4) unmodified MSNPs and pDRIVE-HSP70-GFP; (5) C105Y-functionalised MSNPs and pDRIVE-HSP70-GFP. Experiment was performed in a duplicate. All stock suspensions of nanoparticles (concentration: 2mg/ml) were prepared with nuclease-free water. The doses used for each type of experimental treatment are presented in **Table 2–4.**

***Table 2-4* – Doses for each type of experimental treatment in MSNP-mediated DNA transfer experiments (human sperm)**

Type of treatment	Dose per 10^7 sperm
Free pDRIVE-HSP70-GFP	Equivalent to the dose absorbed on 30µg PEI-coated MSNPs
PEI-coated MSNPs, loaded with pDRIVE-HSP70-GFP	30µg
Unmodified MSNPs and pDRIVE-HSP70-GFP	MSNPs: 30µg per 10^7 sperm; pHL-FcHis-mCherry: equivalent to the dose absorbed on 30µg PEI-coated MSNPs
C105Y-functionalised MSNPs and pDRIVE-HSP70-GFP	MSNPs: 30µg per 10^7 sperm; pHL-FcHis-mCherry: equivalent to the dose absorbed on 30µg PEI-coated MSNPs

Incubation was carried out for 3 hrs at 37ºC under a low-oxygen atmosphere, with gentle mixing by inversion at regular intervals throughout incubation.

2.6.2.2. Removal of non-internalised plasmid DNA from sperm samples and DNA extraction

The remaining aliquots were diluted with PBS to 750µl and washed twice in PBS by centrifugation at 500g for 5 minutes. To eliminate the free plasmid, which had not been incorporated by the sperm, samples were treated with 20 units DNase I in 500µl of DNase buffer for 30 minutes at 37ºC. DNase was then inactivated by heating at 75°C for 5 minutes, and sperm were washed in pre-lysis buffer (see **Section 2.6.1.2.** by centrifugation at 700g for 10 minutes. Sperm DNA extraction was carried out in accordance with the protocol described in **Section 2.6.1.3.**

2.6.2.3. Assessment of pDRIVE-HSP70-GFP delivery into human sperm

Qualitative and quantitative assessment of pDRIVE-HSP70-GFP delivery into boar sperm was performed using real-time polymerase chain reaction (qPCR) with primers designed to detect GFP (sequencing performed by Miss Lien Davidson, a present member of the Coward laboratory) and human glyceraldehyde-3-phosphate dehydrogenase (GAPDH) fragments (GenBank Accession number: NM_002046.5) in DNA extracted from sperm after exposure to various treatments. Primers for the amplification of the target GFP fragment were designed using Primer-BLAST algorithm (Ye *et al.*, 2012) in accordance with the following specifications: length – 18-30 base pairs (bp) length, melting temperature (Tm) – 62-68°C, GC content – 40-60%. Primers for amplification of the target human GAPDH fragment were designed earlier by Miss Siti Nornadirah Amdani, a present member of the Coward laboratory. Characteristics of primers used for amplification of GFP and human GAPDH target fragments are presented in **Table 2–5**.

Singleplex qPCR for amplification of target GFP and human GAPDH gene fragments from each individual sperm sample were set up in 96-well plates (MicroAmp Fast Optical, Life Technologies, UK) in a final volume of 10µl by mixing 5µl Power SYBR Green Master Mix (Life Technologies, UK) with 0.5µl forward and reverse primers (stock concentration: 5µM; final

concentration: 100nM), 50-100ng template DNA, and then nuclease-free water to the final volume. Amplification was carried out in the StepOnePlus Real-Time PCR system (Life Technologies, UK) using the protocol described in **Table 2–6.** DNA from each sperm sample was amplified in a triplicate.

***Table 2-5* – Primer pairs for amplification of target GFP and human GAPDH fragments using qPCR**

	Sequence length (bp)	Primer	Sequence (5'->3')	Primer length (bp)	Start	Stop	Product length (bp)
GFP	695	Forward	CAGTGGAGAGGGTGAAGGTGATGCT	25	81	105	**188**
		Reverse	AACCTTCGGGCATGGCACTCTT	22	268	247	
Human GAPDH	1421	Forward	CACATCGCTCAGACACCATG	20	172	191	**198**
		Reverse	TGACGGTGCCATGGAATTTG	20	369	350	

Primers were synthesised by Invitrogen, UK.

***Table 2-6* – qPCR protocol for amplification of target GFP and human GAPDH gene fragments**

	Cycles	Time	Temperature
Initial denaturation	1	2 min	95°C
Denaturation	45	15 s	94°C
Annealing and elongation (with fluorescence data acquisition)		1 min 30 s	60°C
Final elongation	1	7 min	72°C

To quantify the amount of pDRIVE-HSP70-GFP delivered into human sperm after various treatments, the comparative cycle threshold (Ct) method was applied. Specifically, the relative amount of pDRIVE-HSP70-GFP in relation to the GAPDH sequence was determined using the equation $2^{-\Delta\Delta Ct}$. The ΔΔCt was calculated using the following equation:

$$\Delta\Delta Ct = (\text{mean Ct } (GFP_{treatment}) - \text{mean Ct } (GAPDH_{treatment})) - (\text{mean Ct } (GFP_{control}) - \text{mean Ct } (GAPDH_{control}))$$

Means were calculated within a triplicate of qPCR reactions for each experimental condition (sample and treatment). Exposure to free pDRIVE-HSP70-GFP was used as a control condition.

2.6.2.4. Quality control for detecting DNA transfer into human sperm

Products from qPCR were purified using a QIAquick PCR purification kit (QIAgen, UK) in accordance with the manufacturer's instructions, eluted with nuclease-free water and subject to Sanger sequencing (sequencing performed by Source BioScience, UK). Sequences obtained were visualised in 4Peaks v.1.8 (Nucleobytes BV, The Netherlands; available from www.nucleobytes.com; accessed on 03/08/2015) and aligned with source sequences using Pairwise Sequence Alignment algorithm (http://www.ebi.ac.uk/Tools/psa, accessed on 04/08/2015) to confirm identity.

To confirm the efficacy of digestion of free pDRIVE-HSP70-GFP with DNase I under the conditions used during this protocol, a dose of pDRIVE-HSP70-GFP, equivalent to the dose added to sperm samples during the steps described in **Section 2.6.1.1.** was subjected to treatment with 20 units of DNase I under conditions identical to those applied for removal of free plasmid (**Section 0**Amplification of the digestion product was carried out using the protocol described in **Section 2.6.1.4.** A 1:10 dilution of the stock pDRIVE-HSP70-GFP solution, which was subject to DNase I treatment, was used as a positive control. PCR products were analysed for length by electrophoresis on a 1.3% TAE agarose gel pre-stained with ethidium bromide.

2.7. MSNP-MEDIATED TRANSFER OF PROTEIN INTO SPERM

2.7.1.1. Preparation and exposure of sperm to MSNPs and free/adsorbed protein

For the MSNP-mediated transfer of in-house expressed/purified mCherry into boar sperm, a protocol similar to the one applied for DNA transfer, and described in **Section 2.6.** was used. Specifically, sperm motility was activated by incubation for 15 minutes at 35°C, according to the supplier's instructions. Sperm concentration was assessed in a Bürker-Turk haemocytometer at 200x magnification using a negative contrast phase objective. Following activation, aliquots containing $4x10^7$ sperm each were withdrawn from the sample, centrifuged at 500g for 10 minutes, washed from the extender with PBS, and resuspended to 500µl in pre-warmed (37°C) SFM, supplemented with 0.3% BSA. Washed sperm were then subject to the following treatments: (1) SFM (control); (2) free mCherry; (3) APTES-coated MSNPs, loaded with mCherry; (4) unmodified

MSNPs and mCherry; (5) C105Y-functionalised MSNPs and mCherry. All stock suspensions of nanoparticles (concentration: 2mg/ml) were prepared with PBS. The doses used for each type of experimental treatment are presented in **Table 2–7.** Incubation was carried out for 2 hrs at 37ºC under a low-oxygen atmosphere, with gentle mixing by inversion at regular intervals throughout incubation.

***Table 2-7*– Doses for each type of experimental treatment in MSNP-mediated protein transfer experiments (boar sperm)**

Type of treatment	Dose per 10^7 sperm
Free mCherry	Equivalent to the dose absorbed on 10μg APTES-coated MSNPs
APETS-coated MSNPs, loaded with mCherry	10μg
Unmodified MSNPs and mCherry	MSNPs: 10μg per 10^7 sperm; mCherry: equivalent to the dose absorbed on 10μg APTES-coated MSNPs
C105Y-functionalised MSNPs and mCherry	MSNPs: 10μg per 10^7 sperm; mCherry: equivalent to the dose absorbed on 10μg APTES-coated MSNPs

After incubation, samples were diluted with PBS to 1.5ml and washed three times in PBS by centrifugation at 500g for 5 minutes. After the last wash, pellets were fixed with 500μl 10% formalin solution for 15 minutes. Given that the effects of mCherry-loaded MSNPs upon sperm function had already carried out in the preceding sets of experiments (**Section 3.5**), no separate nanotoxicity assessment was performed in this case.

2.7.1.2. Sperm lysis

In order to lyse sperm, each sperm aliquot was washed from the fixative and resuspended in 1ml lysis buffer (7M urea, 2M thiourea, 1.5M Tris, 4% 3-[(3-Cholamidopropyl)dimethylammonio]-1-propanesulfonate (CHAPS) with protease inhibitors cocktail (cOmplete protease inhibitor cocktail tablets, Roche, UK), 2.4μM PMSF, 18mM DTT; reagents sourced from Sigma-Aldrich, UK). Lysis was carried out for 1 hour at RT under constant agitation. Lysates were then centrifuged to remove cell debris at 3,000g for 5 minutes at 4°C. Total protein concentration in the lysates was determined by spectrophotometry using the Bio-Rad DC protein assay kit, in accordance with the manufacturer's instructions. Long-term storage of samples was carried out at -20°C.

2.7.1.3. Qualitative assessment of mCherry delivery into boar sperm

Qualitative assessment of mCherry delivery into boar sperm was performed via the detection of mCherry in protein lysates using Western blotting (WB). For WB, protein separation was carried out by denaturing electrophoresis of reduced protein samples on 4-12% NuPAGE Novex Bis-Tris minigel (Life Technologies, UK). To achieve the denaturing reduced conditions, each analysed aliquot was mixed with NuPAGE SDS sample buffer (Life Technologies, UK) and NuPAGE reducing agent (Life Technologies, UK) in a 5:4:1 volume ratio, and heated to 101°C for 5 minutes prior to loading onto the gel. Gels were run in NuPAGE MES SDS running buffer (Life Technologies, UK) at 160V for approximately 1 hour, removed from the cassette and equilibrated in transfer buffer (TB: 25mM Tris, 192mM glycine, 10% methanol; all reagents from Sigma-Aldrich, UK) for 15 minutes before protein transfer to polyvinylidene fluoride (PVDF) membrane (Amersham Hybond P 0.45, GE Healthcare Life Sciences, UK) in a semi-dry transfer cell (Trans-Blot SD, Bio-Rad, UK). Protein transfer to PVDF membrane was performed at 15V for 30-40 minutes, after which the membrane was briefly washed in DDW, and blocked in PBS-Tween 0.05% (Sigma-Aldrich, UK) + 5% skimmed milk (Marvel, UK) for 30 minutes. After the removal of blocking buffer, the membrane was incubated overnight in PBS-Tween 0.05% + 1% skimmed milk + primary antibody (mCherry Polyclonal Antibody, PA5-34974, rabbit IgG; Pierce/Thermo Scientific, UK) in a 1:2,500 dilution at 5°C. On the next day, the membrane was washed 3 times in PBS-Tween 0.05% for 5 minutes and incubated in PBS-Tween 0.05% + 1% skimmed milk + secondary antibody (Stabilised Goat Anti-Rabbit IgG (H+L), peroxidase conjugated, Pierce/Thermo Scientific, UK) in a 1:1,000 dilution for 1 hour. The membrane was then washed in PBS-Tween 0.05% thrice, and protein detection performed using the chemiluminescence technique (Amersham ECL Prime, GE Healthcare Life Sciences, UK) in accordance with the manufacturer's instructions. Imaging was carried out via the development of X-ray films (Amersham Hyperfilm ECL, GE Healthcare Life Sciences, UK) exposed to the chemiluminescent reagent-treated membranes, in an

automated X-ray film developer. Digital images of the films were obtained via scanning with a Canon LiDE 200 flatbed scanner (Canon, UK).

To allow the subsequent quantitative evaluation of mCherry delivery into boar sperm, the additional detection of an internal (loading) control, β-tubulin, was carried out. To detect β-tubulin, the membrane was stripped by two washes in acidic stripping buffer (5M glycine, 3.5mM SDS, 1% Tween 20, pH=2.2; all reagents from Sigma-Aldrich, UK) for 10 minutes, two washes in PBS for 10 minutes and two washes in PBS-Tween 0.05% for 5 minutes, all at RT. The membrane was then blocked in PBS-Tween 0.05% + 5% skimmed milk, as described above, and probed for β-tubulin via incubation in PBS-Tween 0.05% + 1% skimmed milk + anti-β-tubulin antibody (anti-β-tubulin antibody – loading control (HRP), rabbit IgG, ab21058; Abcam, UK) in a 1:2,500 dilution for 1 hour. Washing and protein detection was performed as described above.

2.7.1.4. Quantitative assessment of mCherry delivery into boar sperm

Quantitative assessment of mCherry delivery into boar sperm was performed via the quantification of relative band density, corresponding to mCherry, in samples exposed to a combination of any modification of MSNPs and absorbed/free mCherry (APTES-coated MSNPs loaded with mCherry, unmodified MSNPs and mCherry and C105Y-functionalised MSNPs and mCherry) *versus* bands corresponding to mCherry in samples exposed to free protein. The calculated relative density of mCherry bands was adjusted for the relative density of loading control (β-tubulin; relative density of β-tubulin was calculated for MSNP-treated samples *versus* mCherry-only treated samples). Adjusted relative intensity was expressed as arbitrary units (AU). Quantification was performed using the Gel Analysis tool in Fiji/ImageJ 1.48t (Schindelin *et al.*, 2012).

2.8. APPLICATION OF MSNPS TO OOCYTES

Oocytes from superovulated C57BL/6 mice were obtained from the Biomedical Servicesb Unit (University of Oxford) in culture media droplets overlaid with mineral oil (FertiCult, Microm UK). Procedures were carried out with the appropriate Home Office Animals (Scientific Procedures) Act 1986 certification in place.

2.8.1. EXPOSURE OF OOCYTES TO MSNPS

To investigate the possibility of binding with MSNPs, mouse oocytes were incubated in 4-well plates for 2 hours at 37°C under low-oxygen atmosphere in 500µl of M16 media (Sigma Aldrich, UK; control group) or 500µl of M16 media containing either fluorescent unmodified or fluorescent PEI-coated MSNPs, each at a final concentration of 0.3mg/ml (three experimental groups). After 2 hours, oocytes were washed from unbound MSNPs in PBS and fixed with 10% formalin solution for 10 minutes. After washing in PBS post-fixation, oocytes were transferred to 100µl PBS drops on poly-L-lysine pre-coated slides, and incubated in a humidifying chamber with Alexa Fluor 555 wheat germ agglutinin (1 µg/ml; Alexa Fluor 555 WGA, Invitrogen, UK) for 10 minutes at room temperature to stain the plasma membrane. Slides were then carefully washed with PBS, mounted with 4',6-diamidino-2-phenylindole (DAPI)-containing mounting medium (Vectashield H-1200, Vector Laboratories, Peterborough, UK) and examined at 400x magnification under a fluorescent microscope with 330-380nm (blue), 465-495nm (green) and 540-580nm (red) excitation wavelength filters (Nikon UK Ltd.).

2.8.2. OOCYTE MICROINJECTIONS WITH MSNPS

To investigate feasibility of the assisted delivery of MSNPs through the *zona pellucida*, mouse oocytes were microinjected with suspensions of fluorescent unmodified or fluorescent PEI-coated MSNPs in M16 media at a concentration of 0.3mg/ml (two experimental groups). In the control groups, oocytes were either microinjected with equal amounts of M16 media ('sham injection' control) or incubated in M16 ('no intervention' control). Microinjections were performed with a Nikon Narishige micromanipulator mounted on a Nikon Eclipse Ti microscope using a 30º-angled

microinjection pipette with an internal diameter of 5μm (Cook Medical, PA, USA). After the procedure, oocytes were cultured overnight in fresh M16 media at 37°C under low-oxygen conditions. On the next day, all oocytes were assessed for morphology and signs of degradation (irregularity and vacuolisation of the ooplasm) under a stereomicroscope, and then fixed, washed, transferred to poly-L-lysine pre-coated slides, stained with Alexa Fluor 555 WGA, mounted with DAPI-containing medium and imaged as described in **Section 2.6.1**.

2.9. STATISTICAL ANALYSIS

Data are presented as mean±standard error of the mean (SEM), unless specified otherwise. All continuous variables were checked for normality using the Kolmogorov-Smirnoff test and subjected to log-linear or arcsine-square root transformation where appropriate. Continuous variables were analysed using a general linear model (GLM) with post-hoc Bonferroni and Dunnet adjustments and type of treatment, MSNP dose, and incubation time as fixed factors, and ejaculate as a random factor, unless specified otherwise. Categorical values were compared using the chi-square test. Differences were considered significant at $p \leq 0.050$. Statistical analysis was performed using IBM SPSS Statistics v20.0 (IBM, Armonk, NY, USA). Representative figures were constructed in GraphPad Prism v6.0 (GraphPad Software, La Jolla, CA, USA).

CHAPTER 3

EFFECTS OF MESOPOROUS SILICA NANOPARTICLES UPON THE FUNCTION OF MAMMALIAN GAMETES *IN VITRO*

Key messages:

- This chapter presents the first encouraging findings of this thesis, showing that spherical MSNPs with hexagonal pore symmetry and various surface functionalities and/or payloads were biocompatible with boar sperm and mouse oocytes
- MSNPs formed strong associations with approximately one in five boar sperm during incubation *in vitro* and did not exert negative effect upon the main parameters of sperm function
- Exposure of mouse oocytes to MSNPs *in vitro* resulted in surface absorption of nanoparticles to the *zona pellucida* without penetration; assisted delivery into the ooplasm via the use of micromanipulation techniques was possible, but posed technical challenges, and did not result in acute toxicity
- Results presented in this Chapter formed the rationale for subsequent experiments evaluating MSNPs as a platform for the transfer of molecular compounds into mammalian gametes, which are presented in the subsequent chapters of this thesis

3.1. BACKGROUND

Recent progress in biomedical nanotechnology has transformed the concept of targeted biological delivery, allowing the engineering of complex biocompatible nanoscale-sized (1-100nm) platforms with high loading capacity, stability, highly selective affinity, and potential for simultaneous diagnostic and therapeutic ('theranostic') applications (Kunzmann et al., 2011; Lammers et al., 2011). In the last decade, biomedical nanotechnology has noticeably contributed to the diagnostics and treatment of a variety of medical conditions, including cancer, microbial and viral infections, and chronic internal diseases (Uskokovic, 2013; Tsai *et al.*, 2014). Ultimately, this success has triggered an expansion of nanobiotechnological 'vision' to other scientific disciplines, including reproductive biology.

A growing interest in nanomaterial-mediated delivery in reproductive biology is driven by two key factors. Firstly, the evidence that nanomaterials improve the selectivity and efficacy of cargo delivery across a variety of cell types (Tsai *et al.*, 2014). Secondly, there is increasing understanding that the crucial processes of intra-gamete molecular transport underlying gamete development, maturation and acquisition of fertilization potential are mediated by natural cell-secreted nanoparticles, for example, prostasomes and epididymosomes in males (Sullivan and Saez, 2013) and granulosa cell microvesicles in females (da Silveira *et al.*, 2012). These observations form another justification for studies into the feasibility of manipulating these key processes using similar engineered nanoplatforms. Consequently, nanotechnology has great potential to improve the efficacy of reproductive biology techniques associated with the internalisation of molecular compounds into gametes. These techniques include, but are not limited to, gene transfer into reproductive tissues (Ikawa *et al.*, 2002; Ghadami *et al.*, 2010), sperm-mediated gene transfer (SMGT) (Brackett, 1971), and the sorting of sperm into sub-populations driven by the detection of a specific intracellular marker, for example sex sorting (Rath *et al.*, 2013) Although these experimental techniques have been extensively studied over the last few decades, their efficacy remains sub-optimal (Ikawa *et al.*, 2002; Kojima *et al.*, 2008; Eghbalsaied *et al.*, 2013; Rath *et al.*,

2013), and their relative application is thus compromised. There is currently little consensus on which nanomaterial to consider the ideal candidate for reproductive biology, but the general trend is to evaluate the performance of non-biodegradable nanoparticles with a reasonable detection capacity: polyvinylalcohol-functionalised iron oxide (Ben-David Makhluf *et al.*, 2006; Makhluf *et al.*, 2008), magnetic (Kim *et al.*, 2010b) and polystyrene (Fynewever *et al.*, 2007) nanoparticles (NPs), cerium dioxide (Falchi *et al.*, 2014), perfluorocarbon (Jallouk *et al.*, 2014), halloysite clay nanotubes (Campos *et al.*, 2011a), specialised CdSe/ZnS quantum dots (Feugang *et al.*, 2012; Feugang *et al.*, 2015), and nanogold (Taylor *et al.*, 2014b; Tiedemann *et al.*, 2014). Such robust inorganic nanomaterials could be utilised as stable cell tags and permit the visualisation, tracking and sorting of labelled gametes, in addition to their delivery capacity.

This Chapter presents the results of the first series of experiments performed during this thesis. These experiments evaluated the effects of mesoporous silica nanoparticles (MSNPs) upon the function of mammalian gametes during *in vitro* exposure under conditions similar to those used in the ART setting. For the first time, they sought to provide insight into the biocompatibility of MSNPs with mammalian gametes and, therefore, answer the question whether this well-characterised tool for targeted molecular delivery, bioimaging, and tissue engineering (Xia *et al.*, 2009; Hom *et al.*, 2010; Na *et al.*, 2012) can be used for reproductive biology. Findings presented in this Chapter encouragingly demonstrated that spherical MSNPs with hexagonal pore symmetry and various surface functionalities and/or payloads formed strong associations with boar sperm following incubation *in vitro* and did not exert negative effect upon the main parameters of sperm function. *In vitro* exposure of mouse oocytes to MSNPs resulted in surface absorption of nanoparticles to the *zona pellucida*. However, assisted delivery into the ooplasm via the use of micromanipulation techniques was also possible and did not result in acute toxicity. Collectively, these positive results supported further experiments evaluating MSNPs as a platform for the transfer of molecular compounds into mammalian gametes, which are presented in subsequent chapters.

3.2. SPECIFIC DETAILS OF EXPERIMENTAL PROCEDURES

The general materials and methods used to generate the results presented in this Chapter are described in **Chapter 2**. Specific details of the experimental procedures highlighted in this sub-section relate to the exposure of MSNPs to boar sperm.

In particular, for this set of experiments, 1ml aliquots were withdrawn from each boar sperm sample, centrifuged at 500g for 10 minutes, washed from the extender with PBS (Oxoid, UK), resuspended in PBS to 750µl and treated with either MSNPs or PBS (controls). Each experiment was repeated a minimum of three times, using samples obtained from different animals. To evaluate the potential nanotoxicity of MSNPs in sperm, and determine optimal doses and incubation times, washed sperm were exposed to suspensions of three types of unloaded fluorescent MSNPs in PBS (unmodified, PEI-coated, and APTES-coated) in the ratios of 10µg, 15µg and 30µg of particles per 10^7 sperm. In the control group, washed sperm were incubated with PBS. Incubation was carried out for up to 4 hrs at 37ºC under a low-oxygen atmosphere. Sperm motility and viability were assessed after 2 and 4 hrs of incubation. Acrosome morphology and sperm DNA fragmentation were evaluated after 4 hrs of incubation. Binding rates between sperm and unloaded MSNPs were determined after 2, 3 and 4 hrs. For unmodified unloaded MSNPs, binding rates were also recorded after 1 hour of incubation, and used for statistical analysis in **Sections 4.2.2.** and **4.2.3**. To investigate the localisation of MSNPs in sperm, TEM was performed after 4 hours of incubation. After evaluation of potential nanotoxicity and identification of the minimally effective particle/cell ratios and incubation times, washed sperm were exposed to MSNPs carrying prototypes of biological cargo: siRNA- and mCherry-loaded MSNPs in the ratio of 10µg of particles per 10^7 sperm, for 2 hrs. Incubation was carried out under the same conditions. After 2 hours, sperm motility, viability, and binding rates with MSNPs were evaluated.

3.3. RESULTS

3.3.1. CHARACTERISATION OF MSNPS

Synthesis of non-fluorescent MSNPs was performed in a surfactant-templated base-catalysed sol-gel reaction, as previously described by Hom *et al.* (2010). In brief, the reaction is based upon the mixing or a surfactant template with a silica source in hot aqueous solution with alkaline pH, followed by amine and phosphonate surface modification of the forming particles and, finally, removal of the surfactant to expose the porous structure of MSNPs.

Synthesised MSNPs were characterised by electron microscopy. The particles were shown to be slightly non-spherical with elongation in the direction of the pore channels. The mesoporous silica comprised ordered nanometre-sized pores shown by TEM to have hexagonal symmetry when aligned with the beam (**Figure 3–1)**. Unmodified MSNPs had a mean external diameter of 138.4±3.8nm with 2.1±0.1nm-sized pores.

Nanoparticles were coated with PEI or APTES, both representing established methodologies of nanomaterial functionalisation. Efficacy of PEI-and APTES-coating was confirmed by the measurement of electrokinetic (ζ) potential, which indicated an increase or complete reversal of inherently negative ζ potential of unmodified silica (-31.50±0.60mV, -1.91±0.27mV and 37.73±0.27mV for FITC-labelled unmodified, APTES-coated and PEI-coated MSNPs, respectively) (**Table 3–1** and **Table 3–2**). Reduced propensity of PEI-treated MSNPs to agglomerate in suspension was proven by reduced mean hydrodynamic diameter in PEI-coated samples (270nm *versus* 170nm for FITC-labelled unmodified and PEI-coated MSNPs, respectively). In contrast, coating with APTES had little effect upon the agglomeration of MSNPs (270nm *versus* 280nm for FITC-labelled unmodified and APTES-coated MSNPs, respectively).

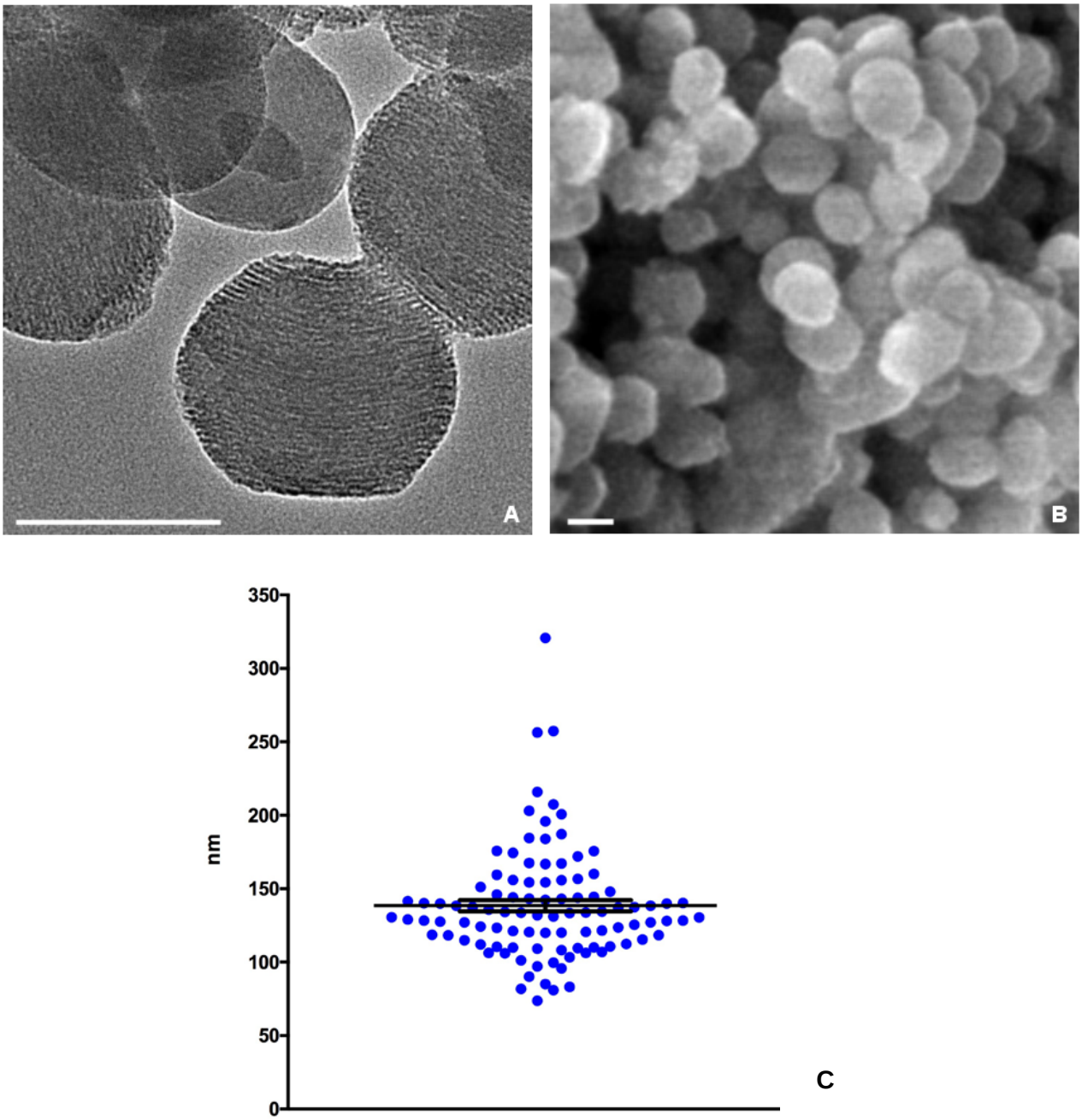

***Figure 3-1* – Characterisation of mesoporous silica nanoparticles (MSNPs).** A) Transmission electron microscopy image of unmodified MSNPs. Scale bar = 0.05µm; B) Scanning electron microscopy image of unmodified MSNPs. Scale bar = 0.1µm. C) Size distribution of synthesised unmodified MSNPs: individual measurements of transmission electron microscopy images (mean±SEM from 100 particles). Synthesised MSNPs were characterised by homogenous size, slightly non-spherical shape with elongation in the direction of the pore channels, and nanometre-sized pores with hexagonal symmetry.

***Table 3-1*– Characterisation of synthesised fluorescent mesoporous silica nanoparticles (MSNPs+FITC): ζ potential and mean hydrodynamic diameter**

	ζ potential (mV)*	**Mean hydrodynamic diameter (nm)**
Unmodified MSNPs	-31.50±0.60	270
PEI-coated MSNPs	37.73±0.27	170
APTES-coated MSNPs	-1.91±0.27	280

*Data presented as mean±SD (automated calculation by Zetasizer Nano ZS proprietary software (Malvern Instruments, UK))

As anticipated, loading with negatively charged lamin A/C siRNA reduced the positive values of ζ potential of unloaded non-fluorescent PEI-coated MSNPs (44.53±0.29mV *versus* 28.13±0.80mV for unloaded and loaded MSNPs, respectively). Adsorption of mCherry protein increased the ζ potential of unloaded non-fluorescent APTES-coated MSNPs (-5.94±0.23mV *versus* 5.29±1.17mV, for unloaded and loaded MSNPs, respectively). Loading with both types of payloads resulted in a slight increase in the mean hydrodynamic diameter of the particles (147nm *versus* 157nm for unloaded PEI-coated and lamin A/C siRNA-loaded MSNPs; 254nm *versus* 286nm for unloaded APTES-coated and mCherry-loaded MSNPs, respectively).

***Table 3-2* – Characterisation of synthesised non-fluorescent mesoporous silica nanoparticles (MSNPs) before and after loading with cargo: ζ potential and mean hydrodynamic diameter**

	ζ potential (mV)*	**Mean hydrodynamic diameter (nm)**
Unmodified MSNPs	-24.03±0.48	275
PEI-coated MSNPs	44.53±0.29	147
Lamin A/C siRNA-loaded MSNPs	28.13±0.80	157
APTES-coated MSNPs	-5.94±0.23	254
mCherry-loaded MSNPs	5.29±1.17	286

*Data presented as mean±SD (automated calculation by Zetasizer Nano ZS proprietary software (Malvern Instruments, UK))

3.3.2. NANOTOXICITY OF UNLOADED MSNPS IN SPERM

3.3.2.1. Sperm motility and viability

Motility and viability were evaluated in sperm samples after 2 and 4 hours of incubation with three types of unloaded MSNPs (unmodified, PEI-coated and APTES-coated) at a ratio of 10, 15 and 30µg of particles per 10^7 sperm using computer assisted sperm analysis (CASA) and eosin Y staining. Collectively, the exposure of sperm to MSNPs did not result in a significant change in the mean proportions of motile, progressively motile and viable sperm compared to control treatment ($p>0.05$ for all comparisons between samples exposed to any type of MSNPs and respective controls at 2 and 4 hours; **Figure 3–2**). Within the experimental samples, there was no significant effect of the type of MSNPs, or the dose and duration of incubation with each type of synthesised MSNPs upon total and progressive sperm motility and viability.

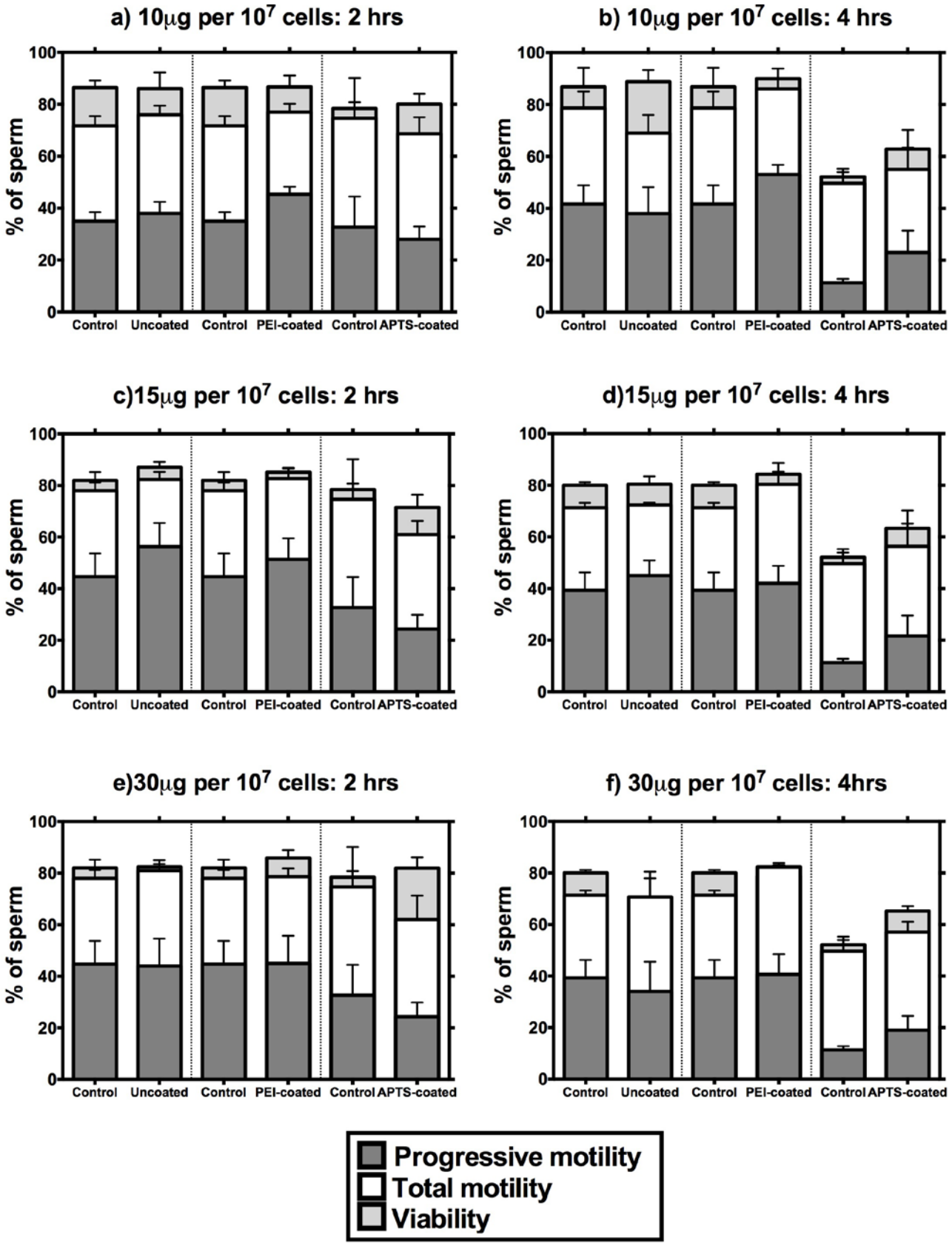

***Figure 3-2* – Proportions of motile, progressively motile and viable boar sperm after 2 and 4 hours of exposure *in vitro* to different modifications of unloaded MSNPs in three particle/cell ratios assessed by CASA and eosin Y staining** (mean±SEM from three repeats in each experimental-control pair; experimental; pairs are divided by vertical dotted lines). Total and progressive motility and viability in samples exposed to different types of unloaded MSNPs did not differ significantly from the time-matched controls, obtained from the same ejaculates as experimental samples.

Similarly, most sperm kinematic parameters evaluated by CASA in MSNP-treated samples remained similar to respective controls at both time points for all types and doses of nanoparticles (**Figure 3–3).** A reduction in the amplitude of lateral head displacement (ALH) was observed after 4 hours of exposure to higher doses of unmodified MSNPs and all doses of coated particles, and was accompanied by an increase in beat cross frequency (BCF) only in sperm samples treated with APTES-coated MSNPs. However, these alterations in sperm kinematic parameters were not associated with changes in other characteristics of sperm motion, and remained within the reference range for fertile boar sperm (Didion, 2008), and consequently, were not likely to have substantial biological significance.

3.3.3. ACROSOME MORPHOLOGY

Integrity of the acrosomal apical ridge in unstained fixed sperm samples exposed to three types of unloaded MSNPs (unmodified, PEI-coated and APTES-coated) in a series of particle/sperm ratios was examined after 4 hours of incubation. This straightforward technique allowed the identification of structural impairments in the sperm acrosomal region directly involved in penetration of the *zona pellucida* during fertilization. Such impairments can arise after acute or prolonged contact with suboptimal environment and correlate with the sperm viability and fertilization potential (Pursel *et al.*, 1972; Tsakmakidis *et al.*, 2012).

Exposure of sperm to MSNPs did not affect acrosome status at selected time points (**Table 3–3**). Mean proportions of sperm with a normal apical ridge (NAR), indicating a structurally intact acrosome, which correlated with preserved sperm capacity to penetrate the *zona pellucida*, consistently exceeded 80% across all experimental and control samples, regardless of the type and dose of MSNPs.

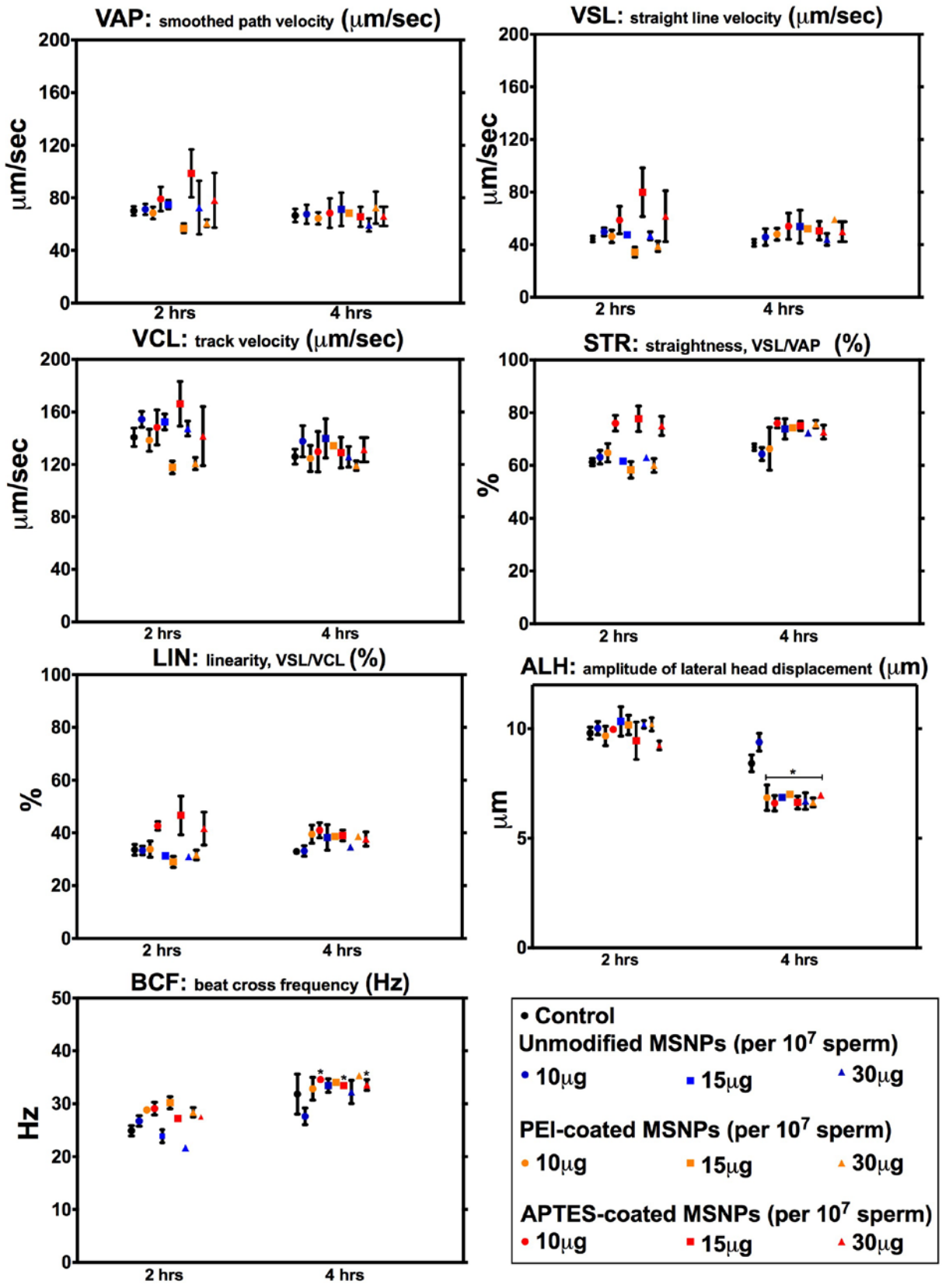

***Figure 3-3* – Motility parameters of boar sperm assessed by CASA after 2 and 4 hours of exposure *in vitro* to different modifications of unloaded MSNPs in three particle/cell ratios** (mean±SEM from twelve repeats in control samples, up to seven repeats in experimental samples for unmodified and PEI-coated particles and three repeats in experimental samples for APTES-coated particles; symbol (*) denotes subsets of categories, whose values are significantly different from time- and ejaculate-matched controls at the 0.05 level. VAP: smoothed path velocity; VSL: straight line velocity; VCL: track velocity; ALH: amplitude of lateral head displacement; BCF: beat cross frequency. STR (ratio of VSL/VAP) = straightness, LIN (ratio of VSL/VCL) = linearity.

***Table 3-3* – Proportions of boar sperm categorised upon the appearance of acrosomal apical ridge and DNA fragmentation after 4 hours of exposure *in vitro* to different modifications of unloaded MSNPs in three particle/cell ratios (mean±SEM)**

		NAR (%)	DAR (%)	MAR(%)	LAC (%)	DNA fragmentation index (%)
Control (PBS)		84.4±3.0	2.1±0.4	2.3±0.5	11.2±2.9*	2.8±0.5
10µg of particles in PBS per 10^7 sperm	Unmodified MSNPs	90.3±2.4	2.7±0.7	2.5±1.0	4.5±1.6	1.1±1.0
	PEI-coated MSNPs	89.0±2.1	4.0±2.9	2.6±1.0	4.4±1.4	1.4±1.0
	APTES-coated MSNPs	89.6±1.4	3.0±0.6	1.0±0.6	6.4±1.9	1.5±0.5
15µg of particles in PBS per 10^7 sperm	Unmodified MSNPs	88.4±3.3	4.3±1.8	1.5±0.5	6.0±2.0	0.7±0.1
	PEI-coated MSNPs	84.6±10.2	2.3±1.8	1.8±1.7	10.6±6.6	1.0±0.5
	APTES-coated MSNPs	85.2±2.4	6.5±2.1	2.5±0.5	5.8±0.7	0.7±0.4
30µg of particles in PBS per10^7 sperm	Unmodified MSNPs	88.2±3.8	4.2±2.2	0.5±0.4	7.2±2.2	0.8±0.2
	PEI-coated MSNPs	86.1±4.8	4.3±3.3	1.8±1.3	7.9±0.3	0.7±0.4
	APTES-coated MSNPs	94.4±2.0	2.3±1.1	1.3±0.3	2.0±0.6*	1.2±0.2

Mean±SEM from six repeats in control samples and three repeats in experimental samples; symbol (*) denotes subsets of categories, whose values are significantly different from time- and ejaculate-matched controls at the 0.05 level; NAR = 'normal acrosomal ridge'; DAR = 'damaged acrosomal ridge'; MAR = 'missing acrosomal ridge'; LAC = 'loosened acrosome cap'

Interestingly, a significantly lower percentage of sperm with a loosened acrosome cap (LAC), in which the acrosomal cap became detached from the sperm head, thus representing acrosomal deterioration, was observed in samples treated with APTES-coated MSNPs at the highest particle/cell ratio, compared to controls. This finding could suggest a protective role of APTES-coated MSNPs in preserving acrosomal morphology during incubation, and, therefore, their favourable effect during *in vitro* culture. Within the experimental samples, there was no significant effect of the type and doses of MSNPs upon integrity of the acrosomal apical ridge, with the exception of APTES-coated particles (significant effect upon the proportion of sperm with LAC; $F_{2,4}=9.670$, $p<0.05$).

3.3.4. SPERM DNA FRAGMENTATION INDEX

The proportion of sperm carrying fragmented DNA is being increasingly considered as an independent marker of sperm quality and capacity to form viable embryos post-fertilization (Shamsi *et al.*, 2011), and can be affected by sub-optimal environment (Fraser *et al.*, 2011). In this set of experiments, sperm DNA fragmentation was visualised in MSNP-treated and control samples using the sperm chromatin dispersion method (**Figure 3–4**), which is based on response variations of

sperm chromatin with fragmented and non-fragmented DNA to protein depletion treatment, and has been previously characterised as a simple, reproducible and inexpensive technique to detect DNA breakage (Enciso *et al.*, 2006).

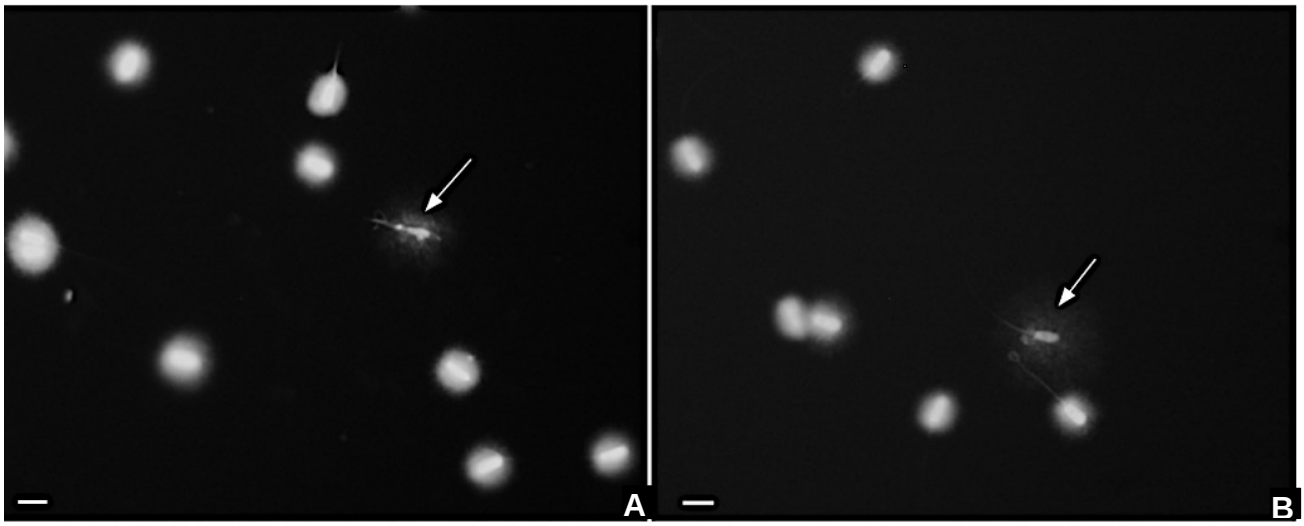

***Figure 3-4* – DNA fragmentations in boar sperm after exposure *in vitro* to unloaded MSNPs: sperm chromatin dispersion test. A) Control; B) A representative image of sperm treated with unloaded MSNPs after 4 hours of incubation.** Sperm with fragmented DNA (indicated with white arrows) are surrounded by disperse halos ('rays') of chromatin, while heads of sperm with non-fragmented DNA have larger area and appear more intense. Staining with DAPI. Images converted to grey scale to facilitate visualisation of the halos. Scale bar = 10µm.

Mean DNA fragmentation index in sperm treated with MSNPs for 4 hours was not significantly different from controls (**Table 3-3**). Across all analysed samples, DNA fragmentation was consistently observed in fewer than 5% of sperm. Within the experimental samples, there was no significant effect of the type and doses of MSNPs upon sperm DNA fragmentation index.

3.4. BINDING BETWEEN SPERM AND UNLOADED MSNPS

Binding rates between boar sperm and unloaded MSNPs were assessed after 2, 3 and 4 hours of incubation to evaluate the effects of time and MSNP dose upon particle-sperm interaction. The term 'binding' was introduced to collectively describe apparent surface attachment and suspected internalisation of MSNPs into sperm, both representing positive outcomes of interaction between the nanoparticles and sperm cells.

MSNPs bound with sperm produced focal fluorescent signals in the sperm head, midpiece or tail region (**Figure 3–5**).

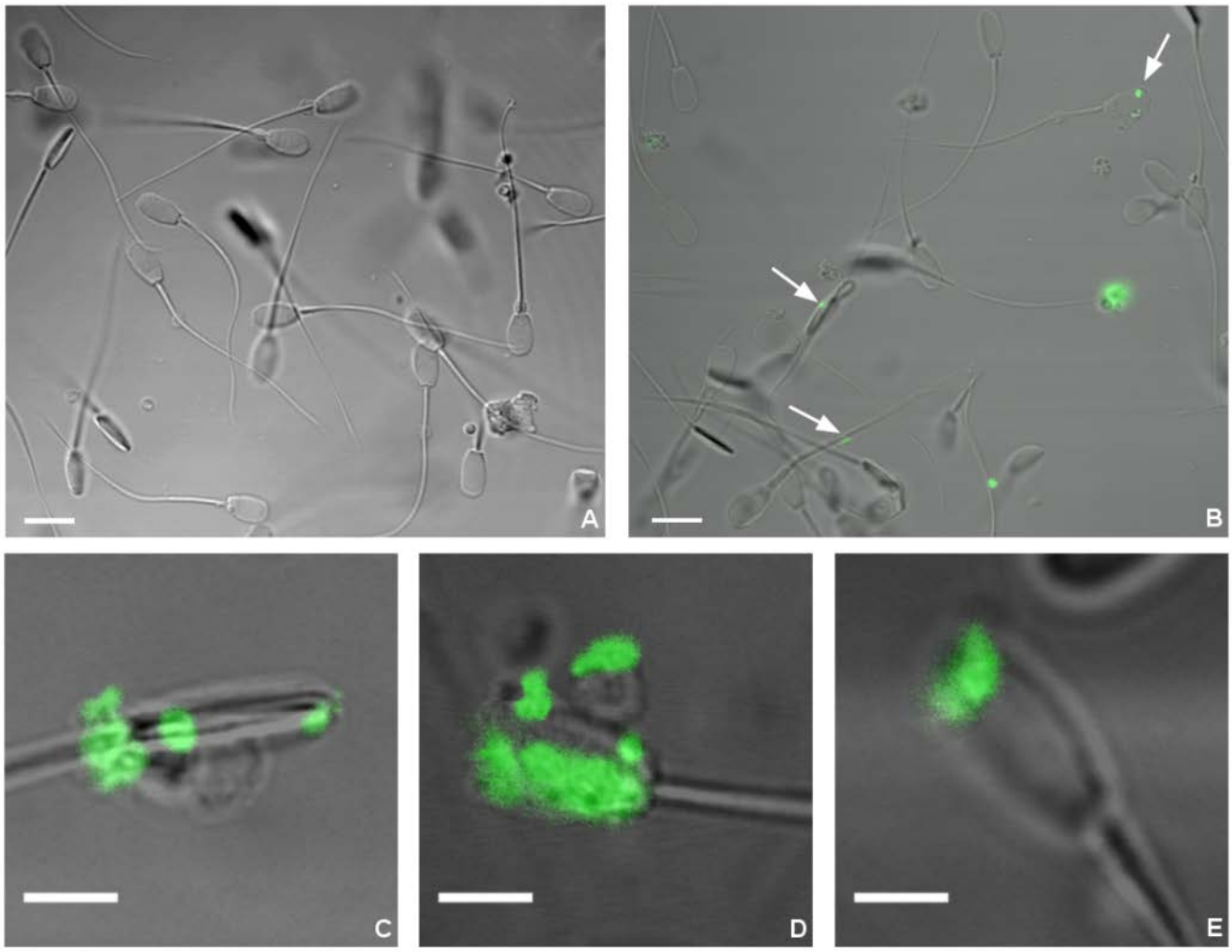

***Figure 3-5* – Binding of unloaded MSNPs with boar sperm after exposure *in vitro*. A) Control; B) A representative image of binding of unloaded MSNPs with sperm.** Nanoparticles bound with sperm produced focal fluorescent signals in the projection of various sperm regions (white arrows indicate MSNP-sperm associations). Scale bar = 10μm. **C-E) Representative images of binding of unloaded MSNPs with sperm.** MSNPs (shown as green fluorescence) bound to the sperm head and midpiece. Scale bar = 5μm.

Binding rate between MSNPs and boar sperm was dependent upon the type ($F_{2,5}$=9.041, $p<0.05$) of MSNPs and their dose for the unmodified MSNP subset ($F_{2,4}$=8.427, $p<0.05$), and did not change significantly throughout incubation (**Figure 3–6)**. A significantly higher proportion of sperm binding with MSNPs was observed after 2 hours of treatment with unmodified particles at the highest particle/cell ratio (30μg per 10^7 sperm), compared to lower doses of the same type of MSNPs (17.4±2.9%, 20.8±5.7% and 41.0±9.2%, for 10, 15 and 30μg per 10^7 sperm, respectively; $p<0.05$). This increase was temporary, as evidenced by a subsequent decline in binding between unmodified MSNPs and sperm at the highest particle/sperm ratio after 3 and 4 hours of exposure. This observation suggested a possibility for temporary weak interaction of sperm with unmodified

mesoporous silica after 2 hours of treatment, followed by dissociation of bound particles from sperm at later stages. On the contrary, MSNP-sperm binding rates in the two remaining types of unloaded MSNPs (PEI-coated and APTES-coated) did not change significantly throughout incubation, and were not markedly influenced by the dose of particles.

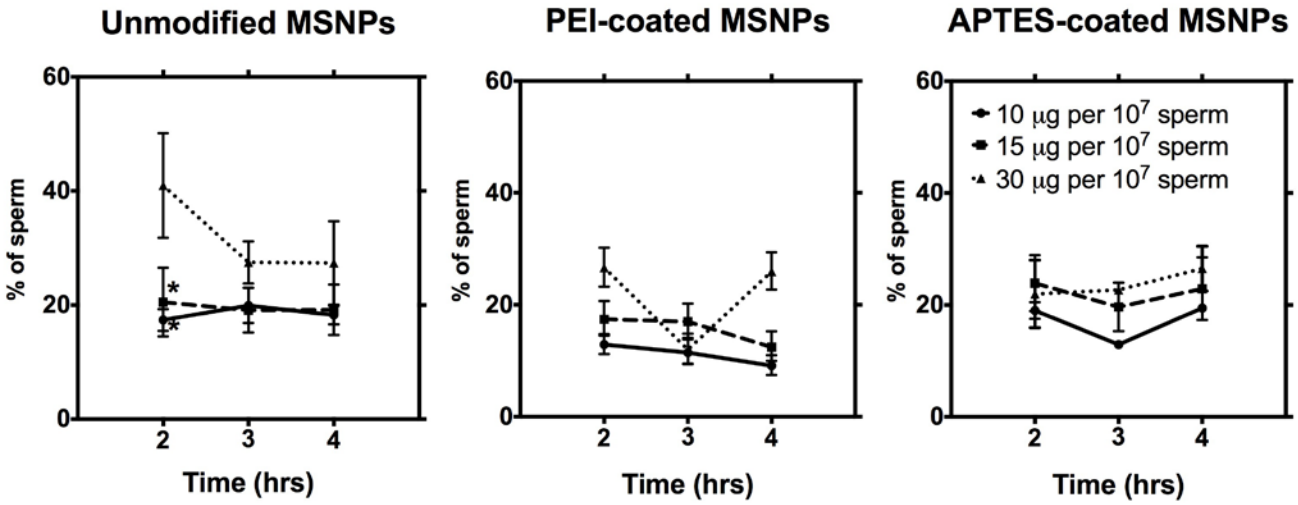

***Figure 3-6* – Binding rates between boar sperm and different modifications of unloaded MSNPs after 2, 3 and 4 hours of exposure *in vitro* in three particle/cell ratios** (mean±SEM from up to seven repeats of the experiment). Binding rate after 2 hours of exposure to unmodified MSNPs in the 30μg per 10^7 sperm ratio was significantly higher compared to lower particle/sperm ratios. Symbol (*) denotes subsets of categories, whose values are significantly different from the binding rate for the 30μg per 10^7 sperm ratio at the same experimental point at the 0.05 level.

For detailed investigation of the localisation of unloaded MSNPs in boar sperm after incubation, thin section TEM was carried out. Although the findings obtained during TEM could suggest that MSNPs adsorb to the sperm plasma membrane and a small proportion of nanoparticles is potentially capable of internalising into sperm, the results were interpreted with caution because of the low number of sperm demonstrating signs of interaction with MSNPs on the TEM images and the possibility of imaging artifacts (**Figure 3–7**). For example, although **Figures 3-7B** and **3-7C** indicated possible localisation of MSNPs in the region of the sperm nucleus and intracytoplasmic compartment, these findings were not used as evidence in favour of particle internalisation.

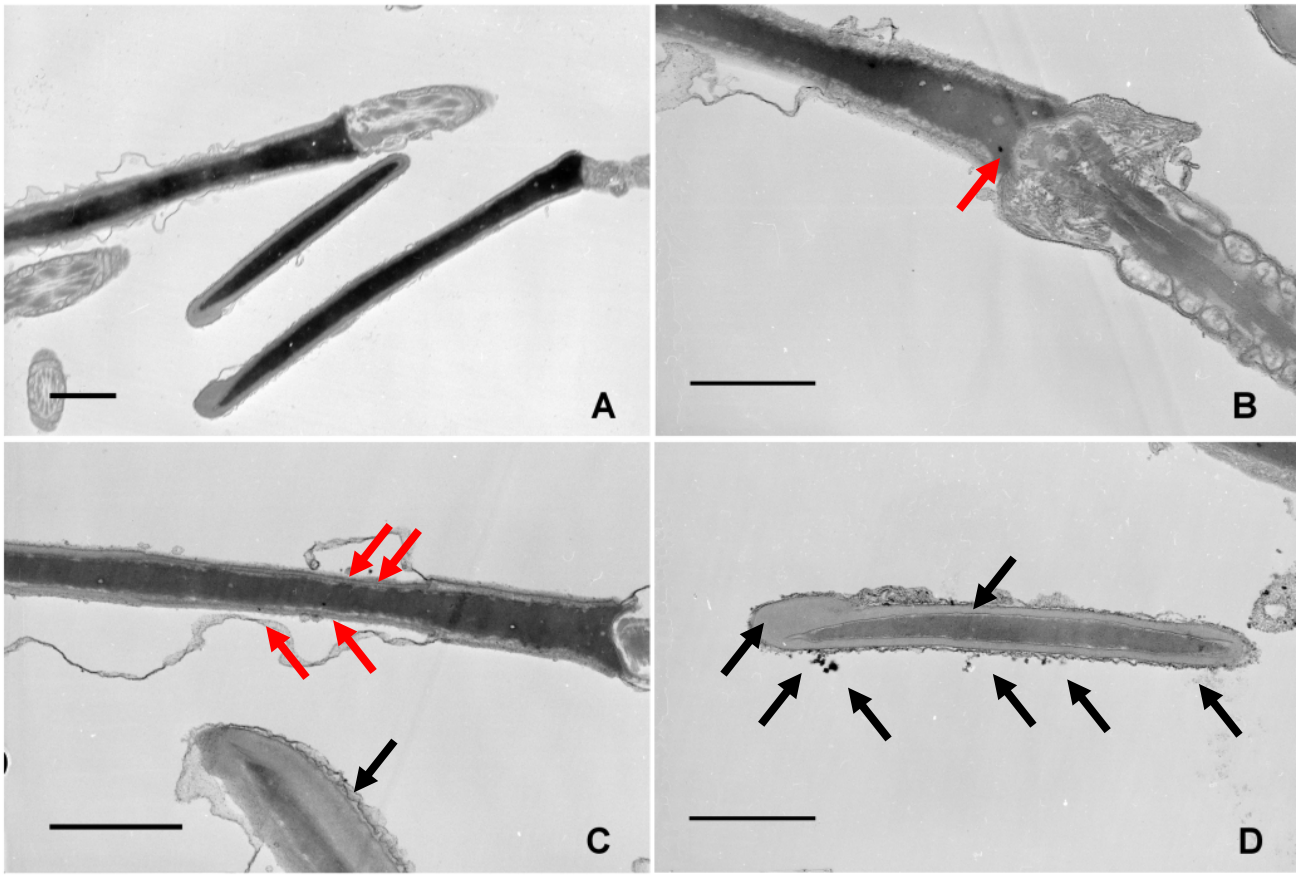

***Figure 3-7* – Localisation of unloaded MSNPs in boar sperm after exposure *in vitro*. A) Control; B) Unmodified MSNPs in sperm. C,D) PEI-coated MSNPs in sperm.** Nanoparticles appear on TEM images as small dense (black) structures absorbed on the outer surface of the boar sperm plasma membrane (black arrows) and inner to the plasma membrane, indicating potential internalisation (red arrows). Scale bar = 1µm.

3.5. NANOTOXICITY AND BINDING BETWEEN SPERM AND LOADED MSNPS

After confirming the biocompatibility of various modifications of MSNPs in boar sperm, a minimally effective dose of 10µg particles per 10^7 sperm and a 2-hour incubation time was chosen for subsequent experimentations with cargo-loaded MSNPs. In this set of experiments, a shorter panel of nanotoxicity tests was applied, focusing mainly upon the effects of exposing boar sperm to loaded MSNPs upon motility and viability.

After 2 hours of incubation, siRNA- and protein-loaded MSNPs had no significant effect upon the mean proportion of motile, progressively motile, or viable sperm, compared to time-matched controls. Similarly to unloaded MSNPs, treatment with MSNPs carrying the two most common candidate types of biological cargo did not alter the key parameters of sperm motion, as assessed by CASA (**Figure 3–8).**

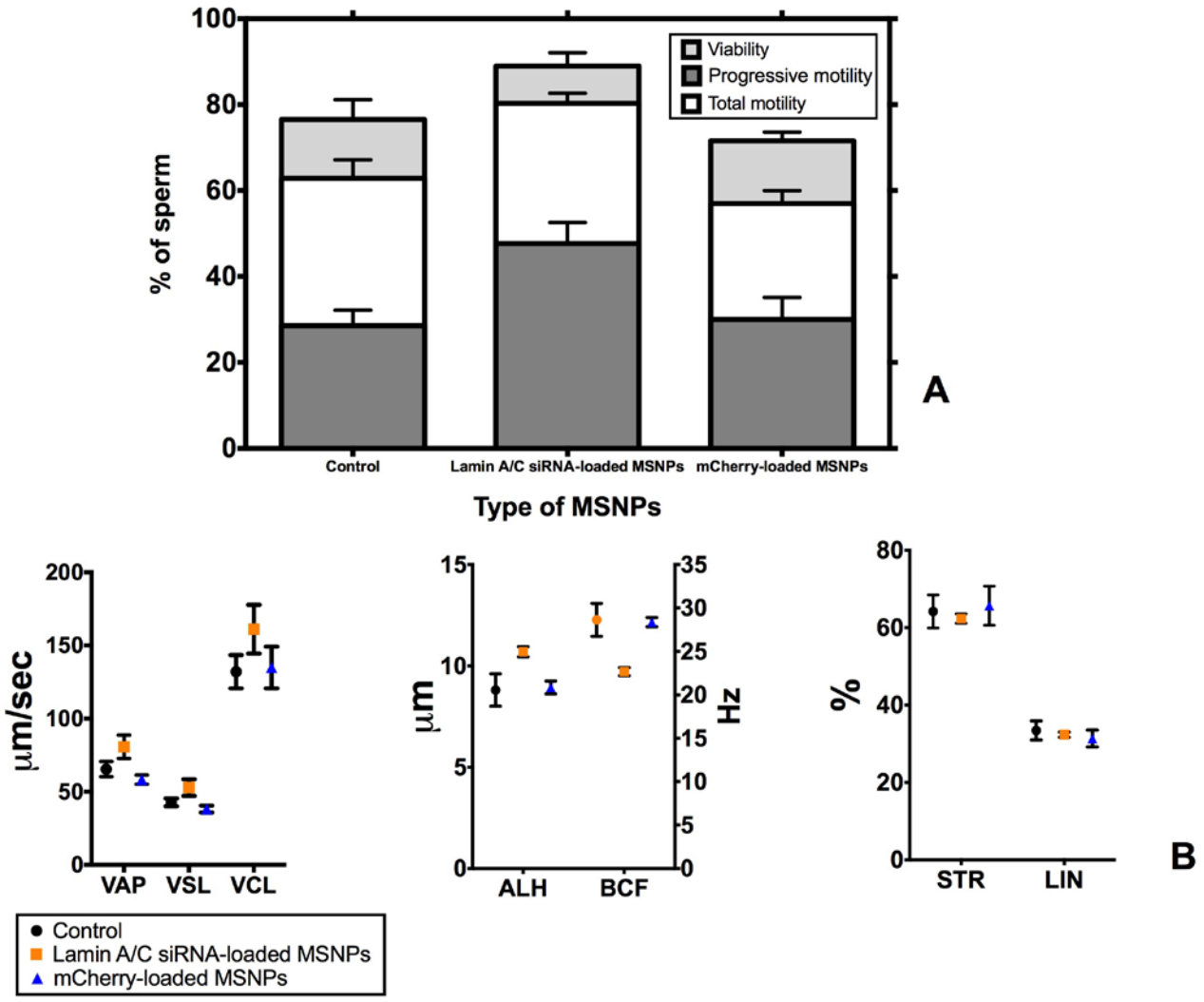

***Figure 3-8* – Motility parameters in boar sperm assessed by CASA after 2 hours of exposure *in vitro* to siRNA- and protein-loaded MSNPs** (mean±SEM from six control samples and three experimental samples). A) Total and progressive motility and sperm viability; B) Sperm motion parameters. VAP: smoothed path velocity; VSL: straight line velocity; VCL: track velocity; ALH: amplitude of lateral head displacement; BCF: beat cross frequency. VAP: smoothed path velocity; VSL: straight line velocity; VCL: track velocity; ALH: amplitude of lateral head displacement; BCF: beat cross frequency. STR (ratio of VSL/VAP) = straightness, LIN (ratio of VSL/VCL) = linearity.

Binding rates between loaded MSNPs and boar sperm were calculated after 2 hours of incubation and compared with the corresponding values for unloaded MSNPs in the 10µg per 10^7 sperm ratio (PEI-coated MSNPs *versus* lamin A/C siRNA-loaded MSNPs and APTES-coated MSNPs *versus* mCherry-loaded MSNPs). Binding rates between sperm and siRNA-loaded MSNPs were significantly lower than for unloaded PEI-coated MSNPs (1.8±0.7% *versus* 12.3±1.9%, respectively; $p<0.05$). In contrast, loading of APTES-coated MSNPs with mCherry had no significant effect upon binding rates with sperm (25.3±4.2% *versus* 19.0±1.5% for mCherry-loaded

and unloaded APTES-coated MSNPs, $p<0.05$). The density of sperm coating with lamin A/C siRNA-loaded MSNPs was lower, compared to mCherry-loaded MSNPs (**Figure 3–9**).

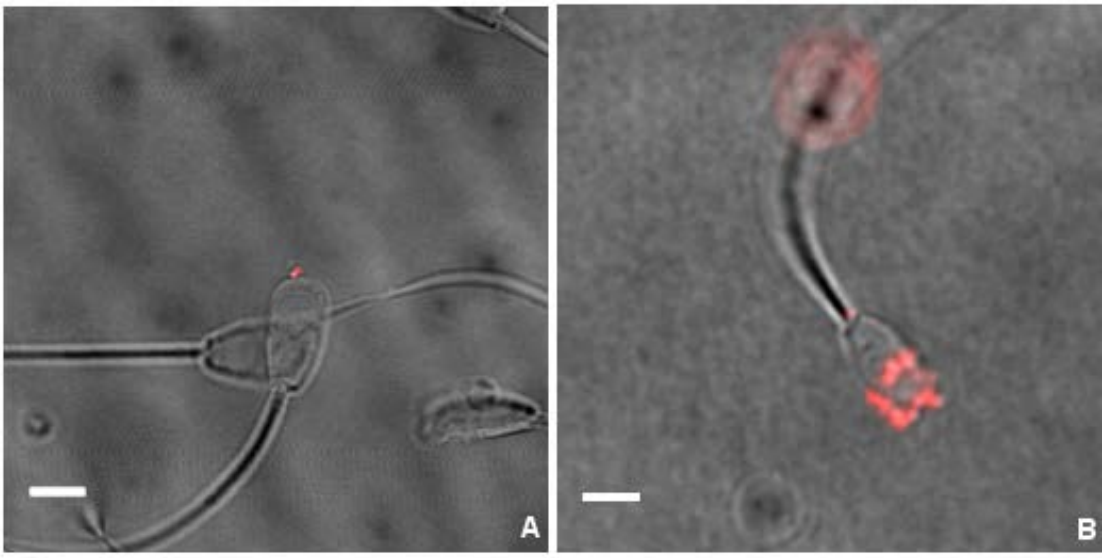

***Figure 3-9* – Binding of loaded MSNPs with boar sperm after exposure *in vitro*. A) Lamin A/C siRNA-loaded MSNPs; B) mCherry-loaded MSNPs.** The density of sperm coating with lamin A/C siRNA-loaded MSNPs was lower, compared to mCherry-loaded MSNPs. Scale bar = 5µm.

3.6. NANOTOXICITY AND BINDING BETWEEN MOUSE OOCYTES AND UNLOADED MSNPS

Fluorescent unmodified and PEI-coated MSNPs adsorbed to the *zona pellucida* of mouse oocytes after 2 hours of incubation, and the density of absorption was not markedly influenced by the physicochemical properties of MSNPs (**Figure 3–10).** All oocytes in the experimental groups (n=8 for fluorescent unmodified, and n=16 for fluorescent PEI-coated MSNPs) showed signs of binding with MSNPs. Although some green fluorescent signals were localised to the *zona pellucida*, which could indicate penetration of MSNPs into transzonal channels, no spontaneous internalisation into the oocytes was observed. No green fluorescence was observed in the control group (n=13).

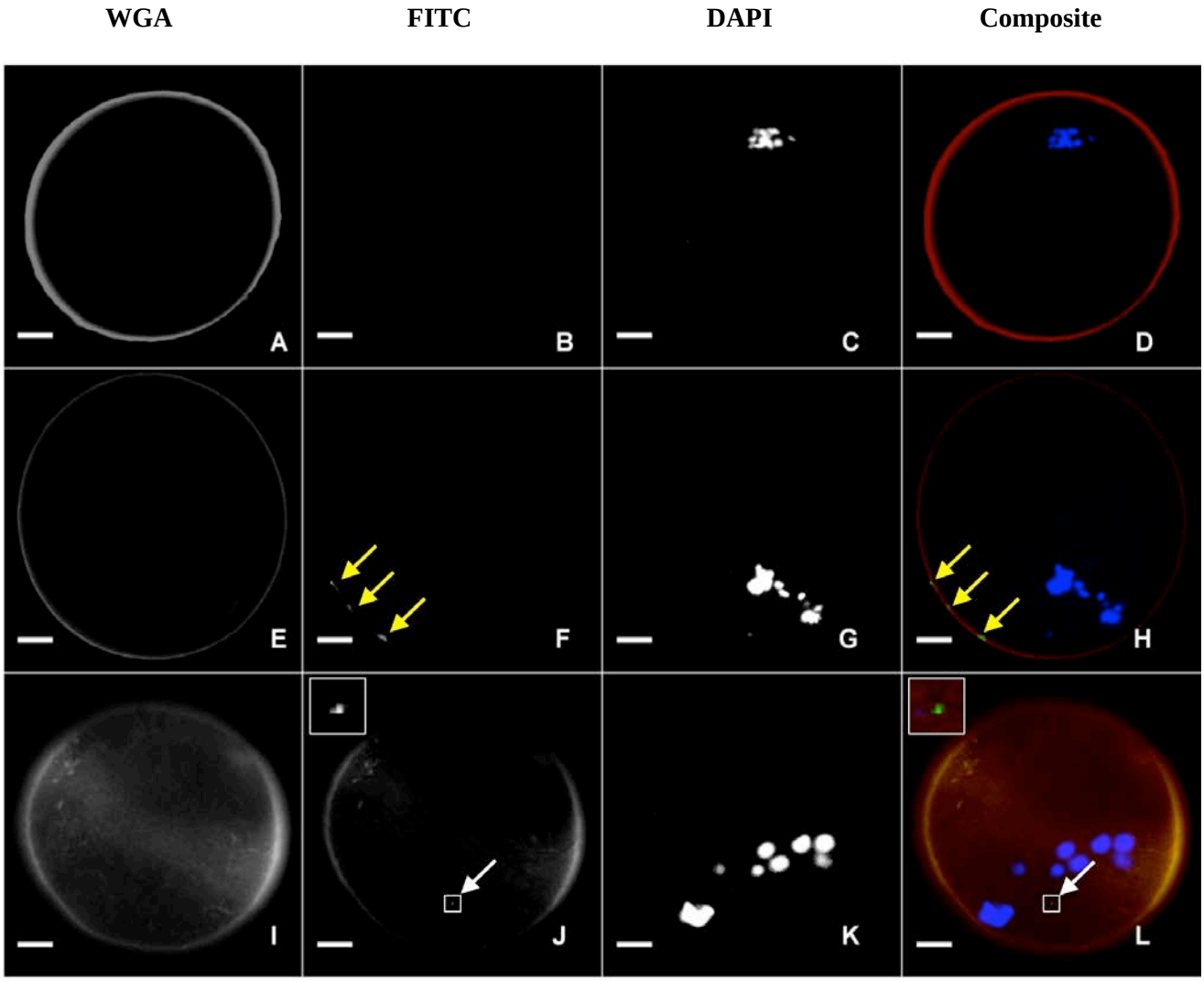

Figure 3-10* – Binding of unloaded MSNPs with mouse oocytes after exposure *in vitro*. A-D) Control (nuclear plane); E-H) Fluorescent unmodified MSNPs (nuclear plane); I-L) Fluorescent PEI-coated MSNPs (apical plane).** Fluorescence from *zona pellucida* captured in the WGA channel, fluorescence from MSNPs – in the FITC channel; nuclear fluorescence – in the DAPI channel. On E-F, 'bleed through' of the WGA signal was observed in the FITC channel in the form of halo (non-specific fluorescence). Nanoparticles bound with the oocytes produced focal fluorescent signals on the surface (white arrows) or in the projection of the *zona pellucida* (yellow arrows*).** Density of adsorption was not markedly influenced by the physicochemical properties of MSNPs. Scale bar = 20µm.

Mouse oocytes were also microinjected with unloaded MSNPs to evaluate their biocompatibility and potential for assisted intracellular delivery. Approximately 18 hours after microinjections, the survival rate of oocytes consistently exceeded 70% and was not significantly different between the MSNP-injected and control groups (**Table 3–4)**. Intracellular fluorescence was detected in 83.3% of the oocytes injected with unmodified MSNPs and only 40% of the oocytes injected with PEI-coated MSNPs (**Figure 3–11**). Collectively, these results indicated an

absence of acute toxicity of MSNPs in the oocytes, but also highlighted the technical difficulties associated with the spontaneous and assisted internalisation of MSNPs into these specialised cells.

***Table 3-4* – Survival rate of mouse oocytes 18 hours after sham microinjections and injections with unloaded MSNPs**

	Survival rate	Proportion of the oocytes with intracellular fluorescence
No intervention (n=10)	100%	N/A
Sham injections (M16) (n=10)	80%	0%
Unmodified MSNPs (n=10)	71.4%	83.3%
PEI-coated MSNPs (n=10)	100%	40%

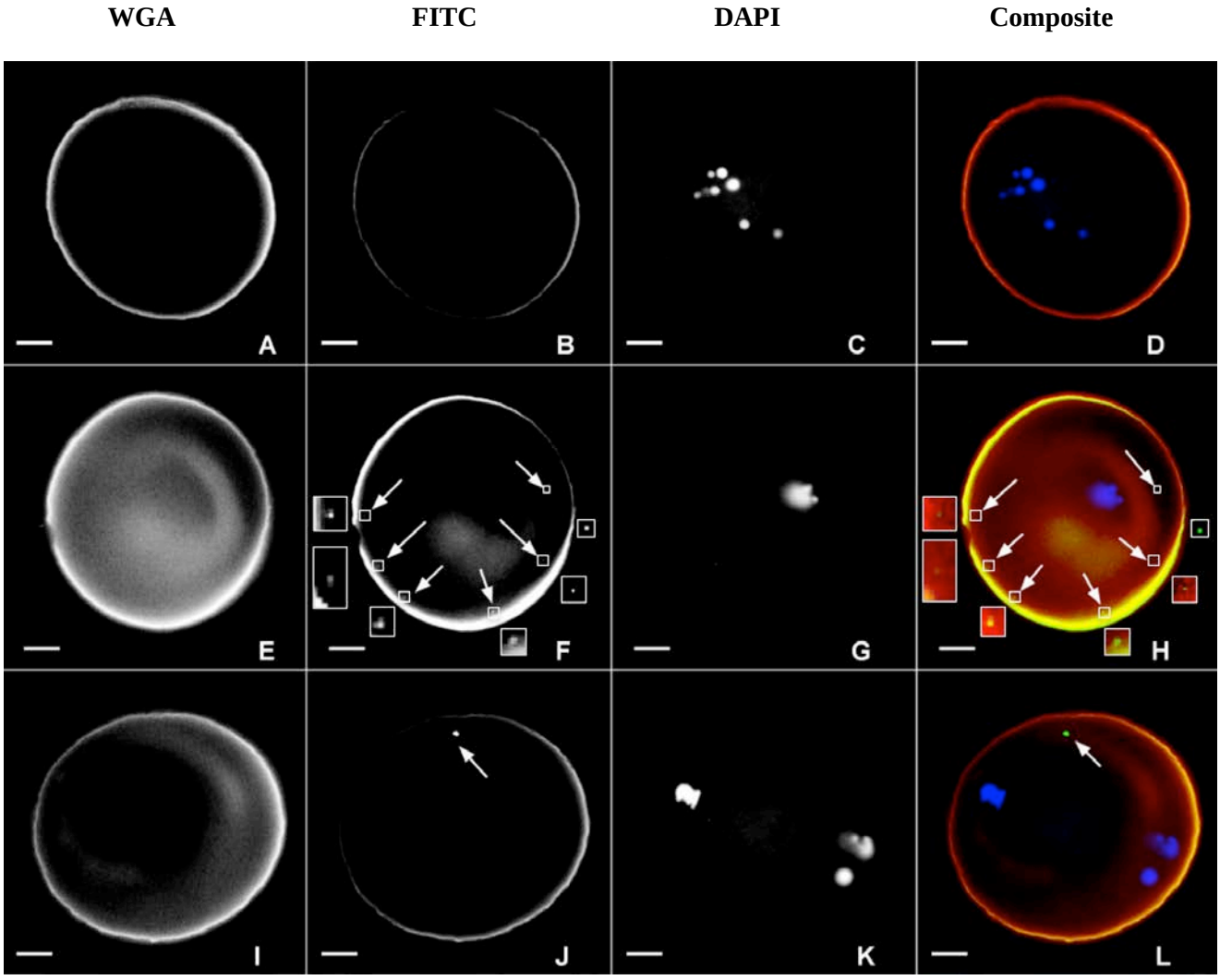

***Figure 3-11* – Unloaded MSNPs in mouse oocytes after microinjections. A-D) 'Sham injection' control); E-H) Fluorescent unmodified MSNPs; I-L) Fluorescent PEI-coated MSNPs**. Fluorescence from *zona pellucida* captured in the WGA channel, fluorescence from MSNPs – in the FITC channel; nuclear fluorescence – in the DAPI channel. 'Bleed through' of the WGA signal was observed in the FITC channel in the form of halo (non-specific fluorescence). Nanoparticles localised inside the oocytes after microinjections produced focal fluorescent signals (white arrows)**.** Scale bar = 20µm.

3.7. DISCUSSION

Research into the mechanisms of reproduction and early stages of embryo development is continuously advancing in response to demands from the assisted reproduction sector (Gianaroli *et al.*, 2012) and regenerative medicine (Chen *et al.*, 2012). Recent reports show that infertility is estimated to affect almost 1.5% of the world population (Mascarenhas *et al.*, 2012), and in approximately 1 in 4 cases the causal factor underlying reproductive failure cannot be established (National Institute for Health and Care Excellence (NICE), 2013). At the same time, the current success rates of available treatments, including assisted reproduction techniques, remain low, with only around 20% of treatment cycles resulting in live births (Sullivan *et al.*, 2013). This justifies the need for development of accurate research tools to investigate and target the fine mechanisms underlying gametogenesis, fertilization and early embryo development.

There is increasing interest towards the use of nanomaterials in reproductive science, supported by evidence that nano-products improve selectivity, affinity and detection limits of existing methodologies, and enhance their performance (Petros and DeSimone, 2010; Lammers *et al.*, 2011; Arvizo *et al.*, 2012). Today, nanomaterials have been applied in pilot experiments involving nanotransfection during SMGT in cows and pigs (Kim *et al.*, 2010b; Campos *et al.*, 2011a), transport of proteins into bovine sperm (Makhluf *et al.*, 2008), experimental *in utero* gene therapy in mice (Yang *et al.*, 2011), sperm and oocyte bioimaging (Feugang *et al.*, 2012; Feugang *et al.*, 2015), sex sorting of gametes in animal breeding (Barchanski *et al.*, 2011), and labelling of pre-implantational embryos during *in vitro* fertilization (Fynewever *et al.*, 2007). However, the range of nanomaterials tested in gametes remains very limited, and their long-term developmental toxicity has not been evaluated extensively. Furthermore, accumulating reports concerning the potential negative effects of many of these nanomaterials upon the DNA integrity in somatic cells (Singh *et al.*, 2009), highlights the need to further investigate the specific genotoxicity of nanomaterials in gametes, and search for an optimal candidate for intra-gamete delivery.

This part of the thesis investigated the effects of MSNPs that had been functionalised with two common types of surface coating (PEI and APTES) and optionally loaded with lamin A/C siRNA or mCherry protein, upon boar sperm and mouse oocytes during *in vitro* incubation. These experiments, for the first time, addressed the use of MSNPs in mammalian gametes from the perspective of a potential compound transfer vehicle. MSNPs had been previously well-characterised as a safe and robust platform for experimental drug development, tissue engineering and gene therapy in a variety of cells and model species (Rosenholm *et al.*, 2012; Sharif *et al.*, 2012; Yang *et al.*, 2012b). However, their performance as research tools in reproductive biology had not been previously tested. Findings obtained during the first stages of this present research supported the biocompatibility and cell binding capacity of MSNPs obtained in various cell types, and extended it to boar sperm and mouse oocytes.

The biocompatibility of MSNPs with boar sperm and mouse oocytes represents an important finding. Potential gameto- and embryo-toxicity of nanomaterials is a matter of continuous concern, since developmental toxicity can be observed regardless of proven safety in somatic cells. Currently, the preservation of sperm function has been reported following treatment with magnetic nanoparticles (Kim *et al.*, 2010b), halloysite clay nanotubes and commercial nanopolymer-based transfection agents (Campos *et al.*, 2011a; Campos *et al.*, 2011b), polyvinylalcohol-functionalised iron oxide nanoparticles (Ben-David Makhluf *et al.*, 2006), and specific types of quantum dots (Feugang *et al.*, 2012; Feugang *et al.*, 2015). At the same time, evidence regarding sperm toxicity of perhaps the most common nanomaterials, such as nanogold and nanosilver, remains contradictory. The effects of these agents vary substantially depending on physical and chemical properties of the particles, dose and model organism (Braydich-Stolle *et al.*, 2005; Wiwanitkit *et al.*, 2009; Barchanski *et al.*, 2011; Moretti *et al.*, 2012). Finally, the outcomes of nanoparticle exposure upon oocytes have only been investigated in a select few studies (Courbiere *et al.*, 2013; Tiedemann *et al.*, 2014; Feugang *et al.*, 2015).

This first set of experiments showed that exposure of boar sperm to unmodified, surface-functionalised and cargo-loaded MSNPs in various particle/sperm ratios did not exert detrimental effects upon the main parameters of sperm function, including motility, viability, kinematic features, and acrosome status, after up to 4 hours of incubation *in vitro*, which represents the conventional timeframe for sperm handling prior to IVF. In this set of experiments, the mean values of key sperm motion parameters assessed by CASA after exposure to various modifications and doses of MSNPs generally remained within reported reference ranges for fertile boar sperm (Didion, 2008). However, it is of worth to note that small insignificant changes in sperm motility parameters between MSNP-treated and control samples were observed. There was, therefore, a possibility that those minor effects at the level of entire sperm population were a direct result of larger effects within the subpopulation of sperm bound with MSNPs.

No reduction in the proportion of sperm exhibiting a normal apical ridge after exposure to unmodified, PEI- and APTES-coated MSNPs using high-magnification light microscopy was observed (Pursel *et al.*, 1972). In this respect, findings were consistent with a previous study reporting the preserved capacity of bovine sperm to undergo acrosome reaction after binding with magnetite nanoparticles (Ben-David Makhluf *et al.*, 2006). In addition, there was no significant increase in the proportion of sperm exhibiting fragmented DNA after incubation with various types and doses MSNPs. This observation suggested their low genotoxicity after short-term exposure. In the case of oocytes, encouraging data were also obtained, showing that although spontaneous intracellular internalisation of MSNPs did not occur in these cells, their persistence in the ooplasm following microinjections did not result in acute toxic effects.

Another significant finding of this set of experiments was that MSNPs spontaneously bound with boar sperm during incubation, which, crucially, did not affect sperm functionality. Since the interaction between sperm and MSNPs has not been characterised previously, the term ‘binding’ was introduced herein to collectively describe the apparent surface attachment and potential internalisation of MSNPs into sperm. Both these types of interaction represent positive outcomes,

since many studies show that nanoparticles, which readily penetrate somatic cells, remain bound to or sequestrated inside the plasma membrane of sperm (Ben-David Makhluf *et al.*, 2006; Kim *et al.*, 2010b; Barchanski *et al.*, 2011). Such a specific pattern of interaction most likely arises as the result of different composition of the sperm plasma membrane, compared to somatic cells. These differences include, for example, a highly compartmentalised structure of the membrane and significantly higher proportion of unsaturated fatty acids, which increases the flexibility and elasticity of the membrane, and allows sperm to travel in a swimming motion (Tapia *et al.*, 2012). Nonetheless, nanoparticles bound to the sperm membrane are reported to preserve their diagnostic and delivery functions, and the lack of cellular internalisation does not compromise the performance of research techniques based upon such methodologies (Kim *et al.*, 2010b; Feugang *et al.*, 2012).

In the set of experiments with unloaded MSNPs, binding rate with sperm was not markedly influenced by the type and dose of the particles, or incubation time. Although coating with PEI was consistently reported to improve nanoparticle uptake in somatic cells (Xia *et al.*, 2009; Hom *et al.*, 2010; Rosenholm *et al.*, 2012), this effect was not observed in sperm, additionally highlighting the highly specialised nature and properties of these cells. The observations of an initially higher MSNP-sperm binding rate after exposure to unmodified MSNPs in the highest particle/cell ratio, followed by a subsequent reduction in binding, correspond to a previous report by Makhluf *et al.* (2006). This earlier study reported that stable binding of magnetite nanoparticles with sperm occurred after approximately 1-2.5 hours of incubation, after an initial transient phase of loose surface attachment (Ben-David Makhluf *et al.*, 2006). Unfortunately, previous studies of interaction between nanomaterials and sperm did not present data regarding the specific size of the sperm population binding with NPs, and it was, therefore, difficult to classify the binding rate observed in this set of experiments as low or high.

At the same time, loading MSNPs with cargo changed their binding rate with sperm. In this study, lamin A/C siRNA and mCherry protein were applied as prototypes of molecular cargo for

delivery into gametes or early-stage embryos. The reduction of binding rates between siRNA-loaded MSNPs and sperm, compared to 'empty' (PEI-coated) MSNPs represented an unexpected observation. In this set of experiments, siRNA was primarily absorbed onto the surface of the particles, as evidenced by changes in ζ potential and hydrodynamic size after loading. Indeed, intra-channel loading of siRNAs into the specific modification of PEI-coated MSNPs used in this project would not be entirely straightforward. Specifically, the size of siRNA, estimated to measure ~2nm (Sinden *et al.*, 1998), was similar to the size of the pores in synthesized particles (2.1nm), which would additionally reduce after coating with PEI. It could be possible that such external localisation of cargo restricted binding of MSNPs only to dedicated regions of the sperm membrane, where interaction with exogenous nucleic acid can occur (Parrington *et al.*, 2007). Nevertheless, despite this particular binding profile between nucleic acid-loaded MSNPs was observed, it was hard to interpret whether such changes in binding would affect the delivery potential of MSNPs in view of the previously discussed evidence that the lack of cellular internalisation into gametes does not compromise the performance of nanomaterials as research tools.

In the set of experiments evaluating internalisation of MSNPs into mouse oocytes, no evidence of spontaneous uptake was observed. These findings largely corresponded to the those reported by other research groups who assessed the potential of nanomaterials to internalise into mammalian oocytes *in vitro.* Specifically, Courbiere *et al*. (2013) report endocytosis of cerium dioxide nanoparticles into mouse follicular cells, but not the oocytes, in which they aggregated around the zona pellucida. In contrast, Tiedemann *et al*. (2014) reported intracellular uptake of gold nanoparticles by porcine oocytes, while silver and alloy particles primarily localised inside the follicular cells. Feugang *et al*. (2015) demonstrated that luciferase-conjugated fluorescent quantum dots injected into porcine ovarian follicles could penetrate the oocyte, presumably via the system of gap junctions between the follicular cells and the oolemma. Collectively, these studies highlighted that spontaneous internalisation of nanomaterials into mammalian oocytes appears challenging and depends on the nature of nanomaterial and, perhaps, animal species in which it is used.

Furthermore, intra-oocyte internalisation occurs only in presence of functional follicular cells around the oocyte, which seem to transport the nanocarrier through the *zona pellucida* into the female gamete. In this Chapter, only mature denuded mouse oocytes were used, and the limited uptake capacity could, therefore, be associated with two factors: firstly, the removal of cumulus cells, and secondly, the physiologically low internalisation capacity of mouse oocytes compared to other species (Courbiere *et al*., 2013; Tiedemann *et al*., 2014; Feugang *et al*., 2015).

In conclusion, this first set of experiments yielded encouraging outcomes regarding the biocompatibility of MSNPs with boar sperm and mouse oocytes, and their potential for binding with these highly specialised cells after exposure *in vitro,* without compromising their essential functions. Therefore, MSNPs can represent a strong candidate for use in reproductive research, including the delivery of molecular constructs into sperm for subsequent transfer into oocytes and early-stage embryos at the time of fertilization. This non-invasive approach can overcome the high costs and complexity of traditionally applied micromanipulation techniques, and facilitate non-invasive genetic modification, targeted bioimaging, and the supplementation of specific molecular deficiencies associated with aberrant fertilization or embryo development. However, despite the overall encouraging findings, these experiments highlighted a number of important issues. Firstly, binding rates between sperm and MSNPs remain at a relatively low level throughout incubation, justifying the need to develop strategies to promote MSNP-sperm binding or selection of the MSNP-sperm bound population. Secondly, although the prototypes of molecular cargo were used in this set of experiments to demonstrate the feasibility of loading and the potential effects of such loading upon the toxicity profiles of MSNPs, the delivery capacity of MSNPs was not evaluated specifically. Finally, lack of evidence supporting the possibility for spontaneous penetration of MSNPs into oocytes during incubation, and the technically challenging nature of microinjection-assisted delivery of MSNPs into these cells, resulted in the research focus for the rest of this thesis shifting predominantly to sperm.

CHAPTER 4

EVALUATION OF STRATEGIES TO IMPROVE BINDING RATES BETWEEN SPERM AND MESOPOROUS SILICA NANOPARTICLES

Key messages:

- This chapter presents the results of experiments investigating three independent strategies to increase binding rates between MSNPs and sperm over those previously reported in Chapter 3. These strategies include: (1) sorting of MSNP-bound sperm from the total sperm fraction using density gradient washing; (2) passive targeting via modification of the size of MSNPs and (3) active targeting via the absorption of specific cell-penetrating peptide C105Y with affinity towards moieties on the surface of MSNPs
- Passive and active targeting of MSNPs towards sperm did not affect the biocompatibility of MSNPs with male gametes
- Both targeting strategies appeared to be incapable of promoting binding of particles with a larger proportion of sperm within the total population, although they facilitated earlier ‘saturation’ of MSNP-sperm binding rates
- Active targeting of MSNPs towards sperm with C105Y represented the most efficient and technically straightforward technique, which allowed to achieve a significantly quicker ‘saturation’ of MSNP-sperm binding rate
- The value of density gradient washing for selection of MSNP-bound sperm remained limited, which additionally highlighted that MSNPs bound with sperm regardless of the first-line parameters of their function

4.1. BACKGROUND

The patterns of interaction between cells and nanomaterials, including uptake mechanisms, intracellular fate and elimination pathways, are fundamentally dependent upon the physicochemical properties of the nanomaterial, including size, shape, surface charge, surface coating and the presence of ligands for active targeting (Petros and DeSimone, 2010; Kunzmann *et al.*, 2011). Intentional manipulation of these parameters would allows us direct nanocarriers to a specific population of cells and promote more specific interaction with a particular cell type. The first set of experiments, described in **Chapter 3**, showed that boar sperm spontaneously bound with MSNPs during incubation *in vitro*, although the proportion of sperm binding with particles fluctuated around a mean value of 20% throughout incubation, regardless of the type, dose and duration of exposure to MSNPs. Quantification of the proportion of sperm binding to nanoparticles out of the total number of sperm in the sample was not carried out previously, and, therefore, interpretation of this number as 'high', 'low' or 'acceptable' remains difficult. Nevertheless, to optimise the technique of nanomaterial-mediated delivery into gametes and, especially, sperm-mediated transfer of compounds into oocytes, it appears logical to develop strategies increasing the proportion of MSNP-bound sperm in samples. Such strategies include: sorting of MSNP-bound sperm from the total sperm fraction, passive targeting via modification of the physicochemical properties of MSNPs, and active targeting via absorption of specific moieties on the surface of MSNPs, which promote binding with sperm.

4.1.1. SORTING OF SPERM ASSOCIATED WITH MSNPS USING DENSITY GRADIENT WASHING

Discontinuous density gradient washing (DGW) is an established procedure for sperm preparation for assisted reproduction in a variety of biological species (Natali, 2011). DGW involves layering of a sperm sample onto a one- or two-layer silica microbead gradient with specific density, and brief centrifugation of the sample, followed by the collection and washing of resulting pellet. The pellet, representing the fraction of 'best-quality' sperm, separated from immotile, dead, immature and

senescent sperm and other cell debris (epithelial cells, white blood cells, bacteria), is then used for downstream applications such as artificial insemination, IVF or ICSI **(Figure 4–1)**.

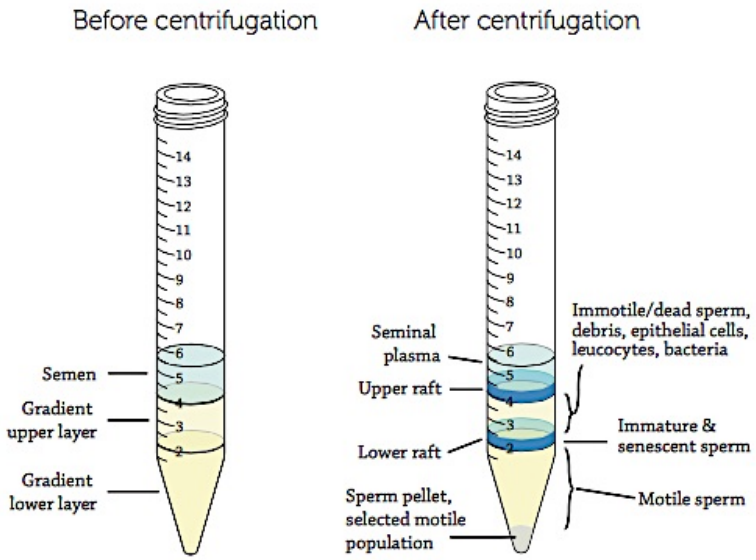

***Figure 4-1* – Density gradient preparation of sperm in a two-layer gradient.** After centrifugation, a pellet containing a selected motile sperm population is formed. Seminal plasma, immotile, dead, immature and senescent sperm, and cell debris, are retained in the various layers of the gradient. (Image sourced from www.nidacon.com, accessed on 16/06/2015).

The specific choice of DGW as a sorting tool for selecting MSNP-bound sperm was motivated by two main factors. Firstly, this technique is quick, inexpensive, does not require dedicated costly laboratory equipment such as a flow cytometer and special training in its use, and can be easily integrated into the existing workflow of ART laboratories. This coincides with the vision of nanomaterials in reproductive science settings as tools to compliment existing procedures in a simple and inexpensive way. Secondly, the technique of fluorescence-activated cell sorting (FACS), an established tool for sperm separation into subpopulations in the field of animal breeding, is known to be unsuitable for boar sperm, the animal model used throughout this thesis. In boars, the multi-step protocol of sperm processing during FACS, involving exposure to laser beam and high pressure, and mechanical damage, results in low sperm concentrations and poor survival (Bonet *et al.*, 2013). Therefore, the use of this costly technique, in its current form, would not add substantial value to the methodology of nanoparticle-mediated delivery into gametes in this particular animal model. Finally, from a purely research perspective, the use of DGW would allow a fast and simple method to assess whether binding of MSNPs with sperm is restricted to a sperm

population with particular functional properties such as motility, viability, or maturity, and, if this is the case, whether this population of sperm is suitable for downstream use.

4.1.2. MODIFICATION OF THE PHYSICOCHEMICAL PROPERTIES OF MSNPS FOR PASSIVE TARGETING TOWARDS SPERM

Passive targeting of nanomaterials is achieved via modification of their size, shape, surface charge and coating, and plays an important role in the facilitation of nanoparticle-cell interaction. Physicochemical properties of nanomaterials can determine the mechanisms of their uptake, intracellular localisation and subsequent fate. For example, small nanomaterials (~20 nm) can be internalised via pinocytosis, while larger nanoparticles can undergo scavenger receptor-, caveolin-, or clathrin-mediated endocytosis depending on the nature of nanomaterial. In addition, carbon nanotubes have been reported to effectively cross the plasma membrane via non-energy-dependent mechanisms, such as diffusion and penetration (Kunzmann *et al.*, 2011) (**Figure 4–2**). With regards to intracellular localisation and subsequent elimination, nanoparticles internalised by somatic cells via endocytotic pathways and entering the endolysosomal system, undergo gradual enzymatic degradation and then are exocytosed from the cell (Albanese *et al.*, 2012). Nanomaterials with free cytoplasmic localisation, on the contrary, are noticeably more robust and can be transmitted to new cell generations after random distribution during mitosis (Rees *et al.*, 2011).

The diameter of MSNPs applied during the experiments described in **Chapter 3** (~138nm) fell within a range of ~50nm to ~450nm, previously characterised as being optimal for intracellular uptake in somatic cells, and was close to the target value of ~100nm for MSNPs (Gan *et al.*, 2012). However, the significantly smaller size of sperm compared to somatic cells could render this specific modification of MSNPs not entirely suitable for this particular cell type. Indeed, most nanomaterials, which have been applied for intra-sperm delivery of molecular cargo thus far, were characterised by a significantly smaller size, ranging, in general, from 5 to 50 nm (**Table 4–1).** Therefore, production of smaller MSNPs for use in sperm could represent a well-justified strategy in order to improve MSNP-sperm binding.

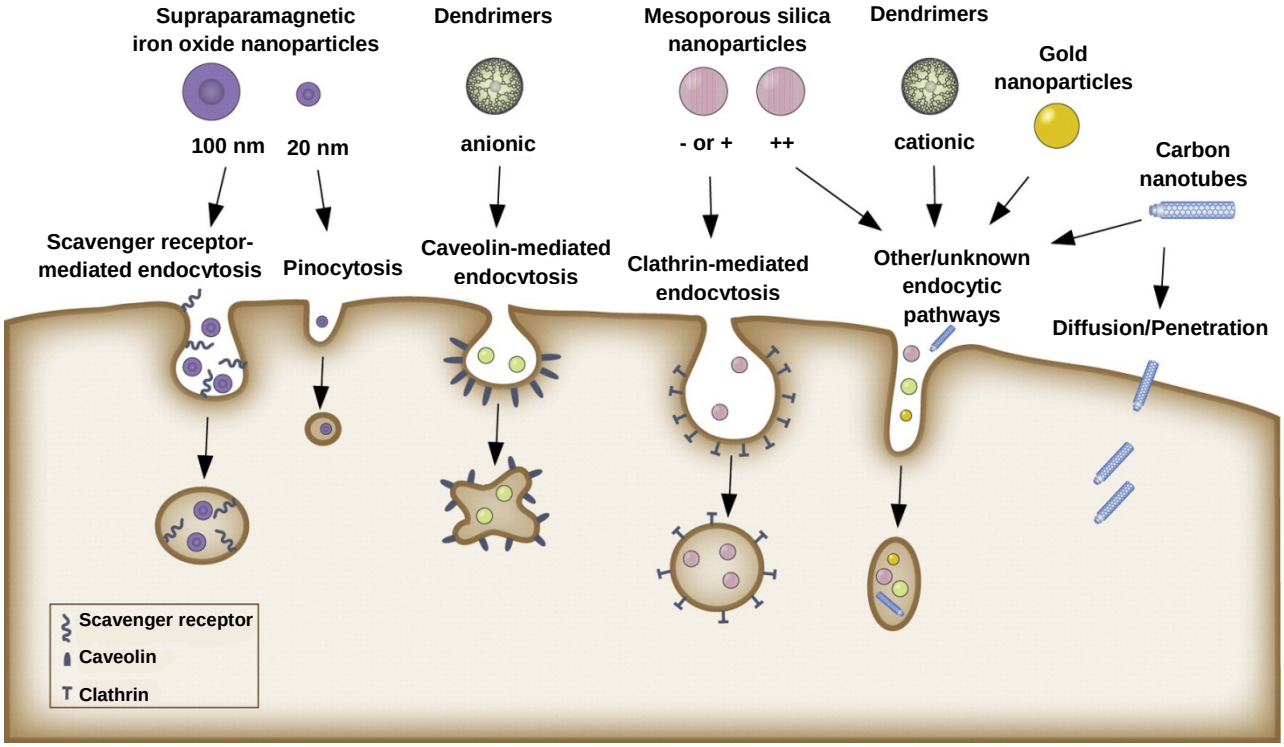

***Figure 4-2* – Mechanisms of intracellular internalisation of nanomaterials.** Nanomaterials undergo internalisation into cells via various intrinsic mechanisms of intracellular uptake. The specific route of internalisation is highly dependent upon the nature, size and surface chemistry of nanomaterials (illustration adapted and modified from Kunzmann *et al.* (2011)).

***Table 4-1* – Nanoparticle-mediated delivery into gametes and cell-labelling *in vitro*: experimental studies in animal models**

Study	Nanomaterial	Size	Application
Makhluf *et al.* (2008)	Polyvinylalcohol-coated magnetic iron oxide NPs (Fe_3O_4)	11±2 nm	Proof-of-principle transfer of anti-protein kinase C-antibody into sperm
Kim *et al.* (2010)	Magnetic NPs (commercial agent)	N/A ~10nm*	Facilitation of SMGT
Campos *et al.* (2011)	PLGA nanopolymer (commercial agent)	N/A	Facilitation of SMGT (‘NanoSMGT’)
Campos *et al.* (2011)	PLGA nanopolymer (commercial agent) and halloysite clay nanotubes (HCN)	N/A HCN: ~50 nm§	Facilitation of SMGT (‘NanoSMGT’)
Feugang *et al.* (2012)	CdSe/ZnS quantum dots	~5-7nm	‘Live’ bioimaging of sperm
Odhiambo *et al.*. (2014)	Magnetic iron oxide NPs (Fe_2O_3)	N/A 50nm or 250nm§	Magnetic removal of defective sperm subpopulation from the ejaculate (‘nanopurification’)
Feugang *et al.* (2015)	CdSe/ZnS quantum dots	8.2±1.7 nm	‘Live’ bioluminescence imaging of mammalian gametes
Barchanski *et al.* (2015)	Nanogold	5-45nm	Proof-of-principle investigation of the potential to label the specific DNA sequences in viable sperm

Symbol (*) denotes approximation from the TEM images of particles bound to sperm; symbol (§) denotes information obtained from the manufacturer’s product characteristics

4.1.3. FUNCTIONALISATION OF MSNPS WITH A SPERM-SPECIFIC CELL-PENETRATING PEPTIDE FOR ACTIVE TARGETING TOWARDS SPERM

Functionalisation of the surface of nanomaterials with specific affinity ligands, including antibodies, aptamers, proteins, peptides, and small molecules, which selectively bind with specific surface receptors in a target cell population, represents a common approach for improving the accuracy of both cargo transport and uptake, and minimising off-target interaction (Lehner *et al.*, 2013). Although active targeting is widely used in the design of nanomaterials for systemic applications, its benefits for the *in vitro* delivery of cargo into gametes have not been extensively studied. Successful active targeting in gametes requires careful selection of affinity ligands which would not interact with gamete surface receptors involved in fertilization and thus result in their premature activation or inhibition. This requirement could limit the use of traditional functionalisation tools, such as antibodies, and require the use of alternative targeting moieties, among which cell-penetrating peptides represent a particularly interesting option.

Cell-penetrating peptides (CPPs) are a specific class of short cationic/amphipathic peptides (<30 amino acids) with the remarkable ability to translocate across the plasma membrane in a receptor- and energy-independent manner, and are able to transport a considerably larger molecular cargo into cells (Patel *et al.*, 2007; Jones and Sayers, 2012). CPPs represent a relatively novel class of functionalisation agents for nanomaterials, with the first studies into the effects of CPP coating upon nanomaterial uptake commencing around fifteen years ago (Santra *et al.*, 2004). Nevertheless, over the last 10 years, CPP-functionalised nanomaterials have been consistently shown to exhibit improved cellular uptake in a variety of cell types, and are currently being proposed as a promising alternative to more conventional active targeting moieties (Farkhani *et al.*, 2014; Shi *et al.*, 2014). In addition, a number of CPPs have been described as possessing affinity towards mammalian gametes and embryos, with several CPPs also demonstrating promising delivery capacity (**Table 4–2**).

***Table 4-2*– Cell-penetrating peptides with affinity towards reproductive tissues and gametes and their delivery potential**

Author	Peptide	Target	Intracellular translocation	Delivery potential
Jones *et al*. (2013)	Penetratin	Bovine sperm	Yes	No
	Tat		Yes	No
	C105Y		Yes	N/A
	Mitoparan		Yes	N/A
	Inverso mitoparan		Yes	N/A
	Inverso mastoparan		Yes	N/A
	Transportan 10		Yes	N/A
Yang *et al.* (2014)	Poly-arginine 11R	Fish (*Takifugu rubripes*) spermary cells	Yes	Yes (Biologically active Oct4)
Kwon *et al.* (2013)	Human papillomavirus L1 capsid protein (LDP12)	Mouse oocytes and embryos	Yes	Yes (EGFP)
Yang *et al.* (2014)	7X-arginine (R7)	Mouse oocytes and embryos	Yes	Yes (Estrogen related receptor β)
Campelo *et al.* (2014)	Crotamine	Bovine embryos	Yes	N/A

Recently, a 17-amino acid synthetic poly-cationic peptide known as C105Y (CSIPPEVKFNKPFVYLI, Mw = 1994.41 g/mol) (Rhee and Davis, 2006), has been characterised as displaying high affinity towards mammalian sperm (Jones *et al.*, 2013). The structure of C105Y is based on the amino acids 346-374 of α1-antitrypsin, and this peptide was initially discovered as a sequence within its C-terminus, which that could facilitate binding with the serpin enzyme complex receptor and intracellular uptake of α1-antitrypsin (Perlmutter *et al.*, 1990). C105Y has been shown to internalise by an energy independent process via lipid rafts and promote DNA transfer into target cells (reviewed by Rhee and Davis, 2006). C105Y was later demonstrated to have encouraging safety profiles in mammalian sperm, and predominantly distribute in the non-acrosomal portion of the sperm head and mid-piece (Jones *et al.*, 2013). C105Y has low toxicity and accumulates in the sperm head, but not in the acrosomal and equatorial regions, which are involved in the earliest stages of fertilization: binding with the *zona pellucida*, exocytosis of acrosomal granules, and binding of the sperm post-acrosomal membrane with the oolemma. These features render C105Y an attractive candidate for the surface functionalisation of nanocarriers for intra-sperm delivery.

This Chapter presents the results of three sets of experiments investigating independent strategies to increase binding rates between MSNPs and sperm in excess of the mean value of 20%, observed in **Chapter 3**. Importantly, these strategies were designed to be applicable to routine laboratory practice to allow their easy integration into the conventional ART laboratory workflow. Findings presented in this Chapter demonstrate that binding of MSNPs with boar sperm during *in vitro* exposure primarily occurred within a specific subset of boar sperm, which cannot be simply assigned to a certain functional category ('motile', 'viable', 'acrosome-reacted'). In addition, this binding occurred independently of the physicochemical properties of MSNPs, such as size, surface coating and presence of targeting moieties, although the reduction in MSNP size and use of active targeting facilitated the earlier formation of MSNP-sperm associations. Collectively, these results indicated the potential for passive and active targeting, but not simple first-line tools for sperm selection, to improve the outcomes of nanoparticle-mediated delivery into gametes.

4.2. SPECIFIC DETAILS OF EXPERIMENTAL PROCEDURES AND DATA ANALYSIS

The general materials and methods used herein are described in **Chapter 2**. Specific details of the experimental procedures highlighted in this subsection relate to: (1) density gradient selection of MSNP-bound sperm; (2) exposure of MSNPs (< 50nm) to boar sperm; and (3) exposure of MSNPs (> 100nm), functionalised with C105Y, to boar sperm. Flowchart outlining the experiments performed in this Chapter is presented in **Figure 4–3**.

4.2.1. DENSITY GRADIENT SELECTION OF MSNP-ASSOCIATED SPERM

For this set of experiments, 1ml aliquots were withdrawn from each boar sperm sample, centrifuged at 500g for 10 minutes, washed from the extender with PBS (Oxoid, UK), resuspended in PBS to 500µl and treated with unmodified, PEI-coated and APTES-coated MSNPs (~138nm) at the previously optimised dose of 10µg per 10^7 sperm or PBS (controls). Incubation was carried out for up to 4 hrs.

Density gradients were prepared using the PureSperm 40/80 kit (Nidacon International AB, Sweden) in accordance with the manufacturer's instructions. Specifically, 2ml of PureSperm 80%

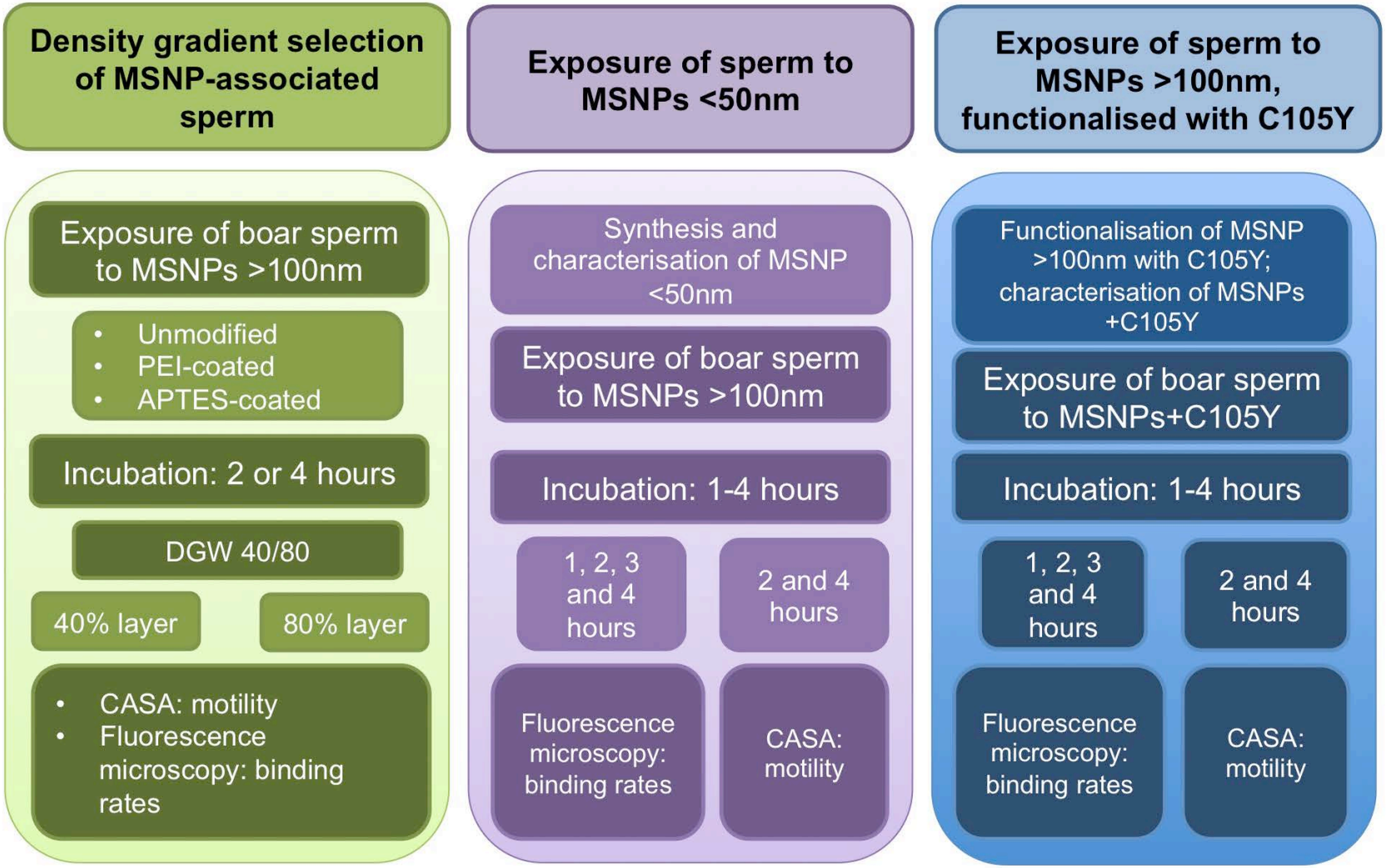

Figure 4-3 – Flowchart outlining the experiments performed for evaluation of strategies to improve binding rates between sperm and mesoporous silica nanoparticles. CASA included quantification of total and progressive sperm motility, and kinematic parameters. MSNPs: mesoporous silica nanoparticles; DGW: density gradient washing; CASA: computer assisted sperm analysis.

was overlaid with 2ml of PureSperm 40% in a 15ml conical tube. After 2 and 4 hours of incubation, experimental and control sperm samples adjusted to 1ml with PBS, were loaded onto individual density gradients and centrifuged at 300g for 20 minutes. After centrifugation, the 40% layer of the gradient was transferred into clean microtubes. The 80% layer was discarded, apart from the bottom fraction, which was covering the pellet. The pellet was thoroughly mixed with the remaining fraction of PureSperm 80%, transferred into a clean microtube and resuspended in washing medium (PureSperm Wash, Nidacon International AB, Sweden) to 1ml. All samples were centrifuged at 500g for 10 minutes. After centrifugation, the supernatant was removed, and the pellets obtained from the 40% and 80% layers of the gradient were resuspended in 50µl and 400µl of PureSperm Wash, respectively. Sperm motility and binding rates with MSNPs in the 40% and 80% layers of the gradient were assessed after 2 and 4 hrs of incubation in accordance with the standard procedure. Given the high degree of concordance between the total motility values obtained during CASA and viability values obtained using eosin Y staining in the previous set of experiments described in **Chapter 3**, and the absence of effects of ~138nm MSNPs upon sperm viability after *in vitro* exposure, this assessment was omitted from the panel of tests. Similarly, since the sperm kinematic parameters after exposure to ~138nm MSNPs were extensively characterised in the previous Chapter, a detailed analysis of sperm motion within each gradient layer was not carried out.

Data obtained in this set of experiments (**Section 4.2.1.**) were analysed using a generalised linear mixed model (GLMM) with post-hoc sequential Bonferroni adjustment, type of treatment (control/MSNPs), gradient layer and time as fixed factors, and with ejaculate as a random factor.

4.2.2. EXPOSURE OF SPERM TO MSNPS < 50nm IN SIZE

For this set of experiments, 1ml aliquots were withdrawn from each boar sperm sample, centrifuged at 500g for 10 minutes, washed from the extender with PBS (Oxoid, UK), resuspended in BTS (37g dextrose hydrate, 6g sodium citrate dehydrate, 1.25g sodium bicarbonate, 1.25g disodium ethylenediamine tetraacetate, 0.75g potassium chloride, 1000ml DDW; pH 7.33 (Pursel and

Johnson, 1976)) to 500µl and subject to treatment with unmodified MSNPs (<50nm) in the doses of 1µg, 10µg, 15µg and 30µg per 10^7 sperm or BTS (controls). Incubation was carried out for up to 4 hrs. Sperm motility and kinematic parameters were evaluated after 2 and 4 hours of exposure. Binding rates between MSNPs and sperm were evaluated after 1, 2, 3 and 4 hours of incubation.

Data obtained in this set of experiments (**Section 4.2.2.**) were analysed using a generalised linear mixed model (GLMM) with post-hoc sequential Bonferroni adjustment, type of treatment (control/MSNPs), gradient layer and time as fixed factors, and with ejaculate as a random factor. Control samples were used as a reference category for the assessment of motility and motion parameters; binding rates between sperm and C105Y-functionalised MSNPs were compared with retrospective data for unmodified MSNPs (obtained during the course of experiments described in **Chapter 3**).

4.2.3. Exposure of sperm to MSNPs > 100 nm in size, functionalised with C105Y

4.2.3.1. Characterisation of MSNPs (>100 nm) functionalised with C105Y

For this set of experiments, an additional panel of MSNP characterisation tests was performed to permit a more detailed evaluation of the physicochemical properties of MSNPs following functionalisation with C105Y for active targeting. Unmodified and C105Y-functionalised MSNPs were characterised for ζ potential in incubation medium (Beltsville Thawing Solution, BTS, pH 7.33) using electrophoretic light scattering (Zetasizer Nano ZS, Malvern Instruments, UK), and hydrodynamic size and number concentrations of particles were determined in phosphate-based saline (Dulbecco's PBS, Sigma-Aldrich UK, pH 7.4) by nanoparticle-tracking analysis (Nanosight LM10, Malvern Instruments, UK). The number of free amine groups on APTES-coated MSNPs was calculated using a colorimetric reaction with 2% ninhydrin reagent solution (Sigma-Aldrich, UK). Binding of C105Y with APTES-coated MSNPs was confirmed by the spectrophotometric measurement of peptide concentration in solution before and after the reaction (BiophotometerPlus, Eppendorf, UK). The average number of ligands adsorbed on each C105Y-functionalised particle, and the proportion of occupied amine groups, was calculated from the estimated quantity of

adsorbed peptide, particle mass and number concentrations, and the quantity of free amine groups before EDC-mediated cross-linking. To evaluate the potential spatial organisation of C105Y after cross-linking on APTES-functionalised MSNPs, three-dimensional models of the peptide were constructed *in silico* using the PEP-FOLD structure prediction server (Alland *et al.*, 2005; Neron *et al.*, 2009), and analysed in Avogadro v1.1.1 (Hanwell *et al.*, 2012). Particle numbers per sperm were approximated from the known mass and number concentrations of C105Y-functionalised MSNPs.

4.2.3.2. Exposure of sperm to C105Y-functionalised MSNPs (>100 nm)

One-millilitre aliquots were withdrawn from each sample, centrifuged at 500g for 10 minutes, washed from the extender with PBS, and resuspended in 750µl of BTS. Sperm were then treated with C105Y-functionalised MSNPs at a ratio of 10µg, 15µg and 30µg of particles per 10^7 sperm, or free C105Y (0.02mM in 10% acetic acid) in a quantity equivalent to that adsorbed on the MSNPs, or BTS (controls). Incubation was carried out for up to 2 hrs at 37ºC under a low-oxygen atmosphere, in accordance with our previous findings indicating that stable binding of MSNPs to sperm can be observed after as little as 2 hrs of *in vitro* exposure Sperm motility, kinematic parameters and acrosome morphology were assessed after 2 hrs of incubation. Binding rates between sperm and C105Y-functionalised MSNPs were determined after 1 and 2 hrs. Levels of cell fluorescence in sperm exposed to C105Y-functionalised MSNPs, and equivalent doses of free C105Y, were also evaluated after 1 and 2 hrs. Corrected cell fluorescence levels were calculated by subtracting the intensity of background fluorescence from the total pixel intensity value (red channel) in approximately 100 individual morphologically-intact sperm per experimental condition (Burgess *et al.*, 2010), and expressed in arbitrary units (AU) per $1\mu m^2$ of sperm surface. Image processing and analysis was carried out using Fiji/ImageJ 1.48t (Schindelin *et al.*, 2012).

Data obtained in this set of experiments (**Section 4.2.3.**) were analysed using a generalised linear mixed model (GLMM) with post-hoc sequential Bonferroni adjustment and type of treatment (control/C105Y-functionalised MSNPs/free C105Y), dose ratio, and time, as fixed factors, and with

ejaculate as a random factor. For a detailed investigation of the effects of dose and the duration of exposure to C105Y-functionalised MSNPs, or free C105Y, upon individual sperm, GLMM was followed by logistic regression analysis of categorical data (total/progressive motility, proportion of sperm with NAR, and binding rate between sperm and C105Y-functionalised MSNPs), controlled for inter-sample variability. Control samples were used as a reference category for the assessment of motility and morphology parameters; binding rates between sperm and C105Y-functionalised MSNPs were compared with retrospective data for unmodified MSNPs (obtained during the course of experiments described in **Chapter 3**).

4.3. RESULTS

4.3.1. DENSITY GRADIENT SELECTION OF MSNP-ASSOCIATED SPERM

Density gradient selection of MSNP-associated sperm was attempted after 2 and 4 hours of incubation with unmodified, PEI-coated and APTES-coated MSNPs with a physical diameter of ~138nm, in a 10µg per 10^7 sperm ratio. This ratio was previously characterised as minimally effective and sufficient to achieve stable binding with MSNPs in approximately 1 in 5 sperm during *in vitro* exposure.

The type of treatment and gradient layer did not have a significant effect upon total and progressive sperm motility at 2 hours of incubation when compared to time-matched controls (**Figure 4–4A,** $p>0.05$). As anticipated, after 2 hours of incubation, total and progressive sperm motility in the 80% layer were higher compared to 40%, although this difference was not significant. However, at 4 hours of incubation, a significant effect of gradient layer, but not the type of treatment, upon total ($F_{1,19}=18.049$, $p<0.05$) and progressive ($F_{1,19}=19.614$, $p<0.05$) motility was observed. Contrary to the anticipated scenario, motility parameters appeared to be higher in the 40% gradient layer, compared to 80%, both in experimental and control samples (**Figure 4–4B)**.

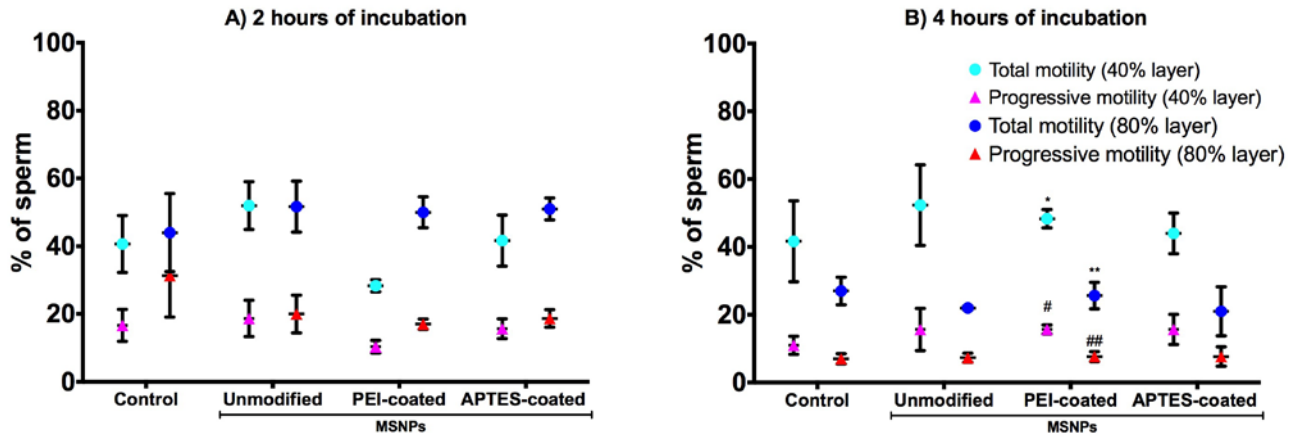

Figure 4-4 – **Proportions of motile and progressively motile boar sperm in the 40% and 80% gradient layers after 2 and 4 hours of exposure *in vitro* to various modifications of MSNPs (~138nm) in a 10µg per 10^7 sperm ratio assessed by CASA** (mean±SEM from three repeats of experiment). Symbols (*, #) denote subsets of categories, whose values are significantly different from each other at the 0.05 level.

Analysis of binding rates between sperm and MSNPs in the two gradient layers for each subtype of MSNPs did not reveal a significant effect of gradient layer or time of incubation upon this parameter for all types of particles ($p>0.05$) (**Table 4–4**). This outcome restricted the use of DGW as a selection tool for MSNP-bound sperm. The profiles of binding between MSNPs and boar sperm remained similar to those previously observed. Specifically, MSNPs bound with sperm produced focal fluorescent signals of variable size in various sperm regions (**Figure 4–5**).

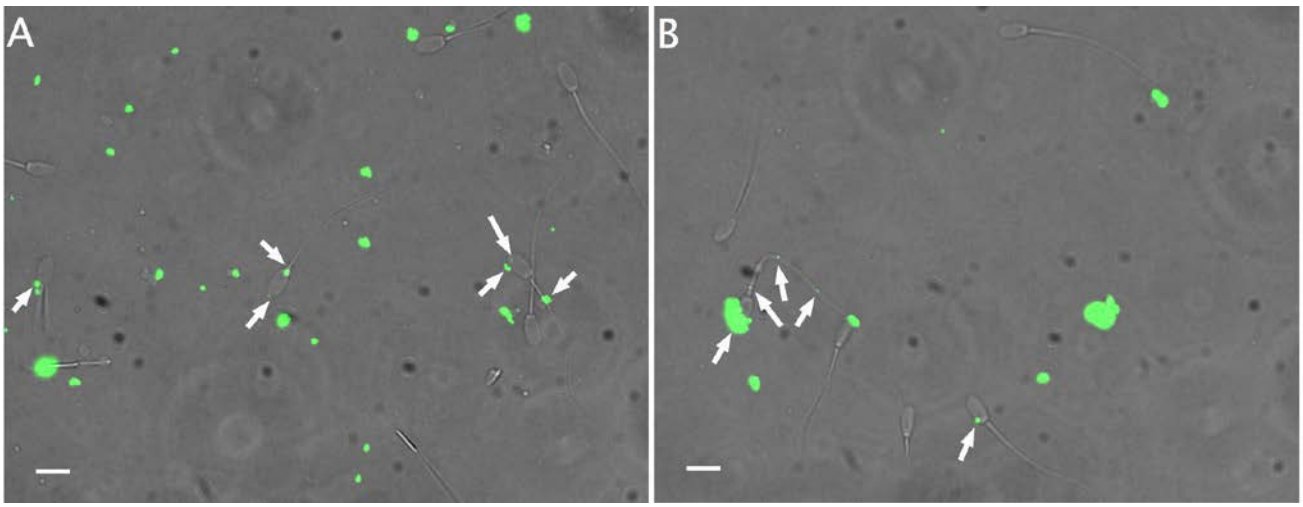

Figure 4-5 **– Binding of unloaded MSNPs with boar sperm after exposure *in vitro* and DGW. A) Representative image of binding of unloaded MSNPs with sperm in the 40% gradient layer; B) Representative image of binding of unloaded MSNPs with sperm in the 80% gradient layer.** Similarly to previous observations, nanoparticles bound with sperm produced focal fluorescent signals in the projection of various sperm regions (white arrows indicate MSNP-sperm associations). Scale bar = 10µm.

***Table 4-3* – Binding rates between sperm and different modifications of MSNPs (~138nm) in the 40% and 80% layers during DGW**

	2 hours			4 hours		
	40% layer	80% layer	P	40% layer	80% layer	P
Unmodified MSNPs	11.9±3.6%	14.8±3.0%	*NS*	24.7±9.2%	21.1±1.7%	*NS*
PEI-coated MSNPs	14.8±7.3%	13.2±4.3%	*NS*	16.5±6.4%	13.2±2.3%	*NS*
APTES-coated MSNPs	22.1±5.9%	24.1±3.5%	*NS*	25.8±10.6%	29.9±5.4%	*NS*

Data presented as mean±SEM from three repeats of experiment; *NS*: not significant (p>0.05)

4.3.2. Exposure of sperm to MSNPs < 50 nm

4.3.2.1. Characterisation of MSNPs

Synthesis of non-fluorescent MSNPs was performed in a surfactant-templated base-catalysed sol-gel reaction, as previously described by Zhu *et al.* (2011). Similarly to the reaction used to produce MSNPs with an average physical diameter of >100nm, this reaction was based upon the mixing or a surfactant template with a silica source in warm aqueous solution with alkaline pH, leading to the assembly of silica nanoparticles, and, finally, removal of the surfactant to expose the porous structure of MSNPs.

Synthesised MSNPs were characterised by electron microscopy. Particles had a mean physical diameter of 24.0±0.4nm, however, the identification of individual MSNPs and their porous architecture was difficult due to high levels of agglomeration on the TEM grids (**Figure 4–6**).

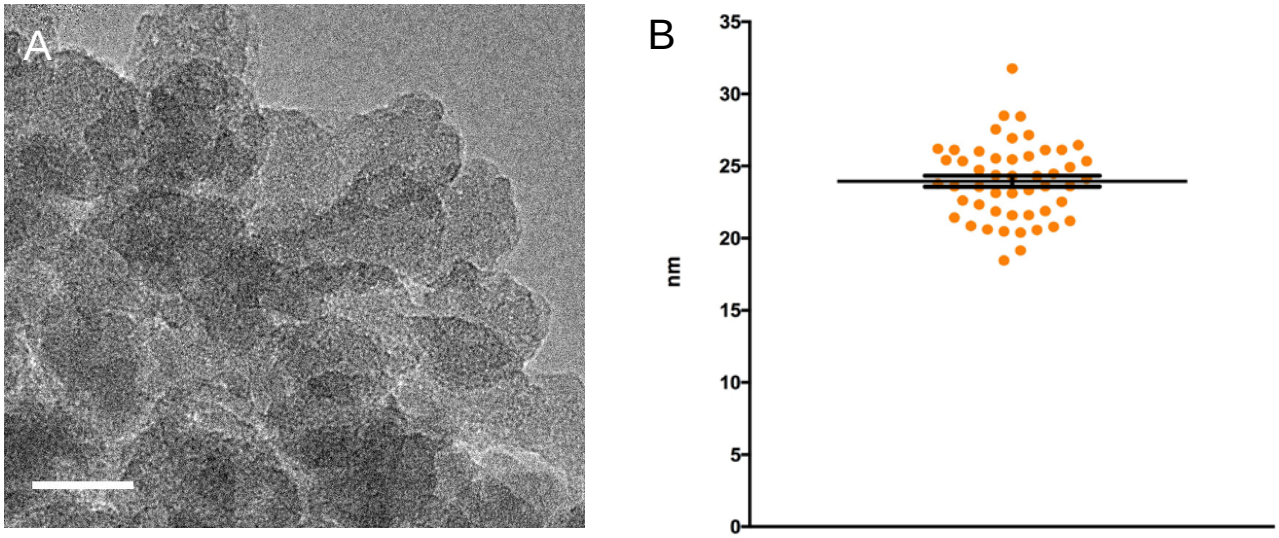

***Figure 4-6* – Characterisation of mesoporous silica nanoparticles (MSNPs).** A) Transmission electron microscopy image of unmodified MSNPs. Scale bar = 0.02µm. B) Size distribution of synthesised unmodified MSNPs: individual measurements of transmission electron microscopy images (mean±SEM from 50 particles). As anticipated, synthesised MSNPs were characterised by a physical size <50nm, but demonstrated the signs of agglomeration.

MSNPs were characterised by an inherently negative ζ potential of unmodified silica (-11.00±9.17mV). Assessment of hydrodynamic diameter in these MSNPs did not yield conclusive outcomes. Specifically, no MSNPs with an anticipated diameter within the 10nm to 100nm range were detected during centrifugation of MSNP suspension through the sucrose gradient. This observation further highlighted the increased propensity of these MSNPs to agglomerate and form larger structures.

4.3.2.2. Sperm motility after exposure to MSNPs < 50nm and MSNP-sperm binding rates

Total and progressive motility were evaluated in sperm samples after 2 and 4 hours of incubation with four dose ratios of MSNPs with a mean physical diameter of 24nm (1, 10, 15 and 30µg of particles per 10^7 sperm) using CASA. There was no significant effect of the type of treatment (MSNPs/control) or dose of particles upon total and progressive motility in sperm exposed to MSNPs (~24nm) at each of the evaluated time points. Moreover, sperm kinematic parameters assessed by CASA were not significantly affected by the type of treatment (MSNPs/control) or dose of particles at 2 and 4 hours of incubation (**Figure 4–7**).

Binding rates between sperm and MSNPs with a mean physical diameter of 24nm in four particle/cell ratios were significantly affected by the dose of the particles ($F_{3,57}$ = 27.706, $p<0.05$), specifically the ratio of 1µg per 10^7 sperm, but not the time of incubation (**Figure 4–8**).

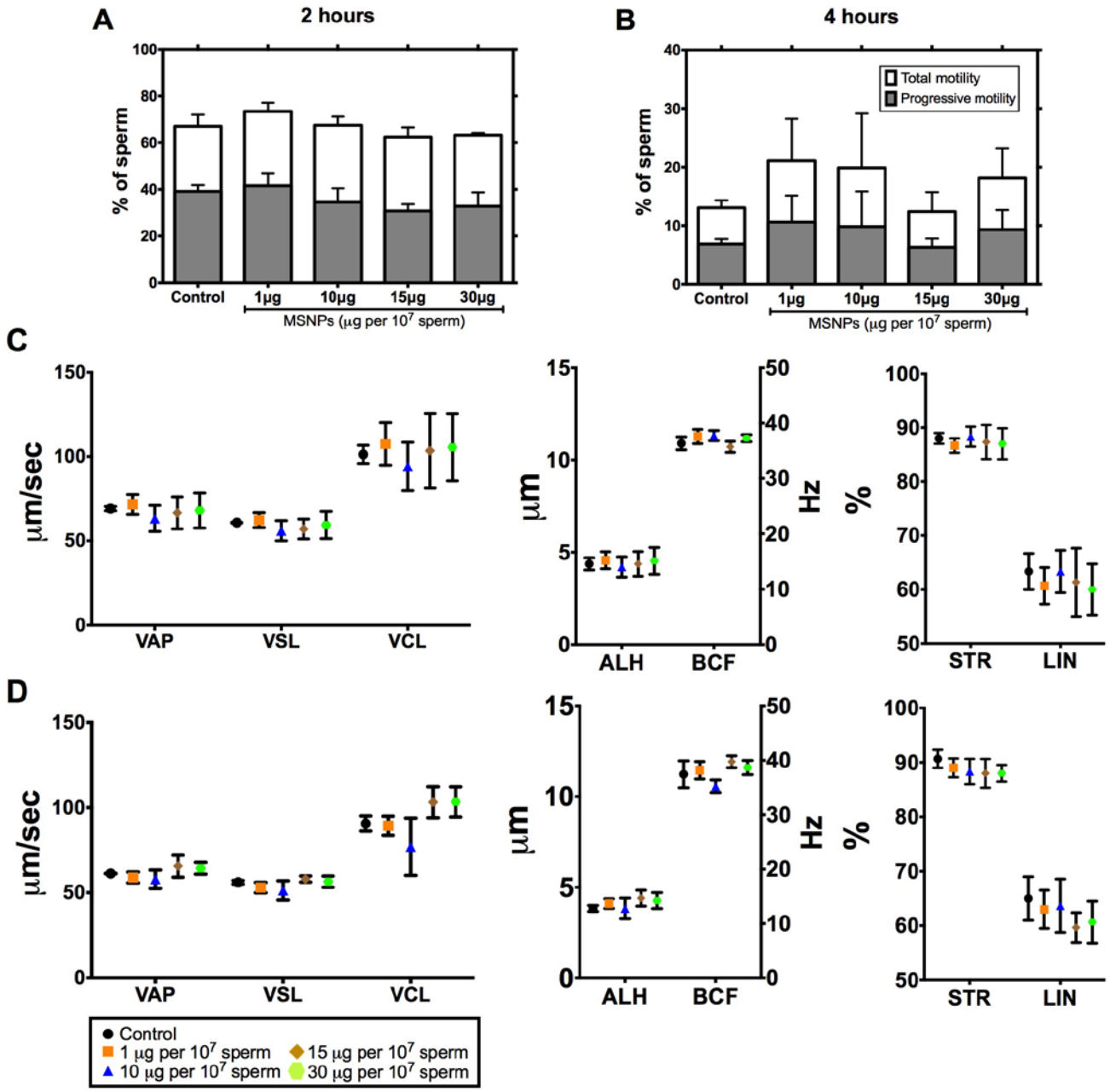

***Figure 4-7* – Motility parameters of boar sperm assessed by CASA after 2 hour and 4 hours of exposure *in vitro* to MSNPs <50nm in four particle/cell ratios (mean±SEM from three samples).** A) Total and progressive motility after 2 hours of exposure; B) Total and progressive motility after 4 hours of exposure C) Sperm motion parameters after 2 hours of exposure; D) Sperm motion parameters after 4 hours of exposure. VAP: smoothed path velocity; VSL: straight line velocity; VCL: track velocity; ALH: amplitude of lateral head displacement; BCF: beat cross frequency. VAP: smoothed path velocity; VSL: straight line velocity; VCL: track velocity; ALH: amplitude of lateral head displacement; BCF: beat cross frequency. STR (ratio of VSL/VAP) = straightness, LIN (ratio of VSL/VCL) = linearity.

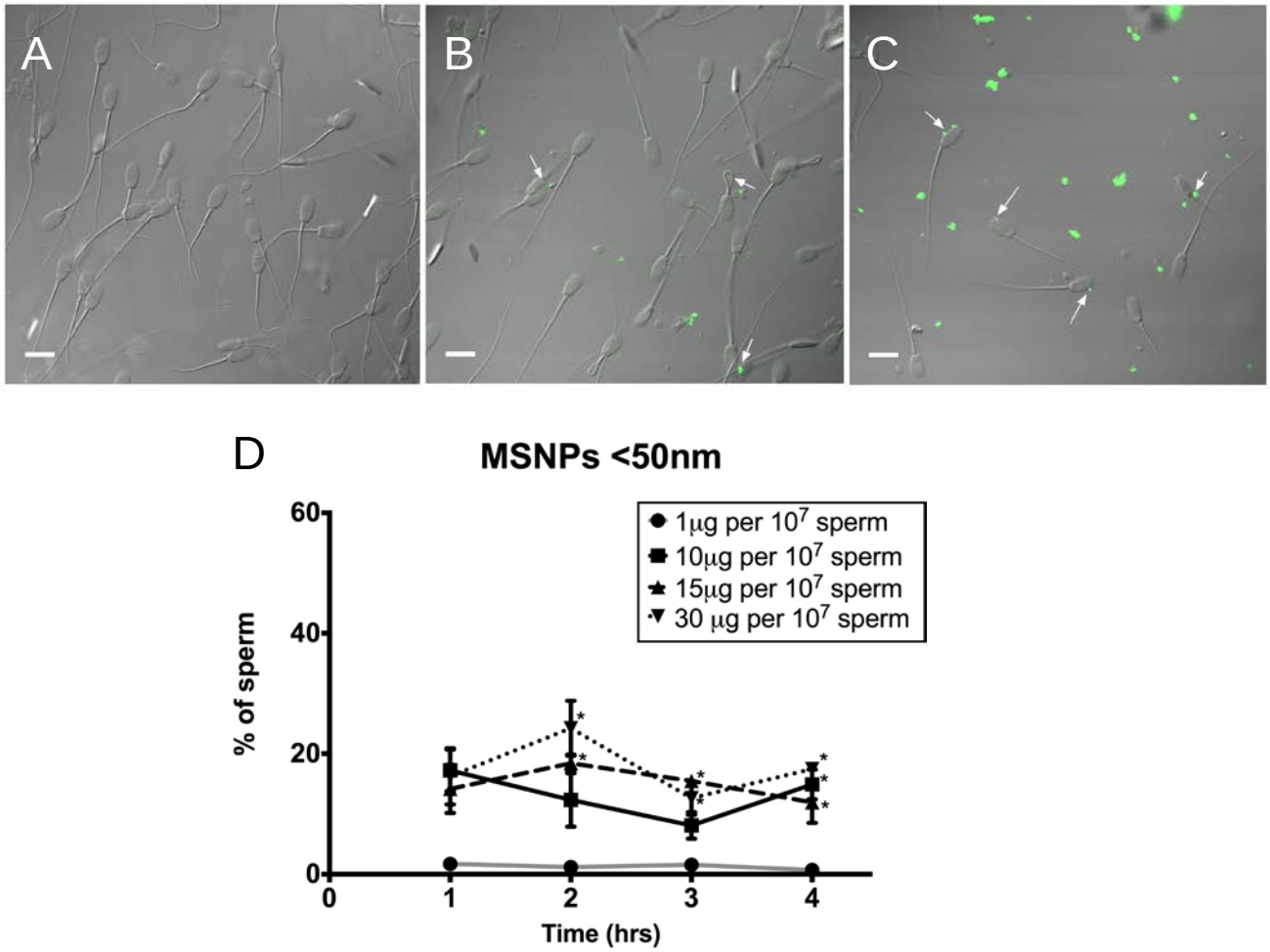

Figure 4-8 **– Binding of MSNPs <50nm with boar sperm after exposure *in vitro*. A) Control; B) Representative image of binding of MSNPs with sperm (1μg per 10^7 sperm ratio). C) Representative image of binding of MSNPs with sperm (15μg per 10^7 sperm ratio). D) Binding rates between boar sperm and MSNPs after 1, 2, 3 and 4 hours of exposure *in vitro* in three particle/cell ratios** (mean±SEM from four repeats of the experiment). Similarly to previous observations, nanoparticles bound with sperm produced focal fluorescent signals in the projection of various sperm regions (white arrows indicate MSNP-sperm associations). Scale bar = 10μm. Symbols (*) denote subsets of categories, whose values are significantly different from the 1μg per 10^7 sperm ratio at the 0.05 level.

The binding rates, observed in this set of experiments utilising 'smaller' MSNPs, remained at the previously observed mean level of ~20% for the particle:cell ratios of 10, 15 and 30 μg per 10^7 sperm, and did not exceed 5% for the smallest particle:cell ratio of 1μg per 10^7 sperm. When the binding rates between sperm and MSNPs <50nm were compared with retrospective data for unmodified MSNPs >100nm, no significant effect of the type of treatment or time of exposure upon this parameter was found. These findings indicated that passive targeting of MSNPs towards sperm via a reduction in their relative size had limited value for improving binding rates compared to the original ~138nm-sized MSNPs. However, the strong possibility for particle agglomeration

represented a serious limitation when interpreting these findings. Interestingly, a trend towards faster 'saturation' of MSNP-sperm binding rate at approximately 20% was observed for 'smaller' MSNPs, compared to ~138nm-sized MSNPs. Specifically, the average binding rates at 1 hour of incubation across all dose ratios for ~24 nm and ~138nm were 15.9±2.2% and 9.4±2.0%, respectively, although the effect did not reach the level of statistical significance.

4.3.3. EXPOSURE OF SPERM TO MSNPS WITH THE SIZE > 100 NM, FUNCTIONALISED WITH C105Y

4.3.3.1. Characterisation of MSNPs (>100nm) functionalised with C105Y

Characterisation data of unmodified MSNPs were reported in **Chapter 3**. In brief, synthesised MSNPs were slightly non-spherical with elongation in the direction of the pore channels, and with ordered nanometre-sized pores displaying hexagonal symmetry when aligned with the beam. Prior to functionalisation with C105Y, MSNPs had an average physical diameter of ~138nm with ~2nm-sized pores. Functionalisation of MSNPs with C105Y had little effect upon ζ potential in incubation medium (-11.23±1.05 mV *versus* -11.57±0.56 mV for unmodified and C105Y-functionalised MSNPs, respectively), and slightly increased their hydrodynamic size in PBS (290±47.2nm *versus* 322±21.5nm for unmodified and C105Y-functionalised MSNPs, respectively), assessed using nanoparticle-tracking analysis. Calculated peptide:MSNP binding ratio was approximately 0.5nmol of C105Y per 10μg of MSNPs or ~$1.4x10^6$ molecules of C105Y per nanoparticle, as estimated from the number concentrations of MSNPs. The average proportion of occupied amine groups on the surface of MSNPs following functionalisation with C105Y, calculated from the ratio between the number of free amine groups before cross-linking and the amount of adsorbed peptide, was ~25%.

Modelling of the possible three-dimensional C105Y configurations *in silico* demonstrated that the approximately 5nm-long string of 17 amino acids could fold into structures measuring ~2.3x1.3x1.5nm and, therefore, approximated the ~2nm pore diameter in synthesised MSNPs

before treatment with APTES. Since the peptide used in this set of experiments was conjugated with TMR (~1nm) (Ebara *et al.*, 2014), resulting in an increase in size, and that MSNPs underwent coating with APTES (~0.9nm), which reduced pore diameter, it was expected that EDC-mediated cross-linking of free amine groups with carboxyl groups in C105Y-TMR was more likely to occur on the surface of the MSNPs, rather than inside the pore channels, thus facilitating the presentation of targeting moieties to sperm.

The previous sets of experiments described in **Chapter 3** did not specifically characterise the number of MSNPs presented to each sperm. This limitation was addressed in this set of experiments, where the number of particles presented to each sperm for all three evaluated dose ratios was estimated based on the known mass concentrations and estimated average number concentrations of C105Y-functionalised MSNPs. As such, the number of C105Y-functionalised MSNPs presented to each sperm in the 10μg of particles per 10^7 sperm ratio was approximated to be in the order of 100. For the 15μg and 30μg of particles per 10^7 sperm ratios, each sperm was exposed to approximately 150 and 300 particles, respectively. Geometric calculations demonstrated that, given that the dimensions of boar sperm head are provisionally 3.5x7μm (ellipse area: ~20μm^2) (Bonet *et al.*, 2013) and the average diameter of the particle is ~138nm (circle area: ~0.015μm^2), nearly 1,330 particles would be required to fully cover the sperm head. Therefore, the ratios of 10μg, 15μg and 30μg of particles per 10^7 sperm would result in coverage of 7.5%, 11.25% and 22.5% of the sperm head in the case of full binding, respectively. It is, however, worth noting that given the possibility of particle agglomeration, the precise number of primary MSNPs presented to each sperm could differ from the values estimated. Therefore, to facilitate more straightforward dosing and consistency of experiments, the dose of MSNPs was continued to be expressed as the mass (μg of MSNPs) per cell number (millions of sperm) ratio.

4.3.3.2. Sperm motility and morphology after exposure to C105Y-functionalised MSNPs and free C105Y

Sperm motility, kinematic parameters and the proportion of sperm with NAR were evaluated using CASA and high-magnification microscopy after 2 hours of incubation with C105Y-functionalised MSNPs at ratios of 10, 15 and 30µg of particles per 10^7 sperm, or equivalent doses of free C105Y, and compared to time-matched controls. Exposure to C105Y-functionalised MSNPs in all nanoparticle/sperm ratios, and equivalent doses of free C105Y, did not result in a significant negative effect upon the total or progressive motility of boar sperm on a population level across all samples (**Figure 4–9A** and **Figure 4–9B**). Neither treatment resulted in a significant change in the kinematic parameters of sperm, compared to time-matched controls (**Figures 4–9D)**. Similarly, a proportion of sperm with NAR, evaluated by high-magnification light microscopy, approximated the reference threshold of 80% across all experimental groups exposed to C105Y-functionalised MSNPs, or free C105Y, and did not deviate significantly from the control group (**Figure 4–9C**).

Interestingly, a separate logistic regression analysis of individual boar sperm data (N=19,880) demonstrated a protective effect of both C105Y-functionalised MSNPs, and free C105Y, upon total sperm motility (**Table 4–4**). The probability for an individual sperm to exhibit motility after 2 hours of incubation with MSNPs+C105Y, or free C105Y, *versus* time-matched controls increased by almost 18% (Odds ratio (OR): 1.177; $p<0.05$) and 20% (OR: 1.203; $p<0.05$), respectively. Similarly, a one-unit increase of the dose of MSNPs+C105Y/free C105Y resulted in an approximately 1% (OR: 1.008) increment in the probability of observing motility in an individual sperm. In contrast, for progressive motility, exposure to C105Y-functionalised MSNPs, but not free C105Y, significantly reduced the likelihood for an individual sperm to move in a progressive fashion after 2 hours of incubation (-15.2%; OR: 0.848; $p<0.05$), compared to controls. This observation prompted further assessment of the effect of both experimental agents upon the sub-proportions of ‘rapid’ sperm, which move within the same velocity range, but in a less straight fashion (VSL/VAP<45%). In this analysis, no significant effect of either C105Y-functionalised MSNPs, or free C105Y, was demonstrated with regard to the probability of an individual sperm

exhibiting 'rapid' motility. Collectively, these findings could indicate that on an individual sperm level, binding of C105Y-functionalised MSNPs prevented sperm from moving at the highest velocity with straight-line trajectory ('progressive'), but did not affect the probability of sperm to exhibit motility in general, including the 'rapid' classification.

Exposure to C105Y-functionalised MSNPs also served as a protective factor for boar acrosome morphology. In logistic regression analysis of data from 2,220 individual sperm, the probability of sperm to demonstrate a NAR following incubation with C105Y-functionalised MSNPs increased by 75% (OR: 1.750, $p<0.05$) *versus* controls. No similar effect was observed in the free C105Y group.

Table 4-4 **– Odds ratios for observing motility, progressive motility and normal apical ridge in individual sperm after 2 hours of exposure to C105Y-functionalised MSNPs or free C105Y***

Outcome		Odds Ratio	95% Confidence Interval for Odds Ratio		P
			Lower	Upper	
Motility[a] (N=12450)	Type:				0.004
	MSNPs+C105Y	1.177	1.060	1.307	0.002
	Free C105Y	1.203	1.073	1.349	0.002
	Dose	1.008	1.004	1.013	0.000
Progressive motility[b] (N=4197)	Type:				0.024
	MSNPs+C105Y	0.848	0.751	0.958	0.008
	Free C105Y	0.896	0.788	1.018	*NS*
	Dose	1.001	0.996	1.006	*NS*
Rapid sperm[c] (N=4569)	Type:				*NS*
	MSNPs+C105Y	0.945	0.839	1.063	*NS*
	Free C105Y	0.980	0.866	1.110	*NS*
	Dose	1.001	0.996	1.005	*NS*
Normal apical ridge[d] (N=1739).	Type:				0.000
	MSNPs+C105Y	1.750	1.137	2.694	0.011
	Free C105Y	0.905	0.596	1.377	*NS*
	Dose	1.001	0.987	1.016	*NS*

* Control group used as a reference category; NS: not significant. Analysis included individual motility data for 19,880 sperm, and individual acrosome morphology data for 2,220 sperm. [a] $\chi^2_7 = 1027.955$, $p<0.05$, correct classification: 63.5% of cases; [b] $\chi^2_7 = 747.513$, $p<0.05$, correct classification: 75.8% of cases; [c] $\chi^2_7 = 600.749$, $p<0.05$, correct classification: 73.7% of cases; [d] $\chi^2_5 = 35.720$, $p<0.05$; correct classification: 82.2% of cases.

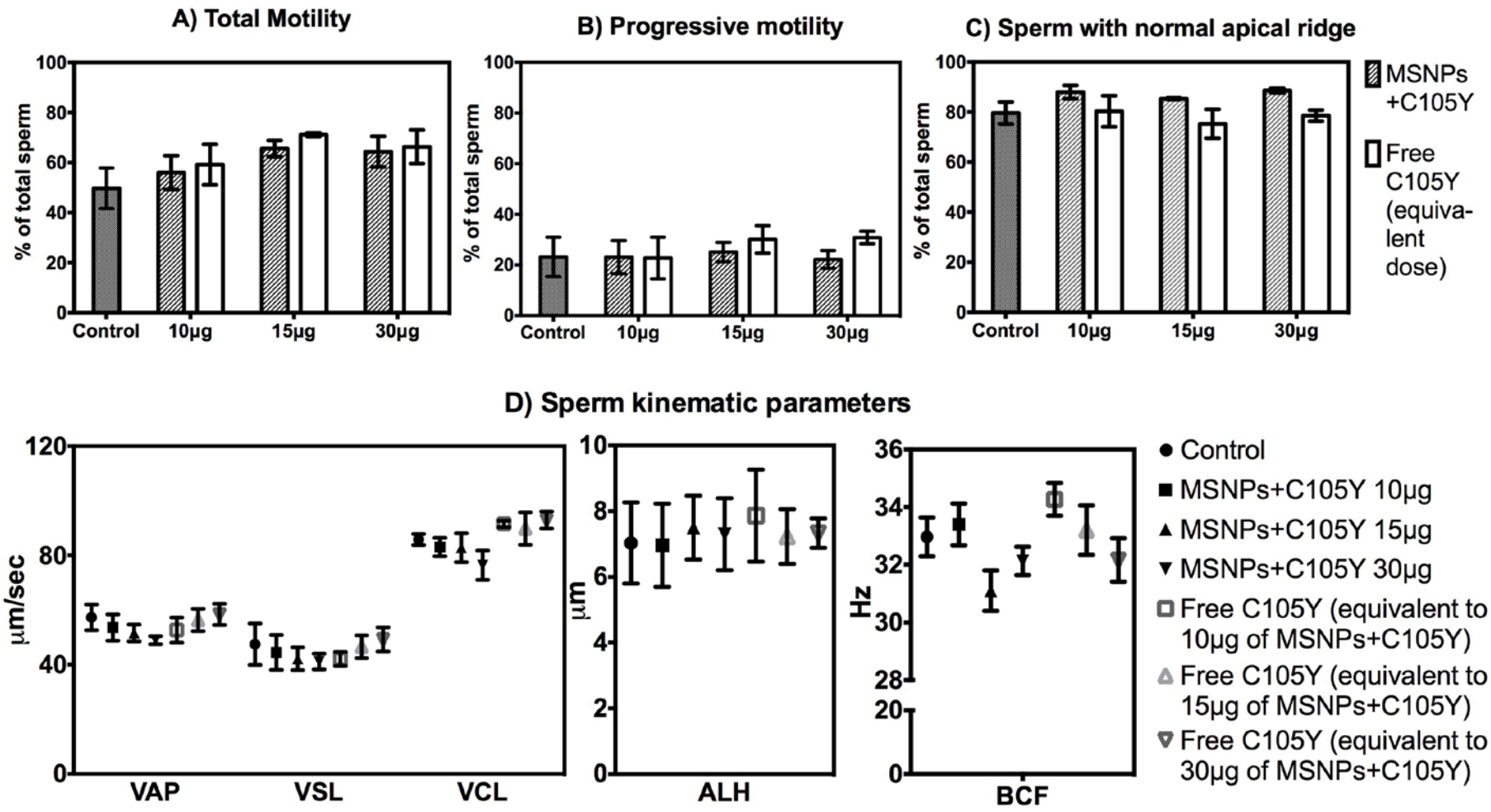

***Figure 4-9*– Motility, kinematic parameters and acrosome morphology of boar sperm assessed by CASA and high-magnification microscopy after 2 hours of exposure to C105Y-functionalised MSNPs in various particle/cell ratios or equivalent doses of free C105Y.** VAP: smoothed path velocity; VSL: straight line velocity; VCL: track velocity; ALH: amplitude of lateral head displacement; BCF: beat cross frequency. For motility and kinematic parameters, data are presented as mean ± SEM from five samples for controls and MSNPs+C105Y, and three samples for free C105Y. For acrosome morphology, data presented as mean ± SEM from three samples control and experimental samples. On the sample level, sperm motility, morphology and kinematic parameters after exposure to C105Y-functionalised MSNPs/free C105Y remained unaltered, compared to time-matched controls ($p>0.05$).

4.3.3.3. Binding of C105Y-functionalised MSNPs with sperm

Binding rates between boar sperm and C105Y-functionalised MSNPs were assessed after 1 and 2 hours of exposure, in accordance with our previous findings, indicating that stable adsorption of MSNPs to the sperm surface occurred after just 2 hours of incubation *in vitro*. Similarly to our earlier observations, C105Y-functionalised MSNPs bound to various sperm regions, including the head, mid-piece and tail, and emitted sharp and focused fluorescent signals on a dark or homogenously stained fluorescent background of variable intensity (**Figure 4–10**). In some sperm, binding of C105Y-functionalised MSNPs followed a distinctive localisation profile of free C105Y, which demonstrated high affinity towards the post-equatorial region of the sperm head and posterior ring (junction of head and mid-piece).

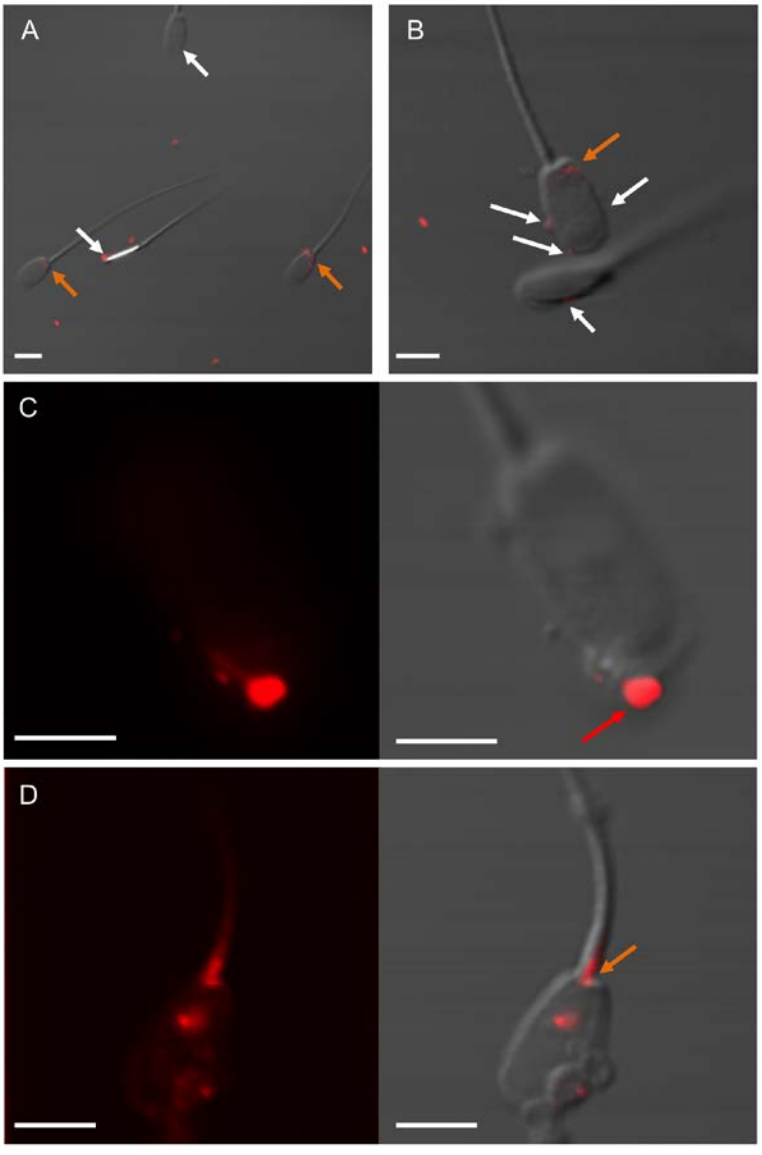

***Figure 4-10*– Binding of C105Y-functionalised MSNPs with boar sperm**. Scalebar = 5 µm. A-B) C105Y-functionalised MSNPs associated with sperm emit sharp and focused fluorescent signals in the projection of various sperm regions (white arrows indicate MSNP-sperm associations; orange arrows indicate associations in post-equatorial region of the head and posterior ring). C-D) Binding of C105Y-functionalised MSNPs with sperm. MSNPs bind to the sperm head and midpiece, and produce a sharp fluorescent signal on a dark or homogenously stained fluorescent background (red arrow indicates a large agglomerate of MSNPs).

Binding rate between sperm and C105Y-functionalised MSNPs was significantly dependent upon the dose of nanoparticles ($F_{1,19}$=20.600, p<0.05), but not the time of exposure (**Figure 4–11**). An increase in particle/sperm ratio from 10μg to 30μg per 10^7 sperm improved the binding rate at both incubation time points by almost a third (23.7±2.7% vs 38.3±0.6% at 1 hour, and 25.4±1.8% vs 35.9±2.2% at 2 hours). At the same time, an increase in the duration of incubation from 1 to 2 hours did not markedly enhance particle-sperm binding. Analysis of individual sperm data (N=4,749, χ^2_6 = 97.924, p<0.05, correct classification: 68.3% of cases) further confirmed these findings, indicating that the probability of observing binding with C105Y-functionalised MSNPs in an individual sperm increased by almost 3% for each one-unit increment of the applied dose of C105Y-functionalised MSNPs (OR: 1.028; 95%CI [1.020-1.035]; p<0.05).

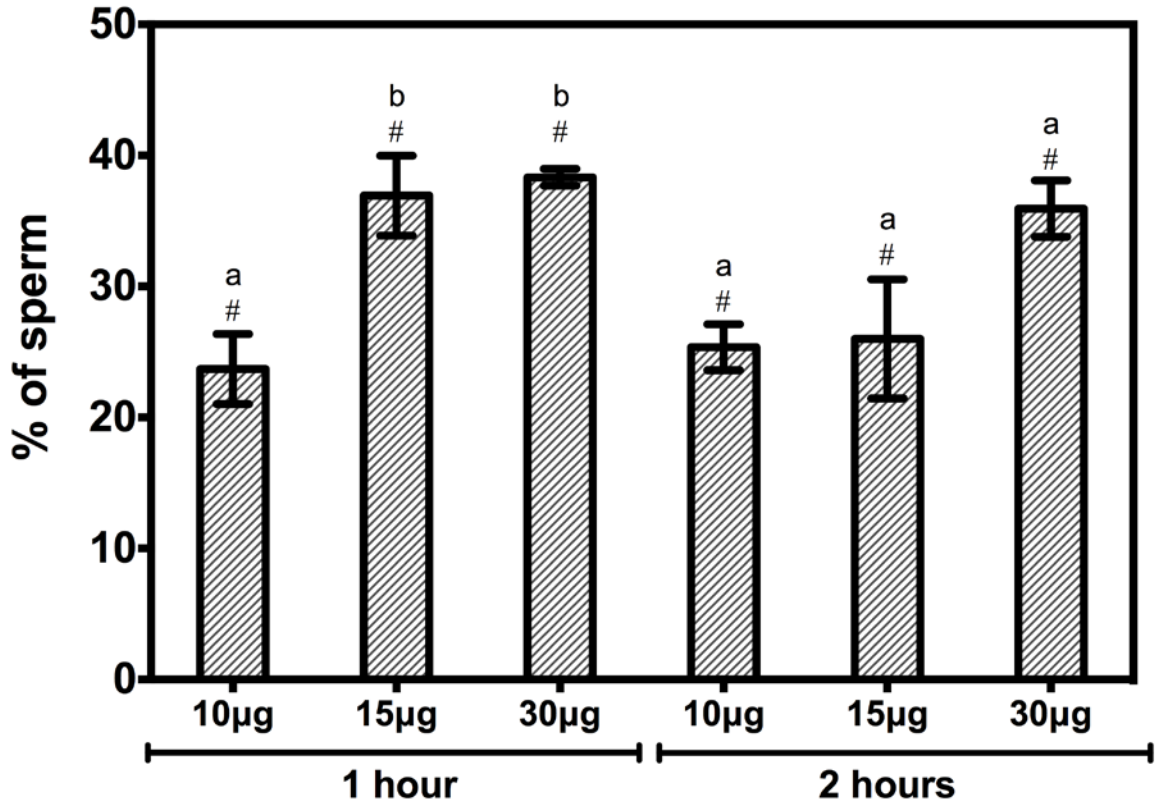

***Figure 4-11* – Binding rates between C105Y-functionalised MSNPs and boar sperm after 1 and 2 hours of incubation *in vitro* in various particle/cell ratios.** Data presented as mean±SEM from five samples. Each letter (a,b) denotes a subset of three dose categories within the same time point, whose values do not differ significantly from each other at the 0.05 level. Symbol (#) denotes a subset of same dose categories at two different time points, whose values do not differ significantly from each other at the 0.05 level.

To evaluate the effects of functionalisation upon the binding capacity between MSNPs and boar sperm, the binding rates of C105Y-functionalised MSNPs were compared with retrospective data for unmodified MSNPs, obtained under similar conditions, and controlled for inter-sample variability (**Table 4–5**). A significant effect of type ($F_{1,37}$=12.100; p<0.05) and dose of nanoparticles ($F_{1,37}$=22.170, p<0.05) upon binding rate was observed. Binding of MSNPs with sperm was significantly promoted by the functionalisation of MSNPs with C105Y (fixed coefficient for MSNPs vs MSNPs+C105Y: -11.110; 95%CI [-17.582;-4.639]; p<0.05) and an increase in the dose of unmodified MSNPs (fixed coefficient: 0.692; 95%CI [0.394; 0.989], p<0.05). Functionalisation of MSNPs with C105Y markedly increased binding rates with boar sperm, especially during the early stages of incubation, where an approximately 3- to 4-fold mean increment was observed, allowing binding levels to be achieved that were similar to those after 2 hours of exposure to unmodified MSNPs, after just 1 hour of treatment.

***Table 4-5* – Binding rates between sperm and C105Y-functionalised/unmodified MSNPs**

	1 hour			2 hours		
	Unmodified MSNPs	C105Y-functionalised MSNPs	P	Unmodified MSNPs	C105Y-functionalised MSNPs	P
MSNP/sperm ratio:						
10ug per 10^7 sperm	7.4±1.7%	23.7±2.7%	<0.05	17.4±1.9%	25.4±1.8%	*NS*
15ug per 10^7 sperm	6.4±4.4%	36.9±3.0%	<0.05	20.8±5.7%	26.0±4.5%	*NS*
30ug per 10^7 sperm	14.5±1.0%	38.3±0.6%	<0.05	41.0±9.2%	35.9±2.2%	*NS*

NS=not significant

4.3.3.4. Cell fluorescence after exposure to C105Y-functionalised MSNPs and free C105Y

Cell fluorescence levels in sperm exposed to C105Y-functionalised MSNPs and equivalent doses of free C105Y, were quantified after 1 and 2 hours of incubation to evaluate the effects of absorption of C105Y on a nanocarrier upon its transport into sperm. Accumulation of free C105Y in boar sperm was consistent with a previously described pattern for bull sperm: C105Y localised primarily to the post-equatorial region of the sperm head, posterior ring and mid-piece (Jones *et al*., 2013). Analysis of cell fluorescence levels, corrected for background fluorescence and expressed as arbitrary units (AU) per 1 μm^2 of sperm surface area, demonstrated a significant effect of the type

of treatment ($F_{1,1151}$=51.338; p<0.05), dose of nanoparticles/free peptide ($F_{1,1151}$= 75.054, p<0.05), and time of exposure ($F_{1,1151}$=91.961, p<0.05) upon fluorescence intensity.

Exposure of sperm to C105Y-functionalised MSNPs resulted in significantly increased levels of cell fluorescence, compared to free C105Y, across all dose ratios and incubation time points (**Figure 4-12**). In most cases, levels of cell fluorescence following exposure to the smallest dose ratio of C105Y-functionalised MSNPs (10µg per 10^7 sperm), or free C105Y, were significantly different than the two larger dose ratios (15µg and 30µg per 10^7 sperm). Corrected fluorescence intensity in sperm exposed to C105Y-functionalised MSNPs remained relatively stable throughout the incubation period. However, in the free C105Y group, a reduction of cell fluorescence at the 2-hour *versus* 1-hour incubation time point in the 15µg- and 30µg-equivalent groups was observed.

4.4. DISCUSSION

According to data reported in **Chapter 3**, MSNPs demonstrated biocompatibility with mammalian sperm and oocytes, and formed strong associations with approximately one in five sperm after simple incubation *in vitro.* These observations render spherical MSNPs with hexagonal pore symmetry as potential compound transfer vehicles for reproductive biology, along with other nanomaterials such as polyvinylalcohol-functionalised iron oxide (Ben-David Makhluf *et al.*, 2006; Makhluf *et al.*, 2008), magnetic nanoparticles (Kim *et al.*, 2010b), halloysite clay nanotubes and commercial polymeric nanotransfectants (Campos *et al.*, 2011a; Campos *et al.*, 2011b), nanogold (Barchanski *et al.*, 2015) and specialised CdSe/ZnS quantum dots (Feugang *et al.*, 2012; Feugang *et al.*, 2015). Although previous studies did not specifically quantify the proportion of sperm demonstrating binding with nanoparticles, but rather focused on the proportion of nanoparticles bound, the average binding rates of 20-25% observed in the set of experiments described in **Chapter 3**, appeared relatively low. From the perspective of reproductive biology, particularly for experiments involving the sperm-mediated delivery of compounds into the oocyte at the time of fertilization, the likelihood of transport should be directly proportionate to the number

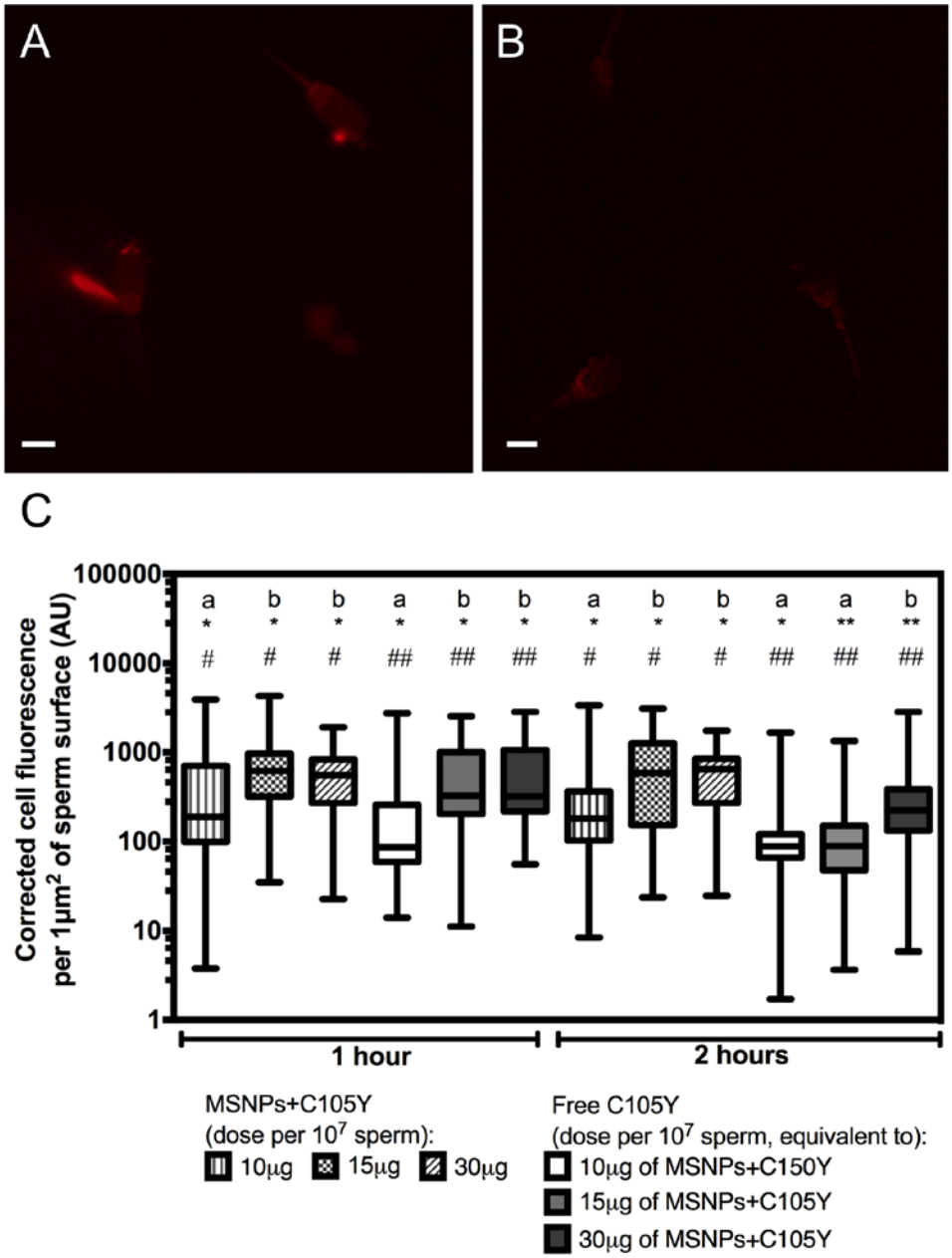

Figure 4-12– **Cell fluorescence after exposure to C105Y-functionalised MSNPs or equivalent doses of free C105Y.** A) Sperm after exposure C105Y-functionalised MSNPs in a 10µg per 10^7 cells ratio. B) Sperm after exposure to free C105Y in a dose, equivalent to absorbed on 10µg of C105Y-funtionalised MSNPs.Scalebar = 5µm. C) Levels of corrected cell fluorescence per $1\mu m^2$ of sperm surface area. Box plots represent distributions (central horizontal line: median; box: 25-75th percentile; whiskers: min-max) of corrected cell florescence per $1\mu m^2$ of surface area of individual sperm from six samples. Each letter (a,b) denotes a subset of three dose categories of each experimental agent within the same time point (i.e. 10 µg vs 15µg vs 30µg of MSNPs+C105Y at 1 hour), whose values did not differ significantly from each other at the 0.05 level. Symbol (*) denotes a subset of same dose categories of each experimental agent at two different time points (i.e. 10 µg of MSNPs+C105Y at 1 hour vs 2 hours) whose values did not differ significantly from each other at the 0.05 level. Symbol (#) denotes a subset of same dose categories of two different experimental agents at the same time point (i.e. 10 µg of MSNPs+C105Y vs an equivalent dose of free C105Y at 1 hour), whose values did not differ significantly from each other at the 0.05 level. Symbols (**) and (##) denote subsets whose values differed significantly from each other at the 0.05 level (i.e. (*) vs (**), $p<0.05$; (#) vs (##), $p<0.05$).

of nanoparticle-carrying sperm. Therefore, the actual size of the sperm cohort carrying particles could play an important role. This vision justified further research into the potential strategies to improve MSNP-sperm binding, which motivated the experiments performed during the next stage of the project and described in this Chapter.

4.4.1. SORTING OF SPERM ASSOCIATED WITH MSNPS USING DENSITY GRADIENT WASHING

Density gradient washing was chosen to select MSNP-bound sperm as a straightforward and time-saving technique for sperm processing in an ART setting. This technique has been successfully applied previously to prepare boar sperm for IVF, and results in reliable separation of sperm with 'better' functionality from cell debris and immotile, dead, senescent or immature sperm (Matás *et al.*, 2011). The main scope of this thesis was to develop a technique for nanomaterial-mediated delivery, which could form a valuable, but at the same time technically simple, addition to current protocols for assisted reproduction. Therefore, DGW was chosen because it does not involve the use of additional expensive equipment and trained operators, and can be easily implemented in any laboratory setting. It is, however, worth noting that the gold standard for cell sorting into sub-populations based upon the detection of fluorescent markers is FACS. As such, FACS has been attempted for the sorting of sperm from buffalo (Lu *et al.*, 2007), ram (Quan *et al.*, 2015), stallion (Mari *et al.*, 2010), goat (Bathgate *et al.*, 2013), boar (Vazquez *et al.*, 2009), dog (Oi *et al.*, 2013), cat (Spinaci *et al.*, 2007), deer (Kjelland *et al.*, 2011), dolphin (O'Brien and Robeck, 2006), and even humans (Karabinus *et al.*, 2014); however, it is most established in cattle breeding. Currently, several research groups are specifically developing nanoparticle-based probes for sperm sorting using FACS as a photostable and more robust alternative to conventional fluorochromes. In addition, nanoparticle-based probes would be able to detect specific DNA sequences inside sperm, rather than quantify the total amount of DNA inside these cells, thereby increasing the accuracy of this technique for sex sorting (Rath *et al.*, 2013). However, the use of FACS for sorting MSNP-bound boar sperm during the current set of experiments could represent a challenge, since sperm from this species do not readily endure the exposure to laser beam, high pressure and mechanical

factors, which are all inherently associated with FACS. As a result, FACS for boar sperm often results in low sperm concentrations and poor survival and, therefore, has only limited value.

Density gradient processing of boar sperm did not result in the enrichment of sperm fractions in MSNP-bound sperm either in the 40% or 80% gradient layers, for any of the synthesised particles tested herein. Although the results of these experiments showed that DGW cannot be used to sort MSNP-bound sperm, they also allowed me to reach an important conclusion: the possibility to bind with MSNPs did not seem to be related to the first-line functional parameters in individual sperm, such as motility, viability, or maturity. Although DGW was not able to separate sperm based on their binding status with MSNP, it could still differentiate cells based on their motility profiles, permitting the relative enrichment of the 80% layer with motile and progressively motile sperm. The relatively small differences between motility parameters in these two layers were attributed to the nature of the sourced sperm samples, which had already been pre-purified from cell debris and poor quality sperm, resuspended in extender, and delivered in a condition ready for artificial insemination.

Interestingly, an unexpected outcome of DGW was observed after 4 hours of exposure, when the proportions of motile sperm appeared to be higher in the 40% gradient layer than in the 80% layer. This phenomenon was observed both in experimental and control samples, which allowed me to eliminate the role of MSNP exposure. Since the principle of DGW relies upon the sorting of sperm into sub-populations on the basis of cell density, this finding could be attributed to possible sperm density changes in more active sperm sub-populations during prolonged handling in PBS at 37°C, as opposed to the recommended long-term storage temperature of 17°C. For human sperm, DGW has been reported to separate sperm with density differences of approximately 0.01 g/ml (1.10 g/ml for mature sperm and 1.06-1.09 g/ml for immature and morphologically abnormal sperm), and therefore, even small density changes could interfere with DGW performance (Malvezzi *et al.,* 2014). These observations have further strengthened the justification that the

minimally effective MSNP-sperm incubation time of 2 hours, after which binding rates appeared to plateau, was, perhaps, associated with better procedural safety.

4.4.2. PASSIVE TARGETING OF MSNPS TOWARDS SPERM

Passive targeting of MSNPs toward sperm was achieved via the synthesis of particles with a substantially smaller physical size, approximating 24 nm. This set of experiments was driven by the hypothesis that the smaller size of MSNPs would better match the substantially smaller size of sperm, compared to somatic cells, and thus facilitate binding and internalisation. Previously, incorporation into the sperm cytoplasmic compartment or sequestration inside the surface membrane has been reported for magnetic iron oxide NPs (Makhluf *et al.*, 2008), CdSe/ZnS quantum dots (Feugang *et al.*, 2012; Feugang *et al.*, 2015) and nanogold (Barchanski *et al.*, 2015), with a diameter almost 3- to 25-fold smaller than the ~138nm-sized MSNPs applied during the experiments described in **Chapter 3**.

One of the benefits of mesoporous silica is its relative ease of production and adjustability of the size of particles within the 10nm to 2μm range (Yamada *et al.*, 2013). Particle size control is usually achieved via simple modification of the types and ratios of chemical reagents used as silica sources during the reaction, and pH/temperature conditions at which the reaction is allowed to proceed. Essentially, these changes direct the reaction towards one of two possible scenarios: nucleation, which results in the formation of new particles, or growth, which increases the size of existing particles (Matsoukas and Gulari, 1988, 1989). The protocol used to produce smaller MSNPs with a size <50 nm for this set of experiments, utilised a different surfactant (CTAC *versus* CTAB), and was carried out in the presence of ethanol and weak base (DEA) at considerably lower temperatures (40°C *versus* 80°C) (Zhu *et al.*, 2011). As anticipated, the protocol allowed to synthesise MSNPs with a much smaller physical diameter than the particles used in **Chapter 3** (24.0±0.4nm *versus* 138.4±3.8nm). The size of 'smaller' MSNPs, synthesised in this set of experiments for passive targeting towards gametes, was generally comparable with values previously described by Zhu *et al*. (approximate range from 28 to 46 nm).

Reduction of MSNP size did not affect their biocompatibility with sperm, which represented an encouraging observation. After 2 and 4 hours of incubation, the proportions of motile/progressively motile sperm, and sperm kinematic parameters, in samples exposed to MSNPs did not differ from time-matched controls. As mentioned previously, due to high concordance of results between sperm viability assessment using eosin Y and evaluation of total sperm motility using CASA, viability staining of sperm in this set of experiment was not carried out, as it was of limited additional value. A reduction in MSNP size did not result in increased binding rates with sperm thereby restricting the use of passive targeting as a strategy to improve binding rates with these specialised cells. The only potentially biologically relevant phenomenon observed in this set of experiments was that the use of MSNPs with a smaller size resulted in considerably quicker saturation of MSNP-sperm binding rate a mean level of approximately 20% after just 1 hour of incubation. The outcomes of nanotoxicity and binding experiments, however, were interpreted with caution, given the possibility of MSNP agglomeration and, therefore, interaction with sperm as much larger physical entities. In addition, the effect of passive targeting upon binding of nanomaterials with gametes has not been investigated before and, therefore, interpretation of these outcomes in the context of available evidence is difficult. Because of the seemingly low value of passive targeting towards sperm and its unlikely application as a strategy to improve binding rates, the panel of nanotoxicity tests in this subset of experiment was much less detailed and did not include assessment of acrosome morphology and DNA fragmentation index.

Nanomaterials are intrinsically prone to agglomeration because of high surface energy, which increases with decreasing particle size. Several independent groups have described that for MSNPs with diameter <50 nm, agglomeration primarily occurs during the process of washing and surfactant removal, and is associated with multiple sedimentation-redispersion cycles (reviewed by Urata *et al.*, 2009). In this set of experiments, the established technique of overnight refluxing in acidic methanol had been chosen to remove CTAC from the mesopores, which, indeed, was associated with multiple washing and redispersion steps. In their original publication, Zhu *et al*.

removed surfactant using the alternative technique of calcination, which involved heating particles to 550°C for 5 hours under low oxygen conditions. This approach, however, did not allow the authors to fully prevent agglomeration, as evidenced by discrepancies between the mean physical (~37nm) and hydrodynamic diameter (~80nm) of MSNPs, assessed by TEM and dynamic light scattering, respectively. To address the issue of MSNP agglomeration during the removal of surfactant, a dialysis technique has been proposed (Urata *et al.*, 2009). This technique has been shown to eliminate the templating agent from the mesopores of particles <20 nm while fully preserving their dispersion. Initially, the set of experiments described in this Chapter planned to evaluate the performance of dialysis for surfactant removal and assess its benefits for preventing agglomeration of MSNPs <50 nm. However, given the time-consuming nature of these experiments, especially the MSNP characterisation steps, and seemingly small benefits of passive targeting of MSNPs towards sperm for improving binding rate, supported by recent evidence demonstrating low permeability of sperm membranes even for sub-10nm-sized nanomaterials (Feugang *et al.*, 2012; Taylor *et al.*, 2014a), these experiments were deemed of insufficient value and not pursued further.

In conclusion, this set of experiments demonstrated that the passive targeting of MSNPs to sperm via modification of particle size did not appear to affect biocompatibility with male gametes. The value of such a targeting approach to improve MSNP-sperm binding rate thus appears limited, although it may facilitate quicker ‘saturation’ of binding rate. Although particle size control for MSNPs theoretically represents a straightforward procedure, for MSNPs with sizes approximating or below 20 nm, like the particles used in this set of experiments, the important confounding factor of agglomeration should be addressed in future.

4.4.3. FUNCTIONALISATION OF MSNPS WITH A SPERM-SPECIFIC CELL-PENETRATING PEPTIDE FOR ACTIVE TARGETING TOWARDS SPERM

This set of experiments aimed to investigate the effects of the functionalisation of MSNPs with a 17-amino acid synthetic poly-cationic cell-penetrating peptide C105Y (CSIPPEVKFNKPFVYLI) (Rhee and Davis, 2006), upon the binding of MSNPs with boar sperm. The specific choice of C105Y for surface functionalisation of MSNPs was driven, firstly, by encouraging evidence of its high affinity towards mammalian sperm, compared to a subset of another 13 well-characterised CPPs, including penetratin, Tat and mitoparan (Jones *et al.*, 2013), and, secondly, its proposed energy- and receptor-independent internalisation profile. The sperm membrane is highly compartmentalised and undergoes continuous dynamic changes during the events preceding fertilization (Garcia-Vazquez *et al.*, 2011); therefore, the availability of a functionalisation agent, which would not interact with a particular subset of surface receptors and potentially interfere with these dynamic modifications, is highly favourable. Similarly to the previous sets of experiments described in **Chapter 3** the term 'binding' was collectively used to describe both surface binding and potential internalisation as a positive outcome of interaction between MSNPs and sperm. There is growing evidence that the uptake of nanomaterials by gametes is not as straightforward as that of somatic cells: most publications describe surface attachment or sequestration within the plasma membrane as the primary outcome of exposure of gametes to nanomaterials, with only a very small proportion of nanocarrier reaching the intracellular compartment (Ben-David Makhluf *et al.*, 2006; Fynewever *et al.*, 2007; Kim *et al.*, 2010b; Feugang *et al.*, 2012; Courbiere *et al.*, 2013; Taylor *et al.*, 2014a), and in some cases, none at all. Nevertheless, such profiles of interaction do not seem to compromise the performance of research techniques based upon such methodologies, and therefore, the precise mapping of C105Y-functionalised MSNPs was beyond the scope of this set of experiments.

Data showed that functionalisation of MSNPs with the sperm-targeting cell-penetrating peptide C105Y increased MSNP-sperm binding rate, and represented a viable strategy for the arsenal of techniques available for reproductive biology. In this set of experiments, C105Y-

functionalised MSNPs started to form stable associations with boar sperm after as little as 1 hour of exposure, compared to 2 hours for unmodified MSNPs. Although a similar outcome was previously observed for passive-targeted MSNPs, in this case, this increase reached the level of statistical significance. Interestingly, the proportion of sperm demonstrating binding with C105Y-functionalised nanoparticles was significantly increased compared to unmodified MSNPs after only 1 hour of exposure, indicating an increased affinity of functionalised MSNPs towards sperm during the early stages of incubation. After 2 hours, although binding rates for C105Y-functionalised MSNPs were mostly higher compared to unmodified particles, the difference was no longer significant. At this point, binding rates in both groups stabilised at a plateau of approximately 20%-30%, which was consistent with results from the previous set of experiments described in **Chapter 3** and the preceding sections in **Chapter 4**. This observation could indicate that binding with MSNPs occurs primarily in a certain subset of sperm, and that functionalisation of nanoparticles with C105Y aids with initial 'anchoring' of MSNPs onto the surface of these cells, but not in the entire sperm population. These findings coincide with the outcomes of all previous experiments in this thesis, evaluating the performance of non-targeted and passively targeted MSNPs, as well as sperm selection using DGW. In all these experiments, average binding rate between MSNPs and sperm throughout incubation with different doses of particles fluctuated within a range from 20% to 30%. These consistent observations could suggest that sperm which bind with MSNPs most likely possess specific plasma membrane properties, rather than belong to a certain motility or viability category. These findings to a certain extent correspond to the results of a recent study by Barchanski *et al.* (2015), who evaluated the effects of polydisperse gold nanoparticle functionalisation with locked nucleic acids (LNAs) and various CPPs (deca-arginine, transactivator of transcription and simian-virus 40 large T antigen nuclear localization signal) upon binding/internalisation into sperm in attempt to design an efficient tool for the genetic labelling and analysis of these specialised cells. In this particular study, the binding, uptake and intracellular distribution of gold nanoparticles inside sperm was markedly influenced by a combination of

particle surface chemistry, in particular dual functionalisation with LNAs and CPPs, and the properties of sperm surface membrane. However, in contrast to findings described in **Chapter 3** and **Chapter 4**, Barchanski *et al*. did not observe the positive effects of nanoparticle functionalisation with CPP only upon the binding with sperm membrane, and emphasised the significance of sperm acrosome status for internalisation of particles – a point which was not addressed specifically during the experiments described in this thesis. In fact, the proportion of sperm with a NAR in these experiments consistently exceeded the proportion of sperm bound with C105Y-functionalised MSNPs. Therefore, sperm acrosome status was not considered an important contributor to this interaction, and the affinity of certain sperm to MSNPs was largely attributed to the particular, yet thus far unknown, combination of physical, chemical or biological properties of their surface membranes.

In the present set of experiments, functionalisation of MSNPs with C105Y resulted in a change of association pattern with boar sperm, with selected cells demonstrating binding of MSNPs in the post-equatorial region of the sperm head and posterior ring – a profile previously described for free C105Yed but rarely documented for unmodified MSNPs. This observation supports the hypothesis that functionalisation of MSNPs with a cell-specific moiety is likely to alter their binding profile with the target.

Exposure of sperm to C105Y adsorbed on MSNPs consistently resulted in a significant increase of corrected cell fluorescence levels per 1 μm^2 of sperm surface area compared to free C105Y, across all dose ratios and incubation time points. Nanoparticles were previously reported to promote the uptake of exogenous DNA into sperm in nanoSMGT experiments (Kim *et al.*, 2010b; Campos *et al.*, 2011a; Campos *et al.*, 2011b), compared to standard SMGT, however similar comparative studies with intracellular transport of proteins and peptides have yet to be carried out. Even though the internalisation of nanomaterials into sperm in nanoSMGT experiments did not occur consistently, the efficacy of cargo delivery was increased, perhaps due to structural modifications of the plasma membrane following contact with nanoparticles (Taylor *et al.*, 2014a).

Interestingly, a reduction in cell fluorescence at the 2-hour *versus* 1-hour incubation time point in the free C105Y group (15μg- and 30μg per 10^7 sperm equivalent groups) was observed. This was an unexpected finding which could be readily interpreted in the context of existing scientific literature, since previous experiments evaluated the delivery of C105Y into sperm only after 1 hour incubation (Jones *et al.*, 2013).

Finally, functionalisation of MSNPs with C105Y did not affect the biocompatibility of mesoporous silica with boar sperm. Although both compounds have been tested for gametotoxicity previously (Jones *et al.*, 2013), confirmation of the biological safety of functionalised MSNPs in sperm remained an essential step, since previous reports had highlighted the detrimental effects of surface modification of nanomaterials, such as the removal of coatings or functionalisation moieties, upon their toxicity profiles in gametes (Hsieh *et al.*, 2009; Taylor *et al.*, 2014a). In this set of experiments, no negative effects upon total and progressive motility, kinematic parameters of sperm, and the proportion of cell with a NAR were observed at the sample level following exposure to various doses of C105Y-functionalised MSNPs, and equivalent amounts of free C105Y, compared to control groups.

Additionally, a separate logistic regression analysis of individual sperm data, accounting for inter-sample variability, was carried out. This analysis investigated the effects of exposure upon cells in greater detail. Interestingly, analysis indicated a protective effect of both compounds upon total sperm motility, and a beneficial role of C105Y-functionalised MSNPs upon the integrity of the acrosomal apical ridge. This observation could be partially explained by the reported ability of mesoporous silica to suppress the production of endogenous reactive oxygen species (Huang *et al.*, 2010), a powerful source of sperm oxidative damage. However, given the scarce nature of such reports, this phenomenon required further investigation.

Another interesting outcome of the analysis of individual sperm data was the isolated negative effect of C105Y-functionalised MSNPs, but not free C105Y, upon progressive motility (VAP>45μm/sec; VSL/VAP>45%), without a similar effect upon the probability to assign sperm to

a ‘rapid’ motility category (VAP>45μm/sec; VSL/VAP<45%). These results suggested that on an individual sperm level, the physical binding of MSNPs does not necessarily result in sperm retardation, but rather changes its swimming trajectory. In this set of experiments, the protective effects of C105Y-functionalised MSNPs, and free C105Y, upon total sperm motility, the beneficial effects of C105Y-functionalised MSNPs upon the integrity of acrosomal apical ridge, and the isolated negative effect upon progressive, were detected at the individual sperm level, but not at the sample level. This discrepancy could be explained by the pilot nature of these experiments and the relatively small sample size.

In conclusion, this subset of experiments, for the first time, evaluated the use of a 17-amino acid synthetic poly-cationic peptide, C105Y, with affinity towards mammalian sperm, for the functionalisation of spherical MSNPs with hexagonal pore symmetry, and the subsequent use of these functionalised MSNPs in boar sperm. Targeting of MSNPs towards sperm with C105Y enhanced their ability to form strong associations with gametes following incubation *in vitro*. This approach allowed earlier binding with the sperm surface, compared to unmodified MSNPs, and the establishment of new binding profiles. The exposure of sperm to MSNP-absorbed C105Y resulted in a significant increase in cell fluorescence levels, compared to free peptide, highlighting the potential effect of nanoparticles upon the permeability of the sperm membrane. Finally, C105Y-functionalised MSNPs retained biocompatibility with mammalian sperm from the perspective of total motility and acrosome morphology. At the same time, interference with the trajectory of sperm motion at the individual sperm level, due to anchoring of MSNPs to the surface membrane, could represent one of the potential outcomes of binding.

Collectively, this set of experiments indicated that active targeting towards sperm with appropriate moieties represented the most effective and technically straightforward tool to promote favourable outcomes of interaction between sperm and MSNPs, compared to the selection of MSNP-bound sperm or passive targeting towards sperm via modification of particle size.

CHAPTER 5

ASSESSMENT OF THE DELIVERY POTENTIAL OF MESOPOROUS SILICA NANOPARTICLES FOR MOLECULAR TRANSFER INTO MAMMALIAN SPERM

Key messages:

- This chapter presents the outcomes of experiments investigating the possibility to apply MSNPs as DNA and protein delivery vectors for mammalian sperm.
- Loading of molecular cargo onto appropriately functionalised MSNPs (PEI- or APTES-coated for delivery of DNA or protein, respectively) allowed the intra-sperm delivery of payloads, however the efficacy of such delivery did not exceed that of free cargo.
- The combined use of C105Y-functionalised MSNPs, and free payloads, resulted in more stable delivery into a larger number of sperm samples in the case of DNA transfer, and a trend towards higher delivery efficacy into individual samples in the case of protein transfer.
- Collectively, these outcomes strengthened the hypothesis that although the specific types of MSNPs used in this thesis did not seem to internalise into sperm, which inhibited the uptake of adsorbed cargo, exposure to actively-targeted particles promoted cargo uptake into these specialised cells. This phenomenon could be attributed to as yet uncharacterised changes in sperm membrane permeability for exogenous compounds in the presence of actively-targeted particles, without their direct intracellular penetration.

5.1. BACKGROUND

The use of nanomaterials for molecular delivery represents, perhaps, the most exciting application for reproductive science. These multi-functional small-scale delivery tools are characterised by unparalleled targeting options, physiological mechanisms of uptake, and ability to carry large amounts of various payloads, including nucleic acids, proteins, peptides, aptamers, and small molecules (Kim *et al.*, 2013b; Lehner *et al.*, 2013; Uskokovic, 2013; Choudhary and Kusum Devi, 2015). Nanomaterials have been consistently shown to promote the intracellular uptake of molecular cargo and protect sensitive payloads from degradation, thereby resulting in a more efficient and controlled drug delivery (Tsai *et al.*, 2014).

The need for molecular delivery platforms for reproductive biology is the result of the relative inefficacy of spontaneous uptake in mature gametes. Mature sperm are characterised by severely compromised membrane recycling mechanisms. Therefore, their endo- and exocytotic capacity appears almost redundant (Gadella and Evans, 2011; Jones *et al.*, 2013). Such quiescence of intracellular uptake in mature sperm renders the plasma membrane as a static, rather than dynamic, barrier, which restricts intracellular transport of molecules in order to maintain the structural and functional integrity of intracellular compartments (Jones *et al.*, 2013). This ensures the preservation of both paternal genetic material (Parrington *et al.*, 2007) and protection from the inadvertent triggering of intracellular signal transduction pathways, which can cause premature acquisition of fertilization potential (Abou-haila and Tulsiani, 2009). In oocytes, which are 'mechanically' protected from the microenvironment by a barrier created by the *zona pellucida*, intracellular delivery occurs via the surrounding cumulus cells. These specialised follicular cells develop long processes which penetrate the *zona pellucida* and come into intimate contact with the oolemma thereby permitting direct molecular exchange with the female gametes (Vanderhyden and Armstrong, 1989; Eppig *et al.*, 2005; Huang and Wells, 2010; Fragouli and Wells, 2012b). Collectively, these protective mechanisms interfere with the performance of research techniques, requiring the internalisation of molecular compounds into gametes. These techniques include, but

are not limited to, gene transfer into reproductive tissues (Ikawa *et al.*, 2002; Ghadami *et al.*, 2010), SMGT (Brackett, 1971), and sperm sorting into sub-populations driven by the detection of a specific intracellular marker, for example sex sorting (Rath *et al.*, 2013). Although these experimental techniques have been extensively studied over the last few decades, their efficacy remains sub-optimal (Ikawa *et al.*, 2002; Kojima *et al.*, 2008; Eghbalsaied *et al.*, 2013; Rath *et al.*, 2013), and their relative application is thus compromised.

An ideal vehicle for the delivery of molecular cargo into gametes should, most importantly, possess the feature of safety. To be deemed safe for reproductive applications, this vehicle should internalise into cells without profound disruption of the plasma membrane, have minimal effects inside the intracellular compartment, preserve DNA integrity and be incapable of integrating into the host genome. These features are essential, since opposite outcomes could lead to the loss of developmental capacity in gametes or trans-generational effects in the offspring and, therefore, are highly undesirable. Unfortunately, most of the existing intracellular delivery techniques, such as electroporation, viral vectors and membrane permeabilisation, can be associated with unfavourable effects in these specialised cells, which limits practical applications of these methodologies (Lamb, 2008; Garcia-Vazquez *et al.*, 2011; Yamauchi *et al.*, 2012). The sub-optimal performance of conventional molecular delivery methods in reproductive science justifies the need to develop novel, safe and effective delivery techniques. These techniques, ideally, should combine the main advantages of viral vectors, such as high specificity and non-invasiveness of delivery, with the key benefit of electroporation: an avoidance of viral integration into the host genome.

From this perspective, the use of nanomaterials for intra-gamete delivery appears particularly advantageous, since they possess most of the requirements for optimal molecular transfer platforms (**Table 5–1**). In addition, there is increasing evidence that the crucial processes underlying gamete development, maturation and acquisition of fertilisation potential *in vivo* are regulated by extracellular vesicles (EVs), natural nanoparticles, universally secreted by most pro- and eukaryotic cells (Sohel *et al.*, 2013; Sullivan and Saez, 2013). Moreover, these processes appear

to be highly conserved across a variety of biological species These observations form another justification for studies into the feasibility of manipulating these key processes using similar 'engineered' nanoplatforms.

***Table 5-1* – Available delivery tools for the transfer of molecular compounds into gametes**

	Electroporation	**Viral vectors**	**Chemical reagents**	**Nanomaterials**
Damage to cell membrane	+	-	+	-
Mechanism of uptake	Passage through membrane openings	Receptor-mediated energy-dependent	Passage through membrane openings	Mediated/non-mediated energy-dependent or independent
Potential for artificial targeting	-	+ (vector engineering)	-	+++ (functionalisation)
Risk of integration into the host genome	-	+	-	-
Risk of host infection	-	+	-	-
Preservation of cell function after cargo transfer	Poor	Possible	Poor	Yes

The number of studies, which utilise nanomaterials for the transfer of molecular compounds into gametes has been steadily growing since the mid-2000s. However, the total number of publications in this area still remains relatively low. Currently, the spectrum of nanomaterials with favourable biocompatibility with gametes/embryos includes polyvinylalcohol-functionalised iron oxide (Ben-David Makhluf *et al.*, 2006; Makhluf *et al.*, 2008), magnetic (Kim *et al.*, 2010b) and polystyrene (Fynewever *et al.*, 2007) nanoparticles (NPs), perfluorocarbon (Jallouk *et al.*, 2014), halloysite clay nanotubes and commercial polymeric nanotransfectants (Campos *et al.*, 2011a; Campos *et al.*, 2011b), specialised CdSe/ZnS quantum dots (Feugang *et al.*, 2012), and, although with more controversy, nanogold (Taylor *et al.*, 2014b; Tiedemann *et al.*, 2014) and cerium dioxide (Falchi *et al.*, 2014; Preaubert *et al.*, 2015). Most of these studies have consistently demonstrated that the use of nanomaterials improves the efficacy of research techniques, based upon the internalisation of molecular compounds into gametes. These techniques primarily involved loading sperm with exogenous genetic constructs for subsequent SMGT into the oocyte at the time of

fertilization (Kim *et al.*, 2010b; Campos *et al.*, 2011a; Campos *et al.*, 2011b), proof-of-principle transfer of proteins into sperm (Makhluf *et al.*, 2008), and sorting into sub-populations (Barchanski *et al.*, 2015) – all with positive outcomes (**Table 5–2**).

***Table 5-2*– Nanoparticle-mediated delivery into gametes and intracellular cell-labelling *in vitro*: experimental studies in animal models**

Study	Nanomaterial	Application
Makhluf *et al.* (2008)	Polyvinylalcohol-coated magnetic iron oxide NPs (Fe_3O_4)	Proof-of-principle transfer of anti-protein kinase C-antibody into sperm
Kim *et al.* (2010b)	Magnetic NPs (commercial agent)	Facilitation of SMGT
Campos *et al.* (2011a)	Nanopolymer (commercial agent)	Facilitation of SMGT ('NanoSMGT')
Campos *et al.* (2011b)	Nanopolymer (commercial agent) and halloysite clay nanotubes	Facilitation of SMGT ('NanoSMGT')
Barchanski *et al.* (2015)	Nanogold	Proof-of-principle investigation of the potential to label the specific DNA sequences in viable sperm

MSNPs have been extensively characterised as reliable delivery tools with large surface area and pore volume, adjustability of physicochemical properties, high levels of safety and potential to simultaneously carry several biological compounds (Vallet-Regi *et al.*, 2007; Wu *et al.*, 2011; Li *et al.*, 2012; Rosenholm *et al.*, 2012; Wang *et al.*, 2015). MSNPs have also been shown to act as effective delivery platforms for drugs, peptides, fluorescent dyes, and nucleic acids in a variety of cell types (Xia *et al.*, 2009; Hom *et al.*, 2010; Zhu *et al.*, 2011; Na *et al.*, 2012; Luo *et al.*, 2014). However, their delivery capacity in gametes has never been tested previously.

The experiments performed thus far in this thesis have provided encouraging findings regarding the biocompatibility of different modifications of MSNPs, including particles targeted towards mammalian sperm, with gametes. This Chapter presents the outcomes of the logical continuation of this research and focuses on the results of investigation into the possibility to apply MSNPs as delivery vectors for mammalian sperm. These results showed that loading molecular cargo onto appropriately functionalised MSNPs (PEI- or APTES-coated) allowed the intra-sperm delivery of payloads, however the efficacy of such delivery did not exceed that of free cargo. At the same time, the combined use of C105Y-functionalised MSNPs and free payloads resulted in more

stable delivery into a larger number of sperm samples in the case of DNA transfer, and a trend towards higher delivery efficacy in the case of protein transfer. Collectively, these outcomes strengthened the hypothesis that although the specific types of MSNPs used in this thesis did not seem to internalise into sperm, exposure to actively-targeted particles promoted cargo uptake into these specialised cells. This phenomenon could be attributed to yet uncharacterised changes in sperm membrane permeability for exogenous compounds in presence of actively targeted MSNPs, without their direct penetration into sperm.

5.2. SPECIFIC DETAILS OF EXPERIMENTAL PROCEDURES AND DATA ANALYSIS

Specific details of the experimental procedures and data analysis used for the generation of results presented in this Chapter are described in **Chapter 2**.

In brief, to assess the delivery capacity of MSNPs into boar sperm, washed sperm were exposed to the following treatments: (1) PBS; (2) free cargo (pHL-FcHis-mCherry or mCherry); (3) MSNPs, loaded with cargo (PEI-coated MSNPs loaded with pHL-FcHis-mCherry or APTES-coated MSNPs loaded with mCherry); (4) unmodified MSNPs and free cargo (pHL-FcHis-mCherry or mCherry); (5) C105Y-functionalised MSNPs and free cargo (pHL-FcHis-mCherry or mCherry). All particle modifications were added to sperm in in the ratio of 10µg of particles per 10^7 cells. Free cargo was added in the dose, equivalent to that adsorbed on 10µg particles. Incubation was carried out for 2 hrs at 37ºC under a low-oxygen atmosphere. All stock suspensions of nanoparticles (concentration: 2mg/ml), in this case, were prepared with nuclease-free water. After 2 hours, the incubation was stopped, unbound cargo removed via DNase I treatment (for DNA transfer) or abundant washing (for protein transfer), and detection of intracellular delivery performed using PCR and Western blot in DNA and proteins extracted from sperm, respectively.

5.3. RESULTS

5.3.1. LOADING OF PEI-COATED MSNPS WITH PLASMID DNA

Non-fluorescent MSNPs (>100nm) were pre-coated with PEI and loaded with pHL-FcHis-mCherry via co-incubation in a 10:1 ratio. Coating with PEI rendered the inherently negative surface charge of MSNPs positive, thereby permitting the electrostatic attachment of DNA. Throughout incubation, the concentration of free pHL-FcHis-mCherry in the supernatant decreased exponentially, resulting in almost complete adsorption of the plasmid to PEI-coated MSNPs after 24 hours on incubation (**Figure 5–1A**).

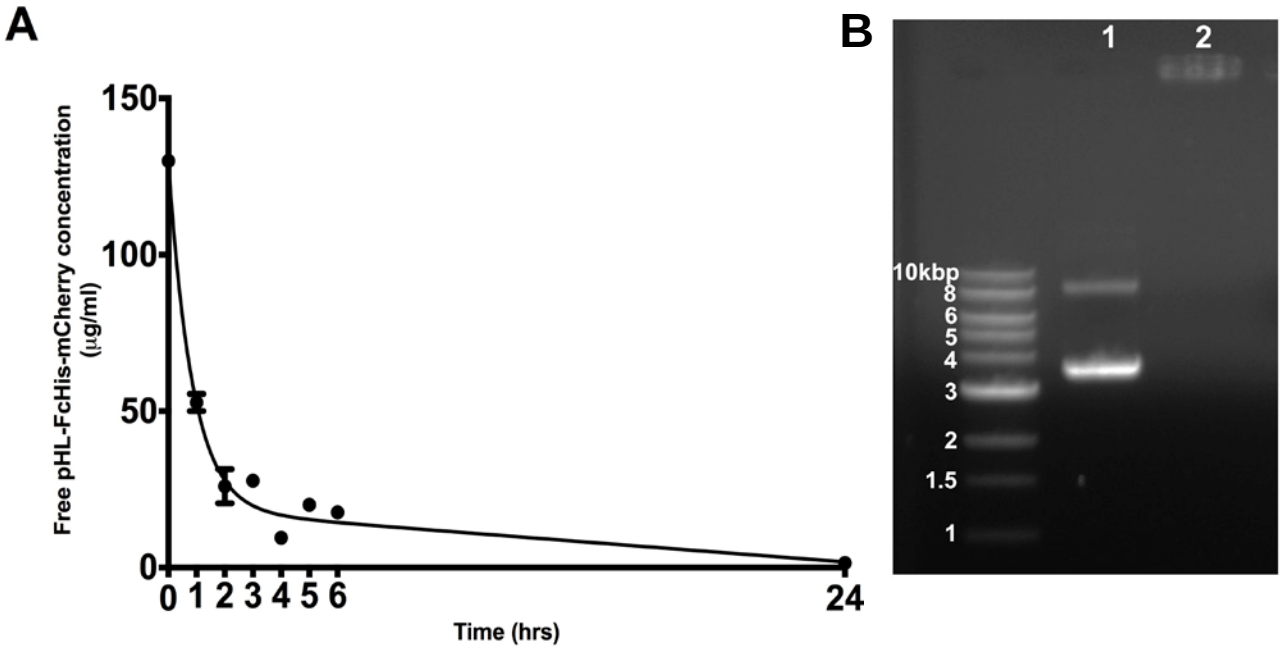

***Figure 5-1* – Loading of PEI-coated MSNPs with pHL-FcHis-mCherry.** A) Concentration of free pHL-FcHis-mCherry in the supernatant from the reaction with PEI-coated MSNPs during 24 hours of co-incubation at 4°C. B) Agarose gel retardation test: Lane 1 – free pHL-FcHis-mCherry; Lane 2 – pHL-FcHis-mCherry loaded onto PEI-coated MSNPs. Loading onto MSNPs prevents the migration of pHL-FcHis-mCherry from the well into the 0.8% TAE agarose gel, in contrast to free plasmid; molecular weight marker – 1kbp DNA ladder (New England Biolabs, UK). Data presented as mean±SEM from a minimum of three repeats.

The agarose gel retardation test confirmed the loading of pHL-FcHis-mCherry on PEI-coated MSNPs, as evidenced by 'retaining' of DNA adsorbed on MSNPs in the well, as opposed to unrestricted migration of free pHL-FcHis-mCherry towards the anode (*Figure 5-1***B**). Since the adsorption of pHL-FcHis-mCherry on PEI-coated MSNPs was almost complete, 10μg particles was estimated to carry 1μg plasmid DNA.

5.3.2. LOADING OF APTES-COATED MSNPS WITH MCHERRY

Non-fluorescent MSNPs (>100nm) were pre-coated with APTES and loaded via covalent immobilisation with mCherry which had been expressed and purified in house. Coating with APTES enriched the surface of MSNPs with free amine groups, thus allowing covalent absorption of mCherry onto the particles via EDC-mediated cross-linking of these functional groups with carboxyl groups in mCherry. Cross-liking was performed in an approximately 2:1 ratio (MSNPs:mCherry), and resulted in almost complete absorption of mCherry on APTES-coated MSNPs after 2 hours of incubation. Given the almost complete binding of mCherry to APTES-coated MSNPs, 10μg particles was estimated to carry 5.5μg mCherry.

5.3.3. MSNP-MEDIATED TRANSFER OF DNA INTO SPERM

Mesoporous silica nanoparticles, pre-coated with PEI and loaded with pHL-FcHis-mCherry, were used for the MSNP-mediated transfer of exogenous DNA into boar sperm. A ratio of 10μg MSNPs per 10^7 sperm and an incubation time of 2 hours, which were characterised as sufficient to achieve stable MSNP-sperm binding in the previous chapters of this thesis, were used for gene transfer experiments. Given the almost complete adsorption of pHL-FcHis-mCherry on PEI-coated MSNPs, the quantity of plasmid presented to each 10^7 sperm was approximated to be 1μg. This amount of DNA fell within the range of doses previously described as sufficient for SMGT, from 200ng to 10μg per 10^7 sperm (Oddi *et al.*, 2012; Lavitrano *et al.*, 2013).

The benefits of loading DNA onto MSNPs were compared with the conventional technique of SMGT, involving simple co-incubation of sperm with exogenous DNA *in vitro* (Lavitrano *et al.*, 2013). In addition, given previous indications of the potential of MSNPs to promote uptake of molecular cargo into sperm, the outcomes of simultaneous sperm exposure to free exogenous DNA and unmodified MSNPs or C105Y-functionalised MSNPs, were assessed. For all treatments, each 10^7 sperm were exposed to 10μg MSNPs and 1μg pHL-FcHis-mCherry, either in free or adsorbed form.

5.3.3.1. Quality control for detection of DNA transfer into boar sperm

Primer specificity was confirmed via the PCR amplification of target sequences using stock pHL-FcHis-mCherry and control pig genomic DNA as templates. Amplicons with the length of 437bp and 151bp, representing the mCherry sequence fragment within pHL-FcHis-mCherry and the swine leptin gene fragment, respectively, were successfully visualised on an agarose gel (**Figure 5–2A**). Alignment of sequencing data from PCR amplicons with source sequences of mCherry and swine leptin confirmed an approximate 99% match (**Figure 5–2C**).

To ensure that the removal of non-internalised pHL-FcHis-mCherry from sperm samples using DNase I was efficient, the efficacy of this step to digest free plasmid was also assessed. Exposure of free pHL-FcHis-mCherry to DNase I in a 1:4 (5 μg: 20 units) ratio for 30 minutes at 37°C resulted in almost full digestion of plasmid DNA, as evidenced by the detection of only trace amounts of the mCherry amplicon on an agarose gel after PCR (**Figure 5–2B)**. These outcomes confirmed that detection of pHL-FcHis-mCherry in boar sperm after exposure to free/adsorbed plasmid and various modifications of MSNPs would be indicative only of the fraction of plasmid transferred into sperm.

5.3.3.2. Efficacy of MSNP-mediated DNA transfer into boar sperm

Transfer of pHL-FcHis-mCherry into boar sperm after exposure to free/adsorbed plasmid and various modifications of MSNPs was performed in 8 ejaculated (two repeats per ejaculate, on average). Evidence of transfer was considered positive when a ~400bp band corresponding to target mCherry sequence (437bp) was detected on agarose gels after PCR amplification of DNA, extracted from boar sperm. A ~150bp band corresponding to the target swine leptin gene fragment (151bp), was used as an internal control for the quantitative assessment of DNA transfer efficacy (**Figure 5–3**).

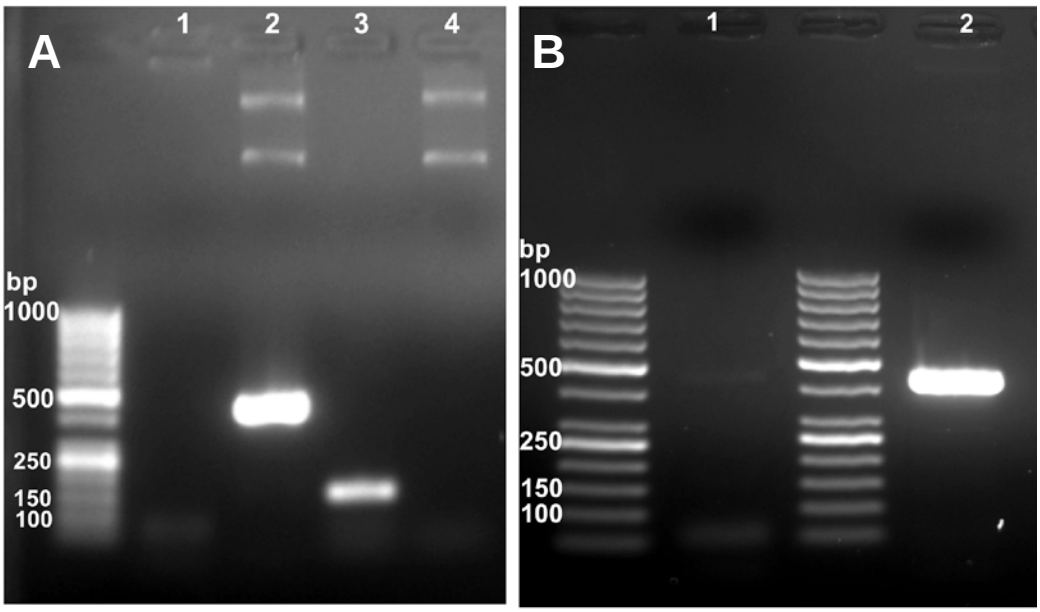

C

```
# Length: 437
# Identity:     431/437 (98.6%)
# Similarity:   431/437 (98.6%)
# Gaps:           0/437 ( 0.0%)
# Score: 2131.0
#
#
#=======================================

Amplicon      1 ACCGCCAAGCTGAAGGTGACCAAGGGTGGCCCCCTGCCCTTCGCCTGGGA   50
                ||||||||||||||||||||||||||||||||||||||||||||||||||
Source        1 ACCGCCAAGCTGAAGGTGACCAAGGGTGGCCCCCTGCCCTTCGCCTGGGA   50

Amplicon     51 CATCCTGTCCCCTCAGTTCATGTACGGCTCCAAGGCCTACGTGAAGCACC   100
                ||||||||||||||||||||||||||||||||||||||||||||||||||
Source       51 CATCCTGTCCCCTCAGTTCATGTACGGCTCCAAGGCCTACGTGAAGCACC   100

Amplicon    101 CCGCCGACATCCCCGACTACTTGAAGCTGTCCTTCCCCGAGGGCTTCAAG   150
                ||||||||||||||||||||||||||||||||||||||||||||||||||
Source      101 CCGCCGACATCCCCGACTACTTGAAGCTGTCCTTCCCCGAGGGCTTCAAG   150

Amplicon    151 TGGGAGCGCGTGATGAATTTCGAGGACGGCGGCGTGGTGACCGTGACCCA   200
                ||||||||||||||||||.|||||||||||||||||||||||||||||||
Source      151 TGGGAGCGCGTGATGAACTTCGAGGACGGCGGCGTGGTGACCGTGACCCA   200

Amplicon    201 GGACTCCTCCCTGCAGGACGGCGAGTTCATCTACAAGGTGAAGCTGCGCG   250
                ||||||||||||||||||||||||||||||||||||||||||||||||||
Source      201 GGACTCCTCCCTGCAGGACGGCGAGTTCATCTACAAGGTGAAGCTGCGCG   250

Amplicon    251 GCACCAACTTCCCCTCCGACGGCCCCGTAATGCAGAAGAAGACCATGGGC   300
                ||||||||||||||||||||||||||||||||||||||||||||||||||
Source      251 GCACCAACTTCCCCTCCGACGGCCCCGTAATGCAGAAGAAGACCATGGGC   300

Amplicon    301 TGGGTGGCCTCCTCCGAGCGGATGTACCCCGAGGACGGCGCCCTGAAGGG   350
                ||||.|||||||||||||||||||||||||||||||||||||||||||||
Source      301 TGGGAGGCCTCCTCCGAGCGGATGTACCCCGAGGACGGCGCCCTGAAGGG   350

Amplicon    351 CGAGAGCAAGCAGAGGCTGAAGCTGAAGGACGGCGGCCACTACGACGCTG   400
                |||||.|||||||||||||||||||||||||||||||||||||||||||||
Source      351 CGAGATCAAGCAGAGGCTGAAGCTGAAGGACGGCGGCCACTACGACGCTG   400

Amplicon    401 AGTTCTGGACCACCTACAAGGCCAAGAAGCCCGTGCA    437
                ||.||..|||||||||||||||||||||||||||||
Source      401 AGGTCAAGACCACCTACAAGGCCAAGAAGCCCGTGCA    437
```

mCherry

```
# Length: 151
# Identity:     151/151 (100.0%)
# Similarity:   151/151 (100.0%)
# Gaps:           0/151 ( 0.0%)
# Score: 755.0
#
#
#=======================================

Amplicon      1 CAGTGTCCCCTGAGCCAGCTAGTGTTCTCTGGGGACGGGAACAGGGTTGG   50
                ||||||||||||||||||||||||||||||||||||||||||||||||||
Source        1 CAGTGTCCCCTGAGCCAGCTAGTGTTCTCTGGGGACGGGAACAGGGTTGG   50

Amplicon     51 GCAGGGAGTTCAGGAAGTGTTTGCTGGAAGAGCGGAGTTTCCAGGCTGAT   100
                ||||||||||||||||||||||||||||||||||||||||||||||||||
Source       51 GCAGGGAGTTCAGGAAGTGTTTGCTGGAAGAGCGGAGTTTCCAGGCTGAT   100

Amplicon    101 TTTGCAGGAGGTGAGGGAAGTGGATTGCCTGGAGGGAGGAGGCTGTTTTG   150
                ||||||||||||||||||||||||||||||||||||||||||||||||||
Source      101 TTTGCAGGAGGTGAGGGAAGTGGATTGCCTGGAGGGAGGAGGCTGTTTTG   150

Amplicon    151 T    151
                |
Source      151 T    151
```

Swine leptin

***Figure 5-2* – Quality control for the detection of DNA transfer into sperm.** A) Amplification of target mCherry (437bp) and leptin (151bp) sequences using the PCR protocol with designed primers: Lane 1 – pig genomic DNA + mCherry primers; Lane 2 –pHL-FcHis-mCherry + mCherry primers; Lane 3 – pig genomic DNA + leptin primers; Lane 4 – pHL-FcHis-mCherry + leptin primers. B) Amplification of target mCherry sequence from pHL-FcHis-mCherry before and after DNase I digestion. Lane 1 – after treatment with DNase I in a 1:4 (5 µg: 20 units) ratio for 30min at 37°C. Lane 2 – before treatment with DNase I (a ~1:10 dilution from the initial sample, subject to DNase I treatment). 1.3% TAE agarose gel, molecular weight marker – GeneRuler 50bp DNA ladder (Life Technologies, UK). C) Pairwise alignment of sequencing data from PCR amplicons with source sequences of mCherry and swine leptin.

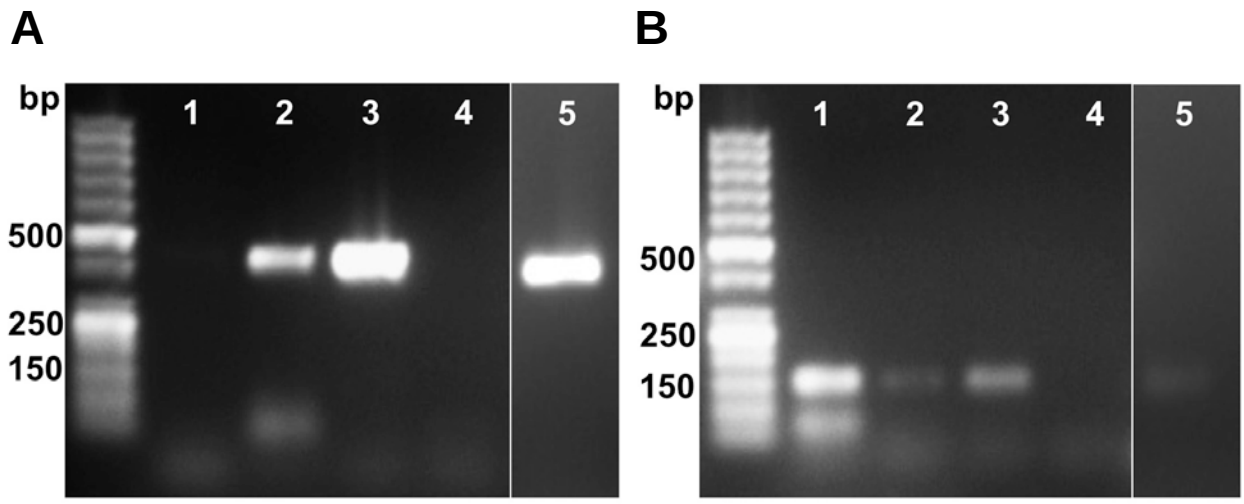

***Figure 5-3* – Detection of pHL-FcHis-mCherry transfer into boar sperm: representative images.** A) Detection of target mCherry fragment (437bp) sequence via PCR amplification of the region of interest in DNA extracted from boar sperm samples. B) Detection of target swine leptin gene fragment (151bp) sequence via PCR amplification of the region of interest in DNA extracted from boar sperm samples. Lanes represent different types of treatment: Lane 1 – control; Lane 2 – free pHL-FcHis-mCherry; Lane 3 – PEI-coated MSNPs, loaded with pHL-FcHis-mCherry; Lane 4 – unmodified MSNPs and pHL-FcHis-mCherry, Lane 5 – C105Y-functionalised MSNPs and pHL-FcHis-mCherry. 1.3% TAE agarose gel, molecular weight marker – GeneRuler 50bp DNA ladder (Life Technologies, UK).

Positive evidence of pHL-FcHis-mCherry transfer into boar sperm was obtained in approximately half of the 13 samples (6/13; 46.2%) available for analysis. In samples, where there was no evidence of the transfer of pHL-FcHis-mCherry into sperm (7/13; 53.8%), the 'true' negative outcomes, caused by failure of transfer, were observed in approximately one third of cases (2/7; 28.5%). In the remaining cases, the lack of evidence of pHL-FcHis-mCherry transfer into sperm was caused by insufficient DNA amplification from experimental samples and, therefore, could be inconclusive (**Figure 5–4**). The highest frequency of pHL-FcHis-mCherry detection was observed in samples exposed to a combination of C105Y-functionalised MSNPs and free pHL-FcHis-mCherry (30.7%; 4/13), followed by a combination of unmodified MSNPs and pHL-FcHis-mCherry (15.4%; 2/13), pHL-FcHis-mCherry adsorbed on PEI-coated MSNPs (7.8%; 1/13) and free pHL-FcHis-mCherry (7.8%; 1/13). The differences in frequencies of DNA transfer into sperm between various treatments were not significant ($p>0.05$).

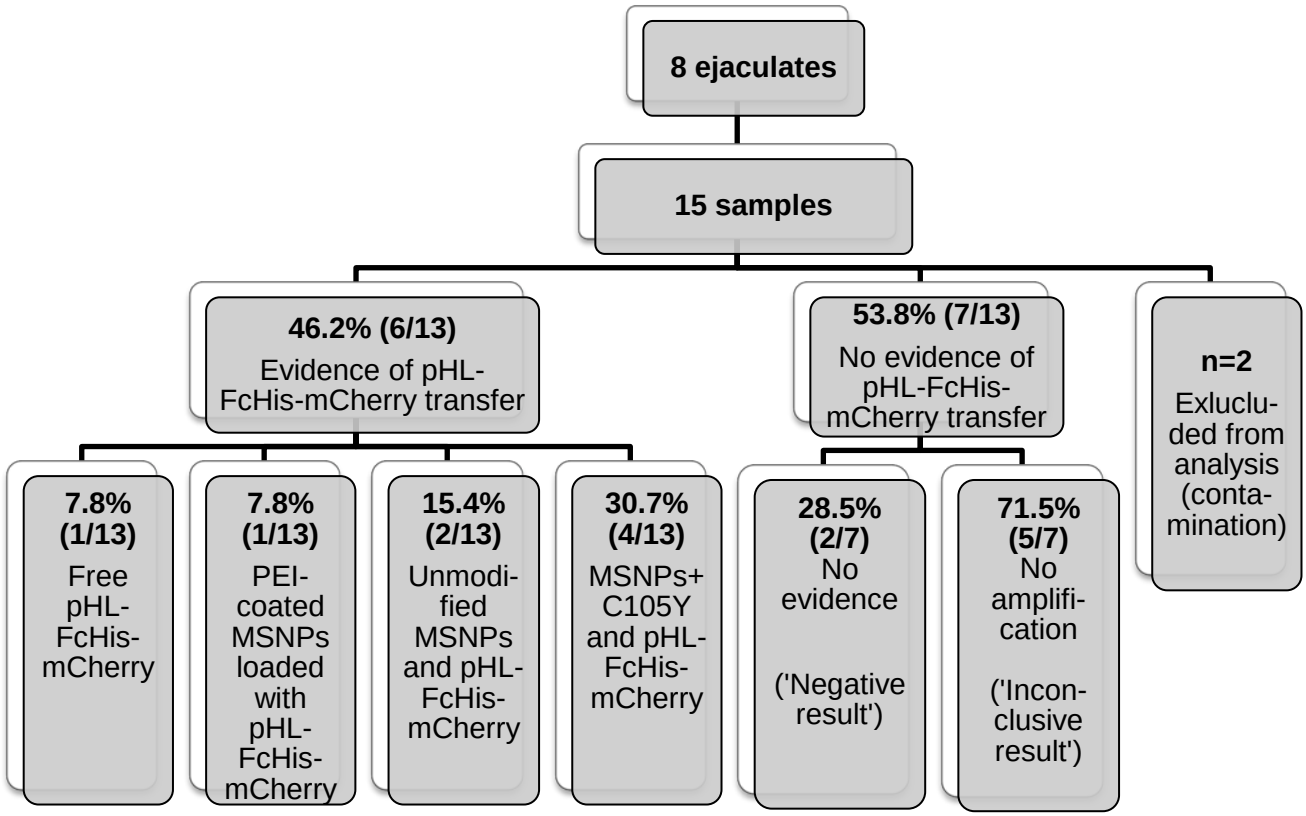

***Figure 5-4* – Transfer of pHL-FcHis-mCherry into boar sperm: qualitative outcomes.** Qualitative assessment of pHL-FcHis-mCherry transfer into boar sperm was based upon detection of a ~400bp band corresponding to target mCherry sequence (437bp) was detected on agarose gels after PCR amplification of DNA, extracted from boar sperm.

Quantitative assessment of the efficacy of MSNP-mediated DNA transfer into boar sperm was performed using the densitometric quantification of relative intensity of bands, corresponding to the mCherry target fragment, *versus* the internal control (swine leptin). Adjusted relative densities were calculated as a ratio between the relative intensity of mCherry target fragment in samples exposed to the combination of free/adsorbed plasmid and any modification of MSNPs *versus* the relative intensity of mCherry target fragment in samples exposed to free plasmid only (**Figure 5–5**). The only type of treatment associated with a higher value of adjusted relative intensity of target mCherry fragment, compared to free plasmid, was the combination of C105Y-functionalised MSNPs and pHL-FcHis-mCherry. Treatment with PEI-coated MSNPs, loaded with pHL-FcHis-mCherry, and the combination of unmodified MSNPs and free pHL-FcHis-mCherry, resulted in a lower adjusted relative density of target mCherry fragment, compared to free plasmid. However, differences between the treatment types were not significant ($p>0.05$).

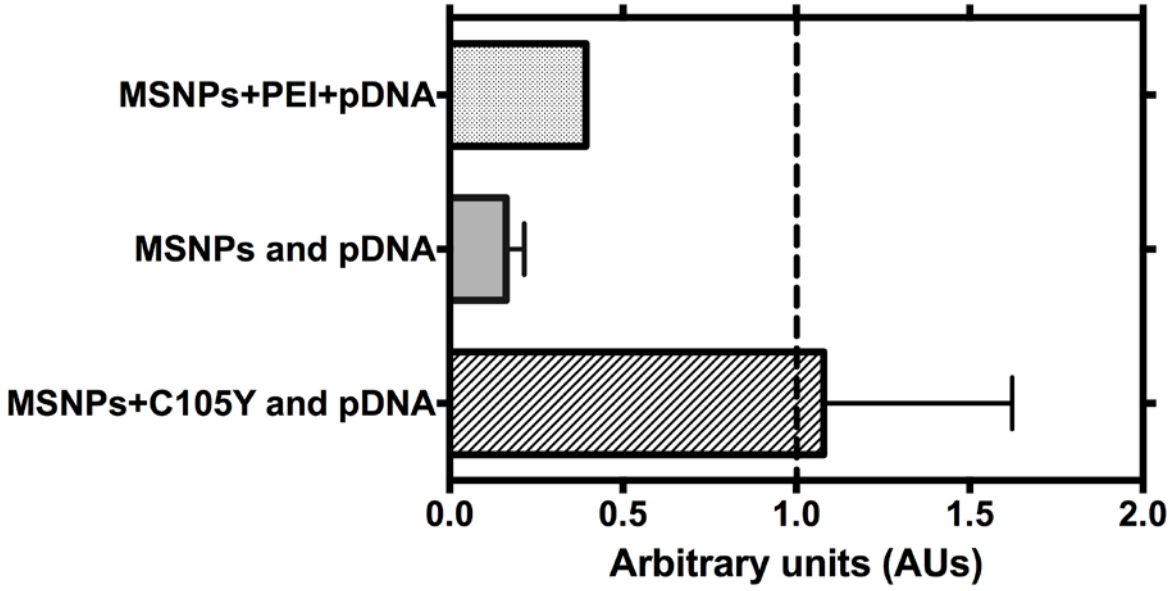

Figure 5-5 – **Transfer of pHL-FcHis-mCherry into boar sperm. Adjusted relative density of target mCherry sequence amplified using PCR and visualused on agarose gels: densitometry assessment.** Mean adjusted relative density of target mCherry fragment in samples exposed to the combination of C105Y-functionalised MSNPs and free pHL-FcHis-mCherry was higher compared to samples exposed to free plasmid ($p>0.05$). Exposure to PEI-coated MSNPs loaded with pHL-FcHis-mCherry and unmodified MSNPs and pHL-FcHis-mCherry resulted in lower adjusted relative density of target mCherry fragment compared to samples treated with free plasmid only ($p>0.05$). Vertical dotted line represents the relative mCherry density in samples exposed to free plasmid only. For 'MSNPs and pDNA' and 'MSNPs+C105Y and pDNA' treatments, data are presented as mean±SEM from two and four replicates, respectively.

5.3.3.3. Safety of exogenous DNA transfer into sperm with respect to sperm function

Sperm motility and viability were evaluated after 2 hours of incubation to confirm that exposure to plasmid DNA in free and adsorbed form did not produce negative effects upon sperm function under the specific conditions used during this set of experiments. The type of treatment had no significant effect upon total and progressive sperm motility, assessed by CASA, and viability, assessed by dual staining with SYBR green/propidium iodide, after 2 hours of incubation *versus* time-matched controls ($p>0.05$) (**Figure 5–6**).

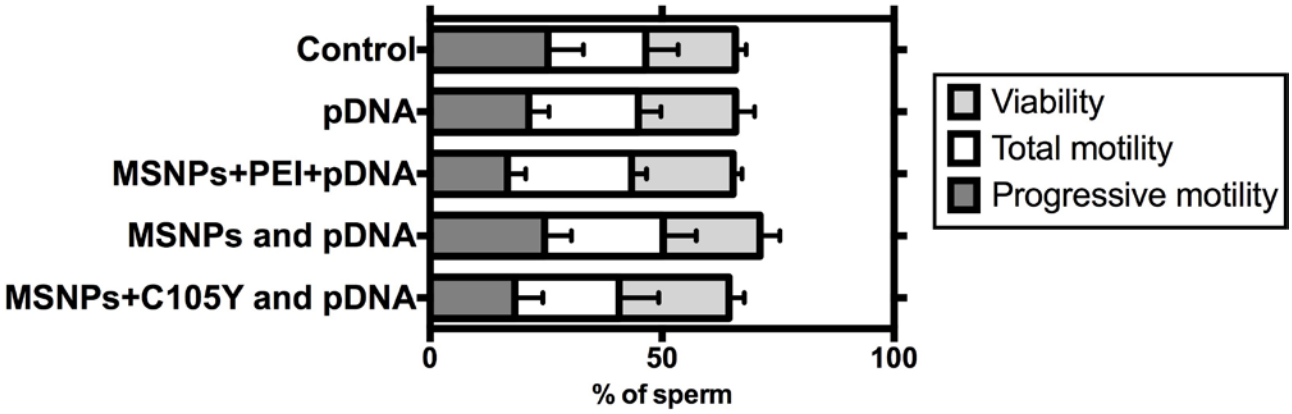

Figure 5-6 – **Proportions of motile, progressively motile and viable boar sperm after 2 hours of exposure *in vitro* to various modifications of MSNPs (~138nm) in a 10µg per 10^7 sperm ratio and free/absorbed pHL-FcHis-mCherry in a 1µg per 10^7 sperm ratio.** Assessment carried out using CASA and SYBR green/propidium iodide dual staining (mean±SEM from four replicates of experiment).

5.3.4. MSNP-MEDIATED TRANSFER OF PROTEIN INTO SPERM

Transfer of mCherry into boar sperm after exposure to free/adsorbed protein and various modifications of MSNPs was performed in 3 ejaculates (three repeats per ejaculate). Evidence of transfer was considered positive by the detection of a ~30kDa band corresponding to mCherry (28.2 kDa) on PVDF membranes after probing with anti-mCherry antibody (**Figure 5–7**). A ~50kDa band corresponding to β-tubulin (50kDa) was used as an internal (loading) control for the quantitative assessment of protein transfer efficacy. Immediately after sperm lysis, the absorbed form of mCherry could be visualised as a band with a higher than expected molecular weight (~50kDa) (**Figure 5–7A**), indicating that adsorption on MSNPs slowed down the migration of mCherry during gel electrophoresis. After freezing/thawing, the 'protein retardation' phenomenon in samples exposed to mCherry adsorbed on APTES-coated MSNPs disappeared, which could indicate the disruption of chemical bonds between the particles, EDC and protein (**Figure 5–7B**).

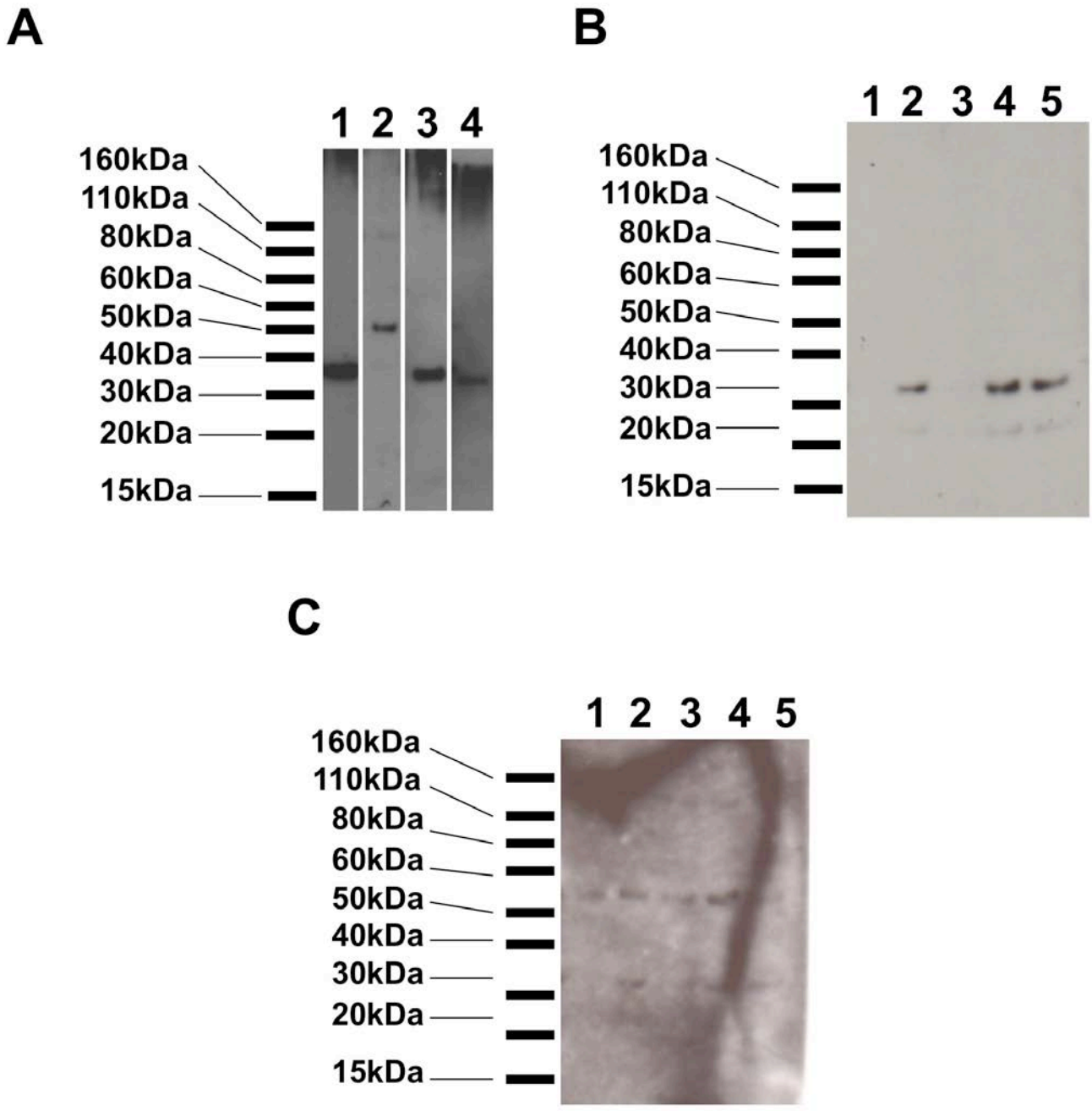

Figure 5-7 **- Detection of mCherry transfer into boar sperm: representative images.** A) Detection of mCherry (~30kDa) in boar sperm lysates. Lanes represent different types of treatment: Lane 1 – free mCherry; Lane 2 – APTES-coated MSNPs, loaded with mCherry; Lane 3 – unmodified MSNPs and mCherry, Lane 4 – C105Y-functionalised MSNPs and mCherry. Immediately after lysis, mCherry adsorbed on APTES-coated MSNPs is visualised as the band with higher molecular weight. B) Detection of mCherry (~30kDa) in boar sperm lysates. After freezing/thawing, the 'protein retardation' phenomenon disappears. C) Detection of internal (loading) control, β-tubulin (~50 kDa), in boar sperm lysates. Lanes represent different types of treatment (B and C): Lane 1 – control; Lane 2 – free mCherry; Lane 3 – APTES-coated MSNPs, loaded with mCherry; Lane 4 – unmodified MSNPs and mCherry, Lane 5 – C105Y-functionalised MSNPs and mCherry. PVDF membranes sequentially probed with rabbit anti-mCherry-IgG (1:2,500) + goat anti-rabbit IgG-HRP conjugate (1:1,000) and rabbit anti-β-tubulin-HRP conjugate (1:2,500), molecular weight marker – Novex Sharp Pre-stained Protein Standard (Life Technologies, UK).

Positive evidence of mCherry transfer was obtained in all 9 samples (**Figure 5–8**). mCherry was successfully detected in sperm lysates from most samples exposed to mCherry absorbed on APTES-functionalised MSNPs (88.9%; 8/9), C105Y-functionalised MSNPs and free mCherry (88.9%, 8/9), and unmodified MSNPs and free mCherry (66.7%; 6/9). Interestingly, mCherry in sperm lysates could be detected in all samples exposed to free protein without MSNPs (100%; 9/9). Differences in the frequency of protein transfer into sperm between various treatments were not significant ($p>0.05$).

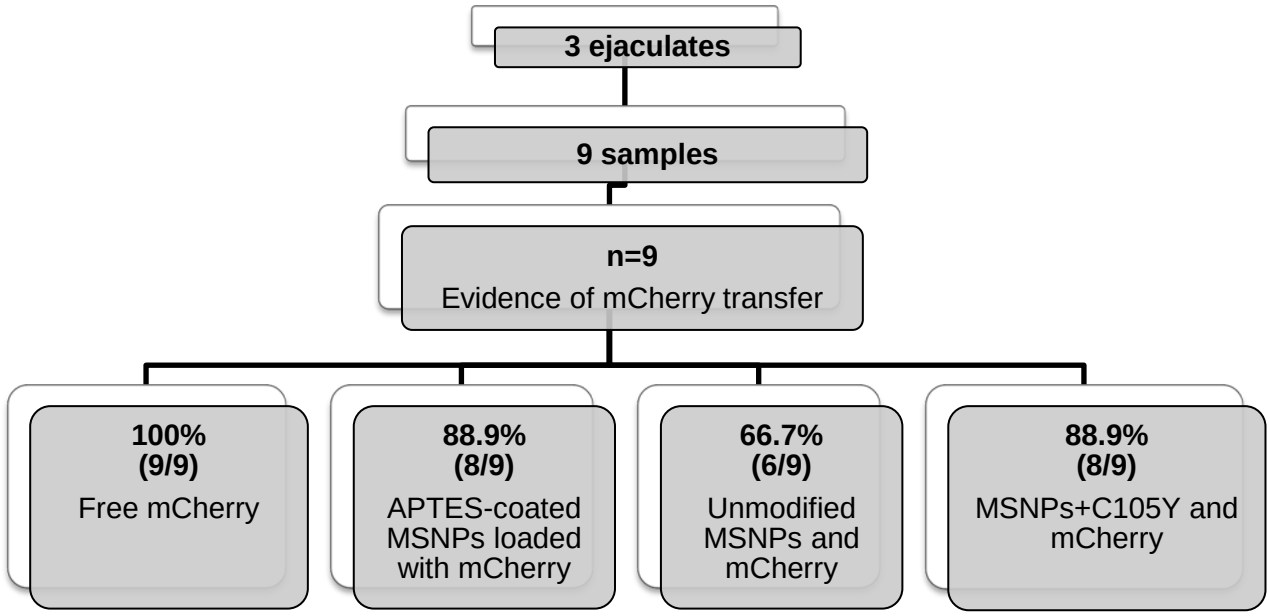

***Figure 5-8* – Transfer of mCherry into boar sperm: qualitative assessment.** Qualitative assessment of mCherry transfer into boar sperm was based upon the detection of a ~30kDa band corresponding to mCherry (28.2 kDa) on PVDF membranes after probing with anti-mCherry antibody.

Quantitative assessment of the efficacy of MSNP-mediated protein transfer into boar sperm was performed using densitometric quantification of relative band intensity, corresponding to mCherry in Western Blots of sperm lysates from samples exposed to the combination of any modification of MSNPs (APTES-coated, unmodified, C105Y-functionalised) and absorbed/free mCherry with *versus* free mCherry. Relative intensity of mCherry bands was adjusted for intensity of the loading control (β-tubulin) (**Figure 5–9**). The highest adjusted relative density of the mCherry band was observed after treatment with C105Y-functionalised MSNPs and mCherry (~3-fold increase *versus* free mCherry), followed by unmodified MSNPs and free mCherry

(~1.5-fold increase *versus* free mCherry). For APTES-coated MSNPs, loaded with mCherry, the adjusted relative density of the mCherry band was lower than in samples exposed to free mCherry (~10-fold decrease), which could indicate that covalent absorption of cargo on MSNPs restricts its intracellular delivery into gametes. Differences in the adjusted relative density of mCherry between various treatments were not significant ($p>0.05$).

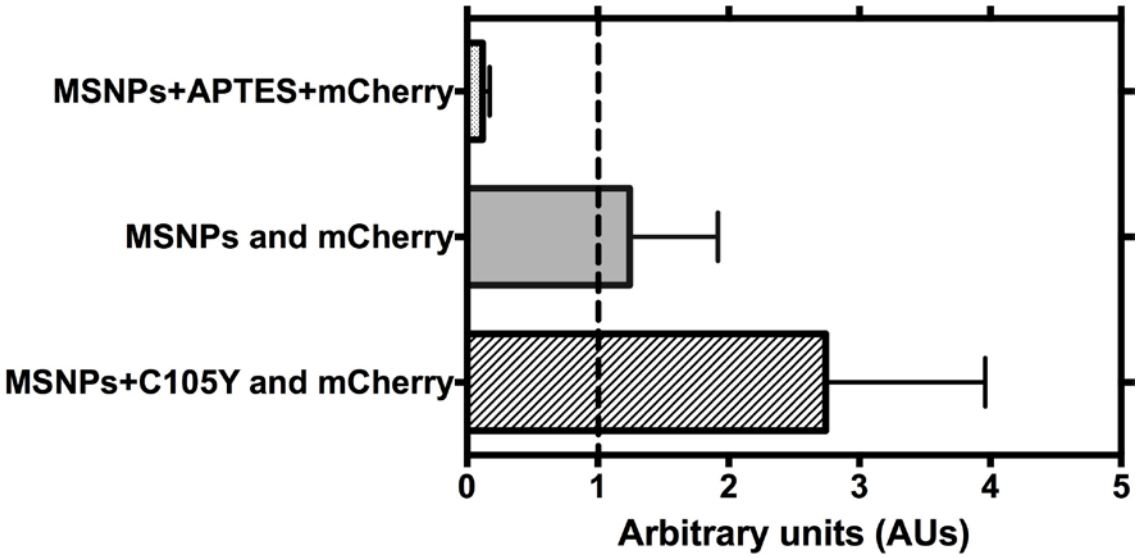

***Figure 5-9* – Transfer of mCherry into boar sperm. Adjusted relative density of mCherry on Western Blots of sperm lysates: densitometry assessment.** Average adjusted relative densities of mCherry in samples exposed to the combination of C105Y-functionalised MSNPs and free mCherry and unmodified MSNPs and free mCherry were higher compared to samples exposed to free mCherry only ($p>0.05$). In lysates from samples exposed to APTES-coated MSNPs loaded with mCherry, average relative densities of mCherry were lower than in free mCherry only ($p>0.05$). Vertical dotted line represents the relative mCherry density in samples exposed to free protein only. Data presented as mean±SEM from eight replicates for 'MSNPs+APTES+mCherry' and 'MSNPs+C105Y and mCherry' treatments, and six replicates for 'MSNPs and mCherry' treatment.

5.4. DISCUSSION

The growing evidence of the superiority of nanomaterials as targeted tools for molecular detection and delivery has triggered their expansion into a variety of research and clinical disciplines, including, but not limited to, oncology (Kim *et al.*, 2013b), cardiology (Psarros *et al.*, 2012), neurology (Holmes, 2013), immunology (Gharagozloo *et al.*, 2015; Serra and Santamaria, 2015), and microbiology (Mahajan *et al.*, 2012; Singh *et al.*, 2014; Choudhary and Kusum Devi, 2015). Reproductive science is a field where the concept of nanomaterial-mediated delivery was particularly well received. Although a certain degree of caution over the long-term safety of these methodologies remains, the universal benefits of nanocarriers such as versatility, large loading capacity, ease of internalisation and non-biological nature, are viewed upon as highly advantageous (Makhluf *et al.*, 2008; Kim *et al.*, 2010b; Campos *et al.*, 2011a; Campos *et al.*, 2011b; Feugang *et al.*, 2012; Rath *et al.*, 2013; Jallouk *et al.*, 2014; Odhiambo *et al.*, 2014; Feugang *et al.*, 2015).

Consequently, over recent years, nanomaterials have been increasingly investigated as potential candidates for intra-gamete delivery, particularly delivery into sperm. These studies have sought to improve the efficacy of SMGT (Kim *et al.*, 2010b; Campos *et al.*, 2011a; Campos *et al.*, 2011b), load sperm with exogenous proteins while preserving their viability (Makhluf *et al.*, 2008), and tag sperm for subsequent sorting based upon sex chromosome (Barchanski *et al.*, 2015) or functional status (Odhiambo *et al.*, 2014). Apart from intracellular delivery, nanomaterials have been used to tag preimplantation embryos (Fynewever *et al.*, 2007), promote embryonic growth and development (Pineda *et al.*, 2012), and assist in the bioimaging of sperm (Feugang *et al.*, 2012; Feugang *et al.*, 2015).

To date, the number of studies investigating nanomaterials specifically for delivery into gametes remains relatively low. Since 2008, there have been only five peer-reviewed publications describing the intentional use of nanoparticles to assist with SMGT, and load sperm with proteins or molecular probes for subsequent sorting (**Table 5–2**). Nevertheless, these publications largely provided encouraging evidence regarding the delivery capacity of specific nanomaterials, including

magnetic iron oxide, halloysite clay nanotubes and nanogold. The promising outcomes of the earlier subset of these publications influenced, to a certain extent, the experiments carried out throughout this thesis in general, and this Chapter in particular.

The current experiments, for the first time, evaluated the ability of MSNPs to transfer molecular cargo into mammalian sperm. Different modifications of MSNPs were first shown to be biocompatible with mammalian sperm in the earlier chapters of this thesis. Therefore, experiments performed in this Chapter represent a logical extension of research into the possibility of using MSNPs as a delivery vector for reproductive biology. Specifically, these experiments assessed the qualitative and quantitative delivery efficacy of MSNPs for DNA and protein transfer using previously optimised incubation conditions such as particle/sperm ratios and duration of incubation. Both types of cargo tested herein represent strong candidates for nanoparticle-mediated delivery into sperm. The enhanced uptake of these compounds into male gametes could help promote the efficacy of such techniques as SMGT, or exogenously supplement infertile sperm which are devoid of specific molecular factors that are essential for fertilization with their analogues (such as sperm-borne oocyte activating factors, for example PLCζ).

This Chapter presents the comparative analysis of qualitative and quantitative delivery efficacy of MSNPs loaded with biological cargo (DNA/protein) *versus* free cargo and two types of MSNPs, unmodified and C105Y-functionalised, which were mixed, but not loaded, with cargo. This particular design of experiments was chosen to answer the following research questions: firstly, does simultaneous exposure to MSNPs and absorbed/free payloads improve uptake into sperm *versus* free payloads only; secondly, does payload adsorption on appropriately functionalised MSNPs (PEI- or APTES-coated for DNA and protein adsorption, respectively) promote uptake *versus* simultaneous treatment with non-adsorbed payloads and MSNPs; and, finally, does the active targeting of MSNPs towards sperm improve their delivery efficacy *versus* non-targeted loaded/non-loaded MSNPs, and cargo-only treatment. Collectively, these experiments sought to assess, for the first time, the feasibility of MSNP-mediated delivery into mammalian sperm and

logically complete this thesis by permitting conclusions to be drawn about the practicality of MSNPs as delivery vectors for these specialised cells.

5.4.1. MSNPS FOR THE DELIVERY OF EXOGENOUS DNA INTO SPERM

The use of nanomaterials to promote exogenous DNA uptake into sperm forms one of the potential strategies to improve the efficacy and reliability of SMGT. SMGT is based on the natural property of sperm from different animal species to bind and uptake exogenous DNA during co-incubation and deliver the construct into the oocyte at the time of fertilization, thus resulting in the production of transgenic/mosaic embryos. SMGT forms an attractive and, in theory, straightforward technique for genetic manipulation, which, in contrast to microinjection approaches, does not require expensive specialised equipment and appropriately trained staff. In addition, SMGT can be used as an alternative to pronuclear injections, or stem cell transfer into the blastocyst, in species where micromanipulation transgenesis is generally challenging. For example, in the case of the porcine model, the introduction of desired genetic traits into embryos via microinjection is compromised by poor visualisation of the pronuclei due to the high lipid content of porcine oocytes (Coward *et al.*, 2007; Lavitrano *et al.*, 2013), thus rendering SMGT the technique of choice.

SMGT was first described by Brackett (1971), who exposed rabbit sperm to simian virus-40 (SV-40) while investigating the possibility of SV-40 transmission into the oocyte during fertilisation and surprisingly found that SV-40 DNA, but not the virus itself, could be internalised into at least one in three sperm and further transmitted into the oocyte. These observations remained largely unnoticed until 1989, when two independent reports of successful SMGT in mice and sea urchins were published (Arezzo, 1989; Lavitrano *et al.*, 1989), rekindling scientific interest in this methodology. To date, the number of publications describing the use of SMGT for the production of transgenic offspring exceeds 70, and the range of species where this technique was deemed successful includes rodents, farm animals, monkeys, birds, insects, frogs and fish (Smith and Spadafora, 2005; Coward *et al.*, 2007; Parrington *et al.*, 2011). However, the efficacy and

reproducibility of SMGT are poor, and stable integration of genetic constructs into F_1 offspring occurs in only approximately 25% of cases (Smith and Spadafora, 2005; Eghbalsaied *et al.*, 2013).

Strategies to improve the efficacy of SMGT include electroporation, use of liposomes, intracytoplasmic injection of oocytes with sperm exposed to free or liposomal forms of transgenes, or linking of a transgene with specific monoclonal antibodies which target the sperm membrane (revewed by Smith and Spadafora, 2005). The use of nanomaterials as carriers of exogenous DNA into mammalian sperm represents another potential strategy to improve the efficacy and reliability of SMGT. To investigate the feasibility of this approach, Kim et al. (2010) applied commercial magnetic iron nanoparticles and an external magnetic field ('magnitofection') to promote uptake of the pCX-EGFP/Neo plasmid into boar sperm, and observed more than a 3-fold increase in the efficacy of this technique compared to simple co-incubation and sperm transfection with lipofectamine. In a further series of studies, Campos *et al.* (2011) showed that a commercial nanotransfectant and halloysite clay nanotubes were also effective in internalising the pEGFP-N1 plasmid into bovine sperm. According to the results of these studies, the efficacy of 'nanoSMGT', assessed as plasmid copy number per sperm, was approximately 2 times higher for halloysite clay nanotubes and 3 times higher for commercial nanotransfectant *versus* free plasmid and lipofection. The efficacy of 'nanoSMGT' for the delivery of exogenous DNA into 4-cell embryos was 4 times higher for both types of nanomaterials *versus* free plasmid and lipofection.

Despite this encouraging evidence from different research groups, the beneficial effects of MSNPs upon the uptake of exogenous DNA into sperm were not confirmed in this thesis. In fact, loading pHL-FcHis-mCherry onto PEI-coated MSNPs did not promote DNA delivery into sperm compared to free DNA, both from a qualitative and quantitative perspective. Specifically, pHL-FcHis-mCherry was detected in the same number of samples (1/13) exposed to free plasmid and plasmid that was electrostatically adsorbed on PEI-coated MSNPs. From a quantitative perspective, the delivery efficacy for PEI-coated MSNPs loaded with pHL-FcHis-mCherry was less than half that recorded for the free plasmid.

The two remaining types of treatment, specifically co-exposure to unmodified or C105Y-functionalised MSNPs and free pHL-FcHis-mCherry, resulted in the transfection of a larger number of samples (2/13 and 4/13, respectively). In the case of unmodified MSNPs and free pHL-FcHis-mCherry, quantitative delivery efficacy was lower than that for free plasmid. However, in the case of C105Y-functionalised MSNPs and free pHL-FcHis-mCherry, comparable efficacy was observed.

Therefore, the only modification of MSNPs, which demonstrated beneficial effects for intra-sperm delivery, involved active targeting towards mammalian sperm via functionalisation with C105Y. These particles demonstrated the potential to deliver DNA into a larger number of samples compared to other types of treatment, but did not promote the uptake of larger quantities of plasmid. It is particularly important to note that the two single cases of DNA transfer into sperm after exposure to free pHL-FcHis-mCherry and pHL-FcHis-mCherry adsorbed on PEI-coated MSNPs, and one out of the four transfer cases after exposure to the combination of C105Y-functionalised particles and free pHL-FcHis-mCherry, were observed in the same sperm sample. This corresponds to previous observations by Lavitrano *et al.* (2013), who consistently demonstrated that sperm from different boars have variable capacity to spontaneously incorporate exogenous DNA. Therefore, in accordance to their recommendations, only sperm from specific animals with proven ability to uptake transgenes should be used to achieve reproducible outcomes of SMGT for transgenesis. In the view of these observations, it appears encouraging that exposure to unmodified and C105Y-functionalised MSNPs allows the delivery of DNA into sperm from animals other than those which seem to be intrinsically prone to uptake exogenous DNA into gametes. It could be hypothesised that co-incubation with MSNPs, especially the C105Y-functionalised MSNPs, alters the permeability of sperm membranes for exogenous cargo, an assumption already made in **Chapter 4** of this thesis. However, this effect was only preserved when payloads were dispersed in culture medium in free form, and not absorbed on the MSNPs.

One possible hypothesis to explain the lack of effect in respect to the loading of plasmid onto PEI-coated MSNPs is that the specific modification of particles used in these experiments had

not been consistently shown to internalise into sperm in the previous chapters of this thesis. Although all three previously discussed studies which applied nanoparticles for SMGT included a step of particle loading with plasmid DNA, the nature of chemical bonds formed between the particles and nucleic acid during this process, and quantities of DNA loaded onto the particles, were not described. As such, in the studies by Campos *et al*. (2011a,b), the internalisation of nanoparticles into sperm was not assessed. It was, therefore, difficult to draw conclusions whether the improved efficacy of plasmid transfer into sperm was indeed the consequence of 'true' particle internalisation or simply changes in sperm membrane permeability without particle penetration. In the study by Kim *et al.* (2010), the enhancement of plasmid delivery into sperm was associated with minimal internalisation of magnetic iron nanoparticles into some gametes thereby highlighting that, for these particles, intracellular uptake might not be necessary for efficient delivery. In contrast to observations by Kim *et al*. (2010), the lack of uptake of the MSNPs used in this thesis appeared to be a limiting factor. However, this thesis utilised particles with substantially larger size than the magnetic iron oxide NPs used by Kim *et al.* (~138nm *versus* ~10nm), which could result in a fundamentally different mechanism of interaction with the sperm membrane.

Collectively, the outcomes of the present set of experiments suggested that although PEI-coated MSNPs could be efficiently loaded with plasmid DNA in doses which had previously been characterised as sufficient for SMGT, such loading, in fact, restricted the delivery of cargo into sperm. In contrast to previous observations by other research groups, which indicated that intracellular penetration of loaded particles was not essential for cargo transport into the cytoplasmic compartment, the lack of intracellular uptake appeared to limit the delivery efficacy of cargo-loaded MSNPs. Interestingly, the co-incubation of sperm with unloaded particles and free cargo seemed to extend the potential application of MSNPs for exogenous DNA transfer to sperm from a wider subset of animals, although the quantities of plasmid internalised into sperm did not differ significantly from those observed after exposure to free payloads. This phenomenon was observed more often for MSNPs actively targeted towards mammalian sperm with C105Y. It could

be hypothesised that in the cases of combined treatment with MSNPs and free cargo, the qualitative improvement in uptake efficiency was related to changes in sperm membrane permeability. The free nature of cargo could allow its unrestricted internalisation into cells, without being 'held back' by the adsorption of a relatively inert and large nanocarrier. It is of particular worth to note that these conclusions, although seeming logical in the view of available evidence, were drawn with a great degree of caution, given the small number of samples analysed and technical limitations of the experimental procedures, primarily related to amplification failures. Importantly, the procedure of DNA transfer into sperm remained safe from the perspective of the first-line parameters of sperm function, including total and progressive motility, and viability.

5.4.2. MSNPS FOR THE DELIVERY OF EXOGENOUS PROTEIN INTO SPERM

Sperm supplementation with exogenous proteins could become a promising strategy for replacement therapy for sperm-specific molecular deficiencies, resulting in aberrant fertilisation and embryo development. Among these, a sub-family of molecules termed 'sperm-borne oocyte activating factors' (SOAFs), and particularly PLCζ, represent particularly strong candidates for exogenous supplementation in the cases of male infertility caused by structural or functional abnormalities of these proteins (Amdani *et al.*, 2013; Amdani *et al.*, 2015). These cases are believed to account for the majority of unsuccessful ICSI procedures in clinical IVF. At present, the only available tool to improve reproductive outcomes in such scenarios is the use of mechanical, chemical or electrical artificial oocyte activators, which remain the source of debate, since their efficacy and safety is still under scrutiny (Sfontouris *et al.*, 2015).

This thesis was under in a research group with a long history of studies into the roles of SOAF in oocyte activation, and the development of methods to produce exogenous replacement therapies for SOAF deficiencies. Development of nanoparticle-based delivery vectors that are capable of transporting proteins inside sperm, therefore, complemented the general research strategy in the group, ultimately aiming to a design a comprehensive solution for the treatment of rare forms of male infertility.

To date, there has been only one study investigating the delivery of proteins into mammalian sperm using nanomaterials. In 2008, Makhluf *et al*. described the use of modified polyvinyl alcohol (PVA) magnetite (Fe_3O_4) nanoparticles for intracellular transfer of anti-proteinkinase C (PKC) α antibody into bovine sperm. This antibody absorbed onto the particles was internalised into sperm after 1 hour of incubation and retained its functional activity, thereby allowing the use of this technique for immunoassays and studies of protein localisation in living cells (Makhluf *et al.*, 2008). This study, however, had a proof-of-concept design and did not compare the efficacy of nanoparticle-mediated delivery of anti-PKCα to the efficacy of free anti-PKCα.

In the set of experiments described in this Chapter, MSNPs were also proven to be capable of protein transfer into sperm. However, the qualitative and quantitative efficacy of such transfer did not significantly exceed the efficacy observed for free protein. The presence of mCherry protein in sperm lysates following exposure to APTES-coated MSNPs loaded with mCherry, and free mCherry, was observed similar numbers of analysed samples. In contrast to anticipated outcomes, the adsorption of mCherry on APTES-coated MSNPs appeared to restrict its delivery into boar sperm from the quantitative perspective, resulting in the transfer of only approximately one-tenth of the amount of mCherry which was delivered into sperm after exposure to free protein only. Combined treatment with unmodified MSNPs and free mCherry resulted in slightly lower qualitative delivery efficacy compared to free protein, but similar amounts of delivered protein. Exposure of sperm to combination of C105Y-functionalised MSNPs led to the uptake of approximately double the amount of mCherry than protein-only treated sperm.

Interestingly, results from the current nanoparticle-mediated protein transfer experiments showed trends similar to those observed during DNA transfer into sperm. Specifically, the adsorption of payloads on appropriately functionalised nanomaterials did not seem to promote their uptake into sperm. In fact, such adsorption appeared to restrict the intracellular delivery of molecular cargo, and was likely to underlie poor MSNP internalisation into sperm. This

phenomenon was even more pronounced for protein-loaded particles, which could be explained by the inherently stronger nature of covalent bonds involved in protein adsorption compared to electrostatic bonds, which were formed between payloads and particles during DNA loading.

Furthermore, active targeting of MSNPs towards mammalian sperm with C105Y seemed to partially rescue transfer outcomes (qualitatively in the case of DNA and quantitatively in the case of protein). It could be hypothesised that active targeting of MSNPs towards mammalian sperm, and earlier formation of MSNP-sperm associations, which was observed in **Chapter 4** of this thesis, indirectly facilitated the uptake of molecular payloads.

In summary, the set of experiments performed in this Chapter demonstrated that MSNPs loaded with cargo were capable of payload delivery into sperm. However, MSNPs did not promote, but rather restricted, uptake compared to free cargo. It is likely that these unexpected outcomes are the result of poor MSNP internalisation into sperm and, therefore, retardation of cargo in the extracellular compartment together with the particles. Exposure of sperm to actively targeted particles resulted in a trend towards better delivery efficacy, either facilitating delivery into a larger subset of samples or increasing the quantity of delivered cargo.

CHAPTER 6

ASSESSMENT OF THE BIOCOMPATIBILITY AND DELIVERY POTENTIAL OF MESOPOROUS SILICA NANOPARTICLES FOR MOLECULAR TRANSFER INTO HUMAN SPERM

Key messages:

- This chapter presents the outcomes of experiments investigating the biocompatibility and delivery potential of MSNPs as DNA carriers into human sperm.
- MSNPs preserved their biocompatibility and potential to bind with cells when applied to human sperm, although MSNP-sperm binding profiles demonstrated inter-species specificity and were significantly affected by the dose of particles and time of exposure.
- All types of MSNPs tested promoted transfer of DNA into human sperm compared to the spontaneous uptake of free exogenous DNA.
- The use of active targeting with C105Y had limited value in human sperm, indicating the potential for species-specific effects.
- Collectively, these outcomes supported the possibility to apply MSNPs as safe delivery vectors into human sperm, although further studies are warranted to evaluate their performance in fresh gametes, and gametes with compromised function, prior to experimental clinical use.

6.1. BACKGROUND

Despite the interest towards nanomaterial-mediated delivery for reproductive biology, the use of this technology in human gametes, even in the context of *in vitro* trials, remains sparse. To date, the spectrum of nanomaterials tested in human gametes, or, more precisely, human sperm, remains narrow, and includes nanogold, nanosilver, cerium dioxide, titanium dioxide and zinc oxide (**Table 6–1**). All of these nanomaterials were shown to exert the negative impact upon sperm function, including reduction in motility and viability, and the promotion of DNA damage.

***Table 6-1*– Nanomaterials in human sperm: *in vitro* nanotoxicity studies**

Study	Nanomaterial	Size (nm)	Final concentration	Effects
Wiwanitkit *et al.* (2009)	Nanogold	9	N/A	Loss of motility in 25% sperm Particle penetration into sperm head and tail Sperm 'fragmentation'
Gopalan *et al.* (2009)	Zinc oxide Titanium dioxide	40-70 40-70	11.5-92.3 μg/ml 3.73-59.7 μg/ml	Sperm DNA damage
Terzuoli *et al.* (2012)	Nanosilver	65	125-500 μM	Decrease in sperm motility and viability
Moretti *et al.* (2012)	Nanosilver Nanogold	65 50	30-500 μM	Decrease in sperm motility and viability
Perrin *et al.* (2014)	Cerium dioxide	N/A (~7)*	0.01-10 μg/ml	Sperm DNA damage

* reported in other publications by the same group (Courbiere *et al.*, 2013; Preaubert *et al.*, 2015)

The only established application of nanoparticles for human sperm is magnetic-activated cell sorting (MACS). This procedure involves the exposure of sperm samples to approximately 50nm superparamagnetic nanoparticles conjugated with annexin V, which bind the externalised phosphatidylserine residues on the surface of sperm undergoing apoptosis, and allows the subsequent removal of these sperm from the sample via binding to an affinity column in the presence of a magnetic field. Although data regarding the efficacy of MACS remain contradictory, and such techniques has not yet been introduced to routine practice in ART laboratories, this approach has been deemed safe and is becoming increasingly accepted (Gil *et al.*, 2013; Romany *et al.*, 2014; Bucar *et al.*, 2015).

The largely encouraging outcomes of the previous chapters of this thesis, and lack of data regarding overall performance of nanomaterials in human gametes, prompted investigation into the biocompatibility and potential uses of MSNPs in human sperm. This Chapter presents the outcomes of a set of experiments which aimed to assess the biocompatibility of MSNPs with human sperm and their ability to deliver payloads into these cells, using exogenous DNA as a prototype for molecular cargo. These experiments confirmed previous observations in that the outcomes of nanoparticle interaction with cells can vary considerably, depending on the cell type within the organism, or within the same cell type from different biological species. MSNPs retained their biocompatibility with human sperm, and did not exert negative effects upon sperm function. However, the binding profiles between MSNPs and human sperm were different than those described for boar sperm in the previous chapters of this thesis, and showed the positive association with dose and time of exposure to MSNPs. Finally, MSNPs were capable of the intracellular delivery of molecular cargo into human gametes and improved uptake of both free and adsorbed cargo compared to free molecules applied to gametes in the absence of MSNPs.

6.2. SPECIFIC DETAILS OF EXPERIMENTAL PROCEDURES AND DATA ANALYSIS

The general materials and methods used for the generation of results presented in this Chapter are described in **Chapter 2**. Specific details of the experimental procedure highlighted in this subsection relate to the exposure of MSNPs to human sperm.

In particular, for this set of experiments, a pooled and washed sperm sample, resuspended in PureSperm Wash medium, was separated into 250µl aliquots, which were subject to treatment with MSNPs or PBS (controls). Each experiment was repeated a minimum of three times. To evaluate the potential nanotoxicity of MSNPs in human sperm and to determine optimal doses and incubation times, washed sperm were exposed to z suspension of unmodified fluorescent MSNPs in PBS in ratios of 5µg, 10µg, 15µg and 30µg of particles per 10^7 sperm. In the control group, washed sperm were incubated with PureSperm Wash. Incubation was carried out for up to 4 hrs at 37ºC under a low-oxygen atmosphere. Sperm motility and viability were assessed after 2 and 4 hrs of

incubation. Sperm DNA fragmentation was evaluated after 4 hrs of incubation. Binding rates between sperm and unloaded MSNPs were determined after 1, 2, 3 and 4 hrs. Sperm motility, viability and DNA fragmentation rates were expressed as a proportional change from controls (in %).

After evaluating potential nanotoxicity and identifying the minimally effective particle/cell ratios and incubation times, I then evaluated the ability of MSNPs to deliver molecular cargo into human sperm. To achieve this, washed sperm were exposed to the following treatments: (1) PBS; (2) free pDRIVE-HSP70-GFP; (3) PEI-coated MSNPs, loaded with pDRIVE-HSP70-GFP; (4) unmodified MSNPs and pDRIVE-HSP70-GFP; (5) C105Y-functionalised MSNPs and pDRIVE-HSP70-GFP. All particle modifications were added to sperm at a ratio of 30µg of particles per 10^7 cells. Incubation was carried out for 3 hrs at 37ºC under a low-oxygen atmosphere. All stock suspensions of nanoparticles (concentration: 2mg/ml), in this case, were prepared with nuclease-free water. After 3 hours, sperm motility and viability were evaluated to ensure safety of the procedure, and cargo transfer into sperm was detected using the protocol described in **Section 2.6.2.**

6.3. RESULTS

6.3.1. NANOTOXICITY OF UNMODIFIED AND UNLOADED MSNPS IN HUMAN SPERM

6.3.1.1. Sperm motility and viability

Motility and viability were evaluated in sperm samples after 2 and 4 hours of incubation with unmodified MSNPs at a ratio of 5, 10, 15 and 30µg of particles per 10^7 sperm using CASA and dual staining with SYBR green/propidium iodide. There was no significant effect of the dose of MSNPs or the duration of incubation upon total and progressive sperm motility, but a significant effect of dose ($F_{1,30}$=3.076, p=0.040) and time of incubation ($F_{4,30}$=13.385, p=0.002) upon sperm viability. A significant difference was observed between sperm viability in samples exposed to the highest dose of MSNPs *versus* controls after 4 hours of incubation (p=0.043), favouring the experimental samples (**Figure 6–1**).

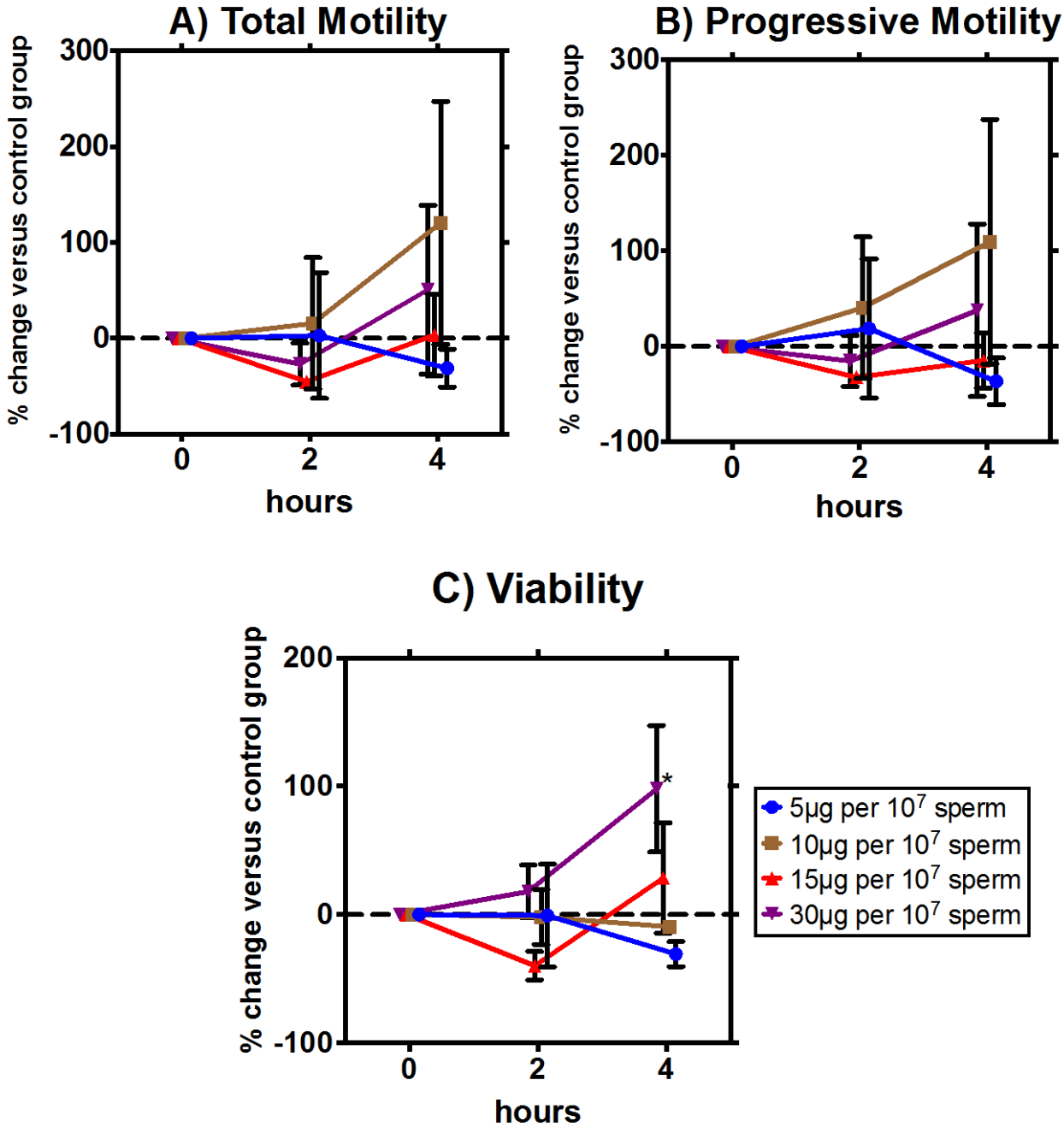

***Figure 6-1* – Proportions of motile, progressively motile and viable human sperm after 2 and 4 hours of exposure *in vitro* to unloaded unmodified MSNPs in four particle/cell ratios assessed by CASA and dual staining with SYBR green/propidium iodide staining** (mean±SEM from three repeats). Total and progressive motility and viability values were plotted as % change from time-matched control aliquots obtained from the same sperm sample as experimental aliquots. Symbol (*) denotes the subset of categories, whose values are significantly different from time-matched controls at the 0.05 level. Dotted horizontal line represents the relative level (100%) in time-matched controls, against which the % change was calculated.

There was no significant effect of the dose of MSNPs, or duration of incubation, upon any of the sperm kinematic parameters assessed by CASA. These parameters in MSNP-treated samples remained similar to time-matched controls at both time points for all doses of nanoparticles (**Figure 6–2**).

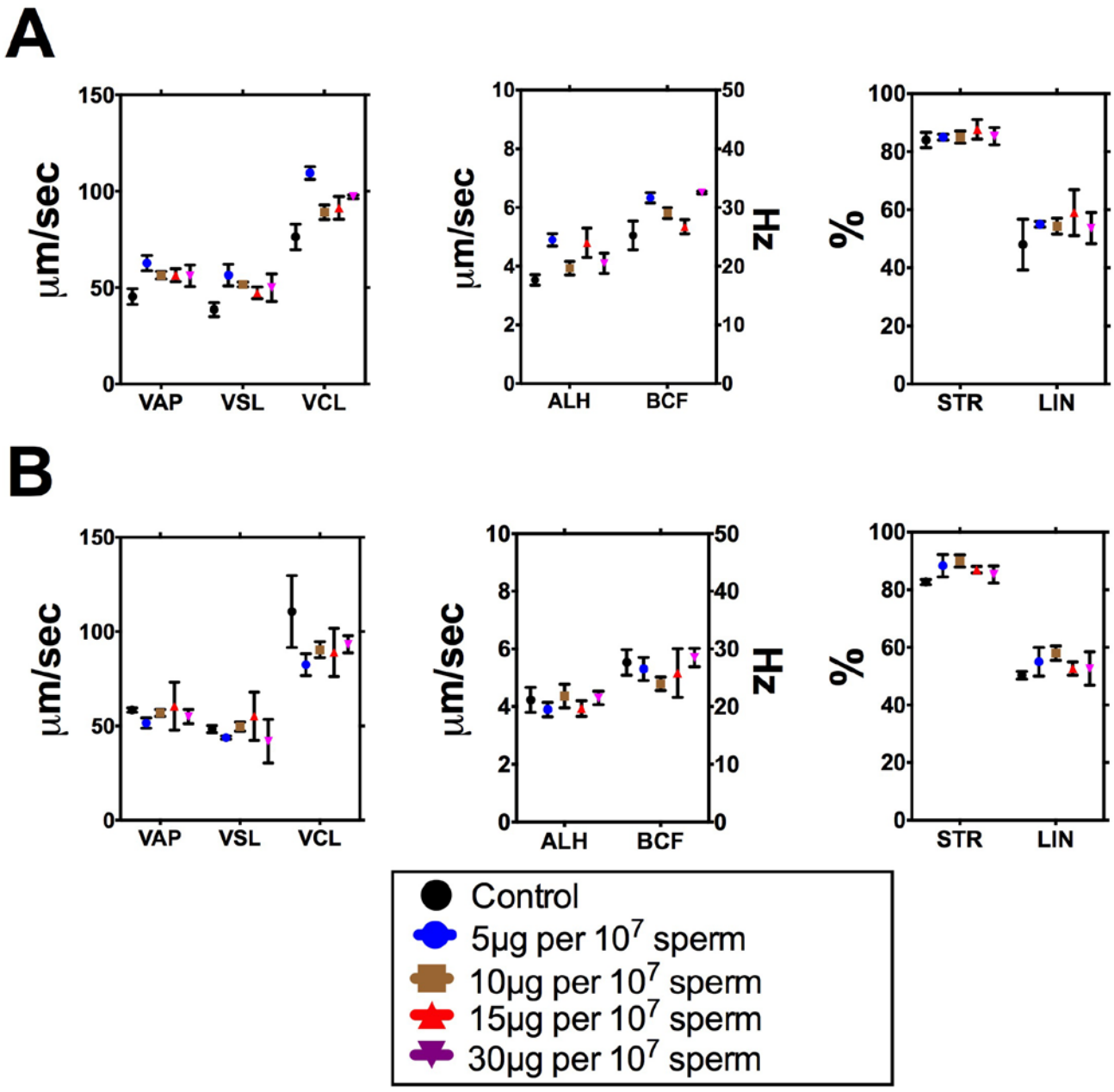

***Figure 6-2* – Kinematic parameters in human sperm after 2 and 4 hours of exposure *in vitro* to unloaded unmodified MSNPs in four particle/cell ratios assessed by CASA** (mean±SEM from three repeats). A) 2 hours; B) 4 hours. VAP: smoothed path velocity; VSL: straight line velocity; VCL: track velocity; ALH: amplitude of lateral head displacement; BCF: beat cross frequency. VAP: smoothed path velocity; VSL: straight line velocity; VCL: track velocity; ALH: amplitude of lateral head displacement; BCF: beat cross frequency. STR (ratio of VSL/VAP) = straightness, LIN (ratio of VSL/VCL) = linearity. There was no significant effect of the dose of MSNPs, or duration of incubation, upon any of the sperm kinematic parameters assessed by CASA.

6.3.1.2. Sperm DNA fragmentation index

Sperm DNA fragmentation was assessed in human sperm samples after 4 hours of incubation with unmodified MSNPs at a ratio of 5, 10, 15 and 30µg of particles per 10^7 sperm using the sperm chromatin dispersion method. There was no significant effect of the dose of MSNPs upon the proportion of sperm with fragmented DNA, which, after denaturation of sperm proteins and membrane lysis during the sperm chromatin dispersion test, appeared as cells without a typical halo of chromatin around the head (**Figure 6–3**).

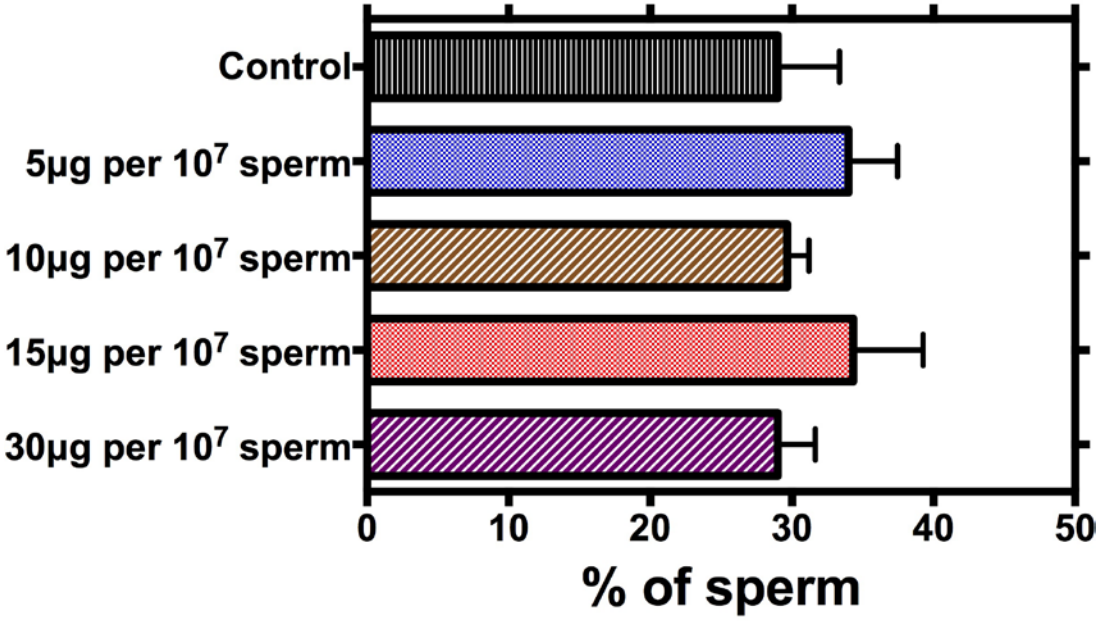

***Figure 6-3* – DNA fragmentation index in human sperm after 4 hours of exposure *in vitro* to unloaded unmodified MSNPs in four particle/cell ratios assessed using the sperm chromatin dispersion method** (mean±SEM from three replicates). There was no significant effect of the dose of MSNPs upon sperm DNA fragmentation index assessed using the sperm chromatic dispersion technique.

6.3.2. *Binding of unmodified and unloaded MSNPs with human sperm*

Binding rates between human sperm and unmodified unloaded MSNPs were assessed after 1, 2, 3 and 4 hours of incubation in order to assess the effects of time and MSNP dose upon particle-sperm interaction. Similarly to the previous chapters of this thesis, the term ‘binding’ was introduced to collectively describe the surface attachment and potential internalisation of MSNPs into sperm, although, given the outcomes of previous experiments, the latter was considered to be an unlikely phenomenon. MSNPs bound with human sperm in a similar fashion to boar sperm, and appeared as focal fluorescent signals in the sperm head, mid-piece or tail region (**Figure 6-4**).

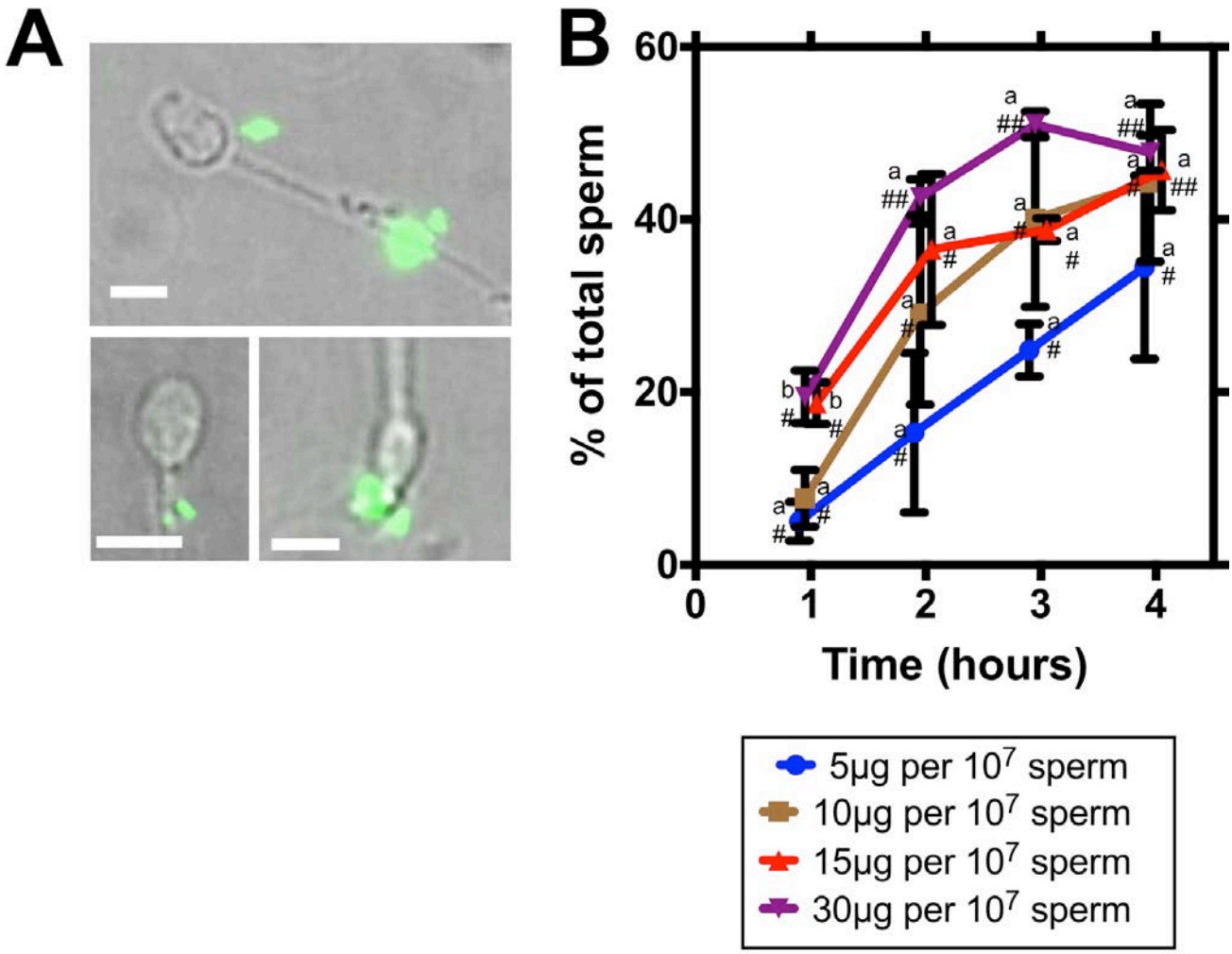

***Figure 6-4* – Binding of unloaded/unmodified MSNPs with human sperm after exposure *in vitro*. A) Representative images of the binding of unloaded unmodified MSNPs with human sperm.** MSNPs (shown as green fluorescence) bound to the sperm head, mid-piece and tail. Scale bar = 5µm. **B) Binding rates between human sperm and unloaded/unmodified MSNPs after 1, 2, 3 and 4 hours of exposure *in vitro* in four particle/cell ratios** (mean±SEM from three repeats). Each letter (a,b) denotes a subset of four dose categories within the same experimental point (i.e. 5µg vs 10µg per 10^7sperm at 1 hour), whose values did not differ significantly from each other at the 0.05 level. Symbol (#) denotes a subset of same dose categories of MSNPs at different time points (i.e. 5µg per 10^7sperm at 1, 2, 3 and 4 hours), whose values did not differ significantly from each other at the 0.05 level. Symbols (##) denote subsets whose values differed significantly from each other at the 0.05 level.

There was a significant effect of MSNP dose ($F_{3,32}$=7.333, $p<0.05$), and time of incubation ($F_{3,32}$=17.665, $p<0.05$), upon the binding rate. At the earliest stages of incubation, the two lower doses of MSNPs (5 and 10µg per 10^7 sperm) resulted in significantly lower binding rates, compared to the two higher particle/sperm ratios (15 and 30 µg per 10^7 sperm). Binding rates increased throughout incubation, and a significant increase was observed for the two higher particle/sperm ratios (15 and 30µg per 10^7 sperm). For the 15µg per 10^7 sperm ratio, a gradual 'accumulation' of the proportion of sperm bound with MSNPs took place. In this subset of samples, the differences in

binding rates reached the level of significance at the 4-hour incubation time point *versus* 1 hour of incubation. For the 30μg per 10^7 sperm ratio, a significant increase in the proportion of sperm bound with MSNPs (over 40% of the total number of sperm) was seen after just 2 hours of incubation, after which the binding rates stabilised. Although the trend towards a time-dependent increase in binding rates was observed in samples exposed to the lower doses of particles (5 and 10μg per 10^7 sperm), substantial variations in the proportions of sperm bound with MSNPs under these conditions accounted for the lack of significance of this trend.

Given the biocompatibility of MSNPs with human sperm in doses of up to 30μg particles per 10^7 sperm after up to 4 hours of *in vitro* exposure, and the significant effect of MSNPs dose, and time of incubation, upon binding rate with human sperm, the highest tolerable dose of 30μg per 10^7 sperm, and the duration of incubation of 3 hours, were chosen for subsequent experiments evaluating the ability of MSNPs to transport molecular cargo into human sperm. The decision to restrict incubation time to 3 hours and not continue *in vitro* exposure of sperm to MSNPs until the 4-hour time point was made to keep the cumulative duration of the protocol below 7 hours.

6.3.3. MSNP-MEDIATED TRANSFER OF DNA INTO HUMAN SPERM

Mesoporous silica nanoparticles, pre-coated with PEI and loaded with pDRIVE-HSP70-GFP, were used to perform the MSNP-mediated transfer of exogenous DNA into human sperm. After loading, 10μg of PEI-coated MSNPs were estimated to carry approximately 0.48μg pDRIVE-HSP70-GFP. Therefore, the quantity of plasmid presented to each 10^7 sperm was approximated to be 1.44μg. Similarly to the previous set of experiments described in **Section 5.3.3.**, this amount of DNA fell within the range of doses previously described as sufficient for SMGT in animal models and varying from 200ng to 10μg per 10^7 sperm (Oddi *et al.*, 2012; Lavitrano *et al.*, 2013).

In this set of experiments, the benefits of loading DNA onto MSNPs were, again, compared with the simple co-incubation of sperm with exogenous DNA *in vitro*, and simultaneous sperm exposure to free exogenous DNA and unmodified MSNPs or C105Y-functionalised MSNPs. For all

treatments, each 10^7 sperm were exposed to 30µg MSNPs and 1.44µg pDRIVE-HSP70-GFP, either in free or adsorbed form.

6.3.3.1. Quality control for DNA transfer/detection in human sperm

To ensure that the removal of non-internalised pDRIVE-HSP70-GFP from sperm samples using DNase I was efficient, the efficacy of the enzyme to digest the free plasmid was assessed. Exposure of free pDRIVE-HSP70-GFP to DNase I in a 1:4 (5 µg: 20 units) ratio for 30 minutes at 37°C resulted in full digestion of plasmid DNA, as evident by the absence of the amplified target GFP gene fragment (~188bp) on agarose gels after PCR (**Figure 6–5A**). Therefore, detection of pDRIVE-HSP70-GFP in human sperm after exposure to free/adsorbed plasmid and various modifications of MSNPs would be indicative only of the fraction of plasmid, transferred into sperm.

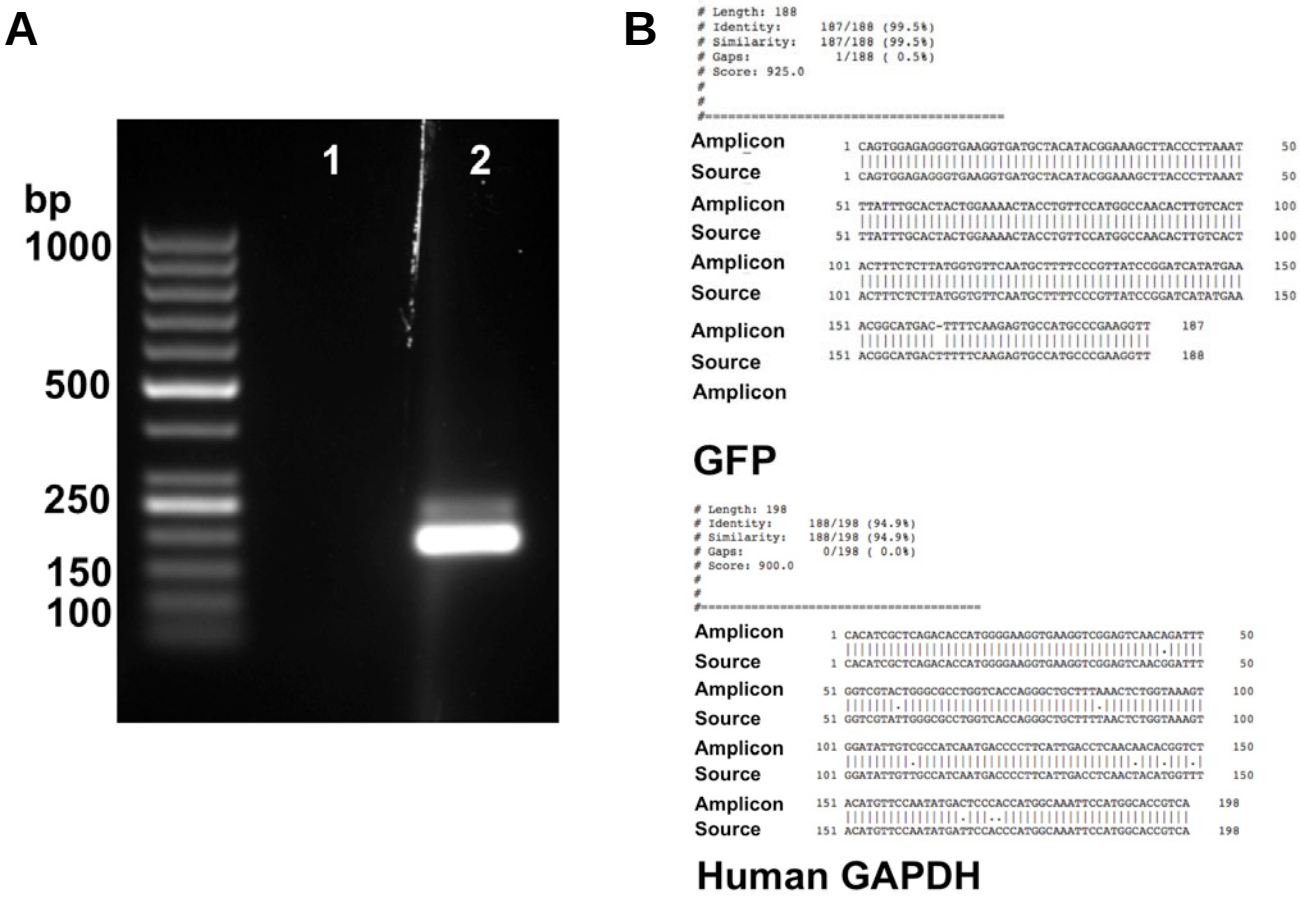

***Figure 6-5* – Quality control for the detection of DNA transfer into sperm.** A) Amplification of target GFP sequence (~188bp) from pDRIVE-HSP70-GFP before and after DNase I digestion. Lane 1 – after treatment with DNase I in a 1:4 (5 µg: 20 units) ratio for 30min at 37°C. Lane 2 – before treatment with DNase I (a ~1:10 dilution from the initial sample, subject to DNase I treatment). 1.3% TAE agarose gel, molecular weight marker – GeneRuler 50bp DNA ladder (Life Technologies, UK). B) Pairwise alignment of sequencing data from qPCR amplicons with source sequences of GFP and human GAPDH.

To confirm the nature of qPCR amplicons, products were subject to Sanger sequencing. Alignment of sequencing data from qPCR products with source sequences of GFP and human GAPDH confirmed a ≥ 95% match (**Figure 6–5B**).

6.3.3.2. Efficacy of MSNP-mediated DNA transfer into human sperm

Transfer of pDRIVE-HSP70-GFP into human sperm via exposure to free/adsorbed plasmid and various modifications of MSNPs was performed in 2 samples obtained from a pool of 10 frozen-thawed sperm aliquots from healthy donors. Transfer was considered successful in the case of qPCR amplification of target GFP sequence in DNA samples extracted from human sperm. Human GAPDH was used as an internal control for quantitative assessment of DNA transfer efficacy.

Positive evidence of pDRIVE-HSP70-GFP transfer into human sperm was obtained in both samples. Specifically, evidence of plasmid DNA transfer into sperm was positive in both samples exposed to pDRIVE-HSP70-GFP adsorbed on PEI-coated MSNPs and the combination of free pDRIVE-HSP70-GFP and C105Y-functionalised MSNPs, and half of the samples exposed to the combination of free pDRIVE-HSP70-GFP and unmodified MSNPs and free plasmid (1 out of 2 samples for each condition). Given the small number of analysed samples, statistical analysis of the differences in frequencies of DNA transfer into sperm between various treatments was not performed.

Quantitative assessment of the efficacy of MSNP-mediated DNA transfer into human sperm was performed using the comparative cycle threshold (Ct) method using qPCR data from samples where simultaneous amplification of target GFP sequence and internal GAPDH control was observed. Overall, all treatments promoted the uptake of plasmid DNA into human sperm. The relative amount of pDRIVE-HSP70-GFP transferred into human sperm in relation to the GAPDH sequence was the highest after exposure to pDRIVE-HSP70-GFP adsorbed on the PEI-coated MSNPs, followed by exposure to combinations of free pDRIVE-HSP70-GFP and unmodified MSNPs, and free pDRIVE-HSP70-GFP and C105Y-functionalised MSNPs (**Table 6–2**). Due to

small sample size and substantial variance in the relative amounts of pDRIVE-HSP70-GFP detected after transfer, the differences between the groups did not reach the level of significance ($p>0.05$).

***Table 6-2* – Relative amount of pDRIVE-HSP70-GFP transferred into human sperm after exposure to free/absorbed plasmid and various modifications of MSNPs**

Type of treatment	**Relative amount of pDRIVE-HSP70-GFP transferred into sperm *versus* the amount transferred after exposure to free plasmid only**			
	N	Mean	SEM	Median (25^{th} %; 75^{th} %)
PEI-coated MSNPs, loaded with pDRIVE-HSP70-GFP	6	$7.0x10^5$	$3.6x10^5$	$4.5x10^5$ ($5.4x10^3$; $1.3x10^6$)
Unmodified MSNPs and pDRIVE-HSP70-GFP	3	567.1	340.7	523.4 (0.04; 1178)
C105Y-functionalised MSNPs and pDRIVE-HSP70-GFP	4	22.24	21.84	0.6 (0.15; 87.77)

Relative amounts of pDRIVE-HSP70-GFP transferred into human sperm were calculated in relation to the GAPDH sequence using the comparative cycler threshold method (Ct) and the $2^{-\Delta\Delta Ct}$ equation. Exposure to free plasmid was used as a control condition.

6.4. DISCUSSION

This Chapter, for the first time, evaluated nanotoxicity and cargo deliver efficacy of MSNPs in human sperm and provided encouraging evidence that MSNPs retained both their biocompatibility when applied to human gametes *in vitro*, and the ability to strongly bind with sperm without compromising sperm function. Exposure of MSNPs to human sperm *in vitro* did not result in a negative effect upon sperm motility, viability or DNA status, which favourably distinguished MSNPs from other nanomaterials previously tested in human gametes, such as nanogold, zinc oxide, titanium oxide, nanosilver and cerium dioxide. In contrast to MSNPs, these nanomaterials produced strong negative effects upon sperm function, ranging from 'silent' sperm DNA damage (Gopalan *et al.*, 2009; Perrin *et al.*, 2014) to reduction in sperm motility and viability (Wiwanitkit *et al.*, 2009; Moretti *et al.*, 2012; Terzuoli *et al.*, 2012) and, finally, sperm 'fragmentation'(Wiwanitkit *et al.*, 2009). Therefore, the biocompatibility of MSNPs with human sperm represents a strong benefit, and enables their use as potential delivery vectors in an investigative or, perhaps, clinical setting.

MSNPs maintained their ability to bind strongly with human sperm during *in vitro* exposure, and the features of binding appeared similar to those previously observed in boar sperm.

Specifically, binding occurred in a 'focal' fashion, and MSNPs bound with sperm produced localised fluorescent signals in the sperm head, midpiece or tail. However, in contrast to findings obtained with boar sperm, the binding rates in human sperm showed a significant association with the dose of particles and time of incubation, both of which promoted MSNP binding. In addition, the size of the cohort of sperm binding with MSNPs was larger in human sperm than in boar sperm: after 4 hours of incubation, the proportion of sperm bound with MSNPs, in most cases, reached or exceeded an average value of 40%, as opposed to 20-30% in boar sperm. These results supported previous observations that the interaction of nanomaterials with cells depends upon a variety of factors, including physical and chemical properties of nanomaterials, but also cell type (Riehemann *et al.*, 2009; Kunzmann *et al.*, 2011; Taylor *et al.*, 2014c). The differences in MSNP binding rates in boar and human sperm could be attributed to a range of factors, including differences in sperm size and shape, membrane structure, and the fact that the human sperm used in this set of experiments was previously cryopreserved, which could have altered the membrane function. In addition, the human sperm used in this set of experiments demonstrated different parameters of sperm motion, compared to boar sperm. Specifically, human sperm generally exhibited lower velocity (VAP, VSL, VCL) and demonstrated less lateral head displacement (ALH), while swimming in a straighter fashion (STR > 80% and LIN ~ 60% in human sperm *versus* STR ~60% ad LIN ~40% in boar sperm). Collectively, these factors could have contributed to the differences in binding profiles of the same type of MSNPs with sperm from different species.

The first stage of experiments performed in this Chapter sought to evaluate the nanotoxicity of MSNPs in human sperm in order to determine the optimum safe and effective incubation conditions for subsequent experiments involving cargo transfer. In this Chapter, nanotoxicity profiles were evaluated for only one type of MSNPs, unmodified MSNPs, which served as 'precursors' for all other particle modifications. This decision was made given the previously observed lack of association between surface modification of particles and their toxicity in sperm, both for polymer (PEI) and aminosilane (APTES) modification, and active targeting with C105Y.

Given the specific features of MSNP binding profiles with human sperm, particularly the positive effect of extended incubation time, and higher doses of MSNPs upon binding rates, the protocol for subsequent cargo transfer was adapted accordingly.

For cargo transfer experiments, human sperm were exposed to free plasmid DNA, plasmid DNA adsorbed on PEI-coated MSNPs, and two combined treatments: unmodified MSNPs and free DNA, or C105Y-functionalised MSNPs and free DNA. In these experiments, MSNPs demonstrated the potential to promote the uptake of both free and absorbed cargo into human sperm during *in vitro* exposure. It is of worth to note, however, that the outcomes of cargo transfer experiments performed in this Chapter were interpreted with caution given the small number of sperm samples tested and, in some cases, inefficient amplification of the internal control, which prevented quantification of the relative amounts of plasmid transferred into sperm.

In contrast to boar sperm, in which exposure to plasmid DNA adsorbed on PEI-coated particles, or the combination of unmodified MSNPs and free plasmid, inhibited cargo transfer compared to free plasmid DNA, the opposite phenomenon was observed in human sperm. In these cells, exposure to plasmid DNA adsorbed on PEI-coated particles, and a combination of unmodified MSNPs and free plasmid, resulted in the transfer of substantially higher amounts of DNA compared to plasmid-only treatment. Another interesting observation was that although exposure to the combination of C105Y-functionalised MSNPs and free DNA resulted in the uptake of a larger amount of cargo, this treatment appeared to be the least effective in human sperm, as opposed to boar sperm. This phenomenon could be attributed to differences in the targeting potential of C105Y in gametes from different species, which remain as yet uncharacterised. It appears that although the targeting potential of C105Y for bovine and boar sperm is consistently strong (Jones *et al.*, 2013), its effects in human sperm are less pronounced, which forms an opportunity for separate investigation.

It could be hypothesised, that the higher delivery efficacy of all modifications of MSNPs in human sperm was caused by a lower intrinsic ability of human sperm to incorporate exogenous

DNA without additional ‘assistance’. Although the potential of boar sperm to internalise exogenous DNA has been consistently proven (Lavitrano *et al.*, 2002; Lavitrano *et al.*, 2013), such experiments have not been carried out for human sperm, and the extent of their natural ability to internalise transgenes remains unknown. For the cargo transfer experiments performed in this thesis, the delivery efficacy of all modifications of MSNPs was compared to the efficacy of spontaneous uptake of free cargo. Therefore, the higher efficacy of PEI-coated and unmodified MSNPs as delivery vectors in human sperm could merely reflect that these particles were able to ‘assist’ with the uptake of plasmid DNA into sperm, which otherwise lacked the natural capacity for plasmid internalisation. At the same time, given the proven ability of boar sperm to uptake transgenes, the use of nanoparticles in this case failed to produce additional benefits, since MSNPs were shown to be non-superior to innate uptake mechanisms in boar sperm. Although the only modification of MSNPs which was capable of improving the outcomes of DNA transfer in boar sperm were C105Y-functionalised MSNPs, their targeting potential appeared to be restricted to boar sperm only.

Collectively, the findings obtained in this Chapter demonstrated that the biocompatibility of MSNPs, and their binding potential, was not restricted exclusively to boar sperm, but was also observed in human male gametes. At the same time, binding rates between MSNPs and sperm seemed to exhibit an element of inter-species variability, which could be attributed to species-specific sperm shape, membrane structure, kinematic parameters and, in the case of human sperm, previous exposure to low temperatures and cryoprotectants. Finally, the delivery potential of MSNPs also showed a species-specific profile, with all of the MSNP treatments tested herein showing a positive effect upon cargo internalisation. However, C105Y-mediated active targeting, which appeared consistently beneficial in boar sperm, failed to produce a similar effect in human gametes.

Interpretation of the results of this Chapter in the context of available evidence represents a challenge, since the number of peer-reviewed publications describing the use of nanomaterials in

human sperm remains scarce (**Table 6–1**). All of these earlier publications exclusively evaluated the toxicity of nanomaterials in human sperm, and did not characterise or quantify the binding of nanoparticles with gametes. Moreover, none of these publications assessed the performance of mesoporous silica, or described the intentional use of nanomaterials as delivery vectors, given the highly unfavourable nanotoxicity profiles of tested nanomaterials in human sperm. Furthermore, active targeting with cell-penetrating peptides has never been attempted in human sperm, and interpretation of lower targeting efficacy of C105Y in this population of gametes is difficult. Further studies are warranted to assess the potential of nanomaterials as cargo delivery vehicles into human gametes, and the species-specific profiles of nanomaterial safety and efficacy. In addition, even though MSNPs demonstrated safety and efficacy in the set of experiments performed in this Chapter, further extensive studies in a larger set of samples, including fresh sperm and sperm with compromised function, are warranted prior to considering this technology for experimental clinical use.

CHAPTER 7

SUMMARY AND CLOSING REMARKS

7.1. SUMMARY

This thesis investigated the use of MSNPs as a potential delivery vector for mammalian gametes in the ART context. The main motivation behind this project was to translate the technique of nanomaterial-mediated delivery into a cutting-edge addition to current assisted reproduction. This new technology could have numerous potential applications, spanning across the fields of fundamental reproductive biology, practical ART in veterinary science, and, perhaps, even IVF in humans. From its earliest stages, this project approached nanoparticle-mediated delivery as a multi-functional tool for reproductive biology and medicine, which could be used in a variety of scenarios. These scenarios include SMGT, the supplementation of molecular deficiencies in sperm, sperm sorting, the delivery of 'nourishing' compounds into existing *in vitro* culture systems for oocytes and embryos, and tracking the fate of specific embryonic cell populations. Therefore, experiments described throughout this thesis essentially aimed to design a simple-to-use versatile chemical reagent, which could be added to gametes and embryos in the IVF setting to exert desirable effects.

The specific choice of MSNPs as a potential delivery tool into gametes was driven by the novelty of this nanomaterial and its inherent features, which made it at a promising candidate for reproductive applications. MSNPs were characterised as structurally robust, relatively inert chemically, easy to produce and capable of carrying carry large amounts of payloads because of their porous architecture. MSNPs were also proven to display low cytotoxicity, and, at the time when this thesis was being planned, a large body of evidence already supported their safety and biocompatibility in different cell types. MSNPs were consistently shown to exhibit strong delivery capacity, including the possibility to internalise nucleic acids into cells, thereby acting as non-viral gene delivery vectors. Moreover, while representing an efficient delivery vehicle for various types of cargo, MSNPs could also be used as a stable cell tag because of their non-biodegradable nature. However, limited data existed regarding the use of MSNPs in gametes in the ART environment,

which made this research particularly exciting. Collectively, all of these features contributed to the choice of MSNPs as a candidate nanovector for this thesis.

7.1.1. BIOCOMPATIBILITY OF MSNPS WITH BOAR SPERM AND MOUSE OOCYTES

The first set of experiments performed for this thesis sought to evaluate the biocompatibility of in-house synthesised MSNPs with gametes, and provide the first insight into the possibility of applying this platform to these highly specialised cells. MSNPs were synthesised using a conventional surfactant-templated base-catalysed sol-gel reaction, optionally coated with PEI or APTES to permit loading with nucleic acids or proteins, and applied to boar sperm and mouse oocytes.

The specific choice of these two animal models for biocompatibility assays was driven by two factors. Firstly, these species are traditionally considered to be good models for human gametes during pre-clinical trials because of morphological and functional similarities. Secondly, mice and farm animals represent important subjects of reproductive biology research themselves. In these species, the investigated technique could be used independently to improve the success rates of existing research methodologies, which positively contributed to the potential ethical benefit of this research.

It is of a worth emphasising again that from the earliest stages, my research tried to gear the technique of MSNP-mediated delivery towards practical ART and view MSNPs as a customisable chemical reagent, which could be added to gametes under *in vitro* conditions in order to improve or modify their function. Therefore, general research methodology, and experimental conditions, were maintained as similar as possible to those used in a practical ART setting, particularly in terms of gamete handling procedures and exposure times.

The first set of experiments demonstrated that the simple *in vitro* exposure of boar sperm to in-house synthesised MSNPs with various surface chemistry (unmodified, PEI-coated and APTES-coated) in a 10-30μg per 10^7 sperm ratio did not produce a negative effect upon total and progressive sperm motility, motion parameters, viability, acrosome morphology or DNA

fragmentation index. During co-incubation, MSNPs could bind with various morphological regions of approximately one in five boar sperm. Stable binding rates were observed after just 2 hours of exposure, and were not affected by an increase in dose or incubation time. MSNPs loaded with nucleic acid or protein as prototypes for molecular cargo still bound to sperm, highlighting the possibility of simultaneous intracellular delivery.

MSNPs could also bind with the *zona pellucida* in mouse oocytes during *in vitro* exposure, although the spontaneous penetration of particles into oocytes was not evident. The persistence of MSNPs in mouse oocytes for up to 24 hours after microinjection did not promote oocyte degradation, which represented an encouraging finding. However, given the absence of spontaneous penetration of MSNPs into the oocytes and technical difficulties associated with intracytoplasmic microinjections of MSNPs, the hypothesis that MSNPs could serve as an easy-to-use and efficient intracellular delivery vector for mammalian oocytes with an intact *zona pellucida* was not pursued further. Therefore, subsequent experiments presented in this thesis focused upon the biocompatibility and delivery potential of MSNPs in sperm.

7.1.2. STRATEGIES TO IMPROVE BINDING BETWEEN MESOPOROUS SILICA NANOPARTICLES AND SPERM

As mentioned previously, in the first set of experiments MSNPs, bound to approximately 20% of sperm in a given sample. Interpretation of this finding in the context of existing literature was challenging, since the proportion of sperm associated with various nanoparticles following *in vitro* exposure had not been quantified before. However, it was hypothesised that for an application such as SMGT, the size of the sperm population associated with MSNPs, and therefore carrying cargo, would be proportionate to the likelihood of cargo transfer into the oocyte. To achieve higher binding rates between MSNPs and sperm, three independent strategies were tested. These included ‘enrichment’ of a given sperm sample with MSNP-associated sperm, modification of the physical properties of MSNPs and the active targeting of MSNPs towards sperm with a cell-penetrating peptide.

In order to ‘enrich’ a given sperm sample with MSNP-associated sperm, a straightforward conventional discontinuous DGW technique was used. This technique is routinely used in embryology laboratories to separate sperm into ‘better’ and ‘worse’ quality sub-populations. In this thesis, DGW was applied to assess how different sperm functionality in these two sub-populations might relate to their binding capacity to MSNPs. As mentioned previously, the choice of DGW as a sperm selection method over other more sophisticated techniques, such as FACS, was driven primarily by our intention to maintain the practicality of MSNP-mediated technology for subsequent translation into a conventional ART setting.

After subjecting MSNP-treated sperm to DGW, no significant differences between binding rates in the ‘better’ or ‘worse’ quality sperm sub-populations were observed. This led to the hypothesis that MSNP binding with sperm occurs independently of the first-line parameters of sperm function, such as motility, assessed by CASA, and viability, assessed via the use of membrane-permeating dyes, and could be related to the specific molecular structure or electrostatic charge of plasma membranes in certain sperm. Furthermore, these experiments led to the conclusion that DGW, in its standard way, cannot be used to ‘enrich’ the sample with MSNP-bound sperm. Therefore, alternative strategies are required for the selection and enrichment of sperm populations with MSNP-bound cells for subsequent downstream applications.

Another strategy tested to improve MSNP-sperm binding rates involved the use of MSNPs with a smaller physical diameter (<50nm). It was anticipated that the use of these MSNPs might promote easier binding and internalisation of particles into sperm because of better size compatibility. This approach, however, was also deemed unsuccessful due to the high propensity of synthesised MSNPs to agglomerate and thereby interact with sperm as large clusters rather than individual particles. Although the potential to optimise the synthesis protocol and reduce particle agglomeration existed, this strategy was not pursued further in view of emerging evidence regarding low nanoparticle internalisation capacity into sperm, even for small nanomaterials.

The final strategy to improve MSNP-sperm binding rates involved the use of a universally deployed technique of actively targeting nanoparticle targeting towards a specific cell population. In this thesis, a cell-penetrating peptide (C105Y) was chosen as an active targeting moiety. C105Y was characterised for its affinity towards mammalian sperm and represents a promising targeting tool with receptor- and energy-independent internalisation into target cells. These unique mechanisms of internalisation are highly advantageous for sperm, since they do not require interaction with surface membrane receptors, many of which play key roles in gamete fusion and fertilisation. Inadvertent blockage of these receptors, could, therefore, have a negative effect upon fertilisation and thus restrict the potential application of nanoplatforms for reproductive biology.

Active targeting of MSNPs towards boar sperm with C105Y resulted in the most encouraging outcomes. This strategy allowed a significantly faster 'saturation' of binding rates – after just 1 hour of incubation, approximately 20% to 30% of sperm showed signs of binding with MSNPs. However, maximal binding rates did not change substantially, showing only a marginal increase to approximately 30% to 35%, which strengthened the assumption that MSNPs preferentially bind to a specific sub-population of sperm. Targeting with C105Y, perhaps, promoted an initial anchoring stage with these cells, rather than facilitated binding to a larger cohort of sperm. Similarly to previous findings, this binding did not affect motility, kinematics and acrosome morphology in boar sperm samples. In addition, the levels of intracellular fluorescence in sperm exposed to MSNPs functionalised with a fluorescent C105Y peptide were higher than those exposed to a free fluorescent C105Y peptide, which could suggest changes in sperm membrane permeability in the presence of MSNPs.

7.1.3. MESOPOROUS SILICA NANOPARTICLES AS A DELIVERY TOOL INTO SPERM

The positive outcomes of studies into biocompatility and binding of MSNPs with sperm formed a rationale for the subsequent testing of these nanoparticles as delivery vectors for exogenous DNA and protein transfer under optimised incubation conditions. It was anticipated that MSNP-mediated delivery would facilitate the 'loading' of sperm with these compounds for SMGT or protein

transfer, respectively. In these experiments, the delivery efficacy of cargo-loaded MSNPs was compared to that of free cargo and two combined treatments: the combination of unmodified MSNPs and free cargo and the combination of C105Y-functionalised MSNPs and free cargo. This experimental design allowed me to evaluate the effect of cargo adsorption on MSNPs upon its availability to sperm, but also how exposure to free cargo in the presence of targeted and non-targeted MSNPs affected its uptake.

Interestingly, these experiments demonstrated that the adsorption of cargo on MSNPs, or co-treatment with unmodified MSNPs and free cargo, had limited benefits for intracellular uptake into boar sperm. The only modification of MSNPs which showed the potential to improve cargo delivery into sperm were C105Y-functionalised MSNPs. Exposure of boar sperm to a combination of C105Y-functionalised MSNPs resulted in the delivery of exogenous DNA into a larger subset of sperm samples, and the transfer of larger quantities of DNA and protein, compared to treatment with free cargo only. Therefore, it appeared that for efficient delivery of cargo into boar sperm the vector itself should undergo internalisation, which was not consistently proven for the MSNPs used throughout this thesis. Since internalisation did not seem to occur, the observed efficacy of MSNP-mediated delivery did not exceed the efficacy of spontaneous cargo uptake into sperm. At the same time, the active targeting of MSNPs towards sperm appeared to promote the delivery of cargo, particularly DNA, into sperm with low intrinsic uptake activity, thereby increasing the number of samples in which positive evidence of DNA transfer was obtained. In addition, MSNPs targeted towards boar sperm with C105Y also showed a trend towards the delivery of larger doses of cargo.

Collectively, these results showed that boar sperm appeared to have a sufficient intrinsic capacity for cargo uptake, and the use of MSNPs as delivery vectors did not substantially facilitate this uptake. Perhaps the limited benefits of MSNPs in this case were associated with the lack of their internalisation. The inability of MSNPs to move freely across the sperm plasma membrane probably narrowed their potential mechanisms of action down to alteration in sperm membrane permeability, which was most commonly seen in the case of C105Y-functionalised MSNPs.

7.1.4. MESOPOROUS SILICA NANOPARTICLES IN HUMAN SPERM: SAFETY AND EFFICACY

Collectively, the favourable biocompatibility of MSNPs with boar sperm, and the benefits of MSNP functionalisation with targeting moieties, formed the basis for the final set of experiments addressed in this thesis. These experiments evaluated the biocompatibility and potential of MSNPs to transport molecular cargo into human sperm.

The experiments were carried out in two stages. Firstly, the biocompatibility and binding rates between MSNPs and human sperm were studied in order to optimise incubation conditions. Secondly, optimised incubation conditions were applied for the MSNP-mediated delivery of exogenous DNA into sperm. Specifically, sperm were exposed to plasmid DNA absorbed on PEI-coated MSNPs or the combinations of unmodified MSNPs and free cargo, or C105Y-functionalised MSNPs and free cargo. Delivery efficacy was confirmed to the outcome of free plasmid-only treatment.

Throughout these tests, MSNPs maintained their biocompatibility and did not produce negative effects upon human sperm motility, viability or DNA status. Furthermore, they maintained their ability to bind with sperm, although inter-species variations in the binding rates were observed in this case. Unlike boar sperm, the time of exposure and dose of MSNPs had a significant effect upon the proportion of human sperm binding with the particle. This observation was taken into consideration during cargo transfer experiments.

In contrast to boar gametes, exposure to MSNPs promoted cargo uptake into human sperm compared to free plasmid-only treatment. Furthermore, the effect of active targeting with C105Y appeared limited, as C105Y-functionalised MSNPs did not facilitate the uptake of larger cargo quantities into human sperm. Such differences in the outcomes of similar experiments in different species were attributed to discrepancies in the innate sperm's innate potential for cargo uptake. In the case of boar sperm with proven ability to undergo SMGT, exposure to MSNPs did not provide additional noticeable benefits. At the same time, the use of MSNPs in human sperm, with perhaps less active innate uptake mechanisms, led to more pronounced effects. The inter-species differences

in sperm structure and function were also highlighted by the lower targeting efficacy of C105Y in human sperm compared to boar sperm, justifying the need to tailor active targeting moieties on a species-by-species basis.

7.2. CONCLUDING REMARKS

Collectively, experiments presented in this thesis demonstrated, for the first time, the potential of MSNPs for reproductive science. MSNPs consistently demonstrated biocompatibility with gametes from different biological species, including boars, mice and humans. They were capable of binding with sperm and oocytes during simple *in vitro* incubation and, crucially, did not exert acute toxicity upon gamete function. MSNPs could be targeted towards sperm or microinjected into oocytes, and both these techniques, aiming to facilitate interaction between MSNPs and gametes, were well-tolerated by cells. MSNPs could also be loaded with molecular cargo, and this action did not prevent particles from binding with gametes, in particular sperm. Finally, MSNPs could deliver cargo into both boar and human sperm, thereby representing a candidate delivery vector for reproductive biology.

Although the experiments presented in this thesis produced encouraging outcomes, they also highlighted many important questions associated with the use of MSNPs for reproductive science. *Firstly, can MSNPs truly internalise into gametes and what are the optimal conditions for this outcome?* In this thesis, the term ‘binding’ was used to collectively describe the surface attachment of MSNPs to sperm and indicate potential intracellular uptake. It is worth mentioning that the data obtained during TEM of sperm exposed to MSNPs did not provide a conclusive answer to the question of whether the internalisation of MSNPs into sperm truly occurred. This seemed to be even less possible for oocytes, as most MSNPs appeared to be retained by the robust mechanical barrier of the *zona pellucida*. There is a growing body of evidence that nanomaterials, in fact, do not undergo intracellular uptake into gametes easily: for example, the proportion of nanoparticles reaching the intracellular compartment in sperm after *in vitro* exposure is remarkably small. In fact, sperm that internalise nanomaterials appear to exhibit altered integrity of the surface membrane,

such as those associated with having undergone the acrosome reaction. Future experiments could address this topic in more detail by applying high-resolution imaging techniques to sperm exposed to MSNPs.

Secondly, is 'true' internalisation of nanomaterials into gametes essential for successful delivery of cargo? At the moment, there seems to be a consensus of opinion that the internalisation of nanocarriers into sperm does not represent a crucial factor for efficient cargo delivery, since the performance of nanoparticle-assisted SMGT is not compromised even when the majority of nanoparticles remain attached to the surface membrane. This point of view, however, did not coincide with the findings of this thesis, at least for the boar model. As such, the intrinsic capacity of boar sperm to take up cargo on most occasions exceeded the potential of what seemed to be mostly non-internalised MSNPs to deliver it. In future, detailed TEM experiments in conjunction with cargo delivery tests using sperm from different animal models could help elucidate whether the efficacy of cargo delivery represents a function of 'true' particle internalisation.

Thirdly, which properties of sperm predispose these cells to binding with MSNPs and what could be done to increase the binding rates above those that are currently observed? Throughout this thesis, MSNPs bound preferentially to a specific population of sperm, which did not exceed 40% of the total population for boar sperm, and 60% of the total population for human sperm. In the case of boar sperm, this level of binding seemed to occur independently of the first-line parameters of sperm function such as motility and viability, and active targeting with C105Y allowed this binding to occur faster, but not in the larger subset of sperm. For human sperm, this association was studied to a lesser extent, but an increase in MSNP doses and incubation times also resulted in the 'saturation' of binding rate at a specific maximum level. It could be anticipated, that a detailed analysis of physical and biological properties of individual sperm, which show binding with MSNPs, could help unravel the fine mechanisms underlying this phenomenon.

Finally, can sperm that have been modified with MSNPs deliver cargo into the oocyte at the time of fertilization and what is the fate and effects of exogenous MSNPs in mammalian embryos?

This is a critical consideration with many potential answers: exclusion, sequestration within a random cell population, or preferential localisation to the embryonic or trophoblastic cells. Given such possibilities, it is vital to investigate how such processes might affect subsequent embryo development. Future studies should aim to address these important questions in order to advance the understanding of how nanomaterials may benefit reproductive biology in the future.

7.3. GENERAL LIMITATIONS

This thesis evaluated the acute toxicity and delivery potential of a specific type of MSNPs (>100nm) during *in vitro* exposure to gametes from selected mammalian species under ART conditions. Therefore, extrapolation of the results obtained in this thesis to MSNPs with other physicochemical features, different incubation parameters or other animal models should be carried out with caution. This thesis did not aim to evaluate the long-term effects of MSNPs upon gamete function of mammalian embryo development, as well as investigate the fate of MSNPs in mammalian embryonic cells. These outcomes should, therefore, form the foundation for separate investigations. The specific limitations associated with each set of experiments are discussed in detail in the relevant chapters.

REFERENCES

Abou-haila, A., Tulsiani, D.R.P., 2009. Signal transduction pathways that regulate sperm capacitation and the acrosome reaction. Arch Biochem Biophys 485, 72-81.

Aitken, R.J., 2014. Age, the environment and our reproductive future: bonking baby boomers and the future of sex. Reproduction 147, S1-S11.

Albanese, A., Tang, P.S., Chan, W.C., 2012. The effect of nanoparticle size, shape, and surface chemistry on biological systems. Annu Rev Biomed Eng 14, 1-16.

Ali, H., Kalashnikova, I., White, M.A., Sherman, M., Rytting, E., 2013a. Preparation, characterization, and transport of dexamethasone-loaded polymeric nanoparticles across a human placental in vitro model. Int J Pharm 454, 149-157.

Ali, H., Kilic, G., Vincent, K., Motamedi, M., Rytting, E., 2013b. Nanomedicine for uterine leiomyoma therapy. Ther Deliv 4, 161-175.

Alland, C., Moreews, F., Boens, D., Carpentier, M., Chiusa, S., Lonquety, M., Renault, N., Wong, Y., Cantalloube, H., Chomilier, J., Hochez, J., Pothier, J., Villoutreix, B.O., Zagury, J.F., Tuffery, P., 2005. RPBS: a web resource for structural bioinformatics. Nucleic Acids Res. 33, W44-49.

Amdani, S.N., Jones, C., Coward, K., 2013. Phospholipase C zeta (PLCzeta): oocyte activation and clinical links to male factor infertility. Adv Biol Regul 53, 292-308.

Amdani, S.N., Yeste, M., Jones, C., Coward, K., 2015. Sperm factors and oocyte activation: current controversies and considerations. Biol Reprod 93, 50.

American Society for Reproductive Medicine (ASRM), 2008. Medical treatment of ectopic pregnancy. Fertil Steril 90, S206-S212.

Ammar, T., Sidhu, P.S., Wilkins, C.J., 2012. Male infertility: the role of imaging in diagnosis and management. Br J Radiol 85 Spec No 1, S59-68.

Antunes, A.M.D., Alencar, M.S.D., da Silva, C.H., Nunes, J., Mendes, F.M.L., 2012. Trends in nanotechnology patents applied to the health sector. Recent Pat Nanotech 6, 29-43.

Arezzo, F., 1989. Sea-Urchin Sperm as a Vector of Foreign Genetic Information. Cell Biol Int Rep 13, 391-404.

Arvizo, R.R., Bhattacharyya, S., Kudgus, R.A., Giri, K., Bhattacharya, R., Mukherjee, P., 2012. Intrinsic therapeutic applications of noble metal nanoparticles: past, present and future. Chem Soc Rev 41, 2943-2970.

Ashby, M.F., Ferreira, P.J., Schodek, D.L., 2009. Nanomaterials, nanotechnologies and design : an introduction for engineers and architects. Butterworth-Heinemann, Amsterdam ; Oxford.

Barchanski, A., Taylor, U., Klein, S., Petersen, S., Rath, D., Barcikowski, S., 2011. Golden perspective: application of laser-generated gold nanoparticle conjugates in reproductive biology. Reprod Domest Anim 46 Suppl 3, 42-52.

Barchanski, A., Taylor, U., Sajti, C.L., Gamrad, L., Kues, W.A., Rath, D., Barcikowski, S., 2015. Bioconjugated gold nanoparticles penetrate into spermatozoa depending on plasma membrane status. J. Biomed. Nanotechnol. 11.

Bartoov, B., Berkovitz, A., Eltes, F., Kogosowski, A., Menezo, Y., Barak, Y., 2002. Real-time fine morphology of motile human sperm cells is associated with IVF-ICSI outcome. J Androl 23, 1-8.

Bathgate, R., Mace, N., Heasman, K., Evans, G., Maxwell, W.M., de Graaf, S.P., 2013. Birth of kids after artificial insemination with sex-sorted, frozen-thawed goat spermatozoa. Reprod Domest Anim 48, 893-898.

Ben-David Makhluf, S., Qasem, R., Rubinstein, S., Gedanken, A., Breitbart, H., 2006. Loading magnetic nanoparticles into sperm cells does not affect their functionality. Langmuir 22, 9480-9482.

Binnig, G., Quate, C.F., Gerber, C., 1986. Atomic Force Microscope. Phys Rev Lett 56, 930-933.

Binnig, G., Rohrer, H., 1982. Scanning Tunneling Microscopy. Helvetica Physica Acta 55, 726-735.

Bonet, S., Casas, I., Holt, W.V., Yeste, M., 2013. Boar Reproduction: Fundamentals and New Biotechnological Trends. Springer Science & Business Media.

Bongioanni, F., Revelli, A., Gennarelli, G., Guidetti, D., Delle Piane, L.D., Holte, J., 2011. Ovarian endometriomas and IVF: a retrospective case-control study. Reprod Biol Endocrinol 9, 81.

Brackett, B.G., 1971. Uptake of heterologous genome by mammalian spermatozoa and its transfer to ova through fertilization. P Natl Acad Sci USA 68, 353-357.

Brakmane, G., Winslet, M., Seifalian, A.M., 2012. Systematic review: the applications of nanotechnology in gastroenterology. Aliment Pharmacol Ther 36, 213-221.

Braydich-Stolle, L., Hussain, S., Schlager, J.J., Hofmann, M.C., 2005. In vitro cytotoxicity of nanoparticles in mammalian germline stem cells. Toxicol Sci 88, 412-419.

Bromley, D.A., 2001. Letter from Dean D. Allan Bromley sent to President Clinton, in: Roco, M.C., Bainbridge, W.S. (Eds.), Societal implications of nanoscience and nanotechnology. International Technology Research Institute, World Technology (WTEC) Division, Loyola College, Arlington, VA, USA, pp. 269-270.

Bucar, S., Goncalves, A., Rocha, E., Barros, A., Sousa, M., Sa, R., 2015. DNA fragmentation in human sperm after magnetic-activated cell sorting. J Assist Reprod Genet 32, 147-154.

Burgess, A., Vigneron, S., Brioudes, E., Labbe, J.C., Lorca, T., Castro, A., 2010. Loss of human Greatwall results in G2 arrest and multiple mitotic defects due to deregulation of the cyclin B-Cdc2/PP2A balance. P Natl Acad Sci USA USA 107, 12564-12569.

Campos, V.F., de Leon, P.M.M., Komninou, E.R., Dellagostin, O.A., Deschamps, J.C., Seixas, F.K., Collares, T., 2011a. NanoSMGT: Transgene transmission into bovine embryos using halloysite clay nanotubes or nanopolymer to improve transfection efficiency. Theriogenology 76, 1552-1560.

Campos, V.F., Komninou, E.R., Urtiaga, G., de Leon, P.M., Seixas, F.K., Dellagostin, O.A., Deschamps, J.C., Collares, T., 2011b. NanoSMGT: Transfection of exogenous DNA on sex-sorted bovine sperm using nanopolymer. Theriogenology 75, 1476-1481.

Cao, G., Wang, Y., 2011. Nanostructures and nanomaterials: synthesis, properties, and applications, 2nd ed. World Scientific, New Jersey.

Chattopadhyay, P.K., Perfetto, S.P., Yu, J., Roederer, M., 2010. The use of quantum dot nanocrystals in multicolor flow cytometry. Wires Nanomed Nanobi 2, 334-348.

Chaudhury, K., Babu K, N., Singh, A.K., Das, S., Kumar, A., Seal, S., 2013. Mitigation of endometriosis using regenerative cerium oxide nanoparticles. Nanomedicine 9, 439-448.

Chen, C., Hu, Z., Liu, S., Tseng, H., 2012. Emerging trends in regenerative medicine: a scientometric analysis in CiteSpace. Expert Opin Biol Ther 12, 593-608.

Chiannilkulchai, N., Driouich, Z., Benoit, J.P., Parodi, A.L., Couvreur, P., 1989. Doxorubicin-Loaded Nanoparticles - Increased Efficiency in Murine Hepatic Metastases. Sel Cancer Ther 5, 1-11.

Choudhary, S., Kusum Devi, V., 2015. Potential of nanotechnology as a delivery platform against tuberculosis: Current research review. J Control Release 202C, 65-75.

Cohen, C.R., Brown, J., Moscicki, A.B., Bukusi, E.A., Paull, J.R.A., Price, C.F., Shiboski, S., 2011. A phase I randomized placebo controlled rrial of the safety of 3% SPL7013 gel (VivaGel (R)) in healthy young women administered twice daily for 14 days. PLoS One. doi:10.1371/journal.pone.0016258.

Cordts, E.B., Christofolini, D.M., Dos Santos, A.A., Bianco, B., Barbosa, C.P., 2011. Genetic aspects of premature ovarian failure: a literature review. Arch Gynecol Obstet 283, 635-643.

Courbiere, B., Auffan, M., Rollais, R., Tassistro, V., Bonnefoy, A., Botta, A., Rose, J., Orsiere, T., Perrin, J., 2013. Ultrastructural interactions and genotoxicity assay of cerium dioxide nanoparticles on mouse oocytes. Int J Mol Sci 14, 21613-21628.

Coward, K., Kubota, H., Hibbitt, O., McIlhinney, J., Kohri, K., Parrington, J., 2006. Expression of a fluorescent recombinant form of sperm protein phospholipase C zeta in mouse epididymal sperm by in vivo gene transfer into the testis. Fertil Steril 85, 1281-1289.

Coward, K., Kubota, H., Parrington, J., 2007. In vivo gene transfer into testis and sperm: developments and future application. Arch Androl 53, 187-197.

da Silveira, J.C., Veeramachaneni, D.N., Winger, Q.A., Carnevale, E.M., Bouma, G.J., 2012. Cell-secreted vesicles in equine ovarian follicular fluid contain miRNAs and proteins: a possible new form of cell communication within the ovarian follicle. Biol Reprod 86, 71.

Damascelli, B., Cantu, G., Mattavelli, F., Tamplenizza, P., Bidoli, P., Leo, E., Dosio, F., Cerrotta, A.M., Di Tolla, G., Frigerio, L.F., Garbagnati, F., Lanocita, R., Marchiano, A., Patelli, G., Spreafico, C., Ticha, V., Vespro, V., Zunino, F., 2001. Intraarterial chemotherapy with polyoxyethylated castor oil free paclitaxel, incorporated in albumin nanoparticles (ABI-007) - Phase I study of patients with squamous cell carcinoma of the head and neck and anal canal: Preliminary evidence of clinical activity. Cancer 92, 2592-2602.

de Oliveira, R., Zhao, P., Li, N., de Santa Maria, L.C., Vergnaud, J., Ruiz, J., Astruc, D., Barratt, G., 2013. Synthesis and in vitro studies of gold nanoparticles loaded with docetaxel. Int J Pharm 454, 703-711.

Dhar, S., Gu, F.X., Langer, R., Farokhzad, O.C., Lippard, S.J., 2008. Targeted delivery of cisplatin to prostate cancer cells by aptamer functionalized Pt(IV) prodrug-PLGA-PEG nanoparticles. P Natl Acad Sci USA 105, 17356-17361.

Didion, B.A., 2008. Computer-assisted semen analysis and its utility for profiling boar semen samples. Theriogenology 70, 1374-1376.

Ebara, M., Kotsuchibashi, Y., Uto, K., Aoyagi, T., Kim, Y.-J., Narain, R., Idota, N., Hoffman, J.M., 2014. Smart nanoassemblies and nanoparticles, in: Ebara, M., Kotsuchibashi, Y., Narain, R., Idota, N., Kim, Y.-J., Hoffman, J.M., Uto, K., Aoyagi, T. (Eds.), Smart Biomaterials. Springer, New York, pp. 67-114.

Eghbalsaied, S., Ghaedi, K., Laible, G., Hosseini, S.M., Forouzanfar, M., Hajian, M., Oback, F., Nasr-Esfahani, M.H., Oback, B., 2013. Exposure to DNA is insufficient for in vitro transgenesis of live bovine sperm and embryos. Reproduction 145, 97-108.

El-Andaloussi, S., Mager, I., Breakefield, X.O., Wood, M.J., 2013. Extracellular vesicles: biology and emerging therapeutic opportunities. Nat Rev Drug Discov 12, 347-357.

Ema, M., Kobayashi, N., Naya, M., Hanai, S., Nakanishi, J., 2010. Reproductive and developmental toxicity studies of manufactured nanomaterials. Reprod Toxicol 30, 343-352.

Eppig, J.J., Pendola, F.L., Wigglesworth, K., Pendola, J.K., 2005. Mouse oocytes regulate metabolic cooperativity between granulosa cells and oocytes: Amino acid transport. Biol Reprod 73, 351-357.

European Commision (EC), 2004. Communication from the Commission – Towards a European strategy for nanotechnology. Office for Official Publications of the European Communities, Luxembourg. [https://ec.europa.eu/research/industrial_technologies/pdf/policy/nano_com_en_new.pdf].

European Commision (EC), 2011. Commission recommendation of 18 October 2011 on the definition of nanomaterial. OJEU, 275/238-275/240.

Falchi, L., Bogliolo, L., Galleri, G., Vlachopoulou, G., Murrone, O., Epifani, G., Pinna, A., Innocenzi, P., Ledda, S., 2014. 266 biocompatibility of nanoceria in ram sperm during 24 hours of incubation. Reprod Fertil Dev 27, 222.

Falcone, T., Parker, W.H., 2013. Surgical management of leiomyomas for fertility or uterine preservation. Obstet Gynecol 121, 856-868.

Farkhani, S.M., Valizadeh, A., Karami, H., Mohammadi, S., Sohrabi, N., Badrzadeh, F., 2014. Cell penetrating peptides: Efficient vectors for delivery of nanoparticles, nanocarriers, therapeutic and diagnostic molecules. Peptides 57, 78-94.

Fassbender, A., Vodolazkaia, A., Saunders, P., Lebovic, D., Waelkens, E., De Moor, B., D'Hooghe, T., 2013. Biomarkers of endometriosis. Fertil Steril 99, 1135-1145.

Felsenstein, K.M., Candelario, K.M., Steindler, D.A., Borchelt, D.R., 2014. Regenerative medicine in Alzheimer's disease. Transl Res 163, 432-438.

Feugang, J.M., Youngblood, R.C., Greene, J.M., Fahad, A.S., Monroe, W.A., Willard, S.T., Ryan, P.L., 2012. Application of quantum dot nanoparticles for potential non-invasive bio-imaging of mammalian spermatozoa. J Nanobiotechnology 10, 45.

Feugang, J.M., Youngblood, R.C., Greene, J.M., Willard, S.T., Ryan, P.L., 2015. Self-illuminating quantum dots for non-invasive bioluminescence imaging of mammalian gametes. J Nanobiotechnology 13, 38.

Feynman, R.P., 1960. There's plenty of room at the bottom, an invitation to enter a new field of physics. Caltech Eng and Sci 23, 22-36.

Fragouli, E., Alfarawati, S., Spath, K., Wells, D., 2014. Morphological and cytogenetic assessment of cleavage and blastocyst stage embryos. Mol Hum Reprod 20, 117-126.

Fragouli, E., Wells, D., 2012a. Aneuploidy screening for embryo selection. Semin Reprod Med 30, 289-301.

Fragouli, E., Wells, D., 2012b. Transcriptomic analysis of follicular cells provides information on the chromosomal status and competence of unfertilized oocytes. Expert Rev Mol Diagn 12, 1-4.

Freire, A.G., Resende, T.P., Pinto-Do-O, P., 2014. Building and repairing the heart: What can we learn from embryonic development? Biomed Res Int. doi:10.1155/2014/679168

Fynewever, T.L., Agcaoili, E.S., Jacobson, J.D., Patton, W.C., Chan, P.J., 2007. In vitro tagging of embryos with nanoparticles. J Assist Reprod Genet 24, 61-65.

Gadella, B.M., Evans, J.P., 2011. Membrane fusions during mammalian fertilization. Adv Exp Med Biol 713, 65-80.

Galli, C., Duchi, R., Colleoni, S., Lagutina, I., Lazzari, G., 2014. Ovum pick up, intracytoplasmic sperm injection and somatic cell nuclear transfer in cattle, buffalo and horses: from the research laboratory to clinical practice. Theriogenology 81, 138-151.

Gan, Q., Dai, D., Yuan, Y., Qian, J., Sha, S., Shi, J., Liu, C., 2012. Effect of size on the cellular endocytosis and controlled release of mesoporous silica nanoparticles for intracellular delivery. Biomed Microdevices 14, 259-270.

Gao, X., Luo, Y., Wang, Y.Y., Pang, J., Liao, C.D., Lu, H.L., Fang, Y.Q., 2012. Prostate stem cell antigen-targeted nanoparticles with dual functional properties: in vivo imaging and cancer chemotherapy. Int J Nanomedicine 7, 4037-4051.

Garcia-Vazquez, F.A., Garcia-Rosello, E., Gutierrez-Adan, A., Gadea, J., 2009. Effect of sperm treatment on efficiency of EGFP-expressing porcine embryos produced by ICSI-SMGT. Theriogenology 72, 506-518.

Garcia-Vazquez, F.A., Ruiz, S., Grullon, L.A., de Ondiz, A., Gutierrez-Adan, A., Gadea, J., 2011. Factors affecting porcine sperm mediated gene transfer. Res Vet Sci 91, 446-453.

Gelperina, S.E., Khalansky, A.S., Skidan, I.N., Smirnova, Z.S., Bobruskin, A.I., Severin, S.E., Turowski, B., Zanella, F.E., Kreuter, J., 2002. Toxicological studies of doxorubicin bound to polysorbate 80-coated poly(butyl cyanoacrylate) nanoparticles in healthy rats and rats with intracranial glioblastoma. Toxicol Lett 126, 131-141.

Geng, F., Song, K., Xing, J.Z., Yuan, C., Yan, S., Yang, Q., Chen, J., Kong, B., 2011. Thio-glucose bound gold nanoparticles enhance radio-cytotoxic targeting of ovarian cancer. Nanotechnology 22, 285101.

Ghadami, M., El-Demerdash, E., Salama, S.A., Binhazim, A.A., Archibong, A.E., Chen, X., Ballard, B.R., Sairam, M.R., Al-Hendy, A., 2010. Toward gene therapy of premature ovarian failure: intraovarian injection of adenovirus expressing human FSH receptor restores folliculogenesis in FSHR(-/-) FORKO mice. Mol Hum Reprod 16, 241-250.

Gharagozloo, M., Majewski, S., Foldvari, M., 2015. Therapeutic applications of nanomedicine in autoimmune diseases: From immunosuppression to tolerance induction. Nanomedicine 11, 1003-1018.

Gianaroli, L., Racowsky, C., Geraedts, J., Cedars, M., Makrigiannakis, A., Lobo, R.A., 2012. Best practices of ASRM and ESHRE: a journey through reproductive medicine. Fertil Steril 98, 1380-1394.

Gil, M., Sar-Shalom, V., Sivira, Y.M., Carreras, R., Checa, M.A., 2013. Sperm selection using magnetic activated cell sorting (MACS) in assisted reproduction: a systematic review and meta-analysis. J Assist Reprod Genet 30, 479-485.

Gopalan, R.C., Osman, I.F., Amani, A., De Matas, M., Anderson, D., 2009. The effect of zinc oxide and titanium dioxide nanoparticles in the Comet assay with UVA photoactivation of human sperm and lymphocytes. Nanotoxicology 3, 33-39.

Grodzik, M., Sawosz, F., Sawosz, E., Hotowy, A., Wierzbicki, M., Kutwin, M., Jaworski, S., Chwalibog, A., 2013. Nano-nutrition of chicken embryos. The effect of in ovo administration of diamond nanoparticles and L-glutamine on molecular responses in chicken embryo pectoral muscles. Int J Mol Sci 14, 23033-23044.

Hafez, E., and Kenemans P, 2012. Atlas of Human Reproduction: By Scanning Electron Microscopy. Springer Science & Business Media.

Handyside, A.H., Lesko, J.G., Tarin, J.J., Winston, R.M., Hughes, M.R., 1992. Birth of a normal girl after in vitro fertilization and preimplantation diagnostic testing for cystic fibrosis. N Engl J Med 327, 905-909.

Hanwell, M.D., Curtis, D.E., Lonie, D.C., Vandermeersch, T., Zurek, E., Hutchison, G.R., Avogadro: an open-source molecular builder and visualization tool [Version 1.1.1].

Hanwell, M.D., Curtis, D.E., Lonie, D.C., Vandermeersch, T., Zurek, E., Hutchison, G.R., 2012. Avogadro: an advanced semantic chemical editor, visualization, and analysis platform. J. Cheminform. 4, 17.

Holmes, D., 2013. The next big things are tiny. The Lancet Neurology 12, 31-32.

Holt, W.V., Brown, J.L., Comizzoli, P., 2014. Conclusions: environmental change, wildlife conservation and reproduction. Adv Exp Med Biol 753, 503-514.

Hom, C., Lu, J., Liong, M., Luo, H., Li, Z., Zink, J.I., Tamanoi, F., 2010. Mesoporous silica nanoparticles facilitate delivery of siRNA to shutdown signaling pathways in mammalian cells. Small 6, 1185-1190.

Hsieh, M.S., Shiao, N.H., Chan, W.H., 2009. Cytotoxic effects of CdSe quantum dots on maturation of mouse oocytes, fertilization, and fetal development. Int J Mol Sci 10, 2122-2135.

Huang, D.M., Hung, Y., Ko, B.S., Hsu, S.C., Chen, W.H., Chien, C.L., Tsai, C.P., Kuo, C.T., Kang, J.C., Yang, C.S., Mou, C.Y., Chen, Y.C., 2005. Highly efficient cellular labeling of mesoporous nanoparticles in human mesenchymal stem cells: implication for stem cell tracking. FASEB J 19, 2014-2016.

Huang, X., Zhuang, J., Teng, X., Li, L., Chen, D., Yan, X., Tang, F., 2010. The promotion of human malignant melanoma growth by mesoporous silica nanoparticles through decreased reactive oxygen species. Biomaterials 31, 6142-6153.

Huang, Z., Wells, D., 2010. The human oocyte and cumulus cells relationship: new insights from the cumulus cell transcriptome. Mol Hum Reprod 16, 715-725.

Hudelist, G., Fritzer, N., Thomas, A., Niehues, C., Oppelt, P., Haas, D., Tammaa, A., Salzer, H., 2012. Diagnostic delay for endometriosis in Austria and Germany: causes and possible consequences. Hum Reprod 27, 3412-3416.

Huyck, K.L., Panhuysen, C.I.M., Cuenco, K.T., Zhang, J.M., Goldhammer, H., Jones, E.S., Somasundaram, P., Lynch, A.M., Harlow, B.L., Lee, H., Stewart, E.A., Morton, C.C., 2008. The impact of race as a risk factor for symptom severity and age at diagnosis of uterine leiomyomata among affected sisters. Am J Obstet Gynecol 198, 168.e161-169.

Ikawa, M., Tergaonkar, V., Ogura, A., Ogonuki, N., Inoue, K., Verma, I.M., 2002. Restoration of spermatogenesis by lentiviral gene transfer: offspring from infertile mice. P Natl Acad Sci USA 99, 7524-7529.

Jain, K.K., 2011. Nanobiotechnology, in: Editor-in-Chief: Murray, M.-Y. (Ed.), Comprehensive Biotechnology (Second Edition). Academic Press, Burlington, pp. 599-614.

Jakop, U., Fuchs, B., SuSZ, R., Wibbelt, G., Braun, B., Muller, K., Schiller, J., 2009. The solubilisation of boar sperm membranes by different detergents - a microscopic, MALDI-TOF MS, 31P NMR and PAGE study on membrane lysis, extraction efficiency, lipid and protein composition. Lipids Health Dis 8, 49.

Jallouk, A.P., Moley, K.H., Omurtag, K., Hu, G., Lanza, G.M., Wickline, S.A., Hood, J.L., 2014. Nanoparticle incorporation of melittin reduces sperm and vaginal epithelium cytotoxicity. PLoS One 9, e95411. doi: 10.1371/journal.pone.0095411.

James, P.S., Hennessy, C., Berge, T., Jones, R., 2004. Compartmentalisation of the sperm plasma membrane: a FRAP, FLIP and SPFI analysis of putative diffusion barriers on the sperm head. J Cell Sci 117, 6485-6495.

Janat-Amsbury, M.M., Peterson, C.M., Kim, S.W., 2009. The role of gene- and drug delivery in women's health--unmet clinical needs and future opportunities. Preface. Adv Drug Deliv Rev 61, 767.

Jiang, J., Bischof, J., 2010. Effect of timing, dose and interstitial versus nanoparticle delivery of tumor necrosis factor alpha in combinatorial adjuvant cryosurgery treatment of ELT-3 uterine fibroid tumor. Cryo Letters 31, 50-62.

Jingting, C., Huining, L., Yi, Z., 2011. Preparation and characterization of magnetic nanoparticles containing Fe(3)O(4)-dextran-anti-beta-human chorionic gonadotropin, a new generation choriocarcinoma-specific gene vector. Int J Nanomedicine 6, 285-294.

Johannsen, M., Gneveckow, U., Eckelt, L., Feussner, A., Waldofner, N., Scholz, R., Deger, S., Wust, P., Loening, S.A., Jordan, A., 2005. Clinical hyperthermia of prostate cancer using magnetic nanoparticles: Presentation of a new interstitial technique. Int J Hyperther 21, 637-647.

Johnson, N., Farquhar, C., 2007. Endometriosis. Clin Evid (Online) 2007, pii: 0802.

Jones, A.T., Sayers, E.J., 2012. Cell entry of cell penetrating peptides: tales of tails wagging dogs. J Control. Release 161, 582-591.

Jones, S., Lukanowska, M., Suhorutsenko, J., Oxenham, S., Barratt, C., Publicover, S., Copolovici, D.M., Langel, Ü., Howl, J., 2013. Intracellular translocation and differential accumulation of cell-penetrating peptides in bovine spermatozoa: evaluation of efficient delivery vectors that do not compromise human sperm motility. Hum Reprod 28, 1874-1889.

Kaitu'u-Lino, T.J., Pattison, S., Ye, L., Tuohey, L., Sluka, P., MacDiarmid, J., Brahmbhatt, H., Johns, T., Horne, A.W., Brown, J., Tong, S., 2013. Targeted nanoparticle delivery of doxorubicin into placental tissues to treat ectopic pregnancies. Endocrinology 154, 911-919.

Karabinus, D.S., Marazzo, D.P., Stern, H.J., Potter, D.A., Opanga, C.I., Cole, M.L., Johnson, L.A., Schulman, J.D., 2014. The effectiveness of flow cytometric sorting of human sperm (MicroSort(R)) for influencing a child's sex. Reprod Biol Endocrinol 12, 106.

Kashir, J., Heynen, A., Jones, C., Durrans, C., Craig, J., Gadea, J., Turner, K., Parrington, J., Coward, K., 2011. Effects of cryopreservation and density-gradient washing on phospholipase C zeta concentrations in human spermatozoa. Reprod Biomed Online 23, 263-267.

Katari, R., Peloso, A., Zambon, J.P., Soker, S., Stratta, R.J., Atala, A., Orlando, G., 2014. Renal bioengineering with scaffolds generated from human kidneys. Nephron Exp Nephrol 126, 119-124.

Kawamura, K., Chen, Y., Shu, Y., Cheng, Y., Qiao, J., Behr, B., Pera, R.A.R., Hsueh, A.J.W., 2012. Promotion of human early embryonic development and blastocyst outgrowth in vitro using autocrine/paracrine growth factors. PLoS One 7, e49328.

Kennedy, S., Bergqvist, A., Chapron, C., D'Hooghe, T., Dunselman, G., Greb, R., Hummelshoj, L., Prentice, A., Saridogan, E., Endometriosis, E.S.I.G.f., Endometrium Guideline Development, G., 2005. ESHRE guideline for the diagnosis and treatment of endometriosis. Hum Reprod 20, 2698-2704.

Kim, C.F., Dirks, P.B., 2008. Cancer and stem cell biology: How tightly intertwined? Cell Stem Cell 3, 147-150.

Kim, D., Jeong, Y.Y., Jon, S., 2010a. A drug-loaded aptamer-gold nanoparticle bioconjugate for combined CT imaging and therapy of prostate cancer. ACS Nano 4, 3689-3696.

Kim, S.H., Chae, H.D., Kim, C.H., Kang, B.M., 2013a. Update on the treatment of endometriosis. Clin Exp Reprod Med 40, 55-59.

Kim, T.H., Lee, S., Chen, X., 2013b. Nanotheranostics for personalized medicine. Expert Rev Mol Diagn 13, 257-269.

Kim, T.S., Lee, S.H., Gang, G.T., Lee, Y.S., Kim, S.U., Koo, D.B., Shin, M.Y., Park, C.K., Lee, D.S., 2010b. Exogenous DNA uptake of boar spermatozoa by a magnetic nanoparticle vector system. Reprod Domest Anim 45, e201-206.

Kjelland, M.E., Gonzalez-Marin, C., Gosalvez, J., Lopez-Fernandez, C., Lenz, R.W., Evans, K.M., Moreno, J.F., 2011. DNA fragmentation kinetics and postthaw motility of flow cytometric-sorted white-tailed deer sperm. J Anim Sci 89, 3996-4006.

Knox, R.V., 2014. Impact of swine reproductive technologies on pig and global food production. Adv Exp Med Biol 752, 131-160.

Kojima, Y., Hayashi, Y., Kurokawa, S., Mizuno, K., Sasaki, S., Kohri, K., 2008. No evidence of germ-line transmission by adenovirus-mediated gene transfer to mouse testes. Fertil Steril 89, 1448-1454.

Koopmans, R.J., Aggeli, A., 2010. Nanobiotechnology — quo vadis? Curr Opin Microbiol 13, 327-334.

Kresge, C.T., Leonowicz, M.E., Roth, W.J., Vartuli, J.C., Beck, J.S., 1992. Ordered Mesoporous Molecular-Sieves Synthesized by a Liquid-Crystal Template Mechanism. Nature 359, 710-712.

Kubota, H., Hayashi, Y., Kubota, Y., Coward, K., Parrington, J., 2005. Comparison of two methods of in vivo gene transfer by electroporation. Fertil Steril 83, 1310-1318.

Kumar, S., Rhim, W.K., Lim, D.K., Nam, J.M., 2013. Glutathione dimerization-based plasmonic nanoswitch for biodetection of reactive oxygen and nitrogen species. ACS Nano 7, 2221-2230.

Kunzmann, A., Andersson, B., Thurnherr, T., Krug, H., Scheynius, A., Fadeel, B., 2011. Toxicology of engineered nanomaterials: focus on biocompatibility, biodistribution and biodegradation. Biochim Biophys Acta 1810, 361-373.

Lamb, D.J., 2008. Would gene therapy for the treatment of male infertility be safe? Nat Clin Pract Urol 5, 594-595.

Lammers, T., Aime, S., Hennink, W.E., Storm, G., Kiessling, F., 2011. Theranostic nanomedicine. Acc Chem Res 44, 1029-1038.

Lammers, T., Kiessling, F., Hennink, W.E., Storm, G., 2010. Nanotheranostics and image-guided drug delivery: current concepts and future directions. Mol Pharm 7, 1899-1912.

Langer, J.E., Oliver, E.R., Lev-Toaff, A.S., Coleman, B.G., 2012. Imaging of the Female Pelvis through the Life Cycle. Radiographics 32, 1575-1597.

Laschke, M.W., Menger, M.D., 2012. Anti-angiogenic treatment strategies for the therapy of endometriosis. Hum Reprod Update 18, 682-702.

Laughlin, S.K., Schroeder, J.C., Baird, D.D., 2010. New directions in the epidemiology of uterine fibroids. Semin Reprod Med 28, 204-217.

Lavitrano, M., Bacci, M.L., Forni, M., Lazzereschi, D., Di Stefano, C., Fioretti, D., Giancotti, P., Marfe, G., Pucci, L., Renzi, L., Wang, H., Stoppacciaro, A., Stassi, G., Sargiacomo, M., Sinibaldi, P., Turchi, V., Giovannoni, R., Della Casa, G., Seren, E., Rossi, G., 2002. Efficient production by sperm-mediated gene transfer of human decay accelerating factor (hDAF) transgenic pigs for xenotransplantation. P Natl Acad Sci USA 99, 14230-14235.

Lavitrano, M., Camaioni, A., Fazio, V.M., Dolci, S., Farace, M.G., Spadafora, C., 1989. Sperm cells as vectors for introducing foreign DNA into eggs - genetic-transformation of mice. Cell 57, 717-723.

Lavitrano, M., Giovannoni, R., Cerrito, M., 2013. Methods for sperm-mediated gene transfer, in: Carrell, D.T., Aston, K.I. (Eds.), Spermatogenesis. Humana Press, pp. 519-529.

Le Broc-Ryckewaert, D., Carpentier, R., Lipka, E., Daher, S., Vaccher, C., Betbeder, D., Furman, C., 2013. Development of innovative paclitaxel-loaded small PLGA nanoparticles: Study of their antiproliferative activity and their molecular interactions on prostatic cancer cells. Int J Pharm 454, 712-719.

Lee, H.J., Lee, H.J., Lee, J.M., Chang, Y., Woo, S.T., 2012. Ultrasmall superparamagnetic iron oxides enhanced MR imaging in rats with experimentally induced endometriosis. Magn Reson Imaging 30, 860-868.

Lee, K.J., An, J.H., Chun, J.R., Chung, K.H., Park, W.Y., Shin, J.S., Kim, D.H., Bahk, Y.Y., 2013. In vitro analysis of the anti-cancer activity of mitoxantrone loaded on magnetic nanoparticles. J Biomed Nanotechnol 9, 1071-1075.

Lehner, R., Wang, X., Marsch, S., Hunziker, P., 2013. Intelligent nanomaterials for medicine: Carrier platforms and targeting strategies in the context of clinical application. Nanomedicine 9, 742-757.

Lemmen, J.G., Agerholm, I., Ziebe, S., 2008. Kinetic markers of human embryo quality using time-lapse recordings of IVF/ICSI-fertilized oocytes. Reprod Biomed Online 17, 385-391.

Lenzi, A., Gandini, L., Picardo, M., Tramer, F., Sandri, G., Panfili, E., 2000. Lipoperoxidation damage of spermatozoa polyunsaturated fatty acids (PUFA): scavenger mechanisms and possible scavenger therapies. Front Biosci 5, E1-E15.

Levy, G., Hill, M.J., Plowden, T.C., Catherino, W.H., Armstrong, A.Y., 2013. Biomarkers in uterine leiomyoma. Fertil Steril 99, 1146-1152.

Li, Z., Barnes, J.C., Bosoy, A., Stoddart, J.F., Zink, J.I., 2012. Mesoporous silica nanoparticles in biomedical applications. Chem Soc Rev 41, 2590-2605.

Liang, C., Yang, Y., Ling, Y., Huang, Y., Li, T., Li, X., 2011. Improved therapeutic effect of folate-decorated PLGA-PEG nanoparticles for endometrial carcinoma. Bioorg Med Chem 19, 4057-4066.

Liang, X.J., Meng, H., Wang, Y., He, H., Meng, J., Lu, J., Wang, P.C., Zhao, Y., Gao, X., Sun, B., Chen, C., Xing, G., Shen, D., Gottesman, M.M., Wu, Y., Yin, J.J., Jia, L., 2010. Metallofullerene nanoparticles circumvent tumor resistance to cisplatin by reactivating endocytosis. P Natl Acad Sci USA 107, 7449-7454.

Lipskind, S.T., Gargiulo, A.R., 2013. Computer-assisted laparoscopy in fertility preservation and reproductive surgery. J Minim Invasive Gynecol 20, 435-445.

Liu, X.X., Rocchi, P., Qu, F.Q., Zheng, S.Q., Liang, Z.C., Gleave, M., Iovanna, J., Peng, L., 2009. PAMAM dendrimers mediate siRNA delivery to target Hsp27 and produce potent antiproliferative effects on prostate cancer cells. Chem Med Chem 4, 1302-1310.

Long, Q.D., Xie, Y., Huang, Y.Q., Wu, Q.J., Zhang, H.C., Xiong, S.Q., Liu, Y.W., Chen, L.J., Wei, Y.Q., Zhao, X., Gong, C.Y., 2013. Induction of apoptosis and inhibition of angiogenesis by PEGylated liposomal quercetin in both cisplatin-sensitive and cisplatin-resistant ovarian cancers. J Biomed Nanotechnol 9, 965-975.

Lu, D., Song, H., Shi, G., 2013. Anti-TNF-alpha treatment for pelvic pain associated with endometriosis. Cochrane Database Syst Rev 3, CD008088.

Lu, Y.Q., Liang, X.W., Zhang, M., Wang, W.L., Kitiyanant, Y., Lu, S.S., Meng, B., Lu, K.H., 2007. Birth of twins after in vitro fertilization with flow-cytometric sorted buffalo (Bubalus bubalis) sperm. Anim Reprod Sci 100, 192-196.

Luo, G.F., Chen, W.H., Liu, Y., Lei, Q., Zhuo, R.X., Zhang, X.Z., 2014. Multifunctional enveloped mesoporous silica nanoparticles for subcellular co-delivery of drug and therapeutic peptide. Sci Rep 4, 6064.

Mahajan, S.D., Aalinkeel, R., Law, W.C., Reynolds, J.L., Nair, B.B., Sykes, D.E., Yong, K.T., Roy, I., Prasad, P.N., Schwartz, S.A., 2012. Anti-HIV-1 nanotherapeutics: promises and challenges for the future. Int J Nanomedicine 7, 5301-5314.

Makhluf, S.B., Abu-Mukh, R., Rubinstein, S., Breitbart, H., Gedanken, A., 2008. Modified PVA-Fe3O4 nanoparticles as protein carriers into sperm cells. Small 4, 1453-1458.

Malvezzi, H., Sharma, R., Agarwal, A., Abuzenadah, A.M., Abu-Elmagd, M., 2014. Sperm quality after density gradient centrifugation with three commercially available media: a controlled trial. Reprod Biol Endocrinol 12, 121.

Mari, G., Rizzato, G., Merlo, B., Iacono, E., Bucci, D., Seren, E., Tamanini, C., Galeati, G., Spinaci, M., 2010. Quality and fertilizing ability in vivo of sex-sorted stallion spermatozoa. Reprod Domest Anim 45, 331-335.

Marina, S., Marina, F., Alcolea, R., Nadal, J., Exposito, R., Huguet, J., 1998. Pregnancy following intracytoplasmic sperm injection from an HIV-1-seropositive man. Hum Reprod 13, 3247-3249.

Marrache, S., Dhar, S., 2012. Engineering of blended nanoparticle platform for delivery of mitochondria-acting therapeutics. P Natl Acad Sci USA 109, 16288-16293.

Martin, G.B., 2014. An Australasian perspective on the role of reproductive technologies in world food production. Adv Exp Med Biol 752, 181-197.

Martin-Romero, F.J., Miguel-Lasobras, E.M., Dominguez-Arroyo, J.A., Gonzalez-Carrera, E., Alvarez, I.S., 2008. Contribution of culture media to oxidative stress and its effect on human oocytes. Reprod Biomed Online 17, 652-661.

Mascarenhas, M.N., Flaxman, S.R., Boerma, T., Vanderpoel, S., Stevens, G.A., 2012. National, regional, and global trends in infertility prevalence since 1990: a systematic analysis of 277 health surveys. PLoS Med 9, e1001356.

Matás, C., Vieira, L., García-Vázquez, F.A., Avilés-López, K., López-Úbeda, R., Carvajal, J.A., Gadea, J., 2011. Effects of centrifugation through three different discontinuous Percoll gradients on boar sperm function. Anim Reprod Sci 127, 62-72.

Matsoukas, T., Gulari, E., 1988. Dynamics of growth of silica particles from ammonia-catalyzed hydrolysis of tetra-ethyl-orthosilicate. J Colloid Interface Sci 124, 252-261.

Matsoukas, T., Gulari, E., 1989. Monomer-addition growth with a slow initiation step: a growth model for silica particles from alkoxides. J Colloid Interface Sci 132, 13-21.

Matsumura, Y., Maeda, H., 1986. A new concept for macromolecular therapeutics in cancer chemotherapy: mechanism of tumoritropic accumulation of proteins and the antitumor agent smancs. Cancer Res 46, 6387-6392.

Matsuura, R., Takeuchi, T., Yoshida, A., 2010. Preparation and incubation conditions affect the DNA integrity of ejaculated human spermatozoa. Asian J Androl 12, 753-759.

May, K.E., Conduit-Hulbert, S.A., Villar, J., Kirtley, S., Kennedy, S.H., Becker, C.M., 2010. Peripheral biomarkers of endometriosis: a systematic review. Hum Reprod Update 16, 651-674.

McGowan, I., Gomez, K., Bruder, K., Febo, I., Chen, B.A., Richardson, B.A., Husnik, M., Livant, E., Price, C., Jacobson, C., Team, M.T.N.P., 2011. Phase 1 randomized trial of the vaginal safety and acceptability of SPL7013 gel (VivaGel) in sexually active young women (MTN-004). AIDS 25, 1057-1064.

Medina-Sanchez, M., Miserere, S., Merkoci, A., 2012. Nanomaterials and lab-on-a-chip technologies. Lab Chip 12, 1932-1943.

Menezes, V., Malek, A., Keelan, J.A., 2011. Nanoparticulate drug delivery in pregnancy: placental passage and fetal exposure. Curr Pharm Biotechnol 12, 731-742.

Menjoge, A.R., Navath, R.S., Asad, A., Kannan, S., Kim, C.J., Romero, R., Kannan, R.M., 2010. Transport and biodistribution of dendrimers across human fetal membranes: implications for intravaginal administration of dendrimer-drug conjugates. Biomaterials 31, 5007-5021.

Meseguer, M., Rubio, I., Cruz, M., Basile, N., Marcos, J., Requena, A., 2012. Embryo incubation and selection in a time-lapse monitoring system improves pregnancy outcome compared with a standard incubator: a retrospective cohort study. Fertil Steril 98, 1481-1489 e1410.

Moretti, E., Terzuoli, G., Renieri, T., Iacoponi, F., Castellini, C., Giordano, C., Collodel, G., 2012. In vitro effect of gold and silver nanoparticles on human spermatozoa. Andrologia 45, 392-396.

Muramatsu, T., Shibata, O., Ryoki, S., Ohmori, Y., Okumura, J., 1997. Foreign gene expression in the mouse testis by localized in vivo gene transfer. Biochem Bioph Res Co 233, 45-49.

Na, H.K., Kim, M.H., Park, K., Ryoo, S.R., Lee, K.E., Jeon, H., Ryoo, R., Hyeon, C., Min, D.H., 2012. Efficient functional delivery of siRNA using mesoporous silica nanoparticles with ultralarge pores. Small 8, 1752-1761.

Nair, H.B., Huffman, S., Veerapaneni, P., Kirma, N.B., Binkley, P., Perla, R.P., Evans, D.B., Tekmal, R.R., 2011. Hyaluronic acid-bound letrozole nanoparticles restore sensitivity to letrozole-resistant xenograft tumors in mice. J Nanosci Nanotechnol 11, 3789-3799.

Nair, H.B., Sung, B., Yadav, V.R., Kannappan, R., Chaturvedi, M.M., Aggarwal, B.B., 2010. Delivery of antiinflammatory nutraceuticals by nanoparticles for the prevention and treatment of cancer. Biochem Pharmacol 80, 1833-1843.

Natali, I., 2011. Sperm preparation techniques for artificial insemination - comparison of sperm washing, swim up, and density gradient centrifugation methods, Artificial insemination in farm animals, Dr. Milad Manafi (Ed.), doi: 10.5772/17026.

National Institute for Health and Care Excellence (NICE), 2013. Clinical guideline (CG) 156 Fertility. RCOG, London.

Navath, R.S., Menjoge, A.R., Dai, H., Romero, R., Kannan, S., Kannan, R.M., 2011. Injectable PAMAM dendrimer-PEG hydrogels for the treatment of genital infections: formulation and in vitro and in vivo evaluation. Mol Pharmaceut 8, 1209-1223.

Neron, B., Menager, H., Maufrais, C., Joly, N., Maupetit, J., Letort, S., Carrere, S., Tuffery, P., Letondal, C., 2009. Mobyle: a new full web bioinformatics framework. Bioinformatics 25, 3005-3011.

Nnoaham, K.E., Hummelshoj, L., Webster, P., d'Hooghe, T., de Cicco Nardone, F., de Cicco Nardone, C., Jenkinson, C., Kennedy, S.H., Zondervan, K.T., 2011. Impact of endometriosis on quality of life and work productivity: a multicenter study across ten countries. Fertil Steril 96, 366-373 e368.

O'Brien, J.K., Robeck, T.R., 2006. Development of sperm sexing and associated assisted reproductive technology for sex preselection of captive bottlenose dolphins (Tursiops truncatus). Reprod Fertil Dev 18, 319-329.

O'Flynn O'Brien, K.L., Varghese, A.C., Agarwal, A., 2010. The genetic causes of male factor infertility: a review. Fertil Steril 93, 1-12.

Oddi, S., Bernabo, N., Di Tommaso, M., Angelucci, C.B., Bisicchia, E., Mattioli, M., Maccarrone, M., 2012. DNA uptake in swine sperm: effect of plasmid topology and methyl-beta-cyclodextrin-mediated cholesterol depletion. Mol Reprod Dev 79, 853-860.

Odhiambo, J.F., DeJarnette, J.M., Geary, T.W., Kennedy, C.E., Suarez, S.S., Sutovsky, M., Sutovsky, P., 2014. Increased conception rates in beef cattle inseminated with nanopurified bull semen. Biol Reprod 91, 97.

Office for National Statistics, 2013. Statistical Bulletin. Cancer Registrations Statistics, England (Series MB1). Office for National Statistics.

Oi, M., Yamada, K., Hayakawa, H., Suzuki, H., 2013. Sexing of dog sperm by fluorescence in situ hybridization. J Reprod Dev 59, 92-96.

Oktay, K., Karlikaya, G., 2000. Ovarian function after transplantation of frozen, banked autologous ovarian tissue. N Engl J Med 342, 1919-1919.

Otsuki, J., Nagai, Y., Chiba, K., 2009. Damage of embryo development caused by peroxidized mineral oil and its association with albumin in culture. Fertil Steril 91, 1745-1749.

Pardal, R., Clarke, M.F., Morrison, S.J., 2003. Applying the principles of stem-cell biology to cancer. Nat Rev Cancer 3, 895-902.

Parrington, J., Coward, K., Gadea, J., 2011. Sperm and testis mediated DNA transfer as a means of gene therapy. Syst Biol Reprod Med 57, 35-42.

Parrington, J., Coward, K., Hibbitt, O., Kubota, H., Young, C., McIlhinney, J., Jones, O., 2007. In vivo gene transfer into the testis by electroporation and viral infection--a novel way to study testis and sperm function. Soc Reprod Fertil Suppl 65, 469-474.

Patel, L.N., Zaro, J.L., Shen, W.C., 2007. Cell penetrating peptides: intracellular pathways and pharmaceutical perspectives. Pharm Res 24, 1977-1992.

Peng, W., Anderson, D.G., Bao, Y., Padera, R.F., Jr., Langer, R., Sawicki, J.A., 2007. Nanoparticulate delivery of suicide DNA to murine prostate and prostate tumors. Prostate 67, 855-862.

Peng, W., Dunton, C., Holtz, D., Parva, M., Stampler, K., Forwood, M., Gogoi, R., Lace, M.J., Anderson, D.G., Sawicki, J.A., 2013. DNA nanotherapy for pre-neoplastic cervical lesions. Gynecol Oncol 128, 101-106.

Perez-Martinez, F.C., Carrion, B., Lucio, M.I., Rubio, N., Herrero, M.A., Vazquez, E., Cena, V., 2012. Enhanced docetaxel-mediated cytotoxicity in human prostate cancer cells through knockdown of cofilin-1 by carbon nanohorn delivered siRNA. Biomaterials 33, 8152-8159.

Perfezou, M., Turner, A., Merkoci, A., 2012. Cancer detection using nanoparticle-based sensors. Chem Soc Rev 41, 2606-2622.

Perlmutter, D.H., Glover, G.I., Rivetna, M., Schasteen, C.S., Fallon, R.J., 1990. Identification of a serpin-enzyme complex receptor on human hepatoma cells and human monocytes. Proc Natl Acad Sci USA 87, 3753-3757.

Perrin, J., Tassistro, V., Auffan, M., Liu, W., Botta, A., Sari-Minodier, I., Bottero, J.Y., Orsiere, T., Rose, J., Courbiere, B., 2014. Cerium dioxide nanoparticles induce DNA damage in human spermatozoa. Hum Reprod 29, i8-i9.

Petros, R.A., DeSimone, J.M., 2010. Strategies in the design of nanoparticles for therapeutic applications. Nat Rev Drug Discov 9, 615-627.

Pineda, L., Sawosz, E., Hotowy, A., Elnif, J., Sawosz, F., Ali, A., Chwalibog, A., 2012. Effect of nanoparticles of silver and gold on metabolic rate and development of broiler and layer embryos. Comp Biochem Physiol A Mol Integr Physiol 161, 315-319.

Preaubert, L., Courbiere, B., Achard, V., Tassistro, V., Greco, F., Orsiere, T., Bottero, J.Y., Rose, J., Auffan, M., Perrin, J., 2015. Cerium dioxide nanoparticles affect in vitro fertilization in mice. Nanotoxicology, 1-7.

Psarros, C., Lee, R., Margaritis, M., Antoniades, C., 2012. Nanomedicine for the prevention, treatment and imaging of atherosclerosis. Nanomedicine 8, Supplement 1, S59-S68.

Pursel, V.G., Johnson, L.A., 1976. Frozen boar spermatozoa: methods of thawing pellets. J Anim Sci 42, 927-931.

Pursel, V.G., Rampacek, G.B., Johnson, L.A., 1972. Acrosome morphology of boar spermatozoa incubated before cold shock. J Anim Sci 34, 278-&.

Qi, X., Song, X., Liu, P., Yi, T., Li, S., Xie, C., Zheng, Y., Bai, Y., Sun, C., Wei, Y., Zhao, X., 2011. Antitumor effects of PLGA nanoparticles encapsulating the human PNAS-4 gene combined with cisplatin in ovarian cancer. Oncol Rep 26, 703-710.

Quan, G.B., Ma, Y., Li, J., Wu, G.Q., Li, D.J., Ni, Y.N., Lv, C.R., Zhu, L., Hong, Q.H., 2015. Effects of Hoechst33342 staining on the viability and flow cytometric sex-sorting of frozen-thawed ram sperm. Cryobiology 70, 23-31.

Raper, S.E., Chirmule, N., Lee, F.S., Wivel, N.A., Bagg, A., Gao, G.P., Wilson, J.M., Batshaw, M.L., 2003. Fatal systemic inflammatory response syndrome in a ornithine transcarbamylase deficient patient following adenoviral gene transfer. Mol Genet Metab 80, 148-158.

Raposo, G., Stoorvogel, W., 2013. Extracellular vesicles: exosomes, microvesicles, and friends. J Cell Biol 200, 373-383.

Rath, D., Barcikowski, S., de Graaf, S., Garrels, W., Grossfeld, R., Klein, S., Knabe, W., Knorr, C., Kues, W., Meyer, H., Michl, J., Moench-Tegeder, G., Rehbock, C., Taylor, U., Washausen, S., 2013. Sex selection of sperm in farm animals: status report and developmental prospects. Reproduction 145, R15-30.

Rees, P., Brown, M.R., Summers, H.D., Holton, M.D., Errington, R.J., Chappell, S.C., Smith, P.J., 2011. A transfer function approach to measuring cell inheritance. BMC Syst Biol 5, 31.

Refuerzo, J.S., Godin, B., Bishop, K., Srinivasan, S., Shah, S.K., Amra, S., Ramin, S.M., Ferrari, M., 2011. Size of the nanovectors determines the transplacental passage in pregnancy: study in rats. Am J Obstet Gynecol 204, 546.e545-549.

Rhee, M., Davis, P., 2006. Mechanism of uptake of C105Y, a novel cell-penetrating peptide. J Biol Chem 281, 1233-1240.

Riehemann, K., Schneider, S.W., Luger, T.A., Godin, B., Ferrari, M., Fuchs, H., 2009. Nanomedicine--challenge and perspectives. Angew Chem Int Ed Engl 48, 872-897.

Roa, W., Zhang, X.J., Guo, L.H., Shaw, A., Hu, X.Y., Xiong, Y.P., Gulavita, S., Patel, S., Sun, X.J., Chen, J., Moore, R., Xing, J.Z., 2009. Gold nanoparticle sensitize radiotherapy of prostate cancer cells by regulation of the cell cycle. Nanotechnology 20, 375101.

Robinson, L., Gallos, I.D., Conner, S.J., Rajkhowa, M., Miller, D., Lewis, S., Kirkman-Brown, J., Coomarasamy, A., 2012. The effect of sperm DNA fragmentation on miscarriage rates: a systematic review and meta-analysis. Hum Reprod 27, 2908-2917.

Rocha, S., Generalov, R., Pereira Mdo, C., Peres, I., Juzenas, P., Coelho, M.A., 2011. Epigallocatechin gallate-loaded polysaccharide nanoparticles for prostate cancer chemoprevention. Nanomedicine (Lond) 6, 79-87.

Romany, L., Garrido, N., Motato, Y., Aparicio, B., Remohi, J., Meseguer, M., 2014. Removal of annexin V-positive sperm cells for intracytoplasmic sperm injection in ovum donation cycles does not improve reproductive outcome: a controlled and randomized trial in unselected males. Fertil Steril 102, 1567-1575 e1561.

Rosenholm, J.M., Mamaeva, V., Sahlgren, C., Linden, M., 2012. Nanoparticles in targeted cancer therapy: mesoporous silica nanoparticles entering preclinical development stage. Nanomedicine (Lond) 7, 111-120.

Rougier, N., Uriondo, H., Papier, S., Checa, M.A., Sueldo, C., Alvarez Sedo, C., 2013. Changes in DNA fragmentation during sperm preparation for intracytoplasmic sperm injection over time. Fertil Steril 100, 69-74.

Ryan, S.M., Brayden, D.J., 2014. Progress in the delivery of nanoparticle constructs: towards clinical translation. Curr Opin Pharmacol 18, 120-128.

Sanna, V., Pintus, G., Roggio, A.M., Punzoni, S., Posadino, A.M., Arca, A., Marceddu, S., Bandiera, P., Uzzau, S., Sechi, M., 2011. Targeted biocompatible nanoparticles for the delivery of (-)-epigallocatechin 3-gallate to prostate cancer cells. J Med Chem 54, 1321-1332.

Santra, S., Yang, H., Dutta, D., Stanley, J.T., Holloway, P.H., Tan, W., Moudgil, B.M., Mericle, R.A., 2004. TAT conjugated, FITC doped silica nanoparticles for bioimaging applications. Chem. Commun. (Camb.) 2810-2811.

Schindelin, J., Arganda-Carreras, I., Frise, E., Kaynig, V., Longair, M., Pietzsch, T., Preibisch, S., Rueden, C., Saalfeld, S., Schmid, B., Tinevez, J.Y., White, D.J., Hartenstein, V., Eliceiri, K., Tomancak, P., Cardona, A., 2012. Fiji: an open-source platform for biological-image analysis. Nat Methods 9, 676-682.

Schmidt, L., Sobotka, T., Bentzen, J.G., Nyboe Andersen, A., Reproduction, E., Society Task, F., 2012. Demographic and medical consequences of the postponement of parenthood. Hum Reprod Update 18, 29-43.

Senapati, S., Barnhart, K.T., 2013. Biomarkers for ectopic pregnancy and pregnancy of unknown location. Fertil Steril 99, 1107-1116.

Serra, P., Santamaria, P., 2015. Nanoparticle-based autoimmune disease therapy. Clin Immunol 160, 3-13.

Sfontouris, I.A., Nastri, C.O., Lima, M.L., Tahmasbpourmarzouni, E., Raine-Fenning, N., Martins, W.P., 2015. Artificial oocyte activation to improve reproductive outcomes in women with previous fertilization failure: a systematic review and meta-analysis of RCTs. Hum Reprod 30, 1831-1841.

Sharif, F., Porta, F., Meijer, A.H., Kros, A., Richardson, M.K., 2012. Mesoporous silica nanoparticles as a compound delivery system in zebrafish embryos. Int J Nanomedicine 7, 1875-1890.

Sharma, B., Ma, W., Adjei, I.M., Panyam, J., Dimitrijevic, S., Labhasetwar, V., 2011. Nanoparticle-mediated p53 gene therapy for tumor inhibition. Drug Deliv Transl Res 1, 43-52.

Shi, N.Q., Qi, X.R., Xiang, B., Zhang, Y., 2014. A survey on "Trojan Horse" peptides: Opportunities, issues and controlled entry to "Troy". J Control Release 28, 53-70.

Sinden, R.R., Pearson, C.E., Potaman, V.N., Ussery, D.W., 1998. DNA: structure and function. Advances in genome biology 5, 1-141.

Singh, N., Manshian, B., Jenkins, G.J., Griffiths, S.M., Williams, P.M., Maffeis, T.G., Wright, C.J., Doak, S.H., 2009. NanoGenotoxicology: the DNA damaging potential of engineered nanomaterials. Biomaterials 30, 3891-3914.

Singh, R., Smitha, M.S., Singh, S.P., 2014. The role of nanotechnology in combating multi-drug resistant bacteria. J Nanosci Nanotechnol 14, 4745-4756.

Skuridin, S.G., Dubinskaya, V.A., Rudoy, V.M., Dement'eva, O.V., Zakhidov, S.T., Marshak, T.L., Kuz'min, V.A., Popenko, V.I., Evdokimov, Y.M., 2010. Effect of gold nanoparticles on DNA package in model systems. Dokl Biochem Biophys 432, 141-143.

Smith, K., Spadafora, C., 2005. Sperm-mediated gene transfer: applications and implications. Bioessays 27, 551-562.

Sohel, M.M., Hoelker, M., Noferesti, S.S., Salilew-Wondim, D., Tholen, E., Looft, C., Rings, F., Uddin, M.J., Spencer, T.E., Schellander, K., Tesfaye, D., 2013. Exosomal and non-exosomal transport of extra-cellular microRNAs in follicular fluid: implications for bovine oocyte developmental competence. PLoS One 8, e78505.

Spinaci, M., Merlo, B., Zannoni, A., Iacono, E., De Ambrogi, M., Turba, M.E., Zambelli, D., 2007. In vitro production of cat blastocysts of predetermined sex using flow cytometrically sorted semen. Theriogenology 67, 872-877.

Steg, A.D., Katre, A.A., Goodman, B., Han, H.D., Nick, A.M., Stone, R.L., Coleman, R.L., Alvarez, R.D., Lopez-Berestein, G., Sood, A.K., Landen, C.N., 2011. Targeting the notch ligand JAGGED1 in both tumor cells and stroma in ovarian cancer. Clin Cancer Res 17, 5674-5685.

Steptoe, P.C., 1969. Laparoscopy: diagnostic and therapeutic uses. Proc R Soc Med 62, 439-441.

Steptoe, P.C., Edwards, R.G., 1978. Birth after the reimplantation of a human embryo. Lancet 2, 366.

Stern, J.M., Stanfield, J., Kabbani, W., Hsieh, J.T., Cadeddu, J.R.A., 2008. Selective prostate cancer thermal ablation with laser activated gold nanoshells. J Urol 179, 748-753.

Stratton, P., Winkel, C., Premkumar, A., Chow, C., Wilson, J., Hearns-Stokes, R., Heo, S., Merino, M., Nieman, L.K., 2003. Diagnostic accuracy of laparoscopy, magnetic resonance imaging, and histopathologic examination for the detection of endometriosis. Fertil Steril 79, 1078-1085.

Su, M.T., Lin, S.H., Chen, Y.C., 2011. Genetic association studies of angiogenesis- and vasoconstriction-related genes in women with recurrent pregnancy loss: a systematic review and meta-analysis. Hum Reprod Update 17, 803-812.

Sullivan, E.A., Zegers-Hochschild, F., Mansour, R., Ishihara, O., de Mouzon, J., Nygren, K.G., Adamson, G.D., 2013. International Committee for Monitoring Assisted Reproductive Technologies (ICMART) world report: assisted reproductive technology 2004. Hum Reprod 28, 1375-1390.

Sullivan, R., Saez, F., 2013. Epididymosomes, prostasomes, and liposomes: their roles in mammalian male reproductive physiology. Reproduction 146, R21-35.

Sun, C., Yi, T., Song, X., Li, S., Qi, X., Chen, X., Lin, H., He, X., Li, Z., Wei, Y., Zhao, X., 2011. Efficient inhibition of ovarian cancer by short hairpin RNA targeting claudin-3. Oncol Rep 26, 193-200.

Suwansa-ard, S., Kanatharana, P., Asawatreratanakul, P., Wongkittisuksa, B., Limsakul, C., Thavarungkul, P., 2009. Comparison of surface plasmon resonance and capacitive immunosensors for cancer antigen 125 detection in human serum samples. Biosens Bioelectron 24, 3436-3441.

Tapia, J., Macias-Garcia, B., Miro-Moran, A., Ortega-Ferrusola, C., Salido, G., Pena, F., Aparicio, I., 2012. The membrane of the mammalian spermatozoa: much more than an inert envelope. Reprod Domest Anim 47 Suppl 3, 65-75.

Tardif, S., Madamidola, O.A., Brown, S.G., Frame, L., Lefievre, L., Wyatt, P.G., Barratt, C.L., Martins Da Silva, S.J., 2014. Clinically relevant enhancement of human sperm motility using compounds with reported phosphodiesterase inhibitor activity. Hum Reprod 29, 2123-2135.

Taylor, U., Barchanski, A., Garrels, W., Klein, S., Kues, W., Barcikowski, S., Rath, D., 2012. Toxicity of gold nanoparticles on somatic and reproductive cells. Adv Exp Med Biol 733, 125-133.

Taylor, U., Barchanski, A., Petersen, S., Kues, W.A., Baulain, U., Gamrad, L., Sajti, L., Barcikowski, S., Rath, D., 2014a. Gold nanoparticles interfere with sperm functionality by membrane adsorption without penetration. Nanotoxicology 8 Suppl 1, 118-127.

Taylor, U., Garrels, W., Barchanski, A., Peterson, S., Sajti, L., Lucas-Hahn, A., Gamrad, L., Baulain, U., Klein, S., Kues, W.A., Barcikowski, S., Rath, D., 2014b. Injection of ligand-free gold and silver nanoparticles into murine embryos does not impact pre-implantation development. Beilstein J Nanotech 5, 677-688.

Taylor, U., Klein, S., Petersen, S., Kues, W., Barcikowski, S., Rath, D., 2010a. Nonendosomal cellular uptake of ligand-free, positively charged gold nanoparticles. Cytom Part A 77A, 439-446.

Taylor, U., Petersen, S., Barchanski, A., Mittag, A., Barcikowski, S., Rath, D., 2010b. Influence of gold nanoparticles on vitality parameters of bovine spermatozoa. Reprod Domest Anim 45, 60.

Taylor, U., Rehbock, C., Streich, C., Rath, D., Barcikowski, S., 2014c. Rational design of gold nanoparticle toxicology assays: a question of exposure scenario, dose and experimental setup. Nanomedicine (Lond.) 9, 1971-1989.

Telfer, E.E., McLaughlin, M., 2012. Strategies to support human oocyte development in vitro. Int J Dev Biol 56, 901-907.

Terzuoli, G., Iacoponi, F., Moretti, E., Renieri, T., Baldi, G., Collodel, G., 2012. In vitro effect of silver engineered nanoparticles on human spermatozoa. J Siena Acad Sci 3, 27.

Thaxton, C.S., Elghanian, R., Thomas, A.D., Stoeva, S.I., Lee, J.S., Smith, N.D., Schaeffer, A.J., Klocker, H., Horninger, W., Bartsch, G., Mirkin, C.A., 2009. Nanoparticle-based bio-barcode assay redefines "undetectable" PSA and biochemical recurrence after radical prostatectomy. P Natl Acad Sci USA 106, 18437-18442.

Thoeny, H.C., Triantafyllou, M., Birkhaeuser, F.D., Froehlich, J.M., Tshering, D.W., Binser, T., Fleischmann, A., Vermathen, P., Studer, U.E., 2009. Combined ultrasmall superparamagnetic particles of iron oxide-enhanced and diffusion-weighted magnetic resonance imaging reliably detect pelvic lymph node metastases in normal-sized nodes of bladder and prostate cancer patients. Eur Urol 55, 761-769.

Tiedemann, D., Taylor, U., Rehbock, C., Jakobi, J., Klein, S., Kues, W.A., Barcikowski, S., Rath, D., 2014. Reprotoxicity of gold, silver, and gold-silver alloy nanoparticles on mammalian gametes. Analyst 139, 931-942.

Tomoda, K., Terashima, H., Suzuki, K., Inagi, T., Terada, H., Makino, K., 2012a. Enhanced transdermal delivery of indomethacin using combination of PLGA nanoparticles and iontophoresis in vivo. Colloids Surf B Biointerfaces 92, 50-54.

Tomoda, K., Watanabe, A., Suzuki, K., Inagi, T., Terada, H., Makino, K., 2012b. Enhanced transdermal permeability of estradiol using combination of PLGA nanoparticles system and iontophoresis. Colloids Surf B Biointerfaces 97, 84-89.

Toro, E., Fernández, S., Colomar, A., Casanovas, A., Álvarez, J.G., López-Teijón, M., Velilla, E., 2009. Processing of semen can result in increased sperm DNA fragmentation. Fertil Steril 92, 2109-2112.

Tsai, N., Lee, B., Kim, A., Yang, R., Pan, R., Lee, D.-K., Chow, E.K., Ho, D., 2014. Nanomedicine for global health. JALA, pii: 2211068214538263.

Tseng, C.-L., Peng, C.-L., Huang, J.-Y., Chen, J.-C., Lin, F.-H., 2013. Gelatin nanoparticles as gene carriers for transgenic chicken applications. J Biomater Appl 27, 1055-1065.

U.S. Cancer Statistics Working Group, 2013. United States Cancer Statistics: 1999–2009 Incidence and mortality web-based report., 03/01/2013 ed. US Department of Health and Human Services, Centers for Disease Control and Prevention and National Cancer Institute, Atlanta.

Urata, C., Aoyama, Y., Tonegawa, A., Yamauchi, Y., Kuroda, K., 2009. Dialysis process for the removal of surfactants to form colloidal mesoporous silica nanoparticles. Chem Commun 34, 5094-5096.

Uskokovic, V., 2013. Entering the era of nanoscience: time to be so small. J Biomed Nanotechnol 9, 1441-1470.

Vallet-Regi, M., Balas, F., Arcos, D., 2007. Mesoporous materials for drug delivery. Angew Chem Int Edit 46, 7548-7558.

Van Gorp, T., Cadron, I., Vergote, I., 2011. The utility of proteomics in gynecologic cancers. Curr Opin Obstet Gynecol 23, 3-7.

van Mello, N.M., Mol, F., Ankum, W.M., Mol, B.W., van der Veen, F., Hajenius, P.J., 2012. Ectopic pregnancy: how the diagnostic and therapeutic management has changed. Fertil Steril 98, 1066-1073.

Vanderhyden, B.C., Armstrong, D.T., 1989. Role of cumulus cells and serum on the in vitro maturation, fertilization, and subsequent development of rat oocytes. Biol Reprod 40, 720-728.

Vazquez, J.M., Parrilla, I., Roca, J., Gil, M.A., Cuello, C., Vazquez, J.L., Martinez, E.A., 2009. Sex-sorting sperm by flow cytometry in pigs: issues and perspectives. Theriogenology 71, 80-88.

Velez, J.M., Velez, J.J., 2011. The eminent need for an academic program in universities to teach nanomedicine. Int J Nanomedicine 6, 1733-1738.

Verlinsky, Y., Rechitsky, S., Schoolcraft, W., Strom, C., Kuliev, A., 2001. Preimplantation diagnosis for Fanconi anemia combined with HLA matching. JAMA 285, 3130-3133.

Wang, A.Z., Bagalkot, V., Vasilliou, C.C., Gu, F., Alexis, F., Zhang, L., Shaikh, M., Yuet, K., Cima, M.J., Langer, R., Kantoff, P.W., Bander, N.H., Jon, S., Farokhzad, O.C., 2008. Superparamagnetic iron oxide nanoparticle-aptamer bioconjugates for combined prostate cancer imaging and therapy. Chem Med Chem 3, 1311-1315.

Wang, N., Liu, B., Liang, L., Wu, Y., Xie, H., Huang, J., Guo, X., Tan, J., Zhan, X., Liu, Y., Wang, L., Ke, P., 2014. Antiangiogenesis therapy of endometriosis using PAMAM as a gene vector in a noninvasive animal model. BioMed Research International 2014, 11. doi: 10.1155/2014/546479.

Wang, Y., Zhao, Q., Han, N., Bai, L., Li, J., Liu, J., Che, E., Hu, L., Zhang, Q., Jiang, T., Wang, S., 2015. Mesoporous silica nanoparticles in drug delivery and biomedical applications. Nanomedicine 11, 313-327.

Waychunas, G.A., 2009. Natural nanoparticle structure, properties and reactivity from X-ray studies. Powder Diffraction 24, 89-93.

Webster, T.J., 2006. Nanomedicine: what's in a definition? Int J Nanomedicine 1, 115-116.

Wells, D., 2014. Next-generation sequencing: the dawn of a new era for preimplantation genetic diagnostics. Fertil Steril 101, 1250-1251.

Williams, V.S., Jones, G., Mauskopf, J., Spalding, J., DuChane, J., 2006. Uterine fibroids: a review of health-related quality of life assessment. J Womens Health (Larchmt) 15, 818-829.

Winer, I., Wang, S.Y., Lee, Y.E.K., Fan, W.Z., Gong, Y.S., Burgos-Ojeda, D., Spahlinger, G., Kopelman, R., Buckanovich, R.J., 2010. F3-targeted cisplatin-hydrogel nanoparticles as an effective therapeutic that targets both murine and human ovarian tumor endothelial cells in vivo. Cancer Res 70, 8674-8683.

Wiwanitkit, V., Sereemaspun, A., Rojanathanes, R., 2009. Effect of gold nanoparticles on spermatozoa: the first world report. Fertil Steril 91, E7-E8.

Woods, N.B., Bottero, V., Schmidt, M., von Kalle, C., Verma, I.M., 2006. Gene therapy: therapeutic gene causing lymphoma. Nature 440, 1123.

Wu, S.H., Hung, Y., Mou, C.Y., 2011. Mesoporous silica nanoparticles as nanocarriers. Chem Commun 47, 9972-9985.

Xia, T., Kovochich, M., Liong, M., Meng, H., Kabehie, S., George, S., Zink, J.I., Nel, A.E., 2009. Polyethyleneimine coating enhances the cellular uptake of mesoporous silica nanoparticles and allows safe delivery of siRNA and DNA constructs. ACS Nano 3, 3273-3286.

Xie, J., Lee, S., Chen, X., 2010. Nanoparticle-based theranostic agents. Adv Drug Deliv Rev 62, 1064-1079.

Yamada, H., Urata, C., Ujiie, H., Yamauchi, Y., Kuroda, K., 2013. Preparation of aqueous colloidal mesostructured and mesoporous silica nanoparticles with controlled particle size in a very wide range from 20 nm to 700 nm. Nanoscale 5, 6145-6153.

Yamauchi, Y., Riel, J.M., Ward, M.A., 2012. Paternal DNA damage resulting from various sperm treatments persists after fertilization and is similar before and after DNA replication. J Androl 33, 229-238.

Yang, J., Li, S., Guo, F., Zhang, W., Wang, Y., Pan, Y., 2013. Induction of apoptosis by chitosan/HPV16 E7 siRNA complexes in cervical cancer cells. Mol Med Rep 7, 998-1002.

Yang, J., Xie, S.X., Huang, Y., Ling, M., Liu, J., Ran, Y., Wang, Y., Thrasher, J.B., Berkland, C., Li, B., 2012a. Prostate-targeted biodegradable nanoparticles loaded with androgen receptor silencing constructs eradicate xenograft tumors in mice. Nanomedicine (Lond) 7, 1297-1309.

Yang, P., Skarsgard, E., Jia, W., 2009. Chitosan-Mediated in Utero Gene Therapy for Cystic Fibrosis. J Invest Med 57, 97-97.

Yang, P.P., Gai, S.L., Lin, J., 2012b. Functionalized mesoporous silica materials for controlled drug delivery. Chem Soc Rev 41, 3679-3698.

Yang, P.T., Hoang, L., Jia, W.W., Skarsgard, E.D., 2011. In utero gene delivery using chitosan-DNA nanoparticles in mice. J Surg Res 171, 691-699.

Ye, J., Coulouris, G., Zaretskaya, I., Cutcutache, I., Rozen, S., Madden, T.L., 2012. Primer-BLAST: a tool to design target-specific primers for polymerase chain reaction. BMC Bioinformatics 13, 134. doi: 10.1186/1471-2105-13-134.

Yelumalai, S., Jones, C., Mounce, G., McVeigh, E., Fatum, M., Coward, K., 2013. Levels of the oocyte activation factor, phospholipase c zeta, in human sperm are reduced following incubation with polyvinylpyrrolidone (PVP). Fertil Steril 100, S88.

Yu, M.K., Kim, D., Lee, I.H., So, J.S., Jeong, Y.Y., Jon, S., 2011. Image-guided prostate cancer therapy using aptamer-functionalized thermally cross-linked superparamagnetic iron oxide nanoparticles. Small 7, 2241-2249.

Yuan, J.L., Duan, R.Q., Yang, H., Luo, X.G., Xi, M.R., 2012. Detection of serum human epididymis secretory protein 4 in patients with ovarian cancer using a label-free biosensor based on localized surface plasmon resonance. International Journal of Nanomedicine 7, 2921-2928.

Yun, J.I., Gong, S.P., Song, Y.H., Lee, S.T., 2013. Effects of combined antioxidant supplementation on human sperm motility and morphology during sperm manipulation in vitro. Fertil Steril 100, 373-378.

Zamboni, W.C., Torchilin, V., Patri, A.K., Hrkach, J., Stern, S., Lee, R., Nel, A., Panaro, N.J., Grodzinski, P., 2012. Best practices in cancer nanotechnology: perspective from NCI nanotechnology alliance. Clin Cancer Res 18, 3229-3241.

Zhang, W., Zhang, D., Tan, J., Cong, H., 2012. Carbon nanotube exposure sensitize human ovarian cancer cells to paclitaxel. J Nanosci Nanotechnol 12, 7211-7214.

Zhang, X., Chen, J., Kang, Y., Hong, S., Zheng, Y., Sun, H., Xu, C., 2013. Targeted paclitaxel nanoparticles modified with follicle-stimulating hormone beta 81-95 peptide show effective antitumor activity against ovarian carcinoma. Int J Pharm 453, 498-505.

Zhao, D., Zhao, X., Zu, Y., Li, J., Zhang, Y., Jiang, R., Zhang, Z., 2010. Preparation, characterization, and in vitro targeted delivery of folate-decorated paclitaxel-loaded bovine serum albumin nanoparticles. Int J Nanomedicine 5, 669-677.

Zhao, M.D., Sun, Y.M., Fu, G.F., Du, Y.Z., Chen, F.Y., Yuan, H., Zheng, C.H., Zhang, X.M., Hu, F.Q., 2012. Gene therapy of endometriosis introduced by polymeric micelles with glycolipid-like structure. Biomaterials 33, 634-643.

Zhou, Z., Wang, L., Chi, X., Bao, J., Yang, L., Zhao, W., Chen, Z., Wang, X., Chen, X., Gao, J., 2013. Engineered iron-oxide-based nanoparticles as enhanced T1 contrast agents for efficient tumor imaging. ACS Nano 7, 3287-3296.

Zhu, J., Wang, H., Liao, L., Zhao, L., Zhou, L., Yu, M., Wang, Y., Liu, B., Yu, C., 2011. Small mesoporous silica nanoparticles as carriers for enhanced photodynamic therapy. Chemistry – An Asian Journal 6, 2332-2338.

Zielinska, M., Sawosz, E., Grodzik, M., Wierzbicki, M., Gromadka, M., Hotowy, A., Sawosz, F., Lozicki, A., Chwalibog, A., 2011. Effect of heparan sulfate and gold nanoparticles on muscle development during embryogenesis. Int J Nanomedicine 6, 3163-3172.

Zou, L., Song, X., Yi, T., Li, S., Deng, H., Chen, X., Li, Z., Bai, Y., Zhong, Q., Wei, Y., Zhao, X., 2013. Administration of PLGA nanoparticles carrying shRNA against focal adhesion kinase and CD44 results in enhanced antitumor effects against ovarian cancer. Cancer Gene Ther 20, 242-250.

APPENDIX 1

RESEARCH OUTPUT

PUBLICATIONS (ORIGINAL RESEARCH PAPERS UNDERLINED)

1. **Barkalina N**, Jones C, Wood MJ, Coward K. 'Extracellular vesicle-mediated delivery of molecular compounds into gametes and embryos: learning from nature' Human Reproduction Update. 2015: pii: dmv027
2. **Barkalina N,** Jones C, Coward K. 'Nanomedicine and mammalian sperm: lessons from the porcine model' Theriogenology. 2015: pii: S0093-691X(15)00289-7. [Invited review]
3. **Barkalina N**, Jones C, Townley H, Coward K. 'Functionalisation of mesoporous silica nanoparticles with a cell-penetrating peptide as a tool to target mammalian sperm *in vitro.*' Nanomedicine (Lond). 2015;10(10):1539-53
4. Jones C, **Barkalina N**, Coward K. 'Highlights from the latest articles in nanomedicine for reproductive oncology.' Nanomedicine (Lond). 2015;10(9):1375-7. [Invited mini-review]
5. **Barkalina N**, Jones C, Coward K. 'Highlights from the latest articles in nanomedicine.' Nanomedicine (Lond). 2014;9(15):2255-8. [Invited mini-review]
6. **Barkalina N**, Jones C, Coward K. 'Mesoporous silica nanoparticles: a potential targeted delivery vector for reproductive biology?' Nanomedicine (Lond). 2014; 9(5):557-60. [Invited editorial]
7. **Barkalina N**, Charalambous C, Jones C, Coward K. 'Nanotechnology in reproductive medicine: emerging applications of nanomaterials' Nanomedicine. 2014;10(5):921-38.
8. **Barkalina N**, Jones C, Kashir J, Huang X, Morrison R, Townley H, Coward K. 'Effects of mesoporous silica nanoparticles upon the function of mammalian sperm *in vitro*' Nanomedicine. 2014; 10(4):859-70.

ORAL PRESENTATIONS

1. **Mesoporous silica nanoparticles in mammalian sperm: effects of in vitro exposure upon fertilization potential'**
   Barkalina N, Charalambous C, Jones C, Coward C.
   5th International Conference 'BioNanoMed 2014', Krems (Austria), 26-28 March 2014
2. **'Mesoporous silica nanoparticles: a potential targeted delivery vector for reproductive biology'**
   The Queen's College Symposium, 4 March 2014
3. **'Mesoporous silica nanoparticle-mediated delivery to mammalian sperm and oocytes: localisation, viability and loading studies'**
   2nd Institute of Reproductive Sciences Research Symposium, Oxford, 22 November 2013
4. **'Mesoporous silica nanoparticle-mediated delivery to mammalian sperm and oocytes: localisation, viability and loading studies'**
   Barkalina N, Kashir J, Jones C, Day C, Townley H, Coward C.
   'Fertility 2013' Conference, Liverpool, 3-5 January 2013

POSTER PRESENTATIONS

1. **'Nanotoxicity of mesoporous silica nanoparticles in human sperm following *in vitro* exposure'**
   Barkalina N, Jones C, Coward C.
   Annual Meeting of the European Society of Human Reproduction and Embryology, Lisbon, 14-19 June 2015
2. **'Mesoporous silica nanoparticles as a delivery platform to mammalian gametes: development of novel research tools and techniques for the transfer of therapeutic compounds'**
   Barkalina N, Kashir J, Jones C, Townley H, Coward C.
   Annual Meeting of the European Society of Human Reproduction and Embryology, London, 7-10 July 2013
3. **'Translational research at the Institute of Reproductive Sciences'**
   Barkalina N, Jones C, Coward C.
   Academic Medical Forum, Oxford, 30 April 2013
4. **'Nanoparticle-mediated delivery to sperm and oocytes: localisation, viability and loading studies'**
   Barkalina N, Kashir J, Jones C, Day C, Townley H, Coward C.
   Annual Oxford Developmental Biology Symposium, 4 December 2012

PATENT APPLICATIONS

1. **Delivery method using mesoporous silica nanoparticles**
   United Kingdom PCT/GB2013/053394 (filed in December 2013)
2. **Delivery method using mesoporous silica nanoparticles**
   US Patent Application No. 61/901,121 (filed in December 2013)

OTHER

1. **Associate Fellow of the Higher Education Academy** (Recognition Ref #PR070076)
2. Together with Dr Kevin Coward and Mrs Celine Jones: **OxTALENT 2014 Teaching Award** (IT Services) and **University Teaching Award** (presented by the Vice-Chancellor of Oxford).

APPENDIX 2

COPYRIGHT

All previously publishes work (for example, figures and images) included in this thesis was reproduced with relevant copyright permission from the original publisher.